Spatiotemporal analysis of Herpesvirus genome presentation and transcriptional progression

Catherine Cherry

2023

Imperial College London

Department of Infectious Disease, Section of Virology

A thesis submitted for the degree of Doctor of Philosophy

Statement of Originality

I declare that I conducted all scientific work presented in this thesis, with the following exception: the TMT labelling and mass spectrometry was performed by Dr Remigiusz Serwa, Proteomics Core Facility, IMoL, CeNT UW. The use of other material has been appropriately referenced and acknowledged.

Copyright Declaration

The copyright of this thesis rests with the author. Unless otherwise indicated, its contents are licensed under a Creative Commons Attribution-Non Commercial 4.0 International Licence (CC BY-NC).

Under this licence, you may copy and redistribute the material in any medium or format. You may also create and distribute modified versions of the work. This is on the condition that: you credit the author and do not use it, or any derivative works, for a commercial purpose.

When reusing or sharing this work, ensure you make the licence terms clear to others by naming the licence and linking to the licence text. Where a work has been adapted, you should indicate that the work has been changed and describe those changes.

Please seek permission from the copyright holder for uses of this work that are not included in this licence or permitted under UK Copyright Law.

Acknowledgements

My deepest thanks to my supervisor, Professor Peter O'Hare. Thank you for your endless patience, words of advice and support during the last few years. I have had the most tremendous time working with you and learning from your experience. Thank you to all the O'Hare Lab members who I had the pleasure of working with. In particular, thank you to Kerina for being the most wonderful friend and colleague, I'm so grateful for your friendship and support.

Thanks also to my co-supervisor, Vanessa Sancho-Shimizu, and my progress review panel Goedele Maertens and Mike Skinner for your advice throughout my PhD. I am very grateful to my funders, the Wellcome Trust, and to the Section of Virology at Imperial College.

Camilla, thanks for being the best flat mate anyone could have. Thank you for cooking dinner for me after late nights, putting up with my complaining and for always having a sympathetic hug ready.

George, thank you for everything. You made everything seem possible and allowed me to see what I could achieve.

Thanks to my Mum and Dad, whose encouragement was invaluable. Thank you for reminding me 'If a PhD wasn't difficult, you wouldn't be doing it!'.

Finally, I would like to pay tribute to the memory of the late Dr Marcus Dorner. Thank you for your mentorship and guidance during the time I spent within your lab. Dr Dorner's contribution to the field of virology cannot be understated and he is greatly missed.

Abstract

The initiation of herpesvirus transcription requires the selective recruitment and activity of the host transcriptional apparatus on virus immediate-early (IE) promoters. Despite general understanding of the broad principles of these early processes that have stemmed from population studies, we have comparatively limited knowledge of transcriptional events at the level of single cell and single genomes. I have developed methods combining click chemistry to visualise individual viral genomes with single molecule RNA transcript analysis and immunofluorescence to gain high resolution insight into the earliest processes of RNA polymerase recruitment, transcriptional bursting and RNA transport during the initiation of herpes simplex (HSV) infection.

Analysing ICP0 and ICP4, as key representatives of the HSV IE class, my results allow quantitative identification of genomes with transcriptionally active IE RNA bursting and the discrimination of active genomes from inactive ones. From simultaneous analysis of the ICP0 intron and exon, I show the highly restricted localisation of intron containing transcripts on genomes within the large mature transcript bursts. The results indicate the highly rapid and likely co-transcriptional splicing of the ICP0 pre-mRNA before general dispersal from the genome. I also show that while genomes show bursting activity for both ICP4 and ICP0, individual genomes can also be highly active for only one or other of these IE genes, indicating a spatial and temporal uncoupling of IE transcription at the single genome level. Combining genome, RNA and protein localisation, and discriminating transcriptionally active genomes from inactive ones, my results also indicate that there is no significant correlation between PML-genome association and transcriptional bursting.

Using pulse labelling with clickable nucleotide precursors to label nascent infected cell DNA synthesis I have examined the organisation and spatial relationship between later DNA synthesis and virus transcription during lytic HSV infection to reveal new qualitative features of the spatial relationship between viral transcription and DNA synthesis. In infected cells that are in S-phase my results

allow the spatial discrimination between cellular and viral DNA synthesis. Moreover, ICP4 shows pronounced selectivity by being recruited only to viral and not cellular sites of DNA replication, in contrast ICP8 is recruited to both types. I also show that different individual replication compartments within a single cell can be functionally distinct in terms of association with transcriptional activity.

These and other results yield insight into the processes of HSV gene expression. They demonstrate the utility of single cell and single molecule based imaging approaches for investigation of DNA virus genomes and their relationship with the host cell during infection. Finally, they prompt a re-evaluation of current models in aspects both of host suppression of viral transcription and the temporal progression of DNA replication.

Contents

Statement of Originality 2

Copyright Declaration 3

Acknowledgements 4

Abstract 5

List of Figures 14

List of Tables 15

Abbreviations 16

1 Introduction **17**

1.1 DNA Viruses 17

1.2 Herpes Simplex Virus 20

1.2.1 Viral Lifecycle 21

1.2.2 Viral Proteins 24

1.3 Transcription 27

1.3.1 DNA Dependent RNA polymerase 27

1.3.2 RNA pol II transcription initiation 28

1.3.3 Promoter proximal pausing 29

1.3.4 P-TEFb 29

1.4 Nuclear environment during early virus entry 31

1.4.1 PML . . . 31
1.4.2 Immune surveillance . . . 36
1.4.3 DNA damage response . . . 36
1.4.4 Chromatin structures . . . 38
1.5 Single cell vs Population Analysis . . . 39
1.5.1 Click Chemistry . . . 39
1.5.2 RNAscope . . . 40
Objectives . . . 43

2 Materials and Methods **44**

2.1 Cell Culture . . . 44
2.1.1 Cell lines and propagation . . . 44
2.1.2 Drug treatments . . . 45
2.2 Virus Culture . . . 46
2.2.1 List of viruses and production cell line . . . 46
2.2.2 Production of Viruses . . . 46
2.2.3 Production of HSV-1^{EdC} . . . 47
2.2.4 Titration of Viral Stocks . . . 47
2.2.5 Adsorption and Visualisation of HSV-1^{EdC} on coverslips . . . 47
2.2.6 Infections . . . 47
2.3 EdC and EU pulse labelling of nascent DNA replication and RNA synthesis . . . 48
2.4 Click chemistry . . . 48
2.5 Immunofluorescence . . . 49
2.6 RNA detection . . . 50
2.6.1 RNAscope . . . 50
2.6.2 DNase treatment before RNA detection . . . 50

2.6.3 RNAscope combined with click chemistry and Immunofluorescence 51
2.6.4 qRT-PCR 51
2.7 Western Blotting 52
2.8 Mass Spectrometry 53
2.9 Widefield microscopy 54
2.10 Quantitative Image Analysis 54
2.10.1 Quantification of Transcription Bursts 54
2.10.2 Quantification of EdC incorporation efficiency 54
2.10.3 Quantification of Genomes or Capsids per cell 55
2.10.4 Quantification of total RNA 55
2.10.5 Quantification of protein levels 56

Results **57**

3 Development of techniques for the simultaneous analysis of individual genomes and their transcriptional activity **57**

3.1 RNA in situ hybridisation allows visualisation of HSV-1 transcripts 58
3.2 Immediate early transcription bursts 60
3.3 Simultaneous detection of ICP4 and ICP0 transcripts 64
3.4 Multiplex analysis within one gene 67
3.5 Combined detection of HSV-1 genomes and analysis of transcriptional activity . . . 70
3.6 Discussion and future perspectives 79

4 Investigation of IE transcription in the absence of new translation and the influence of the autoregulatory function of ICP4 and stimulatory function of VP16 **84**

4.1 Absence of ICP4 autoregulation accounts for increase in transcription during translation inhibition 85

4.2 VP16 induction of viral transcription 89
4.3 Investigation of the role of P-TEFb on viral transcription 91
4.4 A rapidly synthesised protein affects viral gene expression 100
4.5 Discussion and Future Perspectives 105

5 The role of cellular protein PML on transcriptional output from HSV-1 genomes 109

5.1 The fate of PML in early HSV-1 infection 109
5.2 Transcriptional activity of genomes and their proximity to PML domains 114
5.3 Role of PML recruitment to HSV-1 genomes 123
5.4 Discussion and Future Perspectives 128

6 Spatial Relationship between viral transcription and viral DNA replication 130

6.1 Transcripts accumulate inside replication compartments 130
6.2 HSV-1 infection in cells undergoing S phase 133
6.3 ICP8 is recruited to both viral and cell DNA replication sites 142
6.4 Spatial separation of nascent replication sites and RNA transcripts 146
6.5 Heterogeneity between replication and transcription 149
6.6 Discussion and Future Perspectives 153

7 Spatial analysis of host cell transcription during HSV-1 infection 156

7.1 Characterisation of HSV induced transcription territories 157
7.2 Differential effect of inhibition of Cdk9 on virus versus host transcription 163
7.3 Reorganisation of RNA polymerase II during HSV-1 infection 169
7.4 Discussion and Future Perspectives 176

8 General Conclusions and Closing Perspectives 182

8.1 Heterogeneity during HSV-1 infection 183
8.2 Future potential of Azide Biotin Click Chemistry 186

8.3 RNA pol II transcription during HSV-1 infection 189

List of Figures

1.1 HSV-1 Transcription Cascade 23

1.2 RNA pol II CTD Phoshorylation 28

1.3 RNA pol II Transcription 30

1.4 RNAscope Schematic 41

3.1 RNAscope allows visualisation of HSV-1 RNA transcripts. 59

3.2 HSV-1 transcription progression throughout infection. 61

3.3 IE Transcription bursts 63

3.4 Simultaneous detection of ICP0 and ICP4 viral gene transcripts. 65

3.5 Detection of intron containing ICP0 transcripts. 69

3.6 Production of infectious HSV-1^{EdC}. 71

3.7 RNAscope can be combined with click chemistry of EdC labelled cellular DNA . . 72

3.8 Spatial relationship between active genomes and transcription bursts 75

3.9 Optimisation of resolution of transcription bursts 78

3.10 Spatial relationship between genomes and transcription bursts 82

4.1 Effect of CHX on HSV-1 transcription indicates presence of repressor molecules. . . 86

4.2 ΔICP4 HSV1- infection shows role of ICP4 in transcriptional suppression 88

4.3 Genomes are able to reactivate after incubation with ActD 90

4.4 Effect of drugs on plaquing efficiency of ΔVP16 HSV-1. 92

4.5 HMBA present at early timepoints allows successful infection. 95
4.6 HMBA and JQ1 have no effect on viral entry. 96
4.7 HMBA and JQ1 increase levels of ICP0 and ICP4 protein. 97
4.8 HMBA and JQ1 increase levels of IE RNA. 99
4.9 Pretreatment of HaCaT cells with HMBA or JQ1 has differing effects. 101
4.10 HMBA induces rapidly turned over protein which increases viral gene expression. . . 102
4.11 Proteomic analysis to identify targets induced by HMBA. 104
4.12 Models of HMBA induced P-TEFb activation. 107
4.13 Model of JQ1 induced HSV-1 IE transcription 108

5.1 Development of PML IF protocols. 110
5.2 PML is degraded during infection by ICP0. 112
5.3 PML associates with HSV-1 genomes 113
5.4 RNAscope and IF in combination 115
5.5 PML is associated with IE transcription bursts 116
5.6 Transcriptional activity of genomes and their proximity to PML domains. 118
5.7 Association vs colocalisation 120
5.8 Production of FxE^{EdC} 121
5.9 PML is associated with IE transcription of an FxE virus 122
5.10 HSV-1 infection induces DNA damage and activates the DDR 124
5.11 DDR markers are recruited to viral genomes 125
5.12 Damage accumulates around genomes even if they are transcriptionally silenced . . . 127

6.1 Subcellular location of IE and L transcripts pre and post replication 131
6.2 Late transcripts accumulate inside replication compartments 132
6.3 EdC pulse labelling reveals newly synthesised DNA 134
6.4 Heterogeneity of EdC labelling in an asynchronous population. 135

6.5 Classification of EdC labelled HSV-1 infected cells at 8 hpi. 139

6.6 There is no preference for HSV-1 infecting mitotic cells. 141

6.7 ICP8 provides better resolution than EdC patterns. 143

6.8 ICP8 binds both viral and cellular replicating DNA 145

6.9 Withdrawal of protease step in RNAscope protocol improves ICP8 IF staining 146

6.10 Spatial separation between ICP8 foci and RNA transcripts. 148

6.11 Intercellular heterogeneity 151

6.12 Viral Replication compartments may have very low replication. 152

7.1 An EU pulse labels ongoing RNA synthesis 158

7.2 EU labels ongoing RNA synthesis 159

7.3 EU HITTs are not sites of viral transcription 161

7.4 ΔICP4 HSV-1 does not induce EU HITTs 162

7.5 DRB inhibits transcription. 164

7.6 DRB has a profound impact on viral transcription. 166

7.7 EU HITTs are cellular transcription sites. 168

7.8 RNA polymerase can colocalise with EU HITTs 170

7.9 IE proteins are required for RNA pol CTD foci formation 172

7.10 Viral transcription bursts are adjacent to RNA polymerase foci. 175

7.11 Effect of Cdk9 Inhibition on Viral Transcription 177

7.12 HSV-1 Induced Transcription Territories. 181

List of Tables

2.1 Cell lines and culture conditions 45

2.2 Drug treatments 45

2.3 Viruses 46

2.4 Immunofluorescence Primary Antibodies 49

2.5 Immunofluorescence Secondary Antibodies 50

2.6 RNAscope probes 51

2.7 Primers 52

2.8 Western Blot Antibodies 53

List of Abbreviations

ActD	Actinomycin D
CHX	Cycloheximide
CuAAC	Copper catalysed azide-alkyne cycloaddition
DDR	DNA damage response
dsDNA	Double strand DNA
EdC	5-Ethynyl-2'-deoxycytidine
EU	5-ethynyl uridine
FISH	Fluorescent in-situ Hybridisation
G4	G-quadruplex
HBV	Hepatitis B virus
HEXIM1	Hexamethylene bisacetamide-inducible protein 1
HITTs	HSV-1 induced transcription territories
HMBA	Hexamethylene Bisacetamide
hpi	Hours post infection
HSV-1	Herpes Simplex Virus 1
HSV-1^{EdC}	EdC labelled HSV-1
IE	Immediate Early
IFN	Interferon
ISH	In situ hybridisation
MEL	Murine erythroleukemia cell
MOI	Multiplicity of infection
NPC	Nuclear pore complex
PML	Promyleocytic leukemia protein
RNA pol	RNA polymerase
RNA pol II CTD	RNA polymerase II C terminal domain
RT	Room temperature
scRNA-Seq	Single cell RNA Sequencing
snRNA	small nuclear RNA
ssDNA	Single strand DNA
TBP	TATA-binding protein
WT	Wildtype

Chapter 1

Introduction

1.1 DNA Viruses

Over 100 years ago, following the development of germ theory, scientists were confident that infectious diseases could be each explained by a causative agent which could reproduce. The first viruses to be discovered in 1915 were bacterial viruses, the bacteriophage, followed by plant and animal viruses. Purification of the first viruses in 1933 identified DNA contained within the bacteriophage followed by the identification of RNA in tobacco mosaic virus in 1937 [1, 2]. Subsequent experiments throughout the 20th century, and importantly the identification of nucleic acid as genetic material, led to the classification of DNA and RNA viruses and the identification of numerous classes of each with huge diversity. Viral DNA is embedded within our genome, indicating their abundance and longevity in our history. It is likely that every organism on earth has its own range of host specific viruses. The Baltimore classification of viruses divides families of viruses based on how they produce RNA. DNA viruses make up class I (double strand DNA (dsDNA) genomes), class II (single strand DNA (ssDNA) converted to dsDNA) or class VII (dsDNA with an RNA intermediate, 'reversiviruses'). Group I viruses include the Adenoviridae, Papillomaviridae and Polyomaviridae, Hepesviridae and

poxviridae families. Group II contains Paroviridae and Geminiviridae. Hepatitis B virus (HBV) is an example of a Group VII virus.

Infection begins when viruses attach to a cell via receptor molecules on the surface through high affinity interactions leading to pore formation and virus internalisation. The cell receptors have specific viral binding domains, and likewise the viral surface proteins have specific cellular binding regions. Viruses can enter cells via direct fusion with the plasma membrane, releasing their capsid or uncoated genomic content directly into the cytoplasm. Alternatively viruses make use of the endocytic pathway, entering the cell in an endosome and fusing directly with the endosomal membrane [3].

One of the greatest problems for a DNA virus is the necessity for the viral genomes to access the nucleus for transcription and replication. Some viruses have viral proteins associated with the DNA to facilitate replication and nuclear entry, others rely purely on host proteins. Entry into the nucleus occurs through the nuclear pore complex (NPC), a large protein construct in the nuclear membrane. The NPC allows passive diffusion of small molecules and active transport of molecules up to 39 nm in diameter [4]. Viruses have developed unique mechanisms to achieve nuclear delivery. For example, the capsid protein of HBV has an NLS signal, to target it to the nuclear membrane, and the small size of the capsid could mean the entire capsid is imported through the NPC. However the exact mechanism remains unknown, and the capsid may even disassemble in the NPC and reform inside the nucleus. Indeed, this occurs with Adenovirus, whose capsid is partially disassembled inside the NPC. For larger viruses, such as Herpes Simplex virus (HSV), they bind to or 'dock' on the outside of the NPC, and inject their DNA through the NPC into the nucleus [5].

The replication of viral DNA in the nucleus differs depending on the structure of the DNA. Some linear genomes, ie HSV-1, are circularised when they replicate, whereas other linear genomes remain linear throughout replication (adenovirus). Small DNA viruses use host cell enzymes for transcription and replication. Medium sized viruses such as adenoviruses, encode their own DNA

polymerase but use cellular RNA polymerase. Large DNA viruses encode their own DNA polymerases. Circular genomes, like SV40, have a single origin of replication. It replicates, using RNA primers, each strand in the opposite direction. Linear genomes that are circularised, such as HSV-1, are replicated in a rolling circular mechanism producing multiple genomes connected end to end, which are cleaved during incorporation into new progeny virions. Adenovirus genomes use a DNA polymerase and terminal protein precursor complex which uses an amino acid side chain OH as a primer and subsequently proceeds along the length of the genome.

The study of DNA viral infection is vitally important for many reasons. DNA viruses are major public health issue worldwide, responsible for both acute and chronic infections such as smallpox, hepatitis and influenza. Several DNA viruses are cancer causing agents, such as Epstein Barr virus and Human papilloma virus. The manipulation of viruses has been exploited for their therapeutic potential. For example, many vaccines have been developed using viral vectors. The recently developed SARS-CoV-2 vaccine by Oxford/Astrazeneca uses a chimpanzee Adenovirus vector [6, 7]. Gene therapy treatments involve the delivery of a therapeutic gene to the patient by viral vectors, like adenoviruses, either in vivo or ex vivo. [8]. Oncolytic virus therapy is a cancer therapy that uses viruses to target and destroy cancer cells. The first oncolytic virus therapy to be licensed was T-VEC for melanoma in 2015. T-VEC is a modified HSV containing a transgene for granulocyte macrophage-colony stimulating factor along with functional deletions of two viral genes [9]. It is essential to understand the environment that DNA viruses encounter when they enter cells, and more specifically nuclei, and identify the responses targeted against them by our immune responses in order to further develop the therapeutic potential of DNA viruses in addition to combatting infection.

1.2 Herpes Simplex Virus

Within our lab, the model DNA virus we use to study early events in DNA virus infections is Herpes simplex virus 1 (HSV-1). Herpesviruses are split into alpha, beta and gamma families, with HSV-1, HSV-2 and varicella zoster virus in the alpha family, whose defining characteristic is neuronal latent infections. Historically HSV-1 is the most widely studied of the herpesviruses, and could be described as the prototypical herpesvirus, as it infects and replicates in a wide variety of cell types. After infection through skin or mucosa, HSV-1 establishes lifelong infections in neurons with periods of latency and recurrent activations. Most infections are asymptomatic or very mild but in rare cases and immunocompromised individuals HSV-1 can cause severe disease. Reactivation can cause oral and genital lesions and encephalitis. It is estimated by the WHO that two thirds of the global population are infected by HSV-1. Antiviral drugs are the only current treatment and vaccine development has had only limited success [10].

HSV-1 is 180 nm in diameter, with a 152 kbp genome encased in an icosahedral capsid. The capsid is surrounded by a tegument protein layer and finally encased in the viral envelope. The tegument layer comprises two thirds of the total viral volume. Within the envelope the capsid is not situated centrally, with 30-35 nm of tegument space at one side and much less at the other side, which is therefore closer to the envelope. [11]. The tegument consists of many copies of 23 viral tegument proteins, and viral transcripts. The envelope is a lipid bilayer, consisting of 11 viral glycoproteins and some intrinsic membrane proteins. The remainder of the envelope is taken from the host cell. The genome is contained within a spool like structure, and it has recently been shown there are as many as 284 reading frames and at least 84 proteins [12].

1.2.1 Viral Lifecycle

Viral Entry

There are two proposed entry mechanisms for HSV-1; fusion with the plasma membrane or through the endocytic pathway, described above. The type of cell being infected may determine what entry mechanism is used, with the virus entering Vero cells by membrane fusion, and HeLa cells and keratinocytes by the endocytic pathway [13–15]. The fusion process described below either occurs at the cell membrane or in an endosome. HSV-1 cellular entry receptors include heparin sulfate, herpesvirus entry mediator (HVEM) and nectin 1 [16]. On the viral envelope several glycoproteins have key roles; glycoproteins gD, gH/L and gB. Membrane fusion of HSV-1 includes 3 phases. Phase I brings together the membranes through receptor binding. Phase II allows the lipids from the two outer membranes to mix, called hemifusion. Finally, in phase III the inner membranes mix and a pore is formed [17]. gD, gB and gH/L are all essential for fusion. gD and gH/L are required for phases I and II, and gB is essential for the third stage [18]. gD binds to the cellular receptor and transmits a signal through gH/L to the fusion protein gB [19]. In the absence of gB gH/L is not able to cause fusion. The sequential interaction of all 4 components is needed [20]. Transfecting a cocktail of the viral proteins gB, gD and gH/L is sufficient to trigger mass fusion events [21].

After membrane fusion HSV-1 travels to the nucleus by using the host cell microtubule network. This is especially important in neurons, where HSV-1 has to travel big distances along neuronal axons. Microtubules are filaments composed of tubulin heterodimers. They have a structural polarity, one end tethered to the MTOC and a dynamic opposing end. Dynein is the molecular motor responsible for transport from the periphery to the cell centre [22]. Microtubule disrupting drugs reduce transport of HSV-1 capsids to the nucleus [23]. There are conflicting studies over the role of HSV-1 capsid proteins, but the interaction with several tegument proteins is understood to be very important, including UL36 (VP1/2) and UL37 [24].

Transcription

HSV-1 has over 80 genes which are expressed in a regulated temporal cascade by host RNA polymerase II and associated cellular machinery (Figure 1.1, see section 1.3 for mechanistic detail) [25–27]. Immediate early (IE) or alpha genes are transcribed and synthesised by 2 hours post infection (hpi) [28]. Early (E) genes or beta are the next to be transcribed and this requires the presence of the IE proteins. They can be subdivided into two classes, $\beta 1$ and $\beta 2$ based on temporal behaviour. The final class are the late (L) genes, consist of the many structural proteins required for virion formation and are expressed after the onset of DNA replication. The late genes can also be subdivided into two classes, $\gamma 1$ and $\gamma 2$. $\gamma 1$ can be synthesised in the presence of DNA synthesis inhibitors, but $\gamma 2$ are dependent on replication [29]. The three main viral transcriptional regulators are the L protein VP16 and the IE proteins ICP0 and ICP4. All are discussed further below.

Replication, Assembly and Egress

The HSV-1 genome has three origins of replication: two oriS domains and one oriL. There are two unique regions in the genome, unique long (UL) and unique short (US). OriS is present twice in the US genomic region, and oriL is present in UL. Genome replication is initiated after the genome has circularized by a number of viral proteins. Initially, UL9 and ICP8 bind and unwind the DNA. UL9 binds at origin sequences, forming a single strand loop structure that allows ICP8, the ssDNA binding protein, to bind and begin unwinding the DNA. The helicase/primase (H/P) is composed of three viral proteins: UL5, UL8 and UL52. UL5 and UL52 together act as an ATPase, helicase and primase, unwinding DNA and synthesising the initialising primer, and UL8 serves as a nuclear localisation protein. Thirdly, the polymerase is composed of two subunits; UL30 and UL42. UL42 closely resembles PCNA, the mammalian sliding clamp processivity factor, and tethers UL30 to the DNA. It is capable of moving linearly along the DNA. UL30 contains the catalytic subunit of the polymerase. The commonly accepted model for HSV-1 replication is a rolling circle mechanism,

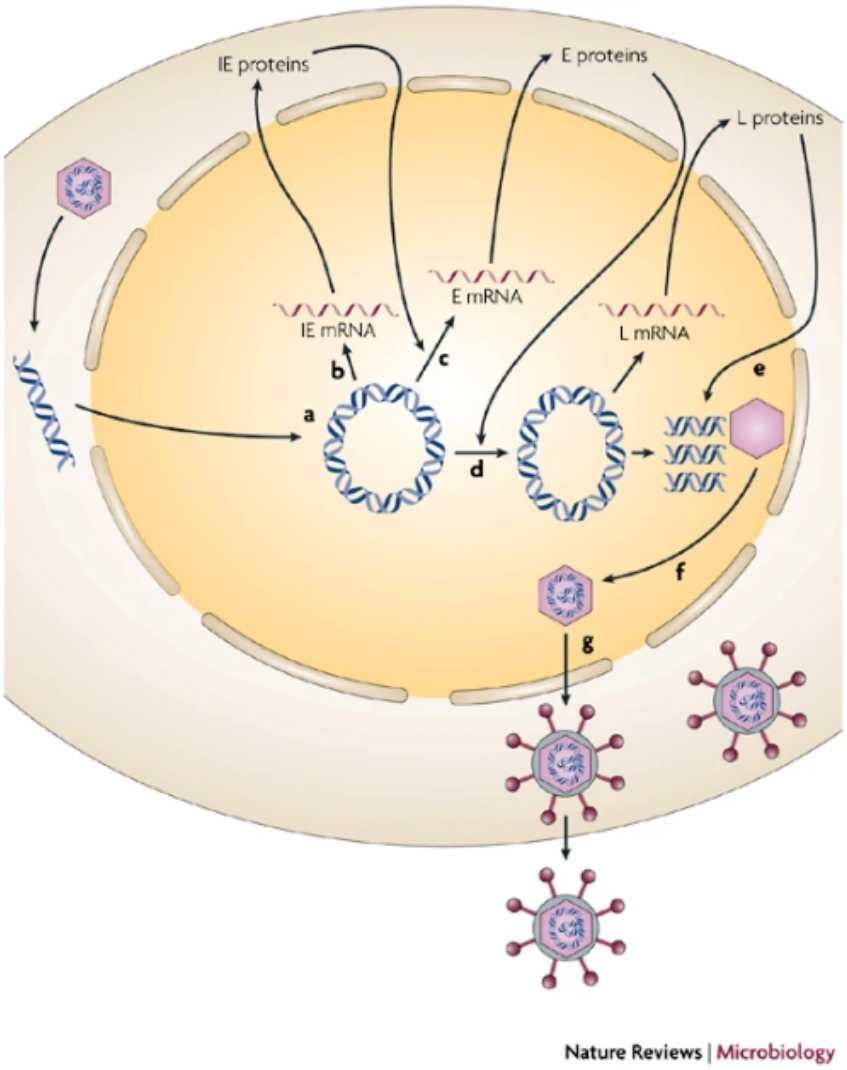


Figure 1.1: HSV-1 Transcription Cascade

Expression of HSV-1 genes in a regulated temporal cascade. Reproduced from [30].

where the DNA is replicated to produce concatamers, but it may be recombination dependent as in late stages of replication the DNA can be found in branched networks [31–33]. Both Y and X structures have been visualised by electrophoresis, resembling replication forks or recombination intermediates.

To produce new virions, structural viral proteins are translated in the cytoplasm and transported back into the nucleus. VP5, VP26 and VP23 move into the nucleus as a complex. The capsid is composed of 161 capsomers - 150 hexon and 11 pentons [34]. The pentamers and hexamers are made of 5 or 6 copies of VP5 respectively, and there is one VP26 molecule on each VP5 in the hexamers. After the capsid has assembled with the help of some scaffolding molecules, the scaffolding

molecules are expelled as the DNA is packaged. DNA packaging requires several proteins for DNA cleavage - UL6 forms the portal structure, UL15/28/33 complex is a terminase, cleaving the concatemeric DNA into monomers. The capsid vertex specific component (CVSC) is composed of UL17, UL25 and UL36. There are 5 CVSC's in every penton. UL25 is an essential encapsidation protein but is not involved in DNA cleavage, and may have a role in preventing the loss of DNA from the capsid [35]. UL15 controls the DNA translocation into the capsid in an ATP dependent manner [36, 37].

Through a process called nuclear egress, the capsids bud through the the inner nuclear membrane into the perinuclear space, gaining an envelope, which then fuses with the outer nuclear membrane and releases the capsid into the cytoplasm. This process relies on the viral proteins UL31 and UL34. In the cytoplasm the majority of tegument proteins are added, before secondary envelopment through glycoprotein membranes of the *trans*-Golgi network, and the now mature virions exit through the secretory pathway [38].

1.2.2 Viral Proteins

Immediate Early Proteins

ICP0 is not an essential viral gene yet ICP0 mutant viruses are severely decreased in viral yield and have a very limited capacity to initiate infection at low multiplicities of infection. ICP0 activates expression from all 3 gene classes, IE E and L, but does not bind DNA directly [39]. ICP0 has a RING finger domain which gives it E3 ubiquitin ligase activity, promoting the degradation of multiple host cell proteins [40], including many components of the antiviral immune signalling pathway. These proteins are numerous and include PML and DNA-PK. Additionally, it is thought to regulate the interaction of chromatin with viral DNA by limiting the amount of interactions and promoting acetylation of histones that are present on viral DNA [41, 42].

ICP4 is a major transcriptional transactivator of viral gene expression. It is a 175 kDa phos-

phoprotein with 4 regions, including DNA binding and C terminal activation domains. ICP4 preferentially binds a specific DNA sequence, yet is also capable of binding dsDNA independent of sequence [43]. It is synthesised early in infection and is associated with viral DNA throughout infection, from the incoming genomes to replicated DNA. ICP4 is not required for IE transcription, but is required for transcription of E and L genes and therefore is essential for viral replication and progeny virion production [44]. In the absence of ICP4, there is reduced recruitment of RNA polymerase II and transcription apparatus to E and L genes and therefore there is no transcription [45]. The tertiary structure of HSV-1 DNA affects ICP4 binding. G-quadruplexes (G4s), which are structures that form in DNA regions with a high guanine content, have been found throughout the HSV-1 genome and in gene promoters. ICP4 binds preferentially to these structures and drives the unfolding of the G4 structures, therefore promoting transcription [46].

In addition to promoting E and L gene expression, it is also capable of autoregulation on its own promoter, restricting its own expression in a negative feedback loop [47–51]. Depending on the promoter and subsequent protein interactions, ICP4 is therefore capable of suppressing or activating transcription. In the promoter of ICP4 it forms a complex with TFIID and TATA-binding protein (TBP) (see section 1.3.2) and this interaction is required for autoregulation.

ICP27 is involved in export of RNA from the nucleus. It binds intronless RNA and exports them from the nucleus through interactions with the export receptor TAP/NXF1 and the Aly/Ref transport adaptor [52]. The RNA poll II binding domain in ICP27 overlaps with the TAP/NXF1 binding domain, so mRNAs are only exported when they have been released from the polymerase. ICP27 interacts with Nup62, a component of the NPC, suggesting that HSV-1 is able to preferentially transport viral RNAs while blocking host RNA transport [53, 54].

Early Protein

ICP8 is a 128 kDa zinc metalloprotein [55]. It is required for DNA synthesis, binding DNA in complex with UL9 (the origin binding protein) and subsequently recruits the other viral proteins involved; the helicase primase complex and the polymerase described above. It binds to non-specific DNA sequences, and in vivo it is many times more likely to bind ssDNA [56, 57]. Several regions within ICP8 are responsible for its nuclear localisation [58]. ICP8 represses transcription from input viral genomes, and is thought to stimualte expression from L genes through it's interaction with ICP27. [47, 59, 60] ICP8 accumulates in replication compartments. An additional function of ICP8 may serve in recruitment of other host proteins. For example, ICP8 and UL12 have been found to interact with Rad50 and Mre11. This may indicate a role for ICP8 to recruit the Mrn11 complex to viral genomes, adapting the role of this host protein to facilitate genome recombination [61, 62].

Late protein

The late tegument protein VP16 is also known as α-gene transactivating factor. VP16 is abundant in the tegument layer, then released by incoming virions with the genome into the nucleus. There, it stimulates IE gene expression by forming a complex with two cellular proteins, Oct1 and HCF, and binding to specific TAATGARAT motifs in IE gene promoters. Oct1 contains two POU DNA binding domains, $\mathrm{POU_H}$ and $\mathrm{POU_S}$, joined by an unstructured linker region. In the standard DNA binding configuration the two POU domains bind on opposite sides of the DNA strand. When it recongises the IE promoter TAATGARAT motif, the flexible linker allows the POU domains to bind in a different relative position. VP16 first binds HCF, and then binds Oct1 through the $\mathrm{POU_H}$ domain [63–67]. When it is bound, VP16 recruits transcription factors such as TFIIB, TFIIH and TBP [68]. After IE proteins have been synthesised they are capable of sustaining the transcription regulation necessary for infection.

VP16 can also negatively regulate host shutdown protein (VHS). VHS degrades host and viral

mRNA by targeting 5' and 3' RNA ends for endoribonucleocytic cleavage [69]. When cellular RNA has been degraded VP16 restricts VHS activity in order for viral RNA to accumulate [70, 71].

1.3 Transcription

1.3.1 DNA Dependent RNA polymerase

Eukaryotic transcription is performed by three RNA polymerases (RNA pol) : RNA pol I, II and III. Non-coding RNAs (ncRNA) such as ribosomal RNA (rRNA) and tRNA (tRNA) are transcribed by RNA pol I and III respectively [72–74]. RNA pol II transcribes protein coding genes into mRNA, as well as ncRNAs such as microRNAs. rRNAs are synthesised within a subnuclear compartment, the nucleolus, by RNA pol I and assembled inside the nucleolus before being exported to the cytoplasm [75]. Work in the 1970s first identified and determined the synthesis of different RNA classes by work using α-amanitin [74]. For all three polymerases, transcription begins with the assembly of initiation complexes on different gene promoters. Despite the functional differences between the polymerases they have a degree of mechanistic and structural conservation. They share a catalytic core of 10 subunits, although the total number of subunits differ between them to achieve specific functions [76, 77].

RNA polymerase II has a long C terminal domain (RNA pol II CTD). The degree of phosphorylation of the RNA pol II CTD influences the binding of various processing factors and controls the progression through various checkpoints. It consists of 52 heptad repeats of YSPTSPS. A generalised view of RNA pol II CTD phosphorylation during transcription is shown below in figure 1.2 adapted from [78]. Serine 5 phosporylation is found at the transcription start site, and serine 2 is associated with elongating polymerases [79]. This has been found to be fairly consistent across most genes [80]. At the end of transcription, the phosphorylation is removed by phosphatases and the polymerase is able to be recycled for another round of transcription. RNA pol II CTD modifications allow for the

interplay between transcription and transcript processing steps, including capping, splicing and 3'end processing.

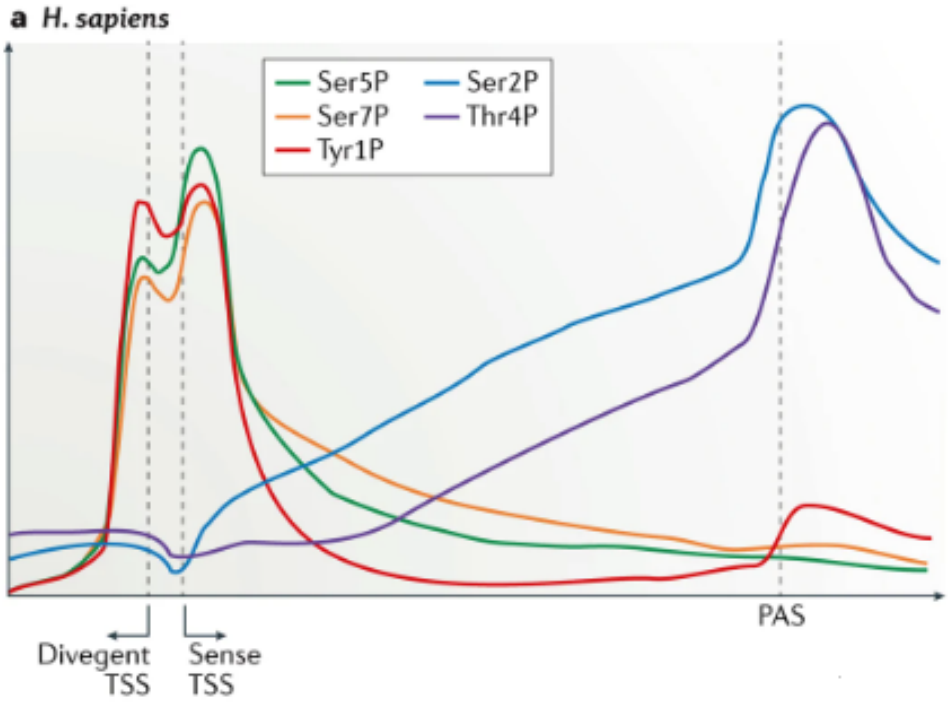


Figure 1.2: RNA pol II CTD Phoshorylation

Adapted from [78].

1.3.2 RNA pol II transcription initiation

There are several regulatory steps involved in the initiation and elongation stages of RNA pol II transcription. The pre initiation complex (PIC) assembles on promoter regions of DNA and consists of many proteins, including TFIID, TFIIA, TFIIB, TFIIF, TFIIE, TFIIH and pol II, and its function is to open DNA ready for transcription [81]. TBP is a component of TFIID and binds DNA, inducing it to bend 90°[82]. TFIID-TBP binding is further stabilised by TFIIB and TFIIA, which then allows the TFIIF-RNA Pol II complex to bind [83]. TFIIE and TFIIH are the last components of the PIC to be recruited [84]. Serine 5 of the RNA pol II CTD is phosphorylated by TFIIH and associated kinases. After the formation of the PIC, the polymerase escapes the promoter and transcribes a short region

of RNA which quickly receives the first post transcriptional modification of a 5' cap for protection from endonucleases. The polymerase stalls at approximately 100 nucleotides downstream of the transcription start site at the pausing region [85, 86].

1.3.3 Promoter proximal pausing

The checkpoint at the entry to elongation is known as promoter proximal pausing. A paused polymerase can be quickly released from pausing to continue transcribing through the body of the gene. Paused polymerases were found on 60% of mammalian genes in a 2016 study [87]. Work using GFP-RNA pol II and fluorescence recovery after photobleaching examined the stability of paused polymerase and progression rate. Of all the polymerases that engage with the promoter, only 10% progress to the paused state. Of these, the time spent paused was on average 42 seconds and only 10% progress to elongation [88]. The remaining polymerases terminate prematurely in abortive elongation. Two factors that induce pol II pausing are negative elongation factor, (NELF) and DRB sensitivity inducing factor (DSIF) [89, 90]. To progress out of the paused state, several changes need to happen. Both NELF and DSIF are phosphorylated, causing NELF to dissociate and a conformational change in DSIF to an elongation permissive state, as well as phosphorylation of Serine 2 within the CTD. The key protein involved with these actions is positive transcription elongation factor b (P-TEFb) (Figure 1.3).

1.3.4 P-TEFb

P-TEFb has been extensively studied. Early experiments using the transcription inhibitor DRB identified P-TEFb as an interaction partner of early elongation complexes after they were paused. P-TEFb allowed them to overcome the negative transcription factors and allow RNA pol II to enter elongation [91]. It is a heterodimer consisting of two subunits, cyclin dependent kinase 9 (Cdk9) and Cyclin T1 [92]. Cdk9 phosphorylates Serine 2 of RNA pol II CTD, NELF and DSIF [93–95]. P-TEFb can

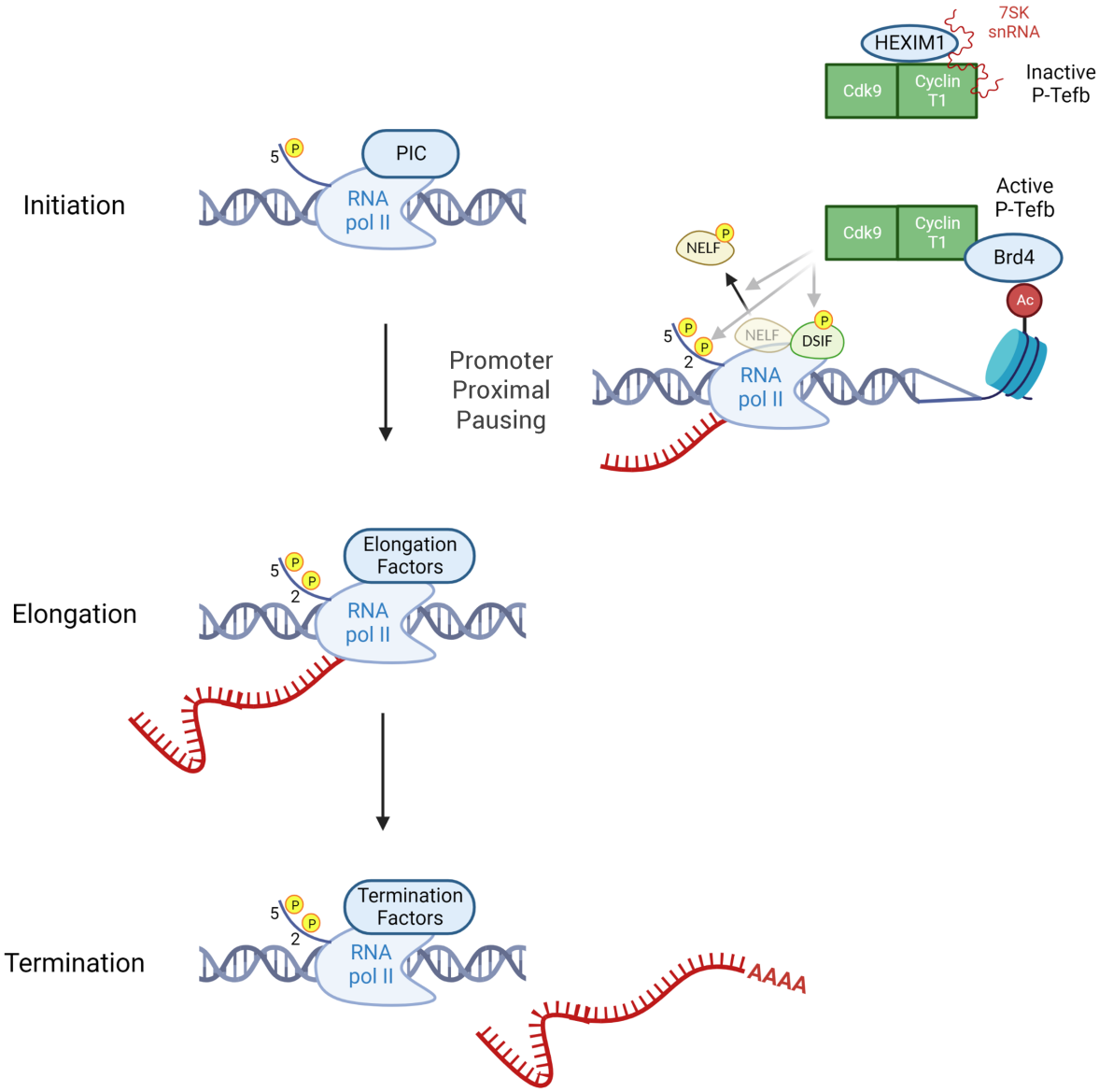


Figure 1.3: RNA pol II Transcription

Stages of transcription of RNA pol II. Produced in Biorender.

be recruited through multiple mechanisms, including through artificial tethering, and intermediaries such as Nf-kappaB and Brd4 [96].

In the cell, a large amount of the Cdk9/CyclinT1 P-TEFb molecules are sequestered in an inactive form with HEXIM1 and 7SK small nuclear RNA (snRNA), with the snRNA acting as a

scaffold for HEXIM1 to inhibit the kinase activity of Cdk9 (Fig 1.3). P-TEFb is also found in an active form when bound to Brd4 [97]. Brd4 is a BET family protein, with 2 bromodomains and an extra terminal (ET) domain and can bind chromatin on acetylated H3 and H4. In this manner, it can recruit P-TEFb to regions of DNA which need to be transcribed. Brd4 has multiple enzymatic activities; kinase activity capable of phosphorylating Serine 2 on the RNA pol II CTD therefore promoting transcription [98], as well as histone acetyltransferase activity allowing it to acetylate histones further opening chromatin structure and promoting transcription [99]. Finally, P-TEFb can exist as part of the super elongation complex (SEC). Both Brd4-P-TEFb and SEC-P-TEFb can phosphorylate RNA pol II CTD [100]. The SEC consists of elongation factors including AFF scaffold proteins, eleven-nineteen Lys-rich leukaemia (ELL) proteins and several mixed lineage leukaemia (MLL) proteins [101]. The release of active P-TEFb from its inactive bound state may be controlled by stress or UV damage activating PP2B and PP1α, post translational modifications such as dephosphorylation or acetylation, or by the action of PI3 kinase [102–104].

1.4 Nuclear environment during early virus entry

When a HSV-1 genome enters a nucleus, it will encounter a complex and densely packaged environment. It will need to overcome many cellular factors which identify it as a foreign threat or damaged DNA and it will need to communicate with transcription machinery to begin gene transcription. Within the fluid yet dense scene which the relatively small genome has to navigate are multiple subnuclear organelles, densely packed chromatin and regions of euchromatin and transcription territories.

1.4.1 PML

Promyleocytic leukemia protein (PML) is a tumor suppressor and the main constituent of PML nuclear bodies (PML-NB's). They also known as nuclear domain 10 (ND-10) bodies, named for the

number of domains that appear in the nucleus. PML was first identified in acute promyelocytic leukaemia (APL), where a chromosomal translocation results in the fusion protein PML-RARα. This fusion protein interferes with normal PML function [105, 106]. PML itself is an interferon inducible gene [107] subject to several post-translational modifications. SUMOylation occurs on three residues: lysine 65, 160 and 490, and has a role in modulating PML degradation and PML-NB assembly. PML contains a SUMO binding domain which enables PML to interact with other SUMOlyated proteins and other PML molecules, interactions which are essential for the formation of PML-NB's. Phosphorylation is another means of regulation of PML. The N and C terminal regions, the NLS, and several other domains all contain phosphorylation sites, and the phosphorylation status of these sites goes on to control PML function. PML also undergoes the other post-translational modifications of ubiquitination and acetylation [108].

PML-NB's are discrete nuclear foci and range in size from 0.1 to 1 microns in diameter. There are on average between 5 to 15 PML-NB's in the nucleus, which in response to stress stimuli increase in size and number. The number and size of PML-NB's also changes during the cell cycle, with numbers increasing as the cells enter and progress through G2 and S phase. During M phase they are disrupted by the movement of chromatin [109]. The role of PML-NB's in the cell is wide-ranging and varied, including transcriptional regulation, the DNA damage response and intrinsic immunity. PML-NB's can act as a damage sensors and participate in DNA repair after activation of the DNA damage response (DDR). In response to DNA damage PML is phosphorylated on at least two residues by ATM and Chk2 [110]. Many other DDR proteins are associated with PML, including MRE1, NBS1, and ATR. The number of PML-NB increases after double strand break induction by UV irradiation [111]. The integrity of PML and it's ability to recruit and therefore direct many interacting proteins is crucial for the DDR. In APL the disruption of PML-NB's is associated with delayed DSB repair. PML-NB's are sites of transcriptional regulation, they associate with transcription factors, and PML-NB's make contact with chromatin in a non-random manner [112]. The mechanism is not known, as it

has been suggested PML has a role in transcriptional suppression and activation. The nuclear bodies can associate with chromatin in a non-random manner, establishing more transcriptionally permissive domains [113]. For example, PML has been shown to regulate transcription from the MHC locus by organising higher order chromatin loop structures [114]. The spatial localisation or composition of the PML bodies may influence the pro or repressive role during transcription.

PML and HSV-1

PML-NB's have long been known to be involved in DNA virus infection. In the 1990s several papers identified PML-NB's as the sites of virus transcription and replication. Using both HCMV and HSV-1, it was shown that only the viral genomes that localise to the ND10 bodies are able to transcribe and proceed to replication [115]. As many as 81% of in situ hybridisation (ISH) DNA signals were associated with PML-NB's [116]. These early papers were evidence for a pro-viral role for PML-NB's in HSV-1 infection. Prior to the publication of these papers, the first published evidence of PML involvement in viral infection was in 1993 when it was discovered that some viruses cause the dispersal of ND10 bodies. During HSV-1 infection it was determined that the immediate early protein ICP0 was the only HSV-1 gene product needed for the loss of ND10, and that upon IE protein synthesis PML-NB's disappeared within 10 minutes [117]. Therefore ICP0 deficient viruses (ΔICP0) are frequently used to prevent the degradation of PML and allow studies to be performed to elucidate the role of PML in viral infection.

The preliminary experiments mentioned above highlight a conflict of views that continue to permeate this field. It is clear that HSV-1 and other DNA viruses encode proteins that degrade and disrupt PML and PML-NB's. However, the virus shows a preference for associating with these bodies and infection progresses from their location. Whether PML is an antiviral factor that has to be eliminated, or whether it is a pro-viral factor whose elimination benefits the virus in other ways remains unresolved.

Following the 1993 study by Maul et al., identifying the degradation of PML by ICP0, the proteasome inhibitor MG132 was shown to prevent HSV-1 induced PML degradation. In human glioblastoma cells overexpressing PML, PML is also degraded, but there is no evidence about the effect the high level of PML had on viral infection [118]. This was one of the first PML overexpression studies. A paper by Weller et al., suggested that the disruption of PML-NB's is critical for productive infection. They categorise HSV-1 infection into several stages, and look at the role of HSV-1 in each. Treatment with arsenic trioxide to stabilise the PML-NB's prevented successful virus infection [119]. One of the first papers to demonstrate PML knockdown in mouse fibroblasts was presented by the Roizman group, who hypothesised that if the effect of IFN in a viral infection is mediated by PML, the IFN should have a greater effect in WT cells than PML knockdown cells. For an HSV ICP0 mutant, there was no difference between wildtype and PML knockdown, indicating that lack of PML did not significantly increase protein synthesis under normal conditions. However in interferon treated cells infection with ΔICP0 virus was impaired in WT cells and yet was only minorly affected in PML-/- cells. They showed that PML is necessary for the IFN response to HSV-1 infection [120]. In human cells, knockdown of PML was achieved in 2006 by Everett et al. The lack of PML enhances plaque forming efficiency of a ΔICP0 virus, but not of a WT virus [121]. This is consistent with the belief that a virus that is unable to disassemble PML-NB's will replicate better if PML is not present. PML knockout lines can be used to express individual PML isoforms, to study the role individual isoforms have in HSV-1 infection. Endogenous PML has to be removed before using vectors to control the expression of the isoforms. PML isoforms I and II are particularly important in the restriction of HSV-1 infection [122].

The majority of PML studies propose an antiviral role to the factor. However, there have been several studies that have claimed the opposite. The proviral aspect may be linked to the proximity of the PML-NB's to the incoming genomes. PML-NB's are disrupted by HSV-1, but rather then eliminating a repressive nuclear structure this may cause the release of stimulatory factors, for example

transcription factors, necessary for the progression of infection. Live microscopy techniques have enabled the ability to follow individual genomes as infection progresses. Initially this was done using small plasmids containing parts of the HSV-1 genome along with fluorescent proteins. In cells over-expressing PML, it was found that replication compartments only develop from genomes that were associated with PML, confirming the studies performed in the late 1990s [123]. In another overexpression study, PML structures could be found many hours after infection but with significantly altered structure and morphology [124]. The discrepancies in PML studies may be partially explained by differences in MOI. For example, at low MOI HSV replication is actually impaired in PML -/- Hep2 cells, while at high MOI there is no difference between WT and PML -/- cells [125, 126]. Merkl et al., discovered in their hands a PML-/- line created by siRNA resulted in a decreased viral yield, in contrast to many other publications. To check their experimental system they obtained PML-/- cells from another source and after infection, saw the increase in viral yield. However upon treatment with their siRNA they again observed a decrease in viral yield. They propose PML depletion blocks the progression to DNA replication as it is required for the efficient formation of replication compartments [127].

An interesting question in PML HSV-1 research concerns PML localisation and structure. Initially it was thought that HSV-1 genomes preferentially recruit PML-NB's or migrate through the nucleus to encounter one. For example, ICP4 and ICP27 were thought to be necessary for genomes to localise to PML-NB [128]. However, several convincing studies emerged to demonstrate the formation of de novo ND10 formation. HSV-1 spreads via cell to cell contact, so in a low MOI infection where virions are spreading from one cell to another they will arrive from one direction. Using a low MOI infection of ΔICP0 and staining for PML and ICP4 protein at 24 hpi, Everett et al., showed asymmetric ICP4/PML complexes at the edge of a spreading plaque, suggesting that the ICP4 foci (representing genomes) arriving at one side of the nucleus are inducing the formation of novel PML-NB's [129]. The PML-NB's are associated with or juxtaposed to the ICP4 domains. In high MOI

infection where a lot of virus is applied onto the monolayer, the virus enters the nucleus in a more random manner. These high MOI infections explain why it was initially thought that viral genomes migrate until they find a PML-NB. Further live cell microscopy experiments indicate that novel PML-NB's form at viral genomes [130]. In this study genomes were directly revealed by FISH rather than relying on ICP4 as a surrogate marker. There remain many outstanding questions in this area, such as the purpose of juxtaposition of PML-NB's rather than precise colocalization, and what drives the initial nucleation of the foci.

1.4.2 Immune surveillance

Innate immunity requires detection of the virus and subsequent cascades of signalling molecules resulting in the production of interferon (IFN) and interferon stimulated genes (ISGs) [131]. This response creates an antiviral environment to limit viral spread and stimulate the adaptive immune response. Against HSV-1, innate signalling is initiated by several molecules including cGMP-AMP synthase (cGAS), simulator of interferon genes (STING) and interferon-γ inducible protein 16 (IFI16). IFI16 is an intracellular DNA sensor, initially discovered as a cytoplamsic sensor but has been found to also detect nuclear viral DNA [132, 133]. IFI16 localises to genomes early during infection [134, 135]. Following its translocation to the cytoplasm IFI16 activates STING [136]. cGAS triggers cGAMP production upon binding HSV-1 DNA and also signals to activate STING [134, 137]. STING will then recruit TANK-binding kinase 1 (TBK-1) which will phosphorylate and activate IRF3 [138]. HSV-1 can destabilise these sensors, fighting back against immune detection, as well as disrupting steps further downstream in the signalling pathway.

1.4.3 DNA damage response

The DNA damage response (DDR) is a network of proteins, modifications and processes that monitors and repairs cellular DNA. DNA can be damaged by multiple factors, including UV radiation,

environmental toxins and oxidative stress. DNA damage is detected by surveillance proteins and causes signalling cascades that can direct the cell to either repair the damage, enter cell cycle arrest or apoptosis. The main proteins involved include three protein kinases; ATM, ATR and DNA-dependent protein kinase (DNA-PK), which phosphorylate many downstream effector proteins. Different forms of DNA damage are recognised and repaired by different pathways in the DDR. For example, dsDNA breaks are recognised by the MRN complex (Mre11-Rad50-Nbs1) which activates ATM. Damage which causes exposure of ssDNA regions, such as errors surrounding DNA replication forks, activates ATR. Finally, DNA-PK is recruited to dsDNA breaks which are eventually repaired through nonhomologous end joining (NHEJ) by XRCC4-DNA ligase IV [139].

DNA viruses can activate the DDR. Upon activation, the DDR components can be pro or anti viral. In addition, there are emerging reports that many of the proteins involved in the DDR recognition are capable of triggering an innate immune response [140]. When HSV-1 enters the cell the genome can cause localised damage to host cell DNA. Additionally, HSV-1 DNA contains many nicks and there are thought to be 15 gaps of approximately 30 nucleotides per genome [141, 142]. The DDR first responder proteins are able to recognise the damage within the HSV-1 genome, including MRN, ATM and DNA-PK. During an HSV-1 infection ATM is activated and phosphorylates p53, Chk1 and NBS [143]. Mre11 and ATM enhance viral replication, whereas DNA-PK is antiviral [143–145]. The requirement of Mre11 and other DDR proteins for HSV-1 replication may be reflected in the branched structures of HSV-1 DNA formed during replication. However, there are conflicting papers suggesting dispensable roles or conflicting results for DDR proteins in HSV-1 infection. For example Mre11 was found to restrict viral replication in a recent paper, in contrast to the evidence presented above [146]. Thus, there is ongoing debate about the role of these proteins in viral infection.

The histone variant H2AX is phosphorylated by ATM and ATR and is a common marker of DNA damage [147, 148]. The phosphorylated form, γH2AX, acts as a platform to recruit other DDR proteins induced by HSV-1 infection and is seen near HSV-1 genomes when ICP4 immunofluores-

cence is used as a surrogate marker. Viral proteins are required for the increase in phosphorylation but it has little impact on viral yield, therefore the role of γH2AX in HSV-1 infection is not clear [149].

1.4.4 Chromatin structures

Human DNA is organised in chromatin, consisting of DNA strands packaged tightly around nucleosomes comprising of histones. Heterochromatin is a dense region with tightly packed chromatin and little to no transcriptional activity, in contrast to euchromatin which is more open and accessible, allowing access for transcription machinery. Chromatin is a dynamic organisational strategy employed by the cell with modifications including acetylation and methylation of histone tails, as well as nucleosome remodellers controlling the density and positioning of nucleosomes. The status of covalent modifications on the histones determine the accessibility of the DNA, for example H3K27me3 (lysine 27 trimethylation on histone 3) is associated with heterochromatin and H3K9ac (histone 3 lysine 9 acetylation) labels transcription regions accessible to RNA polymerase II.

In latent HSV-1 infections, the viral genome is highly associated with histones. An HSV-1 genome in a lytic infection when it first enters the cell will be initially completely devoid of histones, but evidence suggests it is recognised by cellular machinery and histones are quickly deposited, in an attempt to silence genomes in an antiviral response. Histones are initially loaded onto a HSV-1 genome very rapidly, and with time as infection progresses the proportion of DNA associated with histones decreases [150]. VP16 has a role in restricting the depositing of histones on IE promoters, whilst having no impact on the presence of histones throughout the IE gene body and E promoters. Deletion of VP16 causes an increase in histone occupancy on IE promoters [151]. Histone loss as infection progresses is dependent on ICP0 [41]. As histones can present markers of transcriptional activation to cellular machinery, the presence of histones on viral DNA does not immediately correlate with transcriptional repression. Indeed, in addition to histone removal ICP0 promotes histone acetylation, a marker linked with active chromatin [152].

1.5 Single cell vs Population Analysis

Until recently, population level analysis such as sequencing, qPCR and western blots were the standard method of analysis of gene expression. Population analysis however averages a huge number of individual cells and it is becoming increasingly clear that there is a wide degree of heterogeneity both at the tissue level and at the clonal tissue culture monolayer. Averaging analysis over populations therefore masks cellular differences and reduces the chance of finding unique cell types. Highly detailed single cell analysis methods such as single cell RNA sequencing and single cell mass spectrometry demonstrate the heterogeneity at the single cell level [153, 154]. Variability in host gene expression profiles, environmental signalling from neighbouring cells, and cell cycle status all affect the progression of an HSV-1 infection. In addition to host cell variation, variation within the virus population and the random distribution in the number of viruses entering cells affect infection outcome at the single cell level [155]. Single cell analysis allows visualisation of spatiotemporal events that occur during a HSV-1 infection. Within a cell monolayer, single cells exhibit a wide variety of infections, including abortive infected cells and a large range of transcriptional profiles [156]. It is vital to make efforts to understand infections at the single cell level and how this interlinks across populations.

1.5.1 Click Chemistry

Bioorthogonal chemistry refers to a highly selective group of chemical reactions in cells that will not have any side effects against endogenous processes and groups as they are not commonly found naturally, also known as click chemistry [157, 158]. The development of click chemistry by Carolyn Bertozzi, Morten Meldal and Barry Sharpless was awarded the Nobel Prize for Chemistry in 2022. A bioorthogonal precursor, such as an azide group, is incorporated into cells. Subsequently, a probe with the correct functional group (an alkyne group will react to an azide group) reacts to the molecule in the cell that has been labelled. These reactions include the Staudinger ligation (azides and phos-

phines), metal catalysed reactions, and Tetrazine ligations [159]. The use of bioorthagonal chemistry in biological research has increased in the last decade, with it being most commonly utilised in studies of proteins [160].

Of importance within this work are the copper catalysed azide-alkyne cycloaddition (CuAAC) reactions to label nuclei acids. Alkyne derivatised nucleosides are incorporated into newly synthesised DNA and RNA and following the CuAAC reaction an azide-fluorophore is covalently attached [161]. Analysis of DNA synthesis in this way has been used to study cell proliferation and the cell cycle, and DNA synthesis changes in response to external stimuli [162, 163]. The commonly used modified nucleotides include deoxycytidine analogue 5-ethynyl-2'-deoxycytidine (EdC) and deoxythymidine analogue 5-ethynyl-2'-deoxyuridine (EdU) for DNA and EU for RNA.

In viral infections click chemistry has been used to visualise viruses. EdU or EdC is incorporated into the viral genomes, and the progeny virions are used to infect cells. After infection, the cells are processed with the click chemistry reaction and the labelled viral genomes are revealed. This has been achieved for Adenovirus [164], and by this lab and others for HSV-1 [165, 166]. The viruses with the bioorthoganol nucleotides are fully infectious, and allow high resolution spatial analysis of infecting viral genomes within nuclei. Studies into the early stages of infection are permitted, including recruitment and interactions with host proteins as well as genome decompaction.

1.5.2 RNAscope

Population based RNA transcriptional analysis, such as northern blots and qRT-PCR, do not give the level of detail about transcriptional heterogeneity that could be achieved by single cell analysis techniques. In 2009 the first transcriptome from a single cell was published [167]. This method, performed on a mouse blastomere, detected 75% more genes than the previous gold standard microarray assays. In the context of viral infections, single cell RNA sequencing (scRNA-Seq) was first used to investigate Hepatitis C virus [168]. In this study they determined there was diversity between qua-

sispecies within one cell. Since then, there have been multiple scRNA-seq studies examining viral infections [169]. Single cell RNA sequencing has been invaluable in providing omics datasets about the individual transcription profile of cells in conjunction with transcriptional data from an infecting virus [170, 171]. However, this type of analysis is both costly and time consuming, requiring the isolation of single cells and generates large data files for analysis. Another disadvantage of omics studies is that they cannot give any spatial information. The ability to view a monolayer and a viral infection at single molecule level will give insight into infection heterogeneity cell by cell and virus by virus.

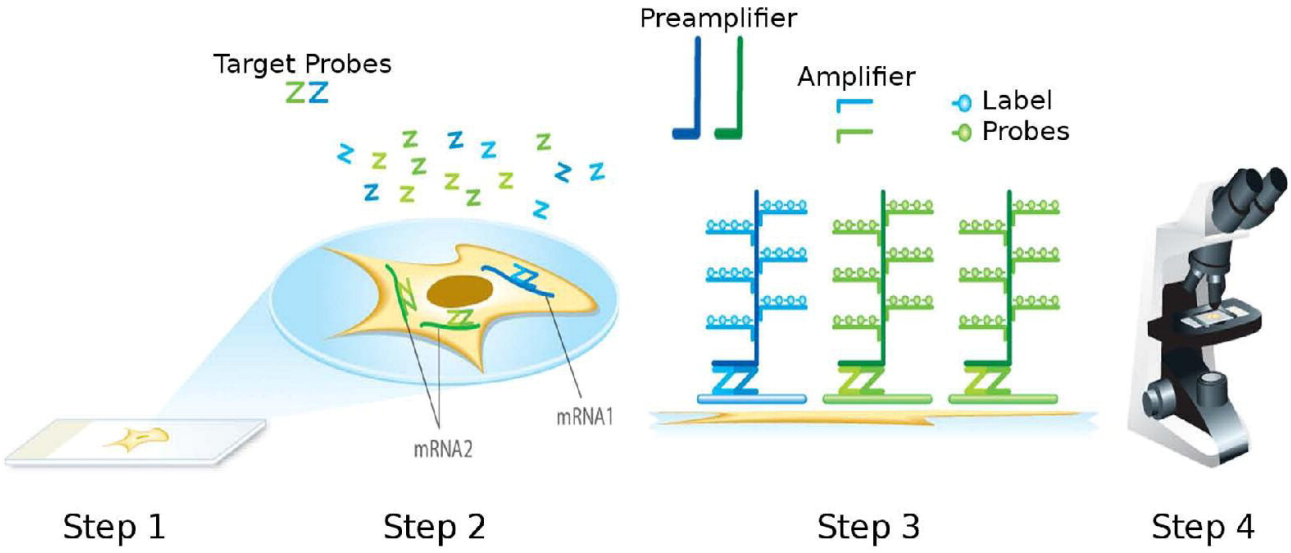


Figure 1.4: RNAscope Schematic

Reproduced from [172]. Step 1, cells are fixed and permeabilised. Step 2, Probes are hybridised to RNA targets. Step 3, Amplification molecules are hybridised in sequence and each unique probe is conjugated to a fluorophore. Step 4, Fluorescent microscopes are used to detect the signal.

RNA Fluorescent in situ hybridisation (RNA FISH) is a widely used technique for detection of emerging transcripts. RNAscope, a commercial assay, is an RNA FISH assay that will provide resolution at the single molecule level, known as single molecule RNA FISH (smRNA FISH). This technique involves the design of highly specific of probes of approximately 18 bases with a tail sequence. These can be thought of as Z shape, where the bottom part is for specific annealing to the

target RNA and the top part, when two adjacent probes are annealed, provides an area of approximately 28 bases. Here, the pre-amplifier can bind, which has 20 binding sites for the next amplifier, which itself has 20 binding sites for the labelled probe. The multiple rounds of amplification result in high specificity and high signal-to-noise ratios allowing detection and visualisation of single RNA molecules [172]. There are RNAscope probes available to purchase for over 100 viruses, and research has been published using RNAscope to investigate many viruses including HIV, Hepatitis E virus and SARS-CoV-2 [173–175].

Objectives

1. Develop techniques of single cell spatial analysis for the simultaneous detection of RNA, protein immunofluorescence and HSV-1 genomes.

2. Investigate transcription in the absence of VP16 or ICP4 function.

3. Investigate the hypothesis that recruitment of specific host restriction factors such as PML are responsible for virus transcriptional repression.

4. Examine the spatial relationship between transcription and DNA replication within viral replication compartments.

5. Examine the changes to nascent global transcription induced by HSV-1 incoming genomes.

Chapter 2

Materials and Methods

2.1 Cell Culture

2.1.1 Cell lines and propagation

Cells were cultured in a humidified incubator at 37 °C with 5% CO_2. The cell lines used are summarised in table 2.1. African green monkey kidney fibroblasts (Vero) cells (both WT and transgenic), Human Bone Osteosarcoma Epithelial Cells (U2OS) and Human epithelial keratinocytes (HaCaT) cells were grown in Dulbecco's Modified Eagle's Medium (DMEM; Gibco) with 10% foetal bovine serum (FBS; Gibco). Human telomerase immortalised retinal pigment epithelial cells (RPE) were grown in DMEM/F12 medium (Sigma) supplemented with 200 mM glutamine and 10% newborn calf serum (NCS; Gibco). All the above cell growth media was supplemented with 100 units/mL penicillin and 100 μg/mL streptomycin (Gibco).

Cells were subcultured from a confluent monolayer approximately 1:6 and twice a week, as required. Culture medium was aspirated and cells were washed in PBS (Sigma), followed by treatment with 0.05% trypsin/EDTA (Invitrogen) for cell detachment. Culture medium was added to neutralise trypsin, and the suspended cells were seeded either in new flasks for continued growth or on

Cell line	Growth Media	Serum	Origin
Vero	DMEM	10% FBS	O'Hare Lab
Vero 49-44	DMEM	10% FBS	Neal DeLuca
HaCaT	DMEM	10% FBS	O'Hare Lab
U2OS	DMEM	10% FBS	O'Hare Lab
RPE	DMEM/F12	10% NCS	O'Hare Lab

Table 2.1: Cell lines and culture conditions

sterile coverslips or multiwell plates for experiments. Cells were counted using a Countess automated cell counter or with a hemocytometer.

2.1.2 Drug treatments

Various drugs used are listed in table 2.2. Dosage length varied in individual expeirments, detailed in the results.

Drug	Concentration	Dilution medium	Source
Actinomycin D (ActD)	5 µg/mL	DMSO	Sigma
Cycloheximide (CHX)	50 µg/mL	Cell culture media	Sigma
Phosphonoacetic acid (PAA)	400 µg/mL	Cell culture media	Sigma
Hexamethylene Bisacetamide (HMBA)	5 mM	Cell culture media	Abcam
JQ1	500 nM	DMSO	Stratech
DRB	50 µg/mL	DMSO	Sigma

Table 2.2: Drug treatments

2.2 Virus Culture

2.2.1 List of viruses and production cell line

Viruses used in this thesis are detailed in table 2.3, alongwith the cell lines used to produce them.

HSV-1 Virus	Description	Producer cell line	Source
HSV-1	Wild-type HSV-1 strain 17	RPE	O'Hare Lab
HSV-1^{EdC}	EdC labelled HSV-1 strain 17	RPE	O'Hare Lab
FxE	HSV-1 strain 17 ICP0 RING finger domain deletion mutant	U2OS	Roger Everett
HSV-1 [KOS]	Wild-type HSV-1 strain KOS	RPE	O'Hare Lab
n12	HSV-1 strain 17 ICP4 deletion mutant	Vero 49-44	Neal DeLuca
in1814	HSV-1 strain 17 VP16 deletion mutant	U2OS	NIBSC

Table 2.3: Viruses

2.2.2 Production of Viruses

Wild-type HSV-1 strain 17 (HSV-1) was produced by infection of confluent RPE monolayers in either T225 flasks or 2L roller bottles at MOI 0.005 in serum free medium. At 2 hpi, an equal volume of medium with 4% NCS was added to give a final concentration of 2% NCS. When cell cytopathy reached 80-100% the infected cells were harvested, normally 48-72 hpi. The cell culture suspension was spun at 2000 rpm for 10 minutes to pellet the cell debris. The supernatant was spun in a Sorvall centrifuge, rotor SS-34, at 19,000 rpm for 90 minutes at 4 °C. The virus pellets were resuspended in PBS and aliquoted and stored at -80 °C.

2.2.3 Production of HSV-1^{EdC}

HSV-1^{EdC} was produced as above, with the following modification. EdC was supplied to the culture media at a final concentration of 10 μM EdC at 6 hpi, and again at 24 hpi.

2.2.4 Titration of Viral Stocks

Cells were seeded in 12 well plates at an appropriate cell density. Cells were infected with three dilutions of virus stock (most often 10^{-6}, 10^{-7} and 10^{-8}). The infection was performed as described below in 2.2.6, with the addition of 1% human serum for neutralising antibodies to reduce viral spread. Plaques are allowed to grow for 72 h before fixation in 4% PFA and stained with crystal violet. Plaques were then counted and titre was calculated as plaque forming units per mL (PFU/mL).

2.2.5 Adsorption and Visualisation of HSV-1^{EdC} on coverslips

5 μL of HSV-1^{EdC} stock containing 25000 PFU was placed on a glass coverslip for 15 minutes. 4% PFA was dropped onto the virus and left for 15 minutes. The coverslips were transferred to a 12 well plate and washed with PBS, and processed for click chemistry and immmunofluorescence (described in sections 2.4 and 2.5 respectively). Quantification of efficiency of EdC incoporation was performed as described in section 2.10.

2.2.6 Infections

When cells were infected by HSV-1, multiplicity of infection (MOI) was calculated based on the titre in PFU/mL. Virus stock was thawed on ice and diluted in DMEM (serum free). 0.5 mL of inoculum per well of a 12 well plate was applied to the cells and incubated on a rotating shaker at 37 °C for 1 h. When the cells are placed in the 37 °C incubator, this defines 0 h. At 1 hpi, the inoculum is removed from the cells and 0.5 mL of 2% FBS DMEM is added. Cells are fixed with 4% PFA at the desired timepoints, or harvested for RNA or protein extraction. Mock infected cells were treated as above

with serum free DMEM, followed by the shift to 2% FBS DMEM.

An exception to this protocol is for the capsid entry studies, where virus entry is synchronised. Cells and inoculum were chilled at 4 °C, the inoculum is added and cells were incubated on a rotating shaker at 4 °C for 45 minutes. This allows viruses to be adsorbed to the cells but not enter. Cells were then transferred to the 37 °C, allowing virus entry.

2.3 EdC and EU pulse labelling of nascent DNA replication and RNA synthesis

Cells were seeded on glass coverslips and were infected or mock-infected with HSV-1. 1 h before fixation, 10 μM EdC or 1 mM EU was added to the media. Cells were fixed in 4% PFA and processed for click chemistry (section 2.4).

2.4 Click chemistry

Cells that had been fixed in 4% PFA were washed in PBS and quenched in 100 mM glycine for 5 minutes. Cells were permeabilised in 0.5 % Triton/PBS for 15 minutes, washed in PBS, and incubated in the click reaction mix for 2 hours; 10 μM Alexa Fluor 488-azide (Invitrogen); 1 mM CuSO4; 10 mM Sodium Ascorbate; 10 mM Amino-guanidine and 1 mM Tris(3-hydroxypropyltriazolylmethyl)-amine (Sigma-Aldrich). For the incubation, coverslips were inverted onto a 35 μL drop of reaction mix on a piece of parafilm. Coverslips were washed in PBS and either processed for Immunofluoresence (section 2.5) beginning at the blocking stage, or directly stained with DAPI (100 μg/ml) and mounted with ProLong gold Antifade Mountant onto a glass slide. Slides were left in the dark overnight and imaged the following day.

2.5 Immunofluorescence

Cells that had been fixed in 4% PFA were washed in PBS, permeabilised in 0.5 % Triton/PBS for 15 minutes, washed in PBS, and blocked in 10% FBS/PBS for 1 hour at room temperature (RT). All antibodies used are shown in tables 2.4 and 2.5. The primary antibody was diluted to the working dilution in 10% FBS/PBS and cells were incubated with the primary antibody for 1 hour, RT. After 3 x PBS washes, the secondary antibody was diluted in 10% FBS/PBS and added to the cells for 1 hour. Cells were washed 3 x PBS stained with DAPI (100 μg/ml) and mounted with ProLong gold Antifade Mountant onto a glass slide.

Antibody target	Host	Dilution	Source
yH2AX	Rabbit	1:1000	Abcam (ab81299)
ICP4	mouse	1:400	Virusys (H1A021)
ICP4	rabbit	1:200	Chris Boutell
ICP8	mouse	1:250	Abcam (20194)
Mx1	Rabbit	1:200	SantaCruz
pDNA-PK	Rabbit	1:100	Abcam (ab18192)
PML (#368)	Rabbit	1:100	O'Hare Lab
PML (5E10)	Mouse	1:10	Prof. Van Driel
RNA pol II CTD	Mouse	1:150	SantaCruz (sc47701)
RNA pol II pSer5	Rabbit	1:250	CST (#13523)
RNA pol II pSer2	Rabbit	1:250	CST (#13499)
VP5	Mouse	1:400	Virusys (HA018)

Table 2.4: Immunofluorescence Primary Antibodies

Antibody	Dilution	Source
Mouse IgG (AlexaFluor 594)	1:1000	Invitrogen (A21203)
Mouse IgG (AlexaFluor 488)	1:1000	Invitrogen (A11029)
Rabbit IgG (AlexaFluor 594)	1:1000	Thermo (35560)
Rabbit IgG (AlexaFluor 488)	1:1000	Invirtogen (A11029)
Rabbit IgG(AlexaFluor 635)	1:1000	Invitrogen (A31577)

Table 2.5: Immunofluorescence Secondary Antibodies

2.6 RNA detection

2.6.1 RNAscope

Cells that have been fixed in 4% PFA are either processed for RNAscope immediately, or if they were to be stored they are dehydrated in ethanol and stored in 100% EtOH at -20 °C. Coverslips were inverted onto parafilm for all subsequent steps. The RNAscope multiplex fluorescent kit v2 was used as described by Advanced Cell Diagnostics, ACD Bio. Briefly, the coverslips were treated with hydrogen peroxide, followed by RNAscope protease III. They were then incubated with the ZZ probe pairs, designed by ACD, for 2 hours at 40 °C in a hybridisation oven (HybEZ oven, ACD Bio). The signal is amplified through a series of amplifiers, then the designated channel for each probe is added and developed with TSA plus Cyanine 3 (Cy3) or TSA Plus Fluoresceine (Fr). Cells were then stained with DAPI, and mounted on glass slides with ProLong Gold Antifade Mountant. The probes use are listed in table 2.6.

2.6.2 DNase treatment before RNA detection

After hydrogen peroxide treatment in the RNAscope protocol, cells were incubated with 8 units of DNase in DNase I Reaction Buffer (Thermo) for 30 minutes at 37 °C. The digestion was stopped by adding 2.5 mM EDTA in H_2O for 10 minutes. Cells were then processed for RNAscope as described

Target	Probe name
ICP0 (HSV-1)	V-HHV1-RL2-C2
ICP0 intron (HSV-1)	V-HHV1-RL2-Intron-O1
ICP0 reduced z (HSV-1)	V-HHV1-RL2-O1
ICP4 (HSV-1)	V-HSV-1-RS1
VP16 (HSV-1)	V-HSV1-UL48-C2
PP1B (Human)	3-plex positive control probe Hs
Mx1 (Human)	Hs-Mx1

Table 2.6: RNAscope probes

above, resuming at the protease step.

2.6.3 RNAscope combined with click chemistry and Immunofluorescence

When the three detection protocols were combined, RNAscope was completed first, followed by click chemistry (excluding the permeabilisation step) and finished by protein immunofluorescence. All three protocols were completed on the same day as cell fixation for optimal results.

2.6.4 qRT-PCR

Cells were grown on 12 well plates and infected with virus as described above. RNA was extracted using Qiagen RNeasy extraction kits as described by the manufactures. Purified RNA was stored at -80 °C. 1 μg RNA was digested with DNase I Amplification Grade (Thermo, 18068015) to remove any contaminating DNA. RNA was then converted to cDNA using the High Capacity cDNA Reverse Transcription Kit (Applied Biosystemts). cDNA was stored at -20 °C. cDNA was diluted 1:4, then 2 μL was used in a 10 μL PCR reaction with 5 μL PowerUp Sybr Green Master Mix in a MicroAmp Optical 384 well reaction plate (Applied Biosystems). Primers used are detailed in Table 2.7. 40 cycles were run on a QuantStudio 7 Flex. Melt curves and Ct values were evaluated using the QuantStudio 7 Flex System Software.

Primer Name	Sequence	Reference
18s F	CCAGTAAGTGCGGGTCATAAGC	[176]
18s R	GCCTCACTAAACCATCCAATCGG	[176]
ICP0 F	GTCGCCTTACGTGAACAAGAC	[177]
ICP0 R	GTCGCCATGTTTCCCGTCTG	[177]
ICP4 F	CGGTGATGAAGGAGCTGCTGTTGC	[177]
ICP4 R	CTGATCACGCGGCTGCTGTACA	[177]

Table 2.7: Primers

2.7 Western Blotting

Cells were grown on 12 well plates and infected with virus or treated with drugs as described above. Protein was extracted by harvesting cells in SDS lysis buffer, or RIPA lysis buffer (150 mM NaCl, 1% NP-40, 0.5% Sodium deoxycholate, 50 mM Tris pH8) + protease inhibitors + phostphatase inhibitors. Two protocols follow from here: for phosphorylated targets the samples were extracted in RIPA buffer and used Tris-buffered saline + 0.1% Tween (TBST) buffer. All other targets used the LI-COR blocking buffer and SDS lysis buffer. Protein samples were boiled for 5 minutes and sonicated for 10 seconds using the Soniprep 150 at maximum amplitude (20 microns). Proteins were loaded on 12% polyacrylamide gels, or 4-12% gradient gels. Proteins resolved by electrophoresis were transferred to nitrocellulose membranes which were blocked with Odyssey blocking solution (LI-COR) or 10% BSA/TBST. Primary antibodies were diluted in blocking buffer and incubated overnight at 4 °C on a roller. Membranes were washed three times with 0.005% Tween in PBS or TBST. Secondary antibodies were diluted in blocking buffer and incubated in the dark for 1h at RT. All antibodies used in western blots are listed in table 2.8. Visualisation of protein bands was performed using the LI-COR Odyssey infrared imaging system.

Antibody Target	Host	Dilution	Source
ICP0	Mouse	1:500	Santa Cruz
RNA pol II CTD pSer2	Mouse	1:2000	MBL
Tubulin	Mouse	1:8000	Sigma

Table 2.8: Western Blot Antibodies

2.8 Mass Spectrometry

HaCaT cells were seeded in 10 cm dishes. 24 h hours post seeding, the cells were either infected with an inoculum of in1814 at MOI 0.1 in 5 mL serum free media per dish, or mock infected with media alone. After 1 hour at 37°C, the inoculum (or virus free media) was removed and replaced with 2% FBS media, +/- 5 mM HMBA, and returned to the 37°C incubator. At 3 hpi (2 h post addition of 2% FBS media), the media was removed and cells were washed 3 times in cold PBS. Cells were lysed in 600 μL 2% SDS in PBS. The lysate was transferred to an eppendorf, sonicated for 10 seconds, centrifuged at 5000 rpm for 10 minutes. Protein was extracted using phenol chloroform precipitation. 600 μL methanol and 150 μL chloroform was added to the lysate, then vortexed vigorously and centrifuged for 5 minutes at 14000 rpm. The upper aqueous layer and lower chloroform layer was removed, leaving behind the protein interphase layer. 1 mL methanol was added to dissolve the protein with the aid of a sonicator. The protein suspension was centrifuged at 14000 rpm for 10 mins. The pellet was washed in methanol and centrifuged again. The methanol was removed and the protein pellet allowed to air dry. Once dry, the pellet was resuspended in in FRESH 600ul AMBIC (50 mM), with TCEP (5 mM) plus 2-chloroacetamide (10 mM) and left to resuspend on a shaker.

Protein concentration was assessed using the nanodrop at 280 nm. Sequencing grade trypsin (Promega) was used to degrade 100 μg protein and incubated at 37 °C overnight. 10% trifluoroacetic acid was used to stop the reaction. The sample was dried in a SpeedVac at 30 °C until dry, approximately 2-3 hours. The dried sample was stored at 4 °C before shipment to Dr Remigiusz Serwa,

Proteomics Core Facility, IMoL.

2.9 Widefield microscopy

Images were acquired with Zeiss Axiovert 135 TV microscope using Zeiss 63x lens (Plan-APOCHROMAT, 1.4 numerical aperture), 20x (Plan-Neofluar, 0.5 numerical aperture) objective lens and Retiga 2000R camera with Image Pro Plus 7.0 software. 3D stacks were acquired with a z-step of 0.5 μm/.

For the 4 colour analysis, images were acquired on a widefield Nikon Ti-Eclipse microscope, with a Plan Apo λ 60x oil immersion objective 1.4NA, a 1.5x zoom, a CoolLED pE-4000 light source and a Hamamatsu Flash 4.0 camera (2048 by 2048 pixels, xy pixel size of 72 nm). 3D stacks were acquired with a z-step of 0.1 μm. Files were deconvolved in NIS-Elements (Nikon, UK), Blind mode, 5 iterations.

2.10 Quantitative Image Analysis

2.10.1 Quantification of Transcription Bursts

For identification of transcription bursts, multichannel fluorescence images were opened in ICY software and transcription bursts were identified using the Spot detector function on the fluorescence channel containing the transcript dye [178]. The bursts were subsequently counted manually. For each field it was confirmed no cytoplasmic transcripts were being detected.

2.10.2 Quantification of EdC incorporation efficiency

For quantification of the efficiency of EdC incorporation into HSV-1^{EdC}, the images of capsid protein (VP5) and EdC genomes from virus on a coverslip were processed using the ComDet v.0.4.1 plugin in ImageJ. The input image was first converted to a two channel format. Approximate particle size of

4 pixels and intensity thresholds for foci in each channel were specified. The plugin identifies foci in each channel with intensities above the detection threshold and classifies them as colocalised if they are within 4 pixels of a foci in another channel. The output of the plugin gives the total number of foci per channel and the number of colocalised particles.

2.10.3 Quantification of Genomes or Capsids per cell

During an HSV-1^{EdC} infection the numbers of capsids or genomes per cell was quantified using ImageJ. The find maxima function identified the total number of genomes or capsids per field and this number was divided by the number of whole nuclei per field.

2.10.4 Quantification of total RNA

To quantify the amount of RNA per cell the DAPI channel was used to segment cells and provide an ROI overlay mask in ImageJ. The background was subtracted from the RNA containing channel, and the pixel intensity per ROI area (therefore per cell) was measured. The integrated density per cell was plotted to analyse the RNA quantity per cell in a field. This method can be extended to quantify the percentage of RNA in a cell that is nuclear. The DAPI field is used to create a second ROI overlay mask restricted to nuclei. Application of this mask onto the RNA channel allows the nuclear RNA signal to be measured. The cytoplasmic RNA signal is calculated by subtraction of the nuclear RNA value from the whole cell RNA value, and expressed as a percentage.

To count the number of nuclei positive for RNA in a field a nuclear ROI mask was created in ImageJ as described above. For each independent experiment a baseline threshold was chosen to remove background signal and applied. Any cell that records a grey value (RNA) above this threshold is identified as positive.

2.10.5 Quantification of protein levels

The percentage of ICP4 protein positive cells was calculated in ImageJ. The dapi channel was used to create a nuclear ROI mask. The ICP4 protein channel was used to measure the grey value of ICP4 per cell, and any cell that was higher than a set threshold was classed as positive.

Chapter 3

Development of techniques for the simultaneous analysis of individual genomes and their transcriptional activity

After HSV-1 genomes enter a cell nucleus, transcription of IE genes is the first step in a successful infection. By examining the de novo transcriptional activity of a genome we can start to understand the progression of infection at level of the single genome as it encounters a variety of counterattacks from within the cell. The first stage of my research was to develop and validate techniques for the high resolution spatial analysis of transcription of representative HSV-1 genes and quantitative analysis. Following this, I developed the ability to visualise transcription simultaneously with individual genome location by click chemistry.

Throughout this thesis I have chosen example cells to represent the features of interest. These cells have been chosen from experiments where a large number of cells were imaged to best illustrate the result. The Vero cell line has been used in the majority of the infections, and was chosen due to both its permissibility to HSV-1 infection and a consistently high performance in the RNAscope assays.

3.1 RNA in situ hybridisation allows visualisation of HSV-1 transcripts

RNAscope, manufactured by ACDBio, is an RNA FISH technology that allows spatiotemporal analysis at the single transcript level. The principles of RNAscope are described in the Introduction, in section 1.5.2. This first gene chosen to be tested was the IE gene ICP0. In mock infected cells, there was no detectable signal from the ICP0 probe, demonstrating the specificity of the signal (Fig 3.1 A).

The probe for ICP0 transcript was used to examine transcription at 3 and 8 hpi in cells infected with MOI 10. At 3 hpi, transcripts were readily detected. The infected cells show a large accumulation of transcript in the cytoplasm as well as small areas of transcript within the nucleus. A detailed examination of transcript localisation and features is developed through the chapter. To ensure that de novo viral transcription is required for probe hybridisation, Actinomycin D (ActD) was added to halt all nascent transcription (Fig 3.1 B). In the presence of ActD, no viral transcripts were detected, demonstrating the requirement for new transcription off the incoming viral genomes as well as the lack of transcripts in the viral capsids.

At 8 hpi, ICP0 RNA accumulates in the nucleus. At this timepoint, there is a large quantity of newly replicated viral DNA in viral replication compartments. To ensure the specificity of the RNAscope probes against viral RNA as opposed to any exposed ssDNA in the actively replicating viral DNA, cells were treated with DNase prior to the probe hybridisation. Figure 3.1 C shows that after the removal of all DNA, confirmed by the absence of DAPI stain, the signal from the RNAscope probe remains. This confirmed that the probes are targeting RNA molecules as opposed to any DNA regions.

After the preliminary experiments establishing the specificity of the RNAscope protocol, a timecourse of infection was performed with probes against two gene classes, an IE gene ICP4 and an

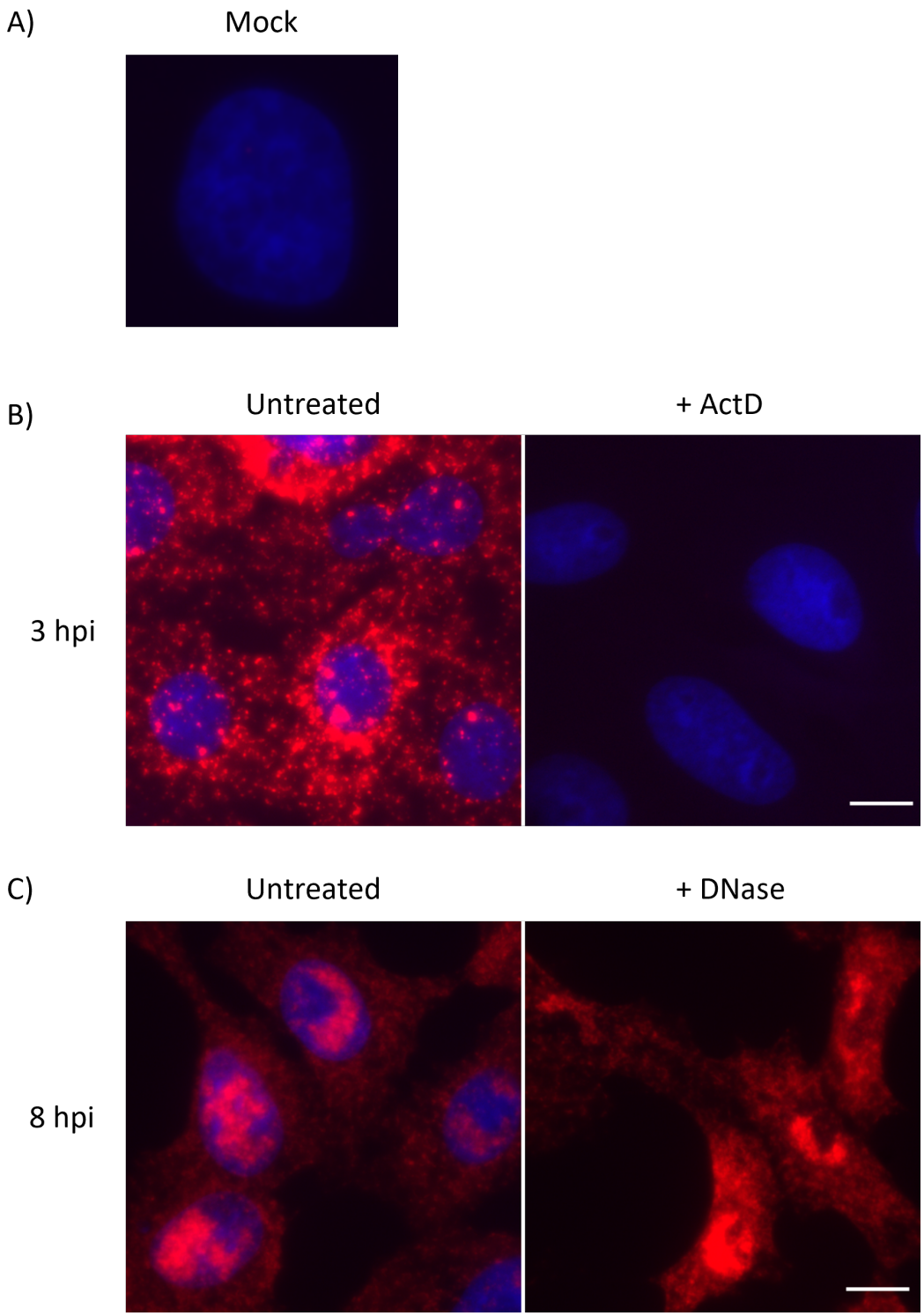


Figure 3.1: RNAscope allows visualisation of HSV-1 RNA transcripts.

A) Uninfected Vero cells B) HSV-1 MOI 10, 3 hpi. Untreated or 5 μg/mL ActD. ICP0 RNA (red), DAPI (blue). C) HSV-1 MOI 10, 8 hpi. Cells fixed, then left untreated or digested with DNase prior to RNAscope. ICP0 RNA (red), DAPI (blue). Scale bar 10 microns.

L gene VP16. ICP4 transcripts appear as early as 1 hpi within the nucleus (Fig 3.2 A). Both single transcripts and large nuclear foci are visible. The large nuclear foci are termed transcriptional bursts

and are discussed further below. At 2 hpi, ICP4 begins to accumulate in the cytoplasm and there are more frequent transcriptional bursts. By 4 hpi, coinciding with the onset of DNA replication, the nuclear burst have mostly disappeared and there is a large amount of cytoplasmic transcript. The virus is preparing for viral replication and there is no ongoing transcription of IE from the incoming genome. At 8 hpi, there is a large viral replication compartment full of ICP4 transcript with little cytoplasmic transcript visible. To summarise, after an initial burst of activity from 1-2 hpi, the number and size of nuclear foci diminished. Then, post replication, transcripts emerge from the replication compartments. To reinforce that this decline and subsequent reactivation is due to the onset of DNA replication, I included PAA in the assay, an inhibitor of HSV-1 viral replication. At 8 hpi there is a large difference in the location of the viral transcripts when PAA is added, as ICP4 does not accumulate in large nuclear regions.

The L gene VP16 requires more time for gene expression due to the requirement of the IE proteins in transcription, with transcripts becoming visual by 2 hpi (Fig 3.2 B). At 8 hpi, VP16 transcript within the nucleus is contained within the replication compartments, but in contrast to the IE ICP4 it has significant quantities of cytoplasmic transcript. The addition of PAA was used to inhibit the onset of viral replication which prevented replication compartment formation and consequently prevents the nuclear accumulation of VP16 transcript. Transcription following the onset of DNA replication will be examined in more detail and discussed in Chapter 6.

3.2 Immediate early transcription bursts

In figure 3.2 A at 1 hpi, in the absence of PAA, two large nuclear foci of ICP4 RNA, or transcription bursts, can be seen. A further example of a transcription burst at 1 hpi is shown in figure 3.3 A and indicated by the arrow. A transcription burst is defined by its large size and intense signal. It must be significantly larger than any single transcript molecules. The current hypothesis, which will be investigated later in this chapter, is that the transcription bursts represent the sites of viral

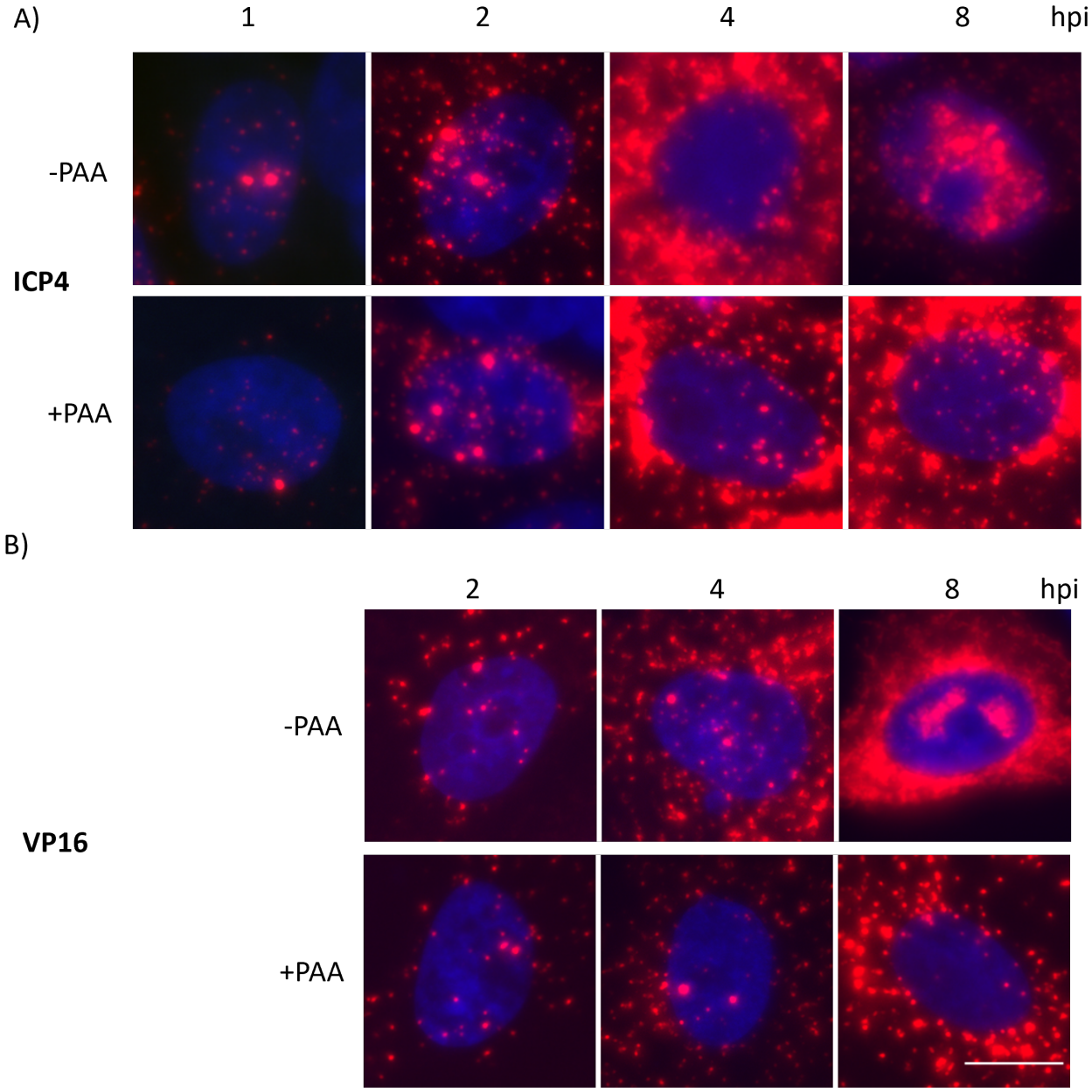


Figure 3.2: HSV-1 transcription progression throughout infection.

Vero cells, HSV-1 MOI 10. A) ICP4 transcript (red) by RNAscope at 1-8 hpi. B) VP16 transcript (red) at 2-8 hpi An example cell from each timepoint is shown.

genomes. Therefore, transcription bursts must also be nuclear. Surrounding the burst are additional single transcript dots representing single transcript molecules. These individual transcripts have been transported away or diffused away from the viral genome.

Quantification of transcription bursts was performed using ICY. Input 63x fields (Fig 3.3 B

i) were processed using the Spot detector function within the ICY software to identify transcription bursts (Fig 3.3 B ii). A new image was generated with nuclear outlines in white and containing only the transcription bursts from the RNA signal (Fig 3.3 B iii). The number of bursts in each cell was then manually counted. Quantification of 230 cells reveals 32% have no transcription bursts, 41% have either 1 or 2 bursts, and the remaining 25% have 3 or more.

Infections used for this image analysis were performed at MOI 10 in an asynchronous cell population. Despite this high MOI, RNAscope reveals significant heterogeneity in transcriptional progression. Statistically, all of these cells will have received at least 1 HSV-1 genome, yet nearly one third have no transcriptional bursts. Some of the negative cells have single transcripts, indicating that the genomes have been transcriptionally active but then have either stopped bursting or have yet to produce a large quantity of transcript. These results from single cell analysis reveal detailed information about heterogeneity during early stages of infection that is not obtainable with bulk population analysis such as RNA sequencing.

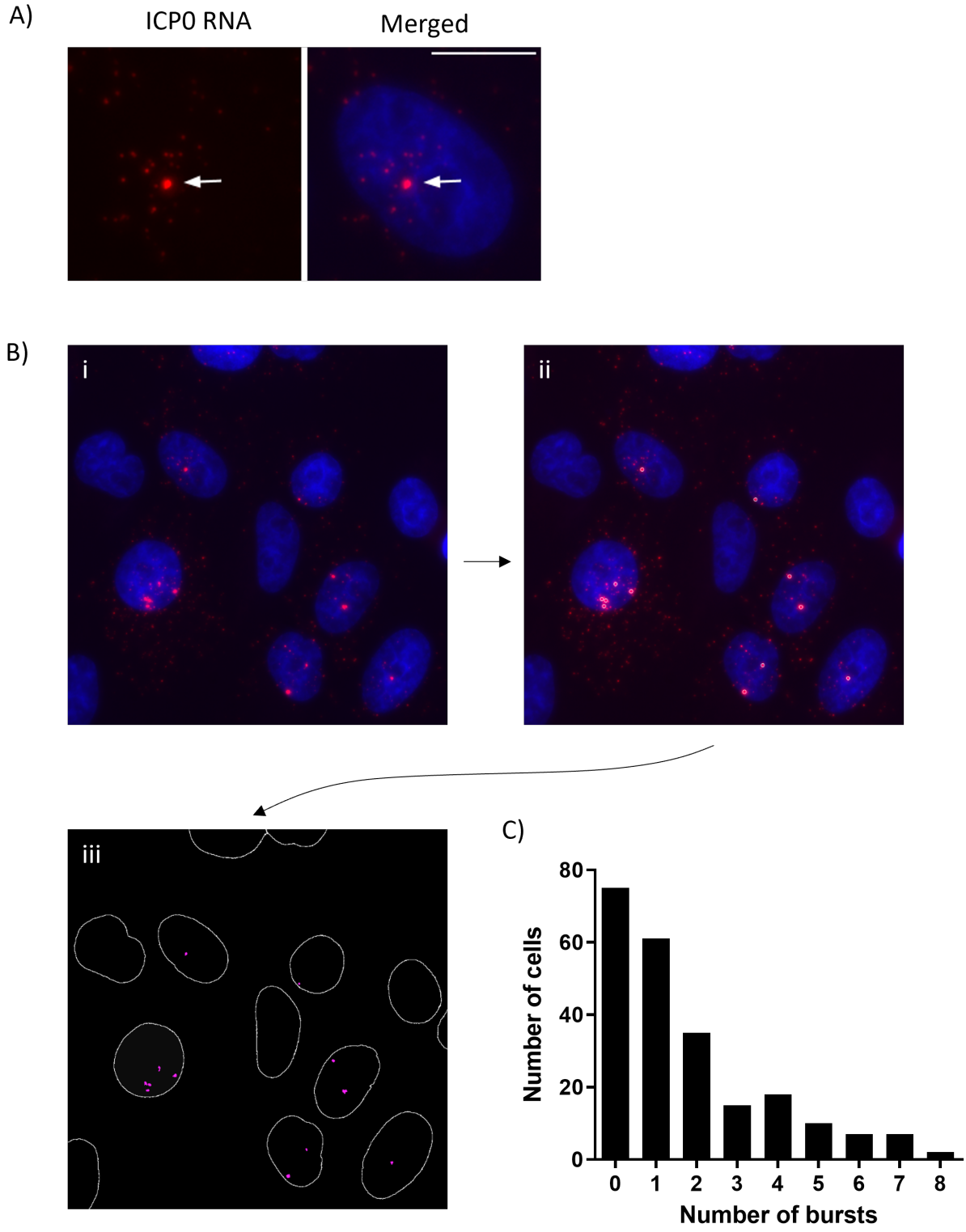


Figure 3.3: IE Transcription bursts

Vero cells, HSV-1 MOI 10, 1 hpi. ICP0 RNA (red), DAPI (blue). A) A single cell with one ICP0 transcription burst, indicated by the arrow. Scale bar 10 microns. B) Example of how a field of cells (i) is processed through ICY. Spot detector selects the transcription bursts (ii), and then the number of bursts per cell are counted manually from a newly generated image with the nuclear outline in white (iii). C) Quantification of the number of ICP0 transcription bursts per cell, n=230.

3.3 Simultaneous detection of ICP4 and ICP0 transcripts

To expand on the transcription analysis presented so far, I wanted to address the transcription of multiple genes simultaneously. Probes against different genes can be multiplexed within the same RNAscope experiment. The design of the amplification reagents allow different probes to be bound to different fluorophores, which therefore means multiple probes can be visualised on the same sample in different channels. This will give spatiotemporal information about the relationship between multiple transcripts within one cell. Probes for two IE genes, ICP0 and ICP4 were used together at 1 hpi (Fig 3.4 A). To aid visualisation of the two transcript types I have chosen a cell with a low transcript level to present in this figure. There is a low level of single transcripts present throughout the nucleus and no large transcription burst is visible. A transcript molecule of ICP0 is indicated by the outline arrow, and a molecule of ICP4 RNA is indicated by the filled arrow. The two transcripts give separate and distinct signals demonstrating that the probes are specific to the individual transcript sequences they are designed to detect and do not cross react.

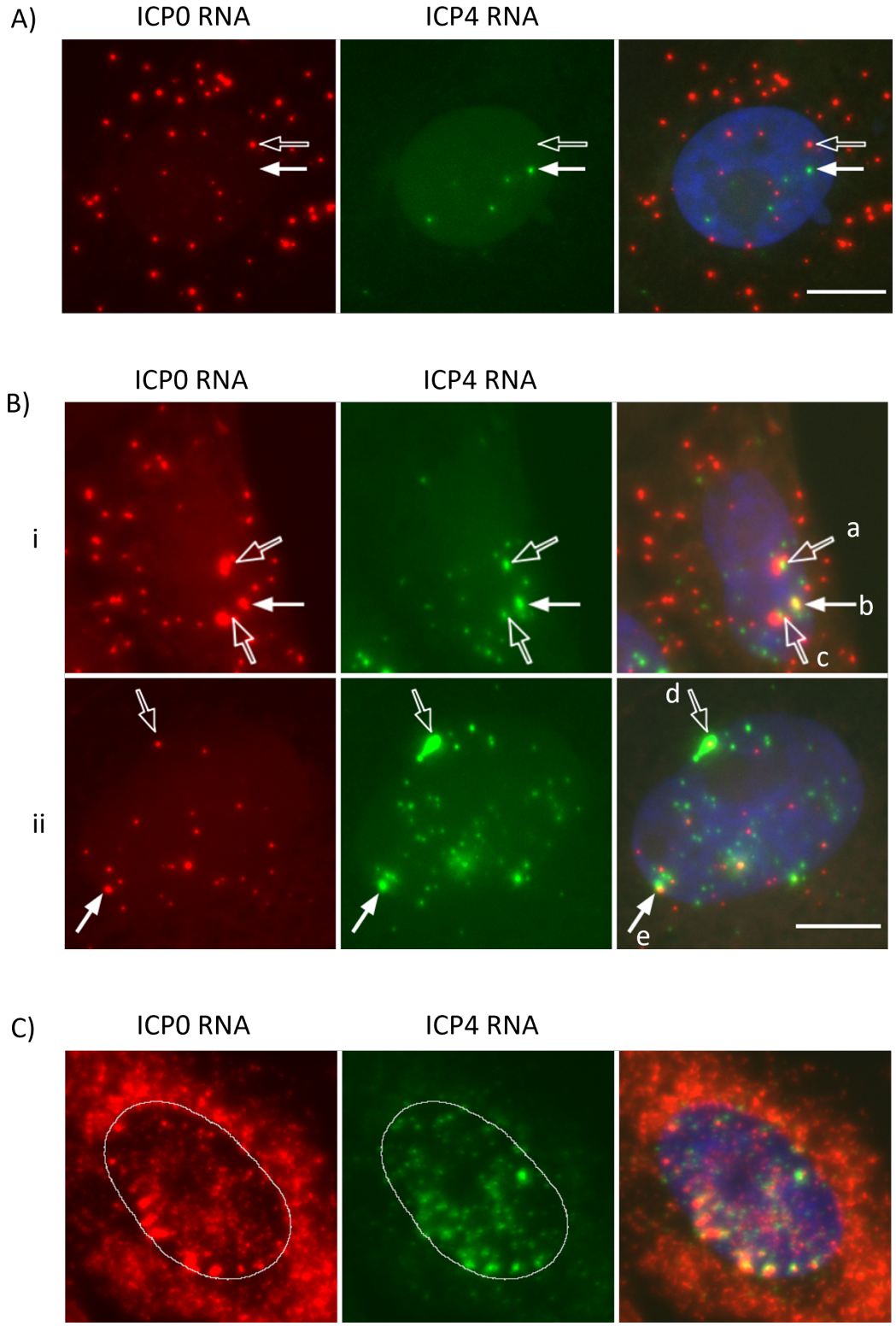


Figure 3.4: Simultaneous detection of ICP0 and ICP4 viral gene transcripts.

Multiplex RNAscope for ICP0 (red) and ICP4 (green) transcript, Vero cells. Scale bar 10 microns. A) HSV-1 MOI 10, 1 hpi. The filled arrow is representing a single ICP4 transcript, and the outline arrow is indicating a single ICP0 transcript. B) HSV-1 MOI 10, 1 hpi. Cell i: arrows indicate ICP0 transcription bursts. Filled arrow (arrow b): ICP0 and ICP4 burst. Cell ii: two ICP4 bursts. Filled arrow (arrow e): small burst, outline arrow (arrow d): large burst. C) HSV-1 n12 MOI 10, 3 hpi. ICP0 and ICP4 RNA. Nuclear outline in white.

In a high MOI infection where there are multiple genomes with transcription bursts, each individual genome may be transcribing both IE genes at the same time, or alternatively only transcribing one or the other. There are two example cells in figure 3.4 B. Cell i has three ICP0 transcription bursts, indicated by the arrows and labelled a, b and c. Of the three ICP0 transcription bursts, burst b (indicated by the filled arrow) is also bursting for ICP4. Bursts a and c, indicated by the outline arrows, are not bursting for ICP4. Bursts a and c have a small amount of ICP4 transcript, suggesting that the genomes are not silent for ICP4, yet there is significantly more ICP0. Cell ii has a large ICP4 burst (burst d) which has only a very low amount of ICP0 transcript associated, most likely a single transcript. The filled arrow at the bottom of the cell highlights an ICP4 burst (burst e), which again is not bursting for ICP0 but is a larger size than a single transcript molecule. Therefore, multiplexing RNA FISH probes has revealed a temporal distinction of transcription kinetics for two IE genes. These were previously thought to be expressed in a highly coordinated manner, yet the transcription burst dynamics suggest different rates of transcription and with heterogeneity between individuals genomes within one cell.

During singleplex experiments using either probes against ICP0 or ICP4 alone, it is not possible to compare relative abundance accurately. This is due to biological and experimental variation. However, one feature of interest that was identified during singleplex experiments was the location of viral transcripts. In order to confirm that the localisation of the two IE genes ICP0 and ICP4 was different, multiplex analysis of the two genes in combination was required. ICP0 is normally present at a greater abundance and with a higher proportion of cytoplasmic transcript. Figure 3.4 A provides an example of this, where there is significantly more ICP0 transcript than ICP4 transcript with a large percentage in the cytoplasm.

To examine this further, a HSV-1 virus with a truncated ICP4 protein was used, n12. The mutant n12 virus is produced in a complementing cell line expressing ICP4, as the ICP4 gene encoded within the virus is non-functional. Therefore, there are two defining features of this virus. Firstly, it

will not replicate. Secondly, as ICP4 is unable to perform the autoregulatory function there will be an increased amount of IE transcripts. The large quantity of transcripts will exaggerate the location phenotype and make any conclusions easier to observe. At 3 hpi with n12 at MOI 10 there are many transcription bursts, in contrast to a WT infection where the bursting rate would be decreasing at the onset of replication. The ICP0 RNA is abundant in the cytoplasm whereas the ICP4 RNA is nuclear (Fig 3.4 C).

3.4 Multiplex analysis within one gene

ICP0 is one of the few HSV-1 genes that is spliced. It has two introns that are removed during post-transcription processing. By designing an RNAscope probe specific for the intron containing regions we aim to view the active area of transcription with increased specificity. The design of the ICP0 probe for RNAscope used thus far spans a large region of the gene. In order to observe intron containing ICP0 transcripts, the binding region of the probe was restricted to the ICP0 intron, a region not covered by the original ICP0 probe. A schematic of the ICP0 RNA probes is given in figure 3.5 A.

The ICP0 intron probe was used in multiplex analysis with the previously used ICP0 probe, now termed the ICP0 exon probe, with the aim of being able to distinguish spliced vs unspliced transcripts. Cell i in figure 3.5 B has one transcription burst, indicated by the arrow. The ICP0 intron domain colocalises with the ICP0 exon transcription burst, but it is a much smaller signal than the ICP0 exon probe. Thus, the ICP0 transcripts containing the intron and therefore unspliced occupy a smaller area than the exon transcripts and the remainder of the transcription burst consists of spliced, processed ICP0 transcript. Splicing of ICP0 must occur quickly after transcription before the intron containing transcripts have had time to diffuse and move away from the genome. Cell ii has two arrows, and additional bursts not indicated by arrows. In the top half of the cell, there are several bursts.

In three of the bursts the intron and exon probes colocalise, while one burst, the one indicated by the filled arrow has no detectable intron signal. Assuming the transcription bursts all represent active viral genomes, this genome may no longer be actively transcribing. Alternatively, the ICP0 transcript is so rapidly spliced no intron remains, having been degraded or diffusing away. The remaining ICP0 transcript, which had been identified as a burst, therefore could represent an accumulation of transcript that has yet to be transported away. The lower half of cell ii, with the magnified insert labelled ii* shows a large transcription burst positive for both probes, and an additional smaller ICP0 intron spot, labelled with the arrow. This single transcript represents a rare single intron containing ICP0 transcript which can be observed diffusing away from transcription bursts.

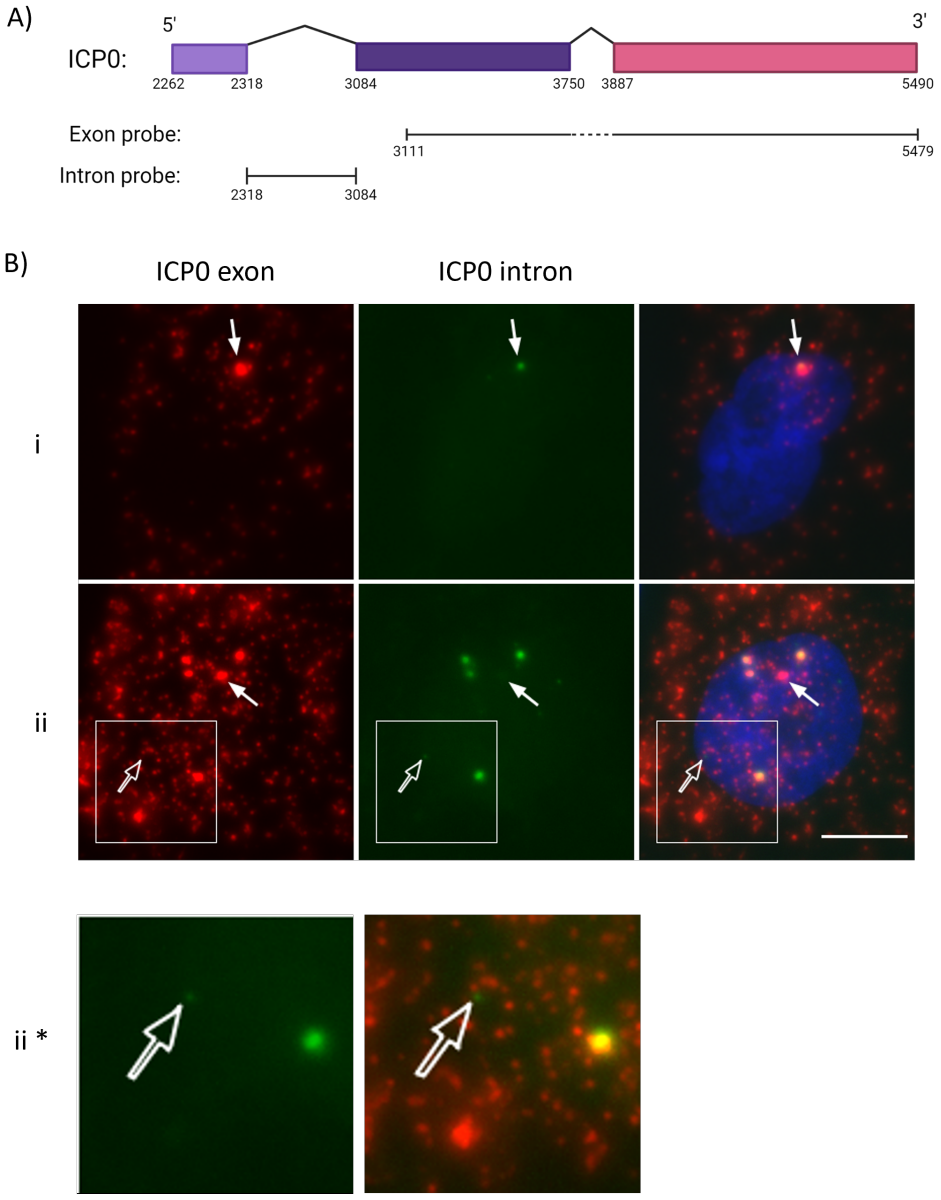


Figure 3.5: Detection of intron containing ICP0 transcripts.

A) Diagram of ICP0 exon and Intron probes. Exons are represented as the coloured boxes, introns are the lines between them. B) Vero cell, HSV-1 MOI 10, 1 hpi Cell i: One ICP0 transcription burst, indicated by the arrow. Cell ii: 5 ICP0 transcription bursts, one is indicated by the filled arrow that is negative for intron. The inset box is expanded in ii*. The outline arrow shoes a single intron transcript. Cell iii: the arrow indicates a colocalised intron exon.

3.5 Combined detection of HSV-1 genomes and analysis of transcriptional activity

As described in the introduction, HSV-1 viral genomes can be visualised through click chemistry reactions if an alkyne nucleotide, such as EdC, is incorporated into the genome. Production of EdC labelled HSV-1 (HSV-1^{EdC}) has been previously detailed by the lab [165]. In brief, HSV-1 is produced in media supplemented with EdC. To assess the efficiency of EdC incorporation, the percentage of labelled viruses can be quantified by application of the purified virus to a glass coverslip. An antibody for the capsid protein VP5 identifies all capsids on the coverslips, and combination with click chemistry to conjugate the Azide-488 fluorophore allows quantification of the percentage of virions with EdC labelled genomes (Fig 3.6 A). The filled arrow is indicating a capsid with a clickable, or EdC labelled genome. The outline arrow is showing a capsid that is either empty, or has a genome that is not labelled with EdC. The ImageJ plugin Comdet calculates colocalisation of VP5 and EdC genomes. Signal maxima that are within 4 pixels are classified as colocalised and appear as a yellow box (fig 3.6 A). It is important that every new virus preparation is evaluated is this manner to ensure there is a high percentage of labelled virions. Quantification of several virus preparations of different ages are presented in the graph in figure 3.6 B. The black bars represent the percentage of VP5 capsids in a field that colocalised with EdC labelled genomes. The grey bars represent the percentage of EdC labelled genomes that are contained within capsids. I evaluated several older stocks and determined that in the two viral stocks from 2015 and 2016, up to 50% of capsids did not contain clickable genomes. The original analysis of these stocks when they were first made resulted in only 10% of capsids without clickable genomes [165]. Older virus stocks are more prone to have both empty capsids and free genomes due to degradation. Therefore, EdC labelled viral stocks should not be stored for extended periods of time.

EdC labelled viruses are fully infectious. When the genome is released from the capsid

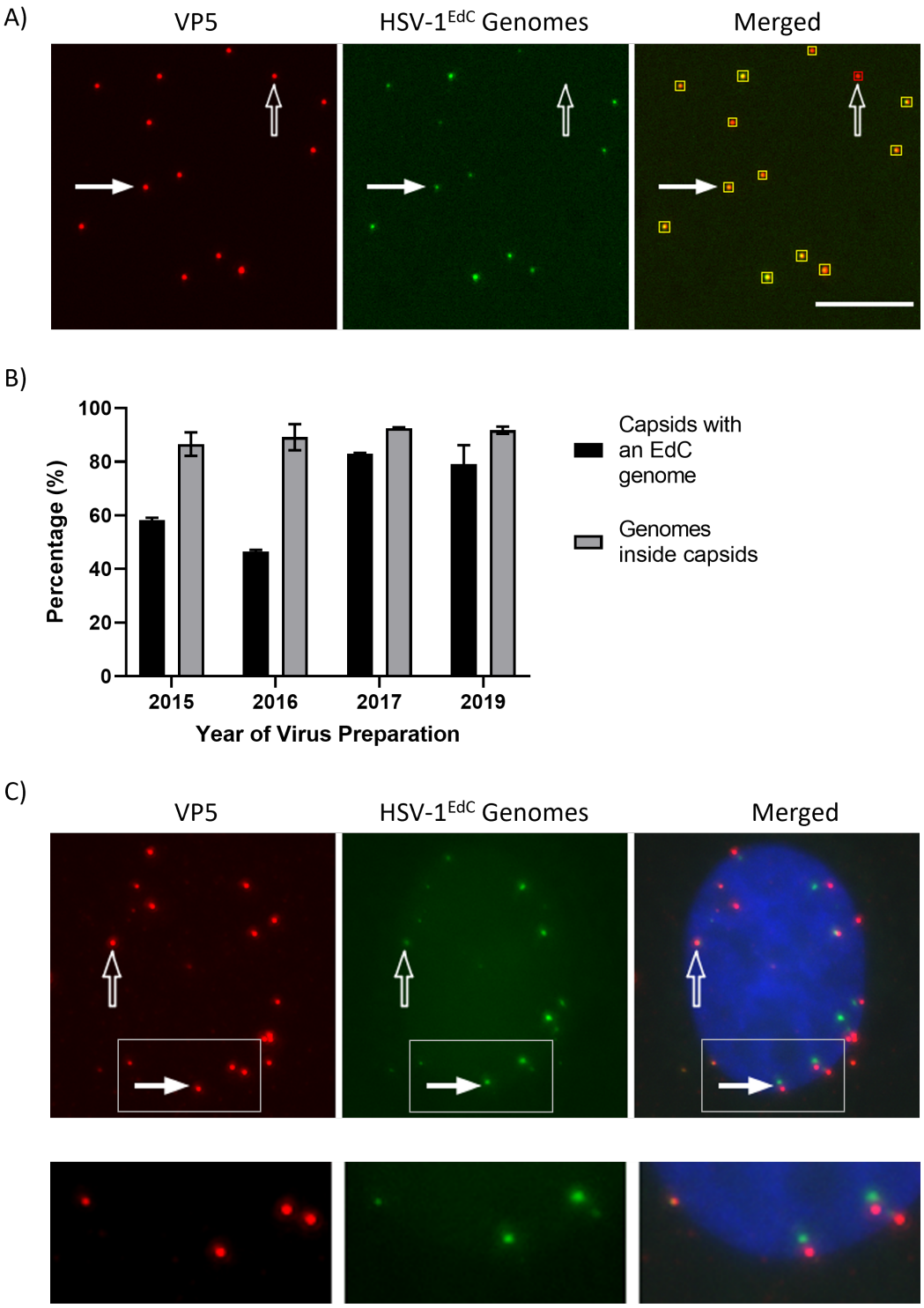


Figure 3.6: Production of infectious HSV-1^{EdC}.

A) HSV-1^{EdC} adhered onto a glass coverslip. Processed for IF (VP5 (capsid protein), red) and click chemistry for EdC genomes (green). ComDet analysis identifies colocalised genomes and capsids in the yellow boxes, shown by the filled arrow. Empty capsids without genomes are in red boxes, shown by the outline arrow. Scale bar 10 microns. B) Analysis of quality of different virus stocks. At least two independent image fields were analysed. Black bars: percentage of VP5 capsids colocalised with genomes. Grey bars: percentage of genomes that colocalised with capsids. C) Vero cell infected with HSV-1^{EdC} at MOI 10, 1 hpi. Processed for IF (VP5) and click chemistry. The vertical filled arrow shows a colocalised genome and capsid. In the expanded inset box, several genomes can be seen leaving the capsid.

through the nuclear pore complex, it is accessible to the click chemistry reaction reagents. At 1 hpi, genomes can be seen inside the nucleus after being released from VP5 capsids (Fig 3.6 C). The outline arrow indicates a genome that has just been released, and the filled arrow in the expanded box shows a genome that has been released from the capsid into the nucleus and has moved slightly from the nuclear pore. These images are initially taken as a z stack and a maximum projection created, so it is important to note that genome indicated by the outline arrow may have moved a distance into the nucleus, but directly beneath so there is no lateral xy movement. Also of interest to note is the capsid to the left of the nuclei. Although this capsid has not released its genome, the genome gives a detectable EdC signal. In the majority of cytoplasmic capsids the genome is undetectable as it is protected by the capsid, but a minority are made visible during sample processing. Occasionally genomes free from capsids are also visualised in the cytoplasm. As mentioned above, the rate of genome free capsids is linked to the quality and therefore the age of the virus stock.

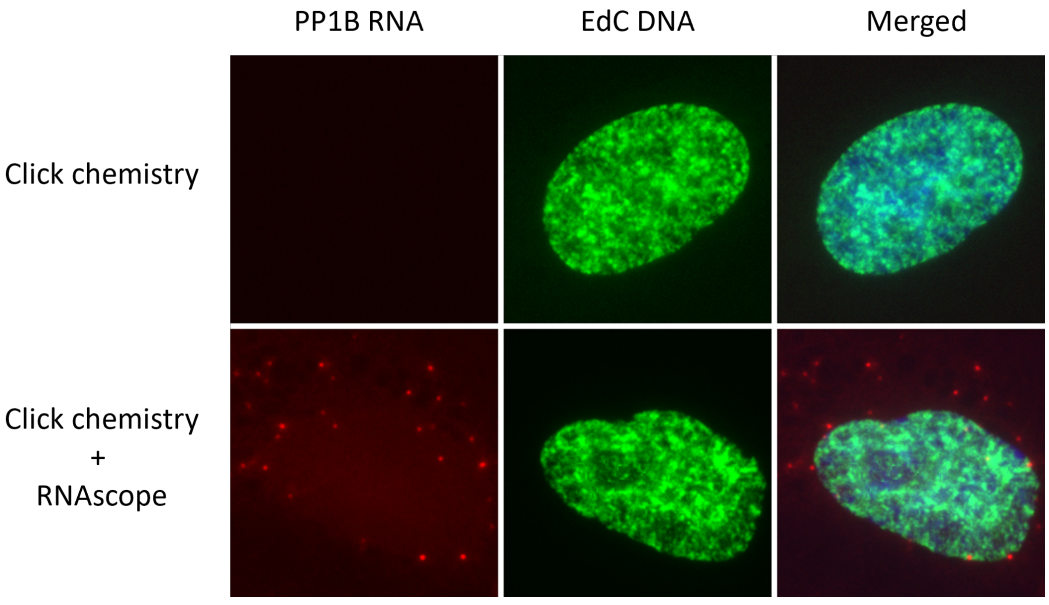


Figure 3.7: RNAscope can be combined with click chemistry of EdC labelled cellular DNA

2h pulse of 10 μM EdC in uninfected Vero cells. Upper panel: Click chemistry analysis. Lower panel: RNAscope for PP1B RNA (red) + Click chemistry (green).

EdC can be supplied to cell culture medium to be incorporated into replicating viral or cellu-

lar DNA, which can then be visualised through a click chemistry reaction. To optimise the protocols for combining RNAscope with bioorthoganol click chemistry reactions, EdC was used to pulse label uninfected cells for 2 hours. Cells were fixed and processed for click chemistry alone, or click chemistry in combination with RNAscope for the cellular gene protein phosphatase 1B (PP1B) (Fig 3.7). When the protocols were combined, there was no loss of EdC DNA signal and the RNA FISH signal remained bright and clear. However, the order of the analysis is important, the RNAscope must be performed before the click chemistry reaction. Additionally, the best fluorescence signals were obtained when the samples were processed on the same day that the cells were fixed.

Having determined that the click chemistry reactions could in principle be combined with RNAscope, the combined protocol was then performed in cells infected with HSV-1^{EdC}. Cells were fixed at 1 hpi, processed for RNAScope (ICP4) and click chemistry for EdC genomes. At 1 hpi, genomes remain in a relatively compact state. As infection progresses, genomes will begin to decompact. In figure 3.8 A, cell i has three transcriptional bursts. Underneath all three bursts there are HSV-1 genomes. Now with the addition of EdC labelled genomes, it can be stated with confidence that the transcriptional bursts represent the sites of active viral genomes. The ability to simultaneously examine genomes and their transcriptional activity demonstrates a significant degree of heterogeneity at the individual genome level. Cell ii in figure 3.8 A has multiple genomes. A genome with a large amount of transcriptional activity is indicated by the open arrow, whilst a genome with little or no activity is illustrated in the same cell with a filled arrow. Therefore within one cell, genomes can be active or inactive with regards to transcription of ICP4. However, this doesn't exclude the possibility that a genome that is inactive for ICP4 at any time could be active for another viral gene in particular other IE genes.

Simultaneous visualisation of infecting genomes and viral RNA allows spatial features of transcription to be analysed. In figure 3.8 B three examples are presented of HSV-1 genomes and their associated transcriptional bursts. The burst may be centred on the genome, as in figure 3.8 B i,

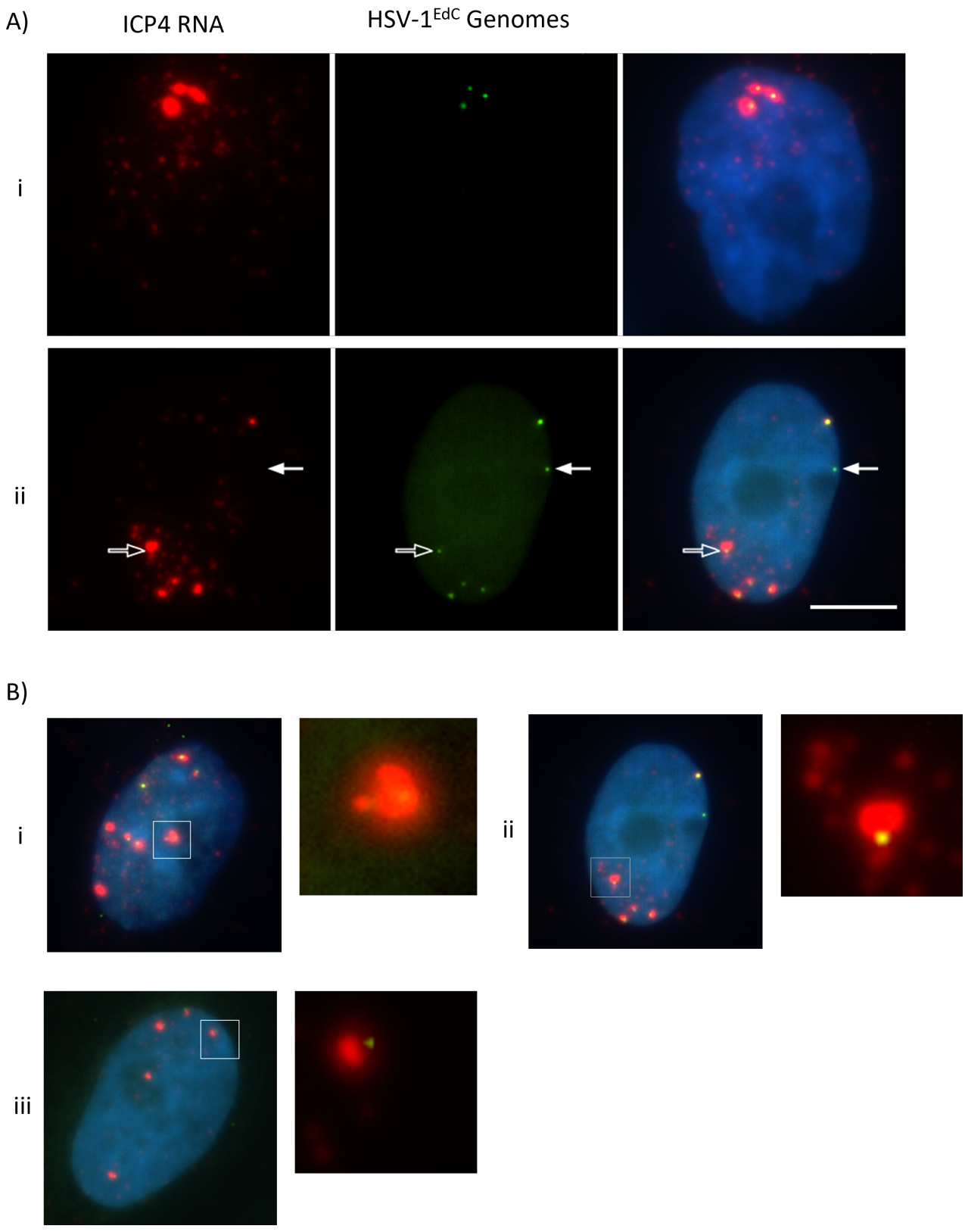


Figure 3.8: Continued on following page.

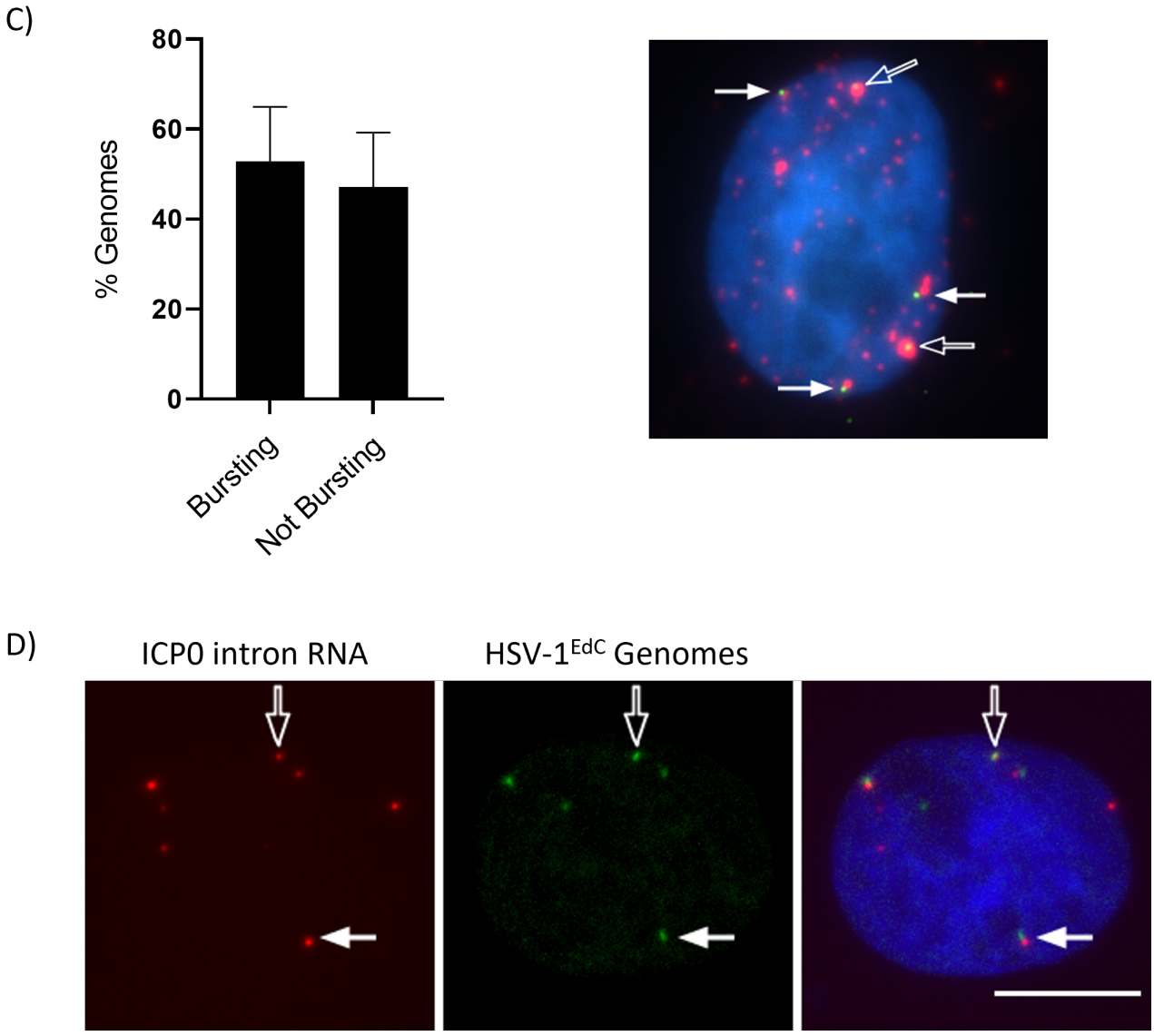


Figure 3.8: Spatial relationship between active genomes and transcription bursts

Infection with HSV-1^{EdC} in Vero cells, MOI 10. A-C) Processed for RNAscope (ICP4) (red) and click chemistry (green). A) 1 hpi. Cell i: ICP4 transcription bursts over HSV-1 genomes. Cell ii: Outline arrow indicates an active genome, the filled arrow indicates an inactive genome. Scale bar 10 microns. B) Three example cells at 1 hpi with three expanded areas illustrating different spatial presentation of genomes and transcription bursts. C) Quantification of bursting and not bursting for ICP4. Active are indicated by the outline arrow, inactive by the filled arrow. n=416. D) Vero cell, HSV-1 MOI 10, 1 hpi. RNAscope for ICP0 intron (red) with click chemistry for genomes (green). Directly associated genomes and transcripts: outline arrow. Closely associated genomes and transcript: filled arrow.

or emerging in one direction, as in figure 3.8 B ii. The example in figure 3.8 B iii would still be classed as a transcription burst, but the associated genome is spatially separated. This may represent loops of actively transcribed viral DNA regions emerging from the compact region, as discussed further in section 3.6.

The transcriptional activity of viral genomes can be quantified. Using the same ICY analysis as introduced in section 3.2, the transcriptional bursts are then compared to genome location. The overwhelming majority of transcription bursts are associated with a viral genome, confirming our hypothesis that transcription bursts represent the location of viral genomes. The few exceptions of a transcription burst without an apparent associated genome is most likely explained by the presence of a small fraction of the genomes that were not efficiently labelled with EdC. Quantification of over 400 genomes and ICP4 RNA reveals no significant difference between the number of genomes Bursting versus Not Bursting. The Not Bursting category includes completely negative or inactive genomes in addition to genomes that may have a small amount of transcript but which were not classified as a burst. As an example, the Vero cell in figure 3.8 C has 5 HSV-1 genomes, two of which are actively bursting, indicated by the open arrows. The other genomes although associated with a small amount of transcript are classified as 'not bursting'. Therefore, significantly higher than 50% of genomes are actively transcribing ICP4, but only 50% are classified as a bursting genome.

As previously stated in section 3.3, the ICP0 intron RNAscope probe represents the location of viral genomes more accurately than the ICP0 exon probe. Analysis of ICP0 intron RNA with viral genomes supports this hypothesis. The Vero cell in figure 3.8 D was infected with HSV-1^{EdC}, fixed at 1 hpi, and processed for RNAscope (ICP0 intron) and click chemistry. It has several viral genomes, and the majority of intron foci colocalise with the genomes. The two indicated with the arrows are either directly colocalised (the outline arrow) or closely associated (the filled arrow). There is one ICP0 intron region which is too large to be a single transcript, but is not associated with a genome. The most probable explanation for this is that there could be an unlabelled genome at this location.

Within an HSV-1 IE transcription burst there are large numbers of RNA transcripts. Attempts to quantify the number of transcripts within the bursts are particularly difficult due to the high intensity of the signal generated with the burst. In an effort to improve resolution within the burst, several protocol modifications were tried. Initially, a reduced amount of fluorophore was added (Fig 3.9 A).

Although transcription bursts are still visible, there was a significant reduction in overall signal and many single transcript foci were lost. A new ICP0 probe was designed with a reduced number of z probes over a smaller binding region on the RNA (Fig 3.9 B). The standard probe contains 20 pairs of z probes, all of which are capable of eventually binding the fluorescent dye. The reduced z probe only consists of 10 z pairs. Compared to the standard probe with a reduced fluorophore, there was better retention of the single molecule signals in the cytoplasm. However, even with the reduced z probe there is no improved resolution within the bursts. They are too densely packed with transcript for single transcript resolution to be obtained.

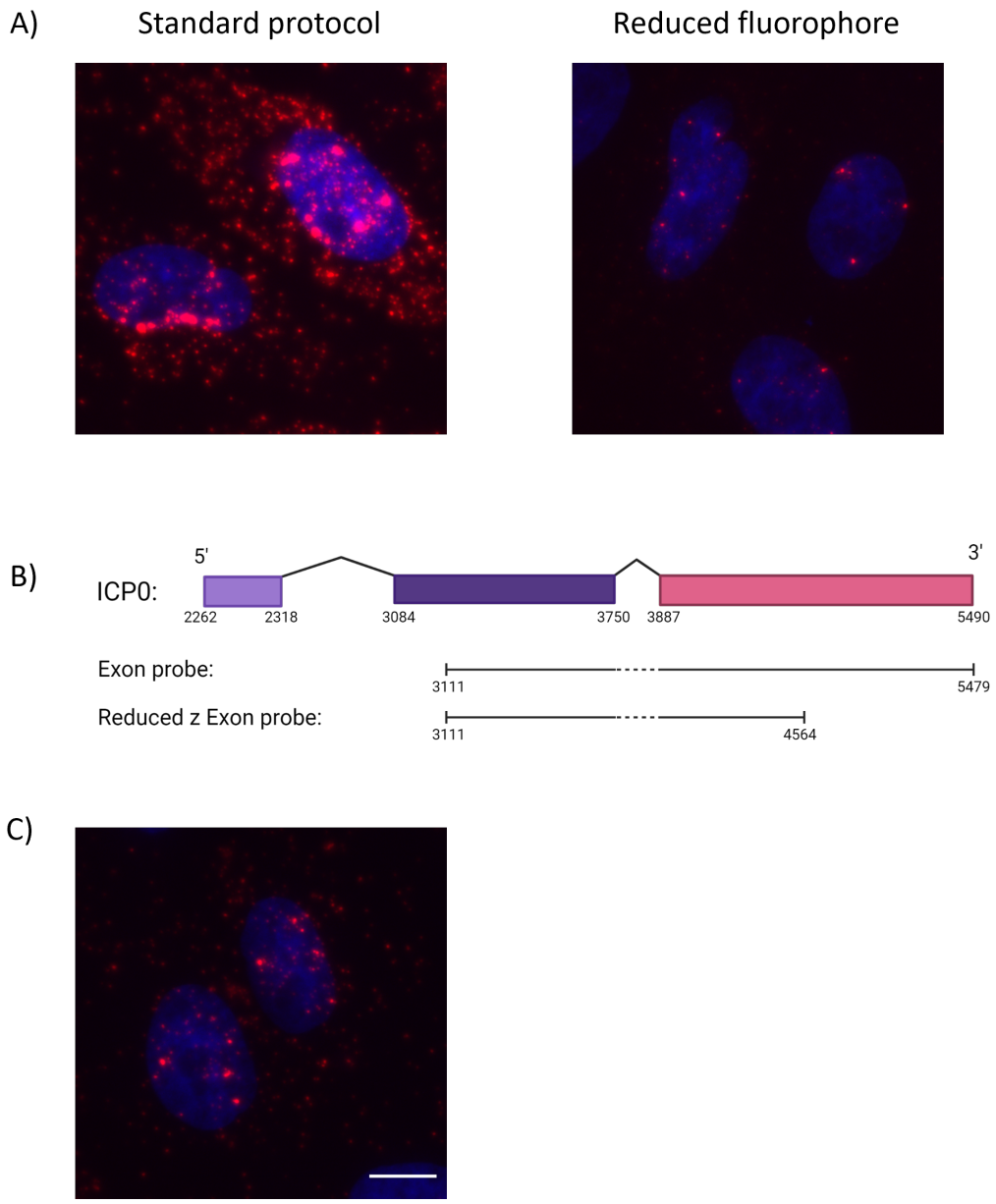


Figure 3.9: Optimisation of resolution of transcription bursts

Vero cells, HSV-1 MOI 10, 1.5 hpi. A) RNAscope for ICP0 (red). Standard protocol with fluorophore concentration at 1:1500. Modified protocol with a reduced fluorophore concentration of 1:5000. B) Design of new ICP0 exon probe. C) RNAscope for ICP0 reduced z exon probe (red) with fluorophore at 1:1500. Scale bar 10 microns.

3.6 Discussion and future perspectives

RNA FISH can be used to examine IE transcription at early timepoints in HSV-1 lytic infections. With the highly detailed subcellular resolution, novel features of viral transcription are revealed. After the genome enters the cell there is rapid transcription of IE genes. A dense region of transcript appears around nuclear genomes, called transcription bursts. Transcripts are exported from these bursts out to the cytoplasm where there is a gradual accumulation of transcript molecules. The rate of transcription from the incoming genomes slows after several hours when transcription bursts are no longer visible. After the onset of DNA replication, transcription resumes at a high rate from inside the viral replication compartments, and this late stage transcription and replication will be addressed in chapter 6.

Transcriptional bursting has been defined in cellular genes which fluctuate between existing in an 'on' or 'off' state. The switch between the two states results in short bursts of rapid RNA synthesis, followed by a period with no transcription [179]. This widely held hypothesis is thought to help explain gene regulation and variation across cells. Single molecule RNA FISH has identified transcriptional bursting as a factor for allele specific expression of individual genes [180]. Once a burst is initiated, the promoter is left in an open state allowing multiple polymerases to engage in gene expression, with as many as 200 polymerases on a single gene being observed [181]. When the promoter switches to an inactive state the burst ends, therefore the time period of accessibility of the promoter has a key role in dictating burst length [182]. There has been limited work studying transcription bursting on virus genomes. In HIV-1, transcription from LAT in integrated HIV DNA showed bursts of RNA expression consisting of up to 10 RNA molecules, essential for reactivation from latency [183, 184].

Here I present evidence for transcriptional bursting on HSV-1 genomes. The appearance of the bursts are similar to published analysis of eukaryotic transcription by smRNA FISH [185]. The

RNAscope images represent a single moment in time and live cell imaging of HSV-1 transcriptional bursting would be a worthwhile next step to pursue. Imaging RNA in live cells relies on proteins such as MS2 or small molecules binding RNA elements, such as the Mango or Spinach aptamers, though many rely on the genetic modification of target RNAs [186]. As viruses do not often cope well with insertions into their genomes, these methods are hard to use successfully. The best results have been achieved for HIV-1 using MS2 [187, 188]. Detection of endogenous RNA in live cell imaging can be achieved with molecular beacons, which are oligonucleotide probes with both a fluorescence and quencher molecule. Upon binding the sequence specific endogenous RNA, the fluorescent molecule and quencher are separated, allowing the molecule to fluoresce [189]. Imaging of endogenous viral RNA has been primarily used for detecting RNA virus genomes such as influenza. To optimise a protocol for live cell imaging of HSV-1 transcription either genetic manipulation of the HSV-1 genome or an endogenous probe could be attempted. However, live cell imaging would inhibit the use of click chemistry to detect HSV-1^{EdC}.

I have successfully been able to combine click chemistry with RNAscope. This allows the detection of single viral genomes and analysis of the transcriptional activity. The RNAscope protocol should be performed first, followed by the click chemistry. This may be due to RNase contamination within the click chemistry reagents, or a process within the click chemistry reaction may prevent the hybridisation of the RNAscope probes to viral RNA. Another observation of combining the two protocols was that a greater number of cytoplasmic genomes were detected than expected. Presumably some stage of the RNAscope protocol, such as the protease digestion, is damaging the viral capsids and making the genomes more accessible to click chemistry reagents. With this being said, it is possible I am overestimating the numbers of viral genomes that I have counted as not transcriptionally active, as quantified in figure 3.8 C. Some of these inactive genomes may not have entered the nucleus. However I am estimating that this proportion will be a low fraction of the whole.

The spatial arrangement I observe between genomes and the transcription bursts opens many

interesting questions. Several of the main spatial associations shown in figure 3.8 are summarised in figure 3.10. Diagrams A, B and C represent the most common arrangements; the genome is either directly underneath the burst (A), the burst is pluming from one side (B), or there is a small gap between the genome and RNA. With A and B, we are very confident that the transcripts have been recently synthesised from the associated genome. However, with C, I would still hypothesise a relationship and would link the burst to the adjacent genome. The spatial separation may be due to the genome no longer actively transcribing RNA, ie the burst has finished, and there has been some movement of the transcript domain away from the genome. Alternatively, the genome may have initiated the process of decompaction after nuclear entry and has prioritised the regions of DNA containing the IE genes. It is conceivable that sections of the 150 kbp genome have looped out from the main body of the genome and transcription is occurring off this region (Figure 3.10, D and E). Evidence that would challenge this hypothesis lies within the ICP0 intron probe RNAscope images. The intron foci are a very good surrogate marker for the site of transcription. I very rarely observe a small spatial separation of the intron foci from the genomes that I would expect to observe if transcription is occurring on a looped region of the genome. We would not be able to accurately investigate this hypothesis using these visualisation methods with widefield microscopy, and future work should most certainly continue to high resolution microscopy.

An additional reason to turn to super resolution imaging is to quantify the size of the viral transcription bursts. Due to the saturation of the signal within the transcription burst it is hard to determine how many single transcripts are contained within a burst. My attempts to improve resolution by reduced probe binding or reduced dye content were not successful. The limiting factor remains the image resolution of widefield and confocal microscopy.

During the acquisition of the images for IE's ICP0 and ICP4 I observed a high degree of heterogeneity. This occurred within a cell monolayer when examining the rate of infection between adjacent cells, and also between infection experiments when taking the population as a whole. Despite

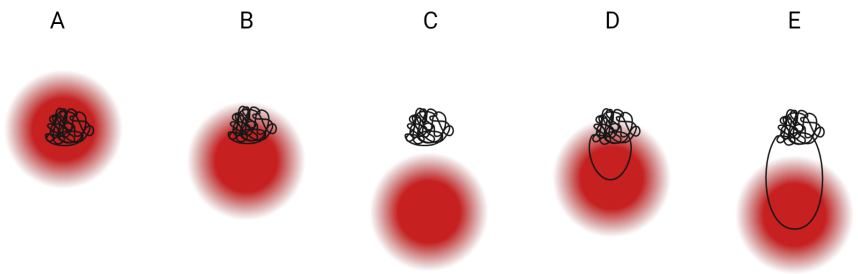


Figure 3.10: Spatial relationship between genomes and transcription bursts

Black HSV-1 genomes with a red transcription burst emerging in various patterns.

this high heterogeneity, there was a trend when comparing the relative spatial localisation of ICP0 and ICP4 transcript. Unexpectedly, ICP0 was often transcribed more rapidly and accumulated to higher levels in the cytoplasm. However, the variability between experiments made this difficult to quantify. Multiplex analysis of ICP0 and ICP4 in an n12 mutant virus infection revealed the differences most starkly, when transcription was occurring at high rates (Figure 3.4). ICP0 is a spliced gene, and I have shown that ICP0 splicing is extremely rapid as very few intron containing transcripts exist away from the genome (Fig 3.8 D). The difference in post translational mechanisms may account for the differences in export from the nucleus. However, by 4 hpi and the onset of DNA replication, there are no observable differences in the localisation of the two IE genes.

The multiplex analysis revealed the potential uncoupling of the two IE genes, which may be another explanation for the differential transport. ICP0 and ICP4 are thought to be under tight temporal transcriptional control, but the ability of genomes to be active for different IE genes suggests a degree of autonomy between the two transcripts. This provides new evidence that the control of IE gene transcription is more complex than previously thought.

To conclude this chapter, I have validated and shown the ability of both RNA FISH and

click chemistry to examine the HSV-1 transcription in lytic infections. The following chapters of this thesis will further develop these tools to investigate HSV-1 transcriptional progression and the host cell defense mechanisms.

Chapter 4

Investigation of IE transcription in the absence of new translation and the influence of the autoregulatory function of ICP4 and stimulatory function of VP16

To extend the analysis we wanted to examine viral transcription in the absence of any new protein translation. HSV-1 encodes powerful regulatory proteins to control gene expression, including promoting both initial transcription and recruitment of cellular proteins as well as regulation of the temporal cascade of expression through the gene classes. When these proteins are absent it is possible to examine the transcriptional potential of an unrestricted virus and how a virus is able to manipulate the host transcriptional environment in greater detail. In this chapter, I will investigate the transcription activity of genomes in the absence of function of two transcriptional regulators; ICP4 and VP16.

4.1 Absence of ICP4 autoregulation accounts for increase in transcription during translation inhibition

In the absence of de novo protein translation, ICP4 protein would not be able to negatively autoregulate expression, yet VP16 would still be present from the incoming capsid. The translation inhibitor CHX was added to cells at 50 μg/mL for 45 minutes before infection and maintained throughout infection. To confirm the block of protein synthesis, infected cells were stained for ICP4 protein (Fig 4.1 A). In untreated cells, ICP4 protein becomes visible in small foci at 1 hpi, likely to represent the location of viral genomes. By 3 hpi there is an increase in foci number and a diffuse staining throughout the rest of the nucleus. At 5 hpi, after the onset of DNA replication, ICP4 is recruited to replication compartments as they form and develop. In the presence of CHX, there is no detectable ICP4 protein expression at any timepoint.

In the absence of CHX, transcription of IE appears as transcription bursts at 1 hpi and an increase in cytoplasmic transcript and decrease in transcription bursts by 3 hpi. When CHX is added, the transcriptional environment at 1 hpi is similar to the untreated cells (Fig 4.1 B). At this early timepoint viral RNA synthesis is not affected by newly synthesised viral proteins. However, at 3 hpi there is a stark difference between the CHX treated and untreated cells. In the absence of any newly synthesised proteins (+ CHX), there is a significant increase in the amount of ICP4 transcript. When the 3 hpi + CHX field is imaged with a lower exposure, multiple transcription bursts are still visible within the nucleus. Therefore, a newly synthesised protein or proteins, either cellular, viral or both is repressing transcriptional output in a normal infection. In the absence of this repressor protein, the huge rate of transcriptional activity that genomes can achieve is revealed. The maintenance of transcription bursts demonstrates the continued activity of genomes.

To confirm my visual observations by RNAscope at the population level, RT-qPCR assays to measure IE proteins were established. RNA was extracted and converted to cDNA. qPCR primers

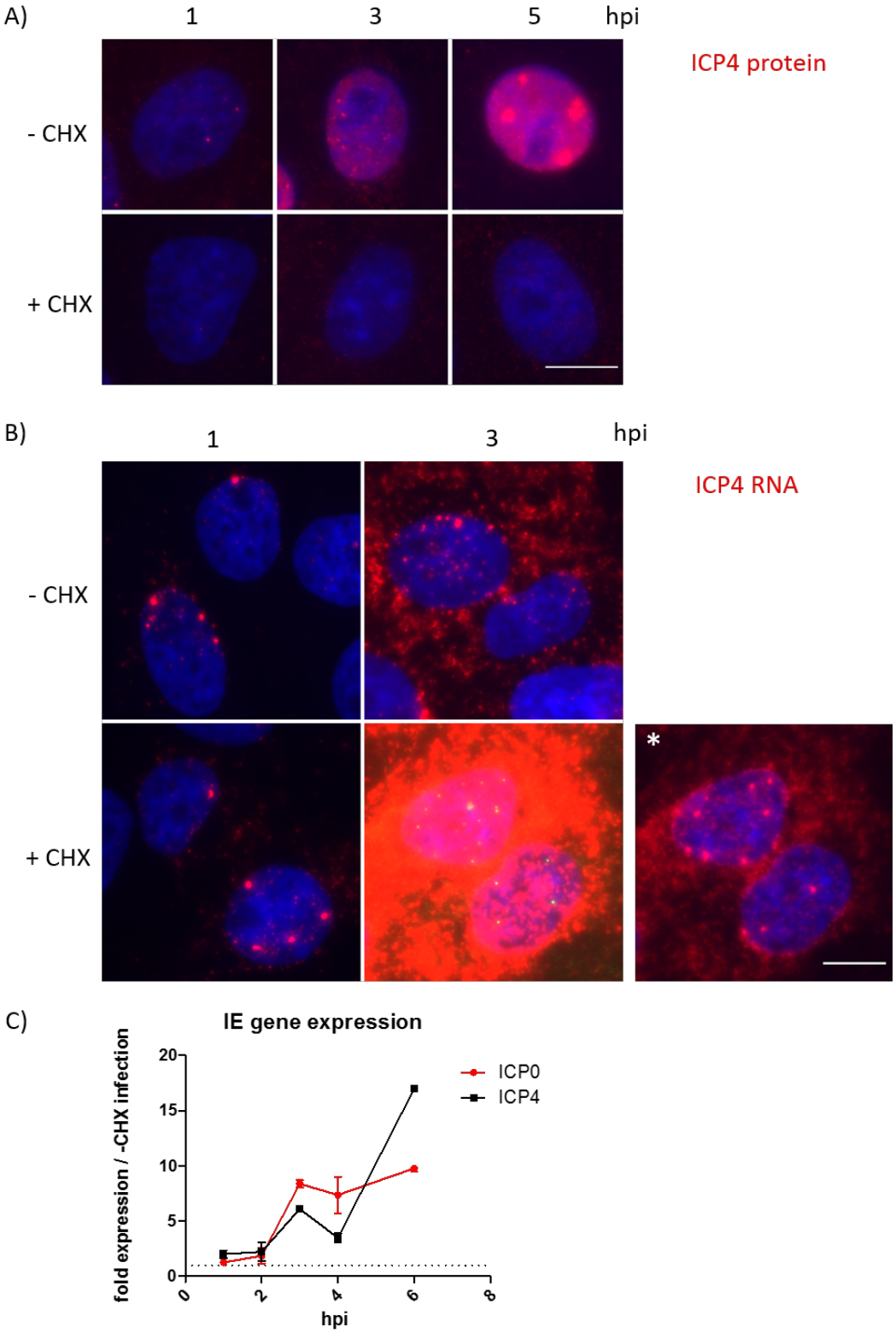


Figure 4.1: Effect of CHX on HSV-1 transcription indicates presence of repressor molecules.

Vero cells infected with HSV-1 MOI 10. Cells pretreated 45 min with 50 μg/mL CHX and present throughout infection. Cells fixed at indicated timepoints (1, 3 and 5 hpi). Scale bar 10 microns. A) ICP4 protein (red) is not synthesised + CHX. B) RNAscope for ICP4 RNA (red). A lower exposure of 3 hpi + CHX is shown with the *. C) qRT-PCR for ICP0 and ICP4 RNA extracted from cells. RNA levels in the presence of CHX presented as fold expression over untreated infection.

were chosen from published literature and efficiency was checked. By plotting expression levels in the presence of CHX as a fold induction over untreated cells, the increase in transcription can be quantified (Fig 4.1 C). ICP0 reaches a nearly 10 fold increase in the presence of CHX, and ICP4 reaches a 15 fold increase. Obvious candidates for the repressor are viral proteins, such as ICP4. As a negative autoregulator, the absence of ICP4 will contribute to the increase of ICP4 RNA. However, there may be additional cellular proteins whose expression is induced by infection which repress viral gene expression.

To investigate the importance of ICP4 repression, the n12 mutant virus with a truncated ICP4 was used. This virus was introduced in section 3.3 and has a non functional ICP4 protein. RNAscope was used to examine ICP0 transcript levels at 3 hpi in WT HSV-1 or n12 infections, in the presence or absence of CHX. Quantification of RNA levels per cell was then performed in ImageJ (Fig 4.2 A). In the absence of CHX, there is an increase in transcript in n12 compared to WT HSV-1 infection. ICP0 RNA in WT infection increased with CHX as expected. However, there was no increase in ICP0 RNA when cells were infected with n12 in the presence of CHX. In the absence of a functional ICP4, preventing protein translation does not further increase viral RNA levels, suggesting the role of a cellular repressor is minimal.

n12 was made from the KOS HSV-1 strain by Neal De Luca. WT HSV-1 strain 17 is the WT strain used in this work, including figure 4.2 A. Due to multiple technical difficulties producing a stable high titre stock of HSV-1 [KOS] it was not possible to produce reproducible RNAscope data for this virus. Consequently, in figure 4.2 A where WT HSV-1 strain 17 is used it is not the most appropriate control. During the optimisation of experiments with the HSV-1 [KOS] strain, RT-qPCR was used to verify the RNAscope data (Fig 4.2 B). For both ICP0 and ICP4, there was a significant increase in HSV-1 [KOS] when CHX was added. However, for n12 there was no significant increase in ICP0 and ICP4 RNA levels. Therefore, ICP4 is the major protein responsible for the increase in transcription seen in a WT infection where protein translation is inhibited. There may be additional

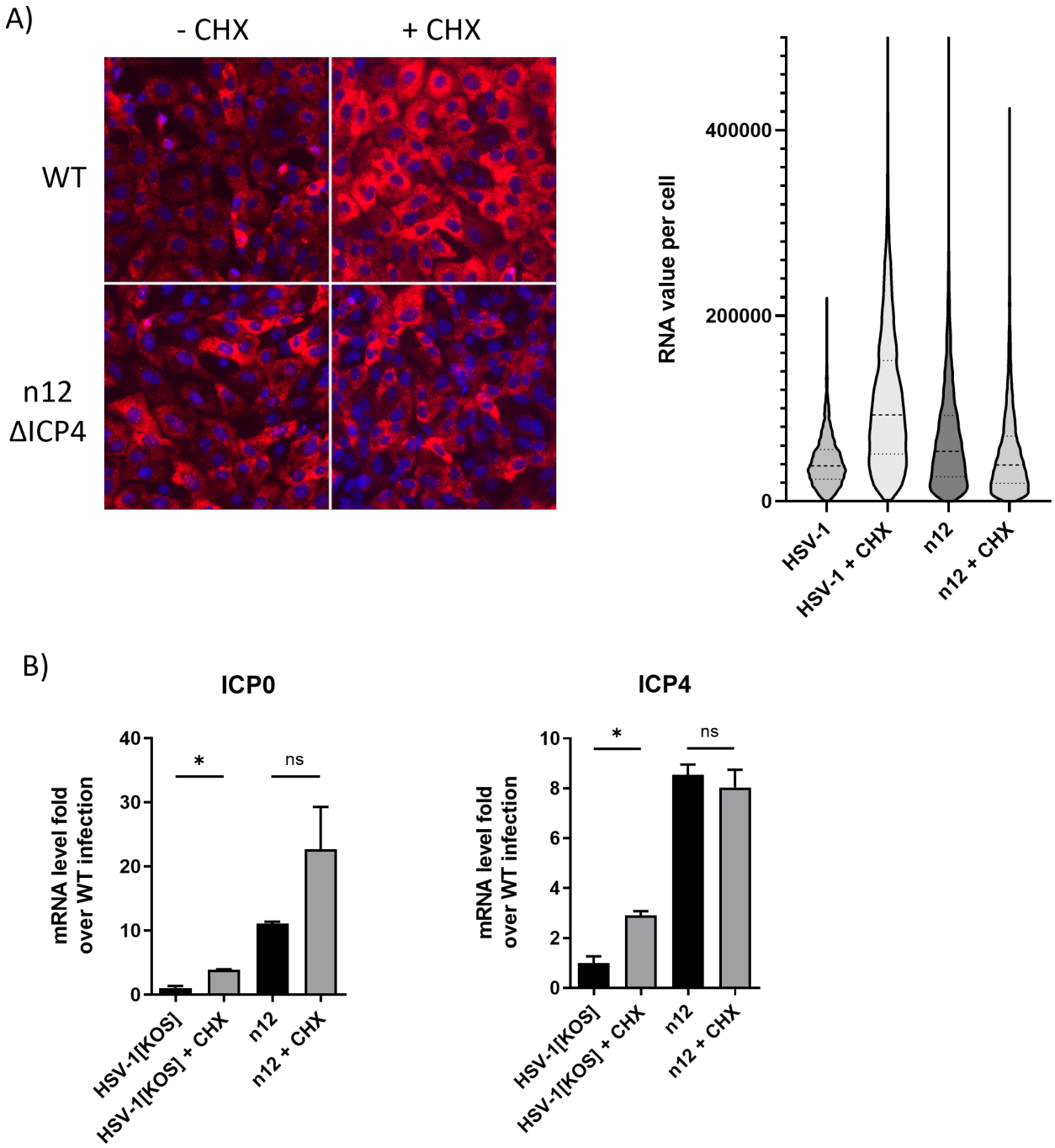


Figure 4.2: ΔICP4 HSV1- infection shows role of ICP4 in transcriptional suppression

A) ICP0 RNA (red) in Vero cells at 3 hpi infected by HSV-1 or n12, MOI 10, in the presence or absence of CHX. Quantification is presented as RNA value per cell. B) qRT-PCR of ICP0 and ICP4 RNA levels at 3 hpi in Vero cells, HSV-1[KOS] or n12, MOI 10. Levels presented as fold expression over HSV-1 [KOS] infection.

rapidly synthesised cellular proteins involved, but compared to the transcriptional repression of ICP4 their effect is modest.

4.2 VP16 induction of viral transcription

VP16 is a tegument protein associated with the capsid and is the driving force of initial IE transcription (see chapter 1.2.2). n12 virions arrive at the nucleus with VP16 to promote transcription, but subsequently lack the transcriptional promotion by ICP4. To further examine the transcriptional potential of VP16 on expression from infecting viral genomes, n12 was allowed to infect Vero cells for 3 h (Fig 4.3 A i). At this point, ActD was added for 1 h to stop all transcription (Fig 4.3 A ii). At 4 h (3 hpi + 1 h ActD) there is still cytoplasmic transcript but nuclear bursts have almost completely disappeared. The 1 h drug treatment stops transcription bursts and allows nuclear transcript to be exported. After the 1 h ActD treatment, the ActD is washed out and the cells allowed to recover for varying times. A 1 h recovery is not long enough for transcription to re-start, but at 3 h after the ActD is removed transcription bursts are beginning to reappear (Fig 4.3 A iii and iv).

Quantification was performed to determine the percentage of total ICP0 transcript present in the nucleus at the treatment timepoints represented in part A. After the addition of ActD for 1h nuclear transcript drops from 15% to 5%. After a 3h recovery from ActD nuclear transcript has increased to nearly 10% (Fig 4.3 B). Quantification of transcription bursts demonstrates a near complete loss of bursts with 1h ActD (4h), and the 3h recovery shows the genomes starting to burst again (7h, Fig 4.3 C). Even if the length of ActD treatment is increased to 6h, the genomes can still reactivate with a 3h recovery period (Fig 4.3 D). Due to the nature of the end point analysis of RNAscope it cannot be determined if the genomes that reactivate are the genomes that were transcriptionally active initially, or what percentage of genomes that were active during the first phase are able to reactivate.

In the above experiments, the virus is allowed to begin a productive infection. During this time period viral proteins such as ICP0 are synthesised and begin altering the cellular environment. During the ActD treatment period, the genomes are vulnerable to any remaining cellular restriction factors that are deposited on the genome. Despite this, with a suitable recovery period the genomes

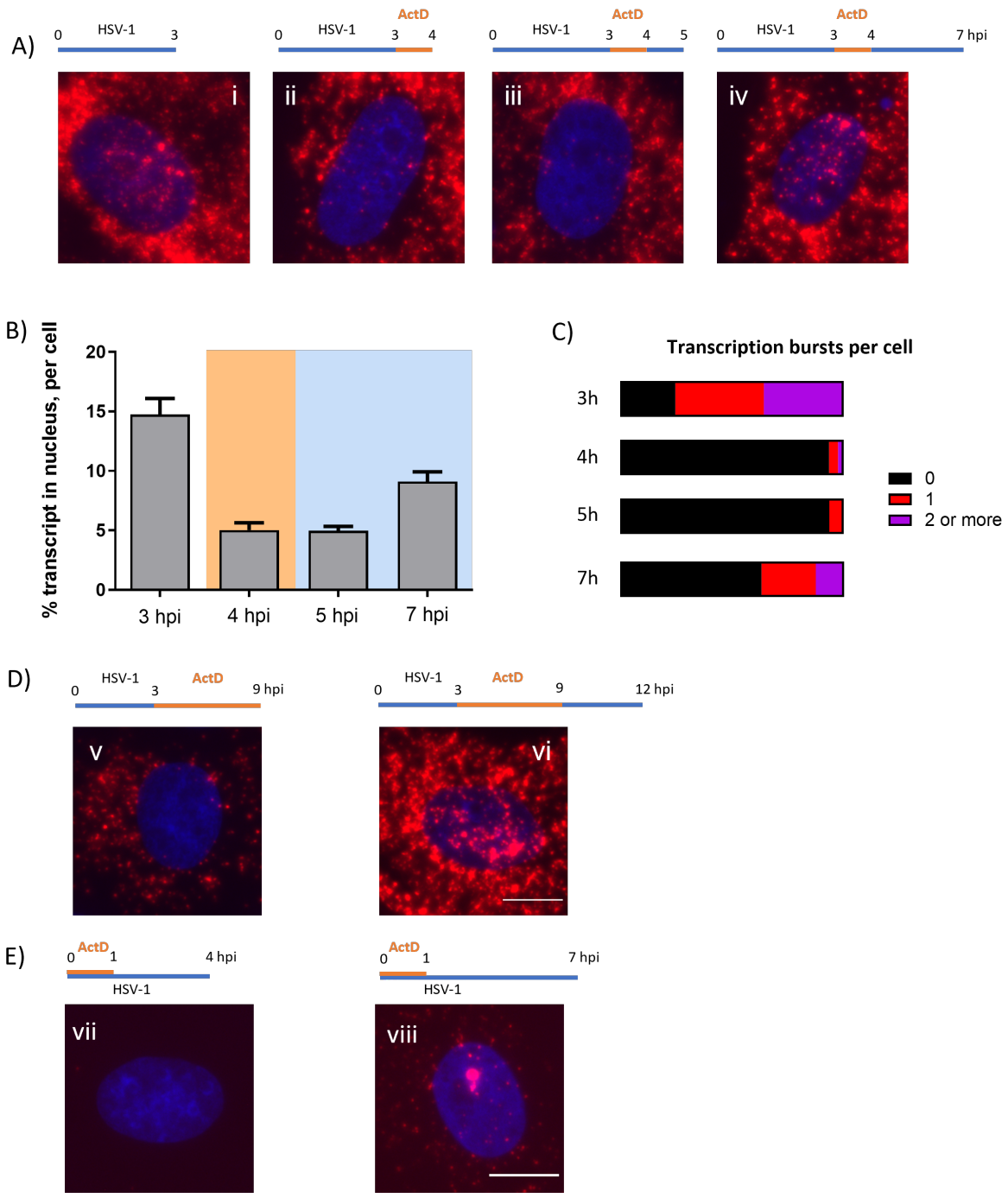


Figure 4.3: Genomes are able to reactivate after incubation with ActD

A) Cell i: ICP0 RNA at 3 hpi. Cell ii: ICP0 RNA at 4 hpi, with ActD added at 3 hpi for 1h. Cell iii: ICP0 RNA at 5 hpi, with ActD added at 3 hpi for 1h and washed out at 4 hpi to give a 1h recovery phase. Cell iv: ICP0 RNA at 7 hpi, with ActD added at 3 hpi for 1h and washed out at 4 hpi to give a 3h recovery phase. B) Quantification of ICP0 transcript per nucleus in the 4 conditions in part (A). C) Quantification of number of ICP0 transcription bursts per cell in the 4 conditions in part (A). Cells with different numbers of bursts are represented by the difference colours, shown in the legend. D) Cell v: ICP0 RNA at 9 hpi, with ActD added at 3 hpi for 6h. Cell vi: ICP0 RNA at 12 hpi, with ActD added at 3 hpi for 6h and washed out at 9 hpi to give a 3h recovery phase. E) Infections are performed in the presence of ActD. At 1 hpi, ActD is washed out to give a 3h recovery (cell vii, 4 hpi) or a 5h recovery (cell viii, 6 hpi).

regain transcriptional activity. However, the cellular landscape will have been altered in the first 3 hours by viral proteins. To investigate the activity of genomes after cellular factors are allowed to recognise viral genomes with no interference from newly synthesised viral proteins, cells were infected in the presence of ActD (Fig 4.3 E). In this scenario, a 3 h recovery was not sufficient for transcription to begin, but after a 5 h recovery transcription bursts were visible. In this experiment HSV-1 genomes are present in the nucleus but transcriptionally inactive for 1 h. Regardless of how many cellular proteins are deposited on the genomes or post translation markers are created, they are not sufficient for the virus to be completely restricted from transcribing. The virion associated proteins such as VP16 are sufficient to overcome the negative cellular factors. This work demonstrates the immense potency and strength HSV-1 has to promote infection.

4.3 Investigation of the role of P-TEFb on viral transcription

In the absence of VP16, viruses are severely compromised but are capable of eventually establishing infections. in1814 is a ΔVP16 HSV-1 virus, with an inactive VP16. It contains a 12 base pair insertion inside the protein coding region of VP16 which prevents the association with HCF-1 and Oct1 [190]. Infections with this mutant virus allow the study of other cellular processes that are involved in the initiation of viral transcription. It has been previously demonstrated that Hexamethylene bisacetamide (HMBA) increases infectivity of in1814 and is used to produce high titre stocks [191]. HMBA is an inducer of murine erythroleukemia (MEL) cell differentiation [192]. A 1998 paper examined other MEL cell differentiation agents, including SBHA and Nicotinamide and their effect on in1814 titre [193]. They found nicotinamide to increase the mutant virus titre, but no effect of SBHA.

On HaCaT cells, HMBA, SBHA and nicotinamide had no effect on the plaque number of a WT virus (Fig 4.4 A). However, HMBA increased the plaque number of in1814 by 100 fold and Nicotinamide had a 30 fold increase (Fig 4.4 B). SBHA had no effect on in1814 titre. in1814 has

been shown to have a high particle to PFU ratio, therefore these experiments demonstrate that in the absence of HMBA there are many viral particles present that do not go on to create a plaque.

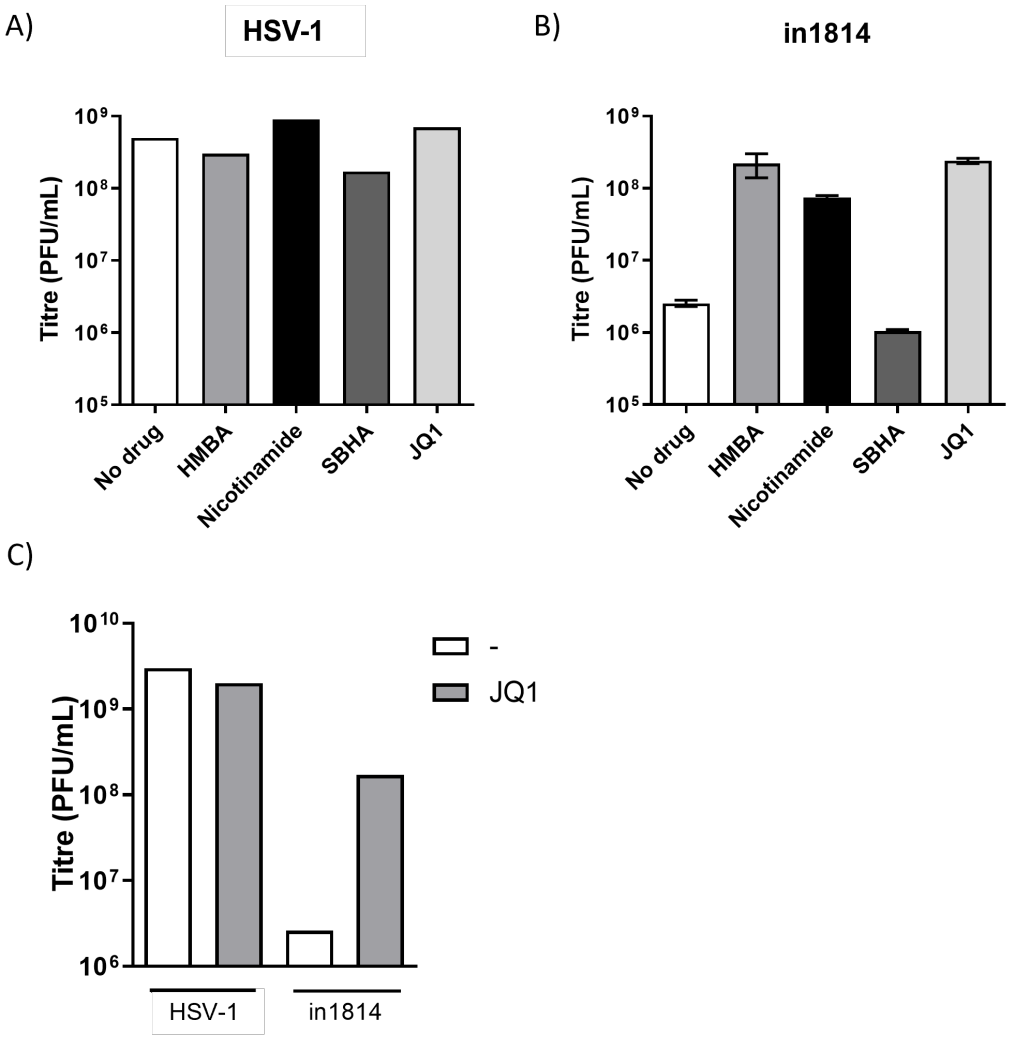


Figure 4.4: Effect of drugs on plaquing efficiency of ΔVP16 HSV-1.

Titre of (A) HSV-1 and (B) in1814 on HaCat cells in the presence of various drugs. All drugs added at 1 hpi. C) Titre of HSV-1 and in1814 on Vero cells in the presence or absence of JQ1.

HMBA induces Hexamethylene bisacetamide-inducible protein 1 (HEXIM1) which together with 7SK RNA inhibits P-TEFb [194, 195]. When P-TEFb is in a complex with Brd4 it is in an active form and can phosphorylate RNA pol II, allowing transcription to progress. The role of P-TEFb on transcription and it's regulation is described in section 1.3 and in figure 1.3. Thus, the HMBA treatment is seemingly causing opposite effects; the increase of viral infection and the inhibition of

P-TEFb, which is normally associated with an inhibition of transcription. Studies looking at the effect of HMBA on various viruses have produced conflicting results. HMBA has been shown to increase the reactivation of HIV-1 from latency [196]. One proposed mechanism for this increase is due to chromatin remodelling around the transcription start site, despite not altering acetylation or methylation of histones [197]. An alternative mechanism is through activation of cellular kinases. HMBA activated Akt via phosphatidylinositol-3-kinase (PI3K) which disrupted the inactive P-TEFb complex by phosphorylation of T270 and S278 in HEXIM1, increasing viral transcription [104]. In contrast, HMBA has also been show to limit viral replication.

As described in section 1.3.4, Brd4 recruits active P-TEFb to acetylated histones. BET domain inhibitors have been developed recently as novel cancer treatments, due to the various roles of BET proteins including Brd4 in cell cycle progression, transcription and DNA replication. JQ1 is a small molecule inhibitor of Brd4 and functions by mimicking acetyl lysines. By this mimicry JQ1 blocks the binding sites the Brd4 would normally utilise to bind to acetylated lysines on histones, displacing Brd4 from chromatin [198]. Brd4 occupancy on genes decreases after JQ1 treatment, and this results in decreased gene expression, for example the transcription of MYC [199].

Conversely, JQ1 has been shown to also play a role in transcriptional activation. JQ1 has been used to shown increased HSV-1 transcription and has been shown to cause reactivation of HSV-1 from latency by releasing it from active chromatin due to an increased level of P-TEFb on the virus genome [200]. A study in 2012 found JQ1 activated transcription of HEXIM1, and that Brd4 was released from it's chromatin bound state in addition to releasing P-TEFb from 7SK RNA [201]. In U2OS cells, 1 h of JQ1 treatment increased EU incorporation into nascent RNA by 35%, an indication of increased transcription. The majority of the upregulated transcripts in this study were determined to be ncRNA or non-polyadenylated transcripts, in comparison to polyadenylated transcripts such as MYC which are downregulated [202]. They propose in this study that JQ1 induces replication stress, which causes P-TEFb dissociation from 7SK RNA.

JQ1 has no effect on the titre of WT HSV-1 virus, however the titre of in1814 increased by 100 fold in the presence of JQ1 (Fig 4.4 A and B). A study investigating the effect of JQ1 on WT HSV-1 infection found an increase in viral titre in Vero cells [200]. The results in Figure 4.4 C directly contradict the results from this study by Ren et al., as we show WT HSV-1 does not increase in infection with the addition of JQ1.

Both HMBA and JQ1 increase the titre of HSV-1 with a defective VP16. Therefore, they must induce cellular changes to compensate for the lack of VP16 transcriptional induction. I therefore investigated the effects of these drugs on viral infection, with the long term goal of understanding how cellular transcriptional machinery can promote viral infection.

Evidence from the McFarlane paper suggests that HMBA presence in the first few hours is sufficient to achieve the increase in titre. To confirm, a plaque assay was performed. Vero cells were infected with in1814 at dilutions from 10^{-5} to 10^{-7} and HMBA was either included in the inoculum and washed out at various timepoints (HMBA exposure length) or added at various timepoints post infection (Time of HMBA addition). After 3 days the number of plaques formed was used to determine titre in these conditions (Fig 4.5). An HMBA exposure of 3h is sufficient to induce the 100 fold increase in plaque number. If HMBA is added up to 2 hpi, an increase in plaque number is seen. However, if the HMBA is not added until 3 hpi the increase is greatly reduced. Therefore, the action of HMBA occurs in the first few hours of infection.

If HMBA or JQ1 increase viral entry into to the nucleus an increased number of viral particle entry would cause an increased plaque number. To investigate the effect of HMBA and JQ1 on viral entry Vero cells were infected with HSV-1 in the presence or absence of HMBA, and the number of capsids per cell was counted at 1 hpi. There was no significant difference in capsid number for either HSV-1 or in1814 (Fig 4.6 A). HSV-1^{EdC} was used to quantify genome entry in the presence of HMBA. There was no significant difference in the number of genomes released into the nucleus in

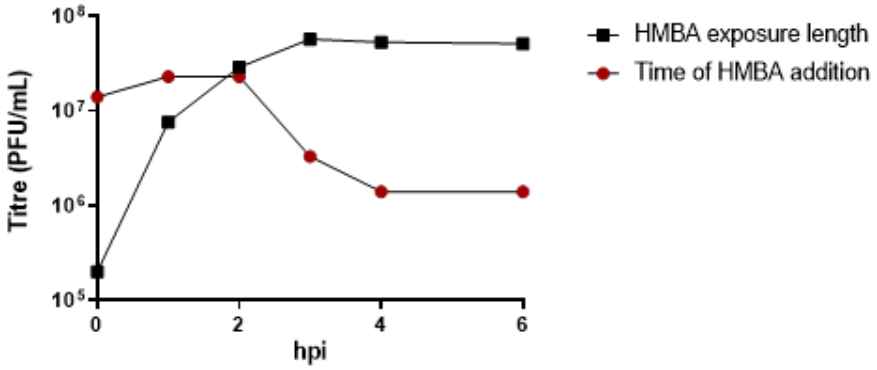


Figure 4.5: HMBA present at early timepoints allows successful infection.

Titre of in1814 when 5 mM HMBA is added at delayed timepoints (Time of HMBA addition) or the titre of in1814 when HMBA is present in the inoculum and removed at various timepoints (HMBA exposure length).

the presence of HMBA (Fig 4.6 B). Similarly, there was no changes to capsid number per cell in the presence of JQ1 in HaCaT cells at 1 hpi (Fig 4.6 C).

Having demonstrated that neither of these drugs inhibited capsid or genome entry into the cells, the results indicated that the in1814 virions in the absence of HMBA or JQ1 are entering cells but failing to form plaques. To begin to investigate where the defect of these virions lie, IE protein expression was examined. Cells infected with HSV-1 or in1814 at MOI 5 (calculated from the titre + HMBA, therefore MOI 0.05 in the absence of HMBA) in the presence or absence of HMBA were fixed at 6 hpi and then probed with an ICP4 antibody (Fig 4.7 A). ICP4 positive cells were counted and expressed as a percentage of total cells (Fig 4.7 B). HMBA failed to increase the number of ICP4 positive cells infected with WT, but significantly increased the percentage of ICP4 positive cells infected with in1814. The percentage of ICP4 positive cells likewise increased in the presence of JQ1 (Fig 4.7 C and D). ICP0 protein measured by western blot also shows a significant increase at 3 hpi due to HMBA or JQ1 (Figure 4.7 E). In summary, HMBA and JQ1 increase IE protein levels.

In the McFarlane paper from 1992 they examined RNA levels after in1814 infection with HMBA. A dot blot experiment with radioactive RNA probes revealed increased IE RNA levels in the

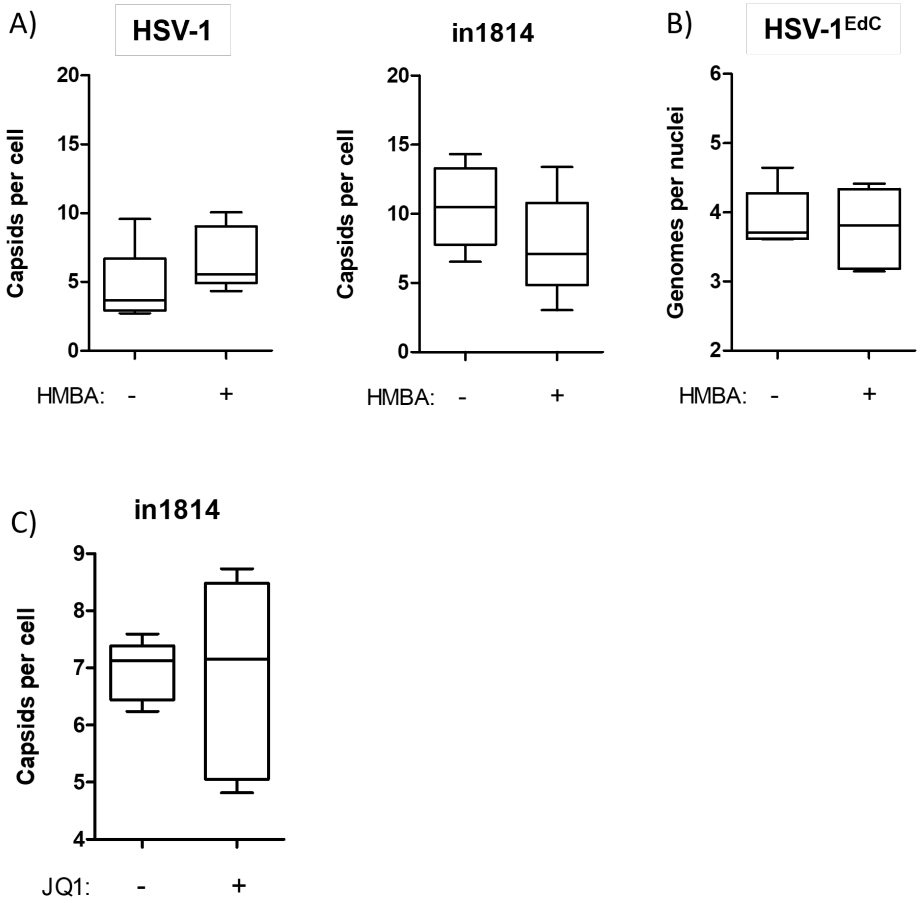


Figure 4.6: HMBA and JQ1 have no effect on viral entry.

A) Vero cells, 1 hpi, HSV-1 MOI 5, in1814 MOI 0.05. +/- 5 mM HMBA. VP5 stained capsids were counted. B) Vero cells, 1 hpi, HSV-1^{EdC} MOI 5. Click chemistry reaction and genomes per nuclei counted. C) HaCaT cells, 1 hpi, in1814 MOI 0.05. +/- 500 nM JQ1. Per field, number of capsids or genomes divided by number of cells or nuclei respectively. 5 separate fields.

presence of HMBA [191]. To examine this with our detailed single cell techniques, RNAscope was used to investigate the effect of HMBA on in1814 transcription. Cells were infected at MOI 0.05 (based on the titre without HMBA) and ICP0 transcript was probed using RNA FISH. At 3 hpi, there was a dramatic increase in ICP0 RNA abundance in the presence of HMBA (Fig 4.8 A). Without HMBA, there were very few cells with nuclear bursts and almost undetectable cytoplasmic ICP0 transcript. In the presence of the drug, almost every cell has multiple ICP0 nuclear bursts with much transcript accumulating in the cytoplasm. Quantification was performed in multiple ways. Firstly,

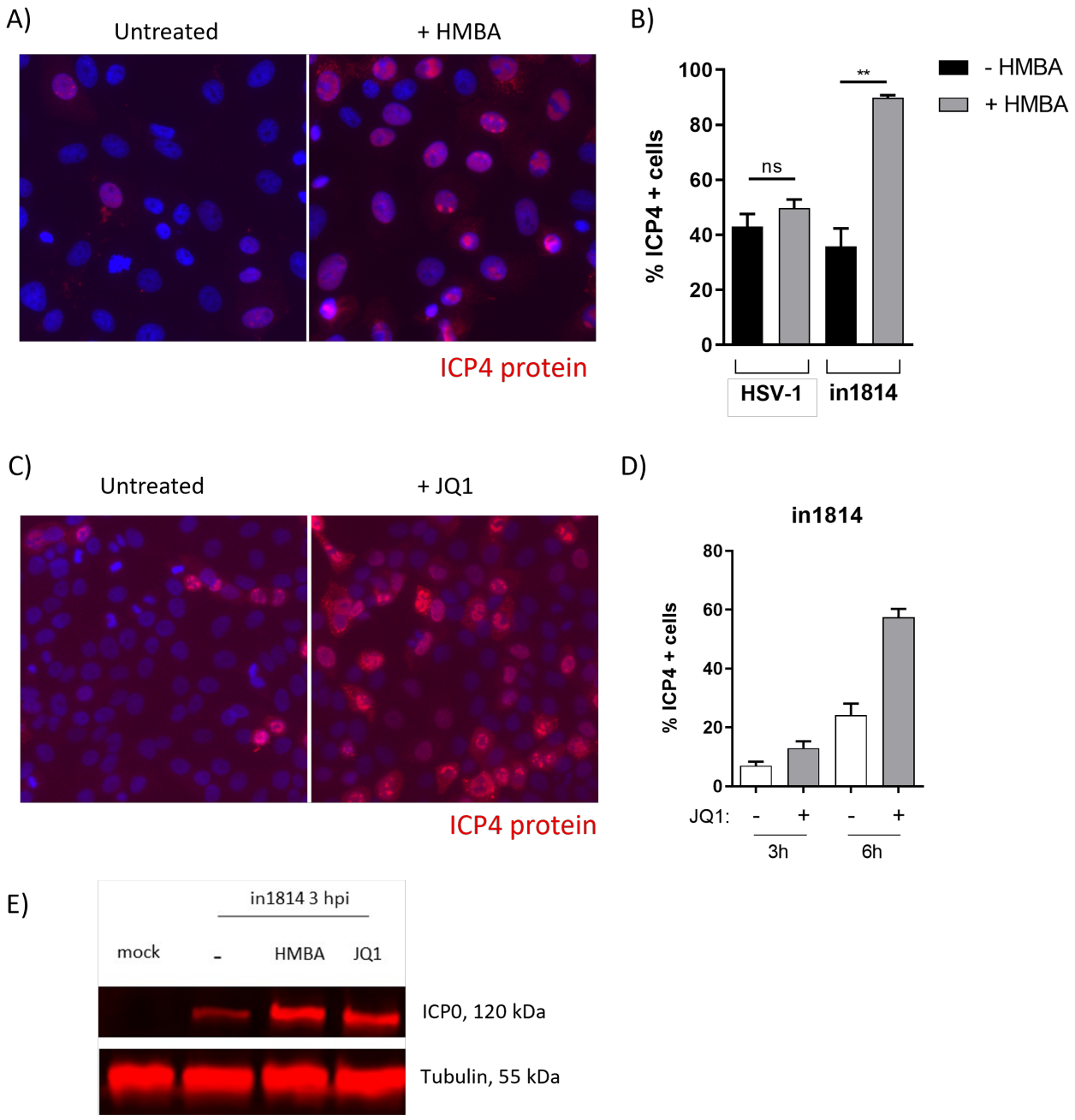


Figure 4.7: HMBA and JQ1 increase levels of ICP0 and ICP4 protein.

A) ICP4 protein in Vero cells at 6 hpi infected by in1814, +/- HMBA. MOI 0.05. B) Quantification of ICP4 positive cells in (A). C) ICP4 protein in Vero cells at 6 hpi infected by in1814, +/- JQ1, MOI 0.05. D) Quantification of ICP4 positive cells in (C). E) ICP0 protein abundance of the total HaCaT cell population. Uninfected cells (mock), 3 hpi in1814 MOI 0.05 untreated (-), 3 hpi + HMBA and 3 hpi + JQ1. Tubulin as loading control.

by analysing total RNA values per cell (Fig 4.8 B) and secondly, by calculating the percentage of nuclei that are positive for RNA signal (Fig 4.8 C). Both analysis show significant increases of RNA in the presence of HMBA. JQ1 produced a similar result, with RNA positive Vero nuclei increasing

significantly at 3 hpi and 6 hpi. Therefore both HMBA and JQ1 stimulate viral IE RNA expression of a VP16 deficient virus at early timepoints. These drugs are inducing cellular changes that promote viral transcription, but only in the absence of VP16. In a WT infection with functional VP16, the cellular changes that HMBA and JQ1 induce are redundant due to the large transcriptional induction that VP16 can achieve.

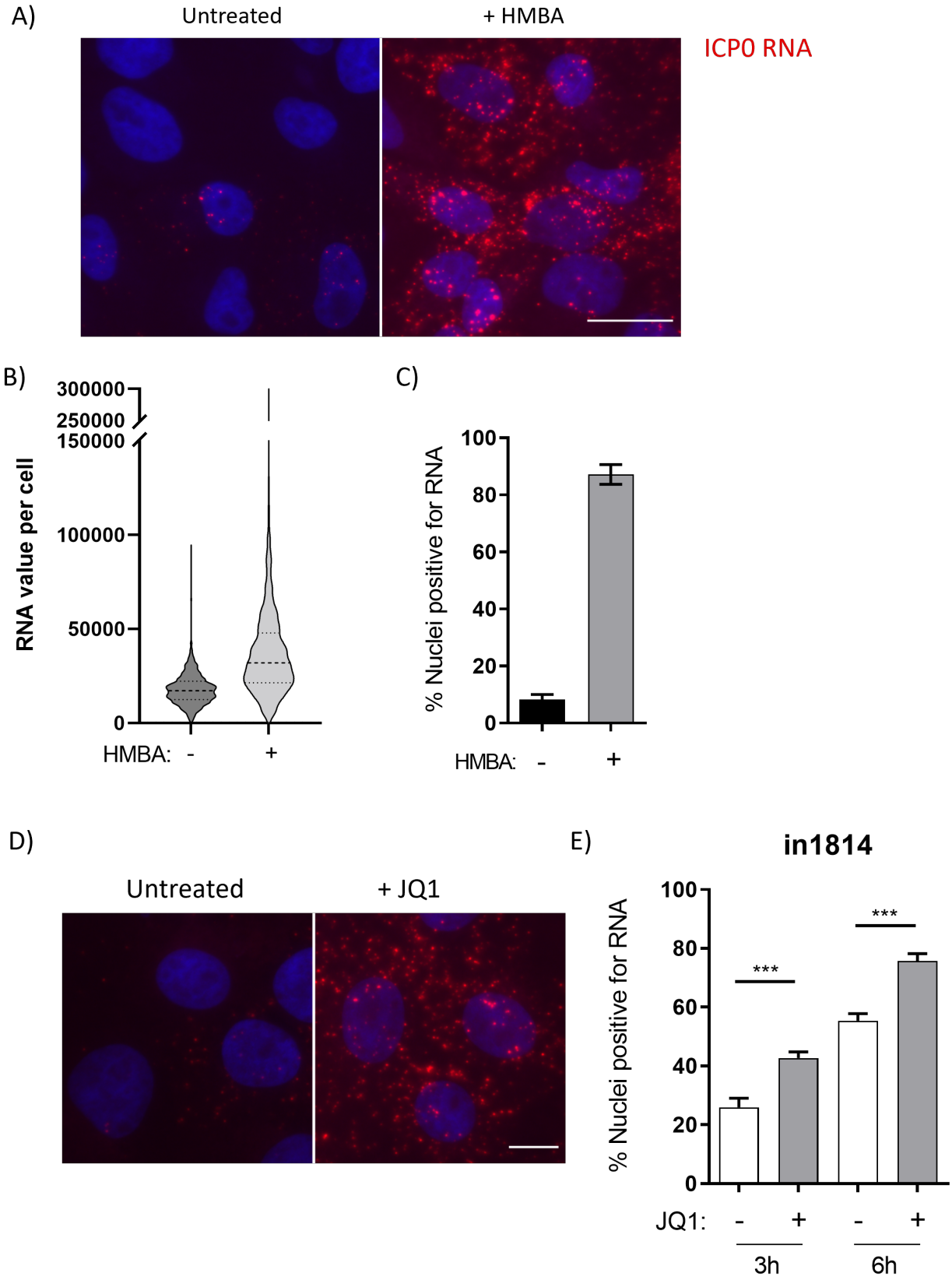


Figure 4.8: HMBA and JQ1 increase levels of IE RNA.

A) ICP0 RNA in Vero cells infected with in1814 MOI 0.05 at 3 hpi in the presence or absence of 5 mM HMBA. Scale bar 10 microns. B) Quantification of total RNA value per cell. C) Quantification of %nuclei positive for ICP0 RNA. D) ICP0 RNA in Vero cells infected with in1814 MOI 0.05 at 3 hpi in the presence or absence of JQ1. Scale bar 10 microns. E) Quantification of %nuclei positive for ICP0 RNA at 3 and 6 hpi.

4.4 A rapidly synthesised protein affects viral gene expression

In the data presented above HMBA and JQ1 have been producing similar effects. Both increased the infectivity of in1814 at the level of RNA transcription. However, the two drugs do have some differing effects. When cells were pre-treated with HMBA prior to infection with in1814, there was no increase in titre (Fig 4.9 A). In contrast, there was increased plaque formation in cells that were treated with JQ1 prior to infection with in1814, though not to the extent seen if JQ1 is provided after infection (Fig 4.9 B). Removal of the JQ1 treatment 1h before infection negated the increase in plaque number caused by the pre-treatment. Thus, HMBA and JQ1 have differing mechanisms of action: the changes induced by HMBA are short lived and quickly reversible, whereas JQ1 induces a change that is more stable yet still reversible and is able to positively promote viral infection of VP16 deficient viruses.

If the induction of HEXIM1 or another protein by HMBA or JQ1 is responsible for the transcriptional increase of the viral genes, then a CHX treatment would reverse the effects. A 4 h pre-treatment of CHX at 50 μg/mL induces a modest 2.8 fold increase in viral titre over the untreated cells (Fig 4.9 C). When the JQ1 pre-treatment of 4 h is combined with a 4 h CHX pre-treatment, the CHX does not decrease the JQ1 induced plaque increase. This suggests that the cellular modifications caused by JQ1 do not involve synthesis of a new cellular protein. This is consistent with the mechanism of action of JQ1 being a small molecule inhibitor binding to Brd4. Yet it is inconsistent with the role of JQ1 as an inducer of HEXIM1, one of the mechanisms it has been reported to act by.

To examine the effect of CHX in combination with HMBA, cells were infected with in1814 and ICP0 transcript was examined in untreated cells at 3 hpi, cells treated with 3 h HMBA or cells treated with 3 h of HMBA and CHX (Fig 4.10). The 3 h HMBA treatment produced the expected increase in ICP0 RNA levels. However, the presence of CHX drastically reduced the HMBA induction. As CHX prevents the synthesis of any new proteins, the results therefore strongly suggest that

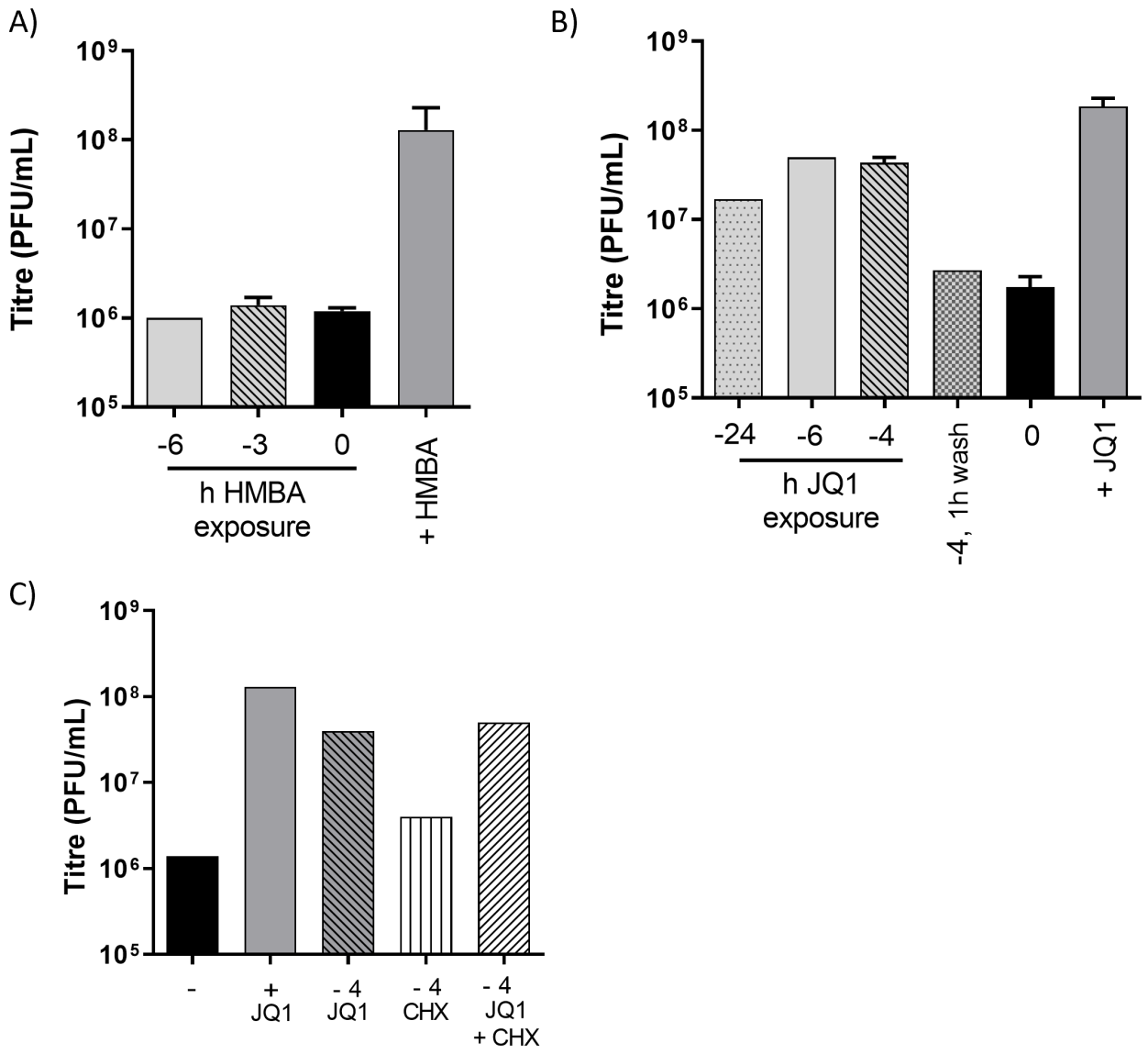


Figure 4.9: Pretreatment of HaCaT cells with HMBA or JQ1 has differing effects.

A) HaCaT cells were pretreated with 5 mM HMBA for 6 or 3 h before infection and then washed. Titre of in1814 in the pretreated cells is compared to the titre of untreated cells (0 h HMBA exposure) and 72 h HMBA post infection (+HMBA). B) HaCaT cells were pretreated with 500 nM JQ1 for 24, 8 or 4 h before infection. These cells were infected immediately after JQ1 removal, and a further condition was included of a 1h recover (-4 h JQ1, 1h wash). The titre of in1814 in the pretreated cells is compared to the titre of untreated cells (0) and 72 h JQ1 post infection (+ JQ1). C) Titre of in1814 in untreated cells (-), 72 h JQ1 (+ JQ1), a 4 h JQ1 pretreatment (-4 JQ1), a 4 h CHX pretreatment (-4 CHX) and a 4 h pretreatment of JQ1 and CHX (-4 JQ1 + CHX).

a newly synthesised cellular protein is induced by HMBA and promotes the increase in transcription early during infection with a VP16 defective virus. In a WT infection, the action of this induced protein is unnecessary due to the activity of VP16. In a VP16 deficient virus infection, this cellular

protein affects transcriptional machinery in a profound way to benefit viral transcription.

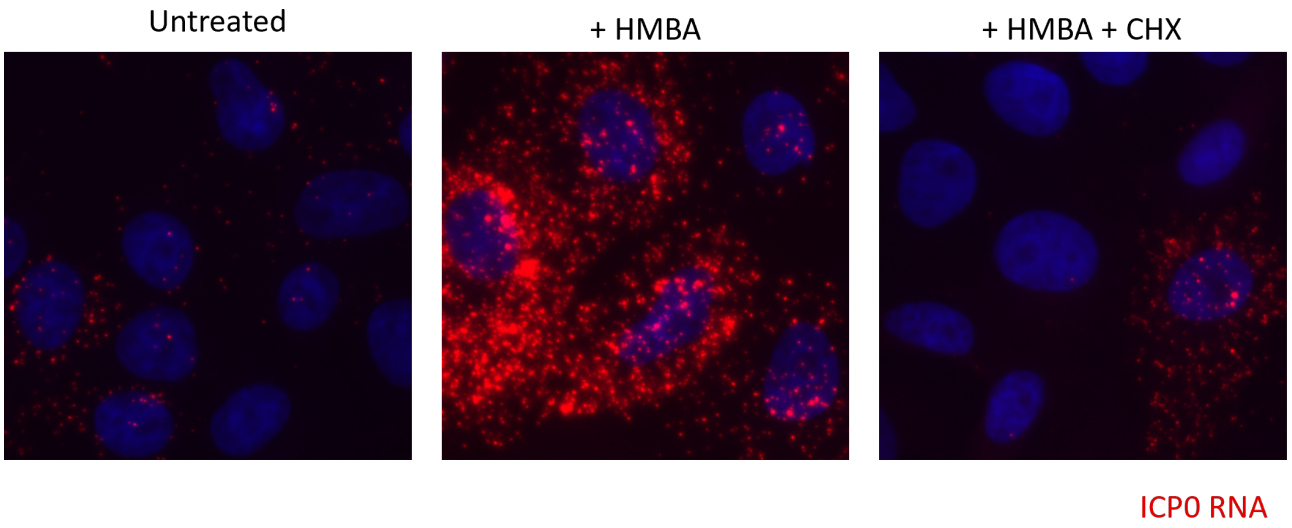


Figure 4.10: HMBA induces rapidly turned over protein which increases viral gene expression.

ICP0 RNA (red) levels at 3 hpi in Vero cells infected with in1814 MOI 0.05. Cells were untreated, treated with 5 mM HMBA or treated with both HMBA and 50 μg/mL CHX.

HEXIM1, one of the key targets induced by HMBA, could be a strong candidate for a newly translated factor that might induce HSV-1 transcription when VP16 was defective. HEXIM1 would therefore need to be transcribed and translated very rapidly, however there is conflicting evidence about the rate of HEXIM1 protein induction by HMBA. For example, in MEL cells HEXIM1 induction by western blot is not observed until 8 hours post treatment [203, 204]. However, in Jurkat cells an increase in HEXIM1 protein abundance is seen at 2 hours [104]. To investigate if additional cellular proteins are rapidly synthesised in response to HMBA, and possibly contributing to the HSV-1 transcriptional response, a proteomics based approach was chosen. The experimental plan is outlined in figure 4.11 A. In triplicate, cells were infected with in1814, or left uninfected. At 1 hpi, when the inoculum was removed, one sample was left untreated whilst the other was incubated with HMBA. At 3 hpi, all cells were harvested and the protein extracted using phenol chloroform precipitation. The total cell protein was then subjected to digestion and dried in a speedvac. The samples were then

analysed by mass spectrometry after labelling by TMT reporter tags.

During optimisation, extracted proteins were run on an SDS PAGE gel and total protein was stained with Coomassie. Lane 1 in figure 4.11 B shows phenol chloroform extracted protein. Lane 2 was loaded with the equivalent amount of protein after the trypsin digest, and the lack of visible bands represent a successful digestion.

After the TMT analysis, 44 proteins were identified as significantly upregulated in the uninfected cells after 2 hours with HMBA, indicated by the pink dots (Fig 4.11 C). GO analysis failed to identify significantly affected biological processes. Importantly, HEXIM1 was not significantly upregulated. In the infected vs infected + HMBA, no proteins were identified as being significantly different. This was not expected, as the viral IE proteins should have been significantly increased. Overall, the results from this proteomics analysis were inconclusive. It is possible there was a small increase in HEXIM1 protein level which was sufficient to induce the functional affect but was an undetectable change in this experiment. The three triplicate experiments were performed on separate days. Each set had newly plated cells, and a fresh inoculum of virus prepared. Although the statistical tests were performed in both paired and non-paired methodologies, if the triplicates were performed on the same day with cells of the same passage perhaps this would have reduced the sample variation enough to generate stastical significance. Despite the unsuccessful attempt, identification of a new target in this scenario has to be performed at the population based omics level, and cannot be achieved with single cell analysis. Therefore, further optimisation beyond this project will hopefully yield successful candidates for validation.

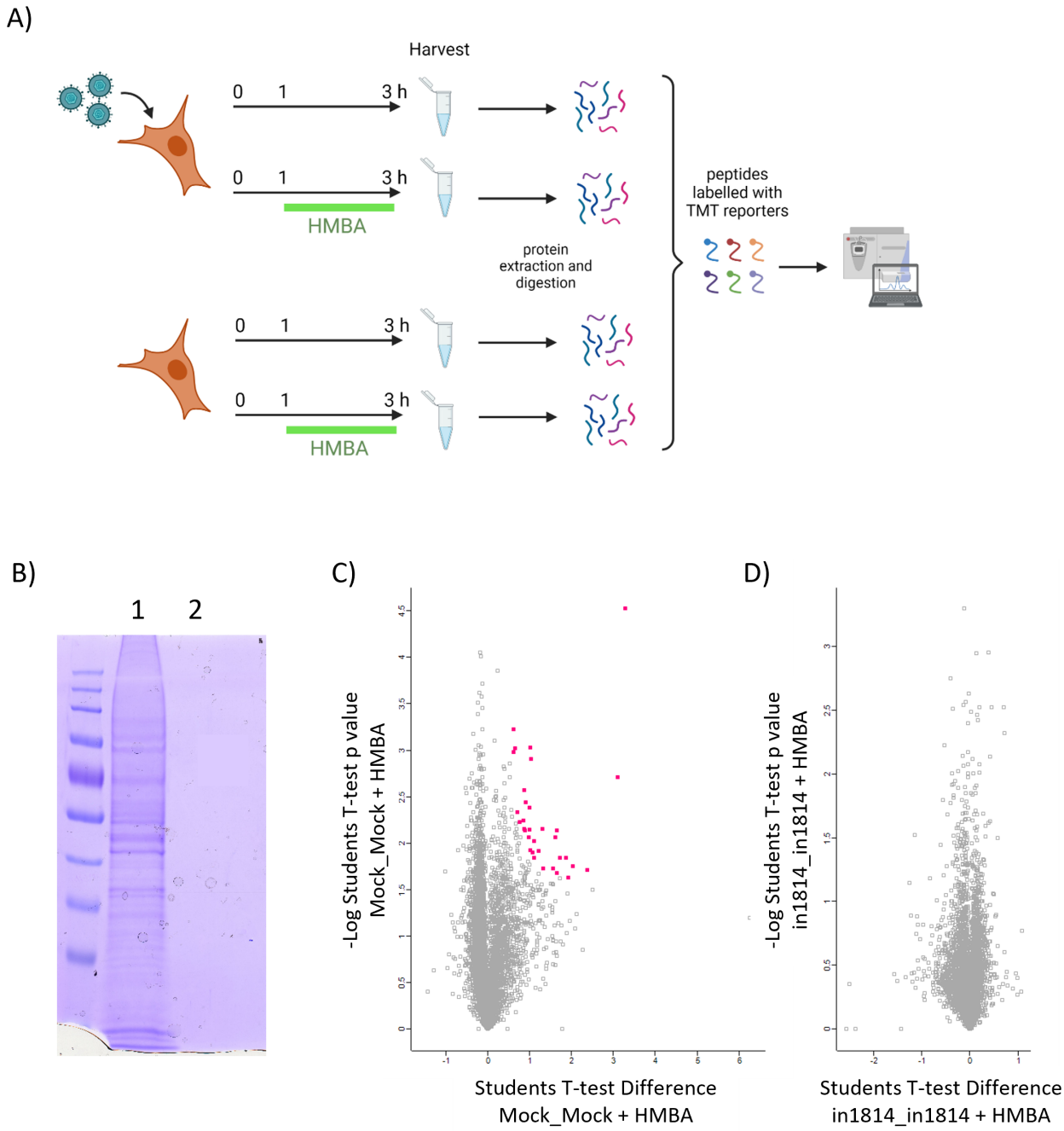


Figure 4.11: Proteomic analysis to identify targets induced by HMBA.

A) Experiment design for proteomic analysis. B) Coomassie stain of proteins extracted by phenol chloroform extraction from HaCaT lysates before trypsin digest (lane 1) or after trypsin digest (lane 2). C) All proteins identified in the TMT analyses. Significantly different proteins between uninfected and uninfected + HMBA are labelled in pink. D) There are no significantly different proteins in cells infected with in1814 and cells infected with in1814 and treated with HMBA.

4.5 Discussion and Future Perspectives

Within this chapter I have examined the transcription of several mutant HSV-1 viruses. The aim was to first identify the importance of the role of the transcriptional regulators ICP4 and VP16 on transcription output. Despite initial experiments inhibiting protein translation suggesting there may be rapidly induced cellular proteins inhibiting viral transcription in an antiviral manner, I demonstrated this was primarily due to the actions of ICP4 autoregulation. Secondly, I wanted to investigate the influence of cellular proteins on viral transcription in the absence of VP16. I demonstrated with high resolution the effect of both HMBA and JQ1 on HSV-1 transcription. I concluded that that population based analysis would be required to identify candidates. This did not yield definitive results but has enabled future analysis.

In a WT virus VP16 plays the role of an important transcriptional inducer, as described previously. However, in its absence the virus must rely on cellular transcription machinery, which it does with limited success giving a severely inhibited infection. The use of small molecule drugs that influence transcription, particularly through the modulation of proteins involved in the P-TEFb equilibrium, allowed me to examine how these cellular changes can influence viral transcription. It is difficult to reconcile the different state of Cdk9 in P-TEFb, whether inactive, active or chromatin bound, with the actions of HMBA and JQ1 and the corresponding information available about transcriptional increases and decreases. As described in the Introduction, P-TEFb exists in active and inactive forms (Figure 1.2). Overwhelmingly in the literature, when it is bound with Brd4 it is considered active and Brd4 recruits P-TEFb to gene promoters. Brd4 is either chromatin bound, free or in protein complexes.

The effect of HMBA on in1814 viral infection initially present a contradiction. HMBA increases the transcription of IE genes within the first few hours of HSV-1 infection in the absence of VP16. However, one of the main functions of HMBA is to induce the expression of HEXIM1,

a molecule that keeps P-TEFb in an inactive state. This conflict has been acknowledged previously, with several interpretations given for this disparity centering in the disruption of HEXIM1-7SK-RNA-P-TEFb by AKT, which HMBA activates (figure 4.12, A) [104]. I attempted to confirm the affect of HMBA on AKT phosphorylation by Western blot, but I was unable to successfully optimise the use of the antibodies. Further validation of this method of P-TEFb activation should be continued, particularly in keratinocyte cell lines. An alternative explanation was proposed by He et al. In the first few hours post HMBA treatment, HMBA induces the disruption of the inactive P-TEFb complex. One of the genes activated by P-TEFb is HEXIM1, resulting in a large increase of the HEXIM1 concentration within the nucleus by up to 5 fold. This creates a negative feedback loop, where the HEXIM1 pushes the P-TEFb status back towards the inactive state (Figure 4.12 B) [205]. VP16 can recruit P-TEFb to RNA pol II [206]. In the absence of VP16, this recruitment is therefore diminished. During an in1814 infection the absence of P-TEFb recruitment by VP16 is a key component of the reduced infectivity and HMBA alleviates some of this effect. Unfortunately I was not able to provide detailed insight into the molecular explanation for HMBA induced transcription of IE genes, and this will be the focus of ongoing future work.

JQ1 is BET domain inhibitor which is also involved in the P-TEFb equilibrium. As described in section 4.3 JQ1 may employ the same negative feedback loop as illustrated by HMBA in figure 4.12 B. Additionally, it has been proposed JQ1 promotes dissociation of inactive P-TEFb by inducing replication stress. Aside from these proposals, I believe JQ1 increases viral transcription by a different mechanism. My results indicate this pathway differs from the HMBA mode of action (Figure 4.9).

Histone acetylation is associated with transcription. The addition of a negatively charged acetyl group promotes an open chromatin structure [207]. As described in section 1.3.4, Brd4 recognises acetylated histones in promoters and recruits P-TEFb to transcription start sites. JQ1 binds competitively in the acetyl lysine binding site on Brd4, preventing it from binding chromatin. Therefore this would suggest there is a large population of Brd4 that is unable to recognise acetylated

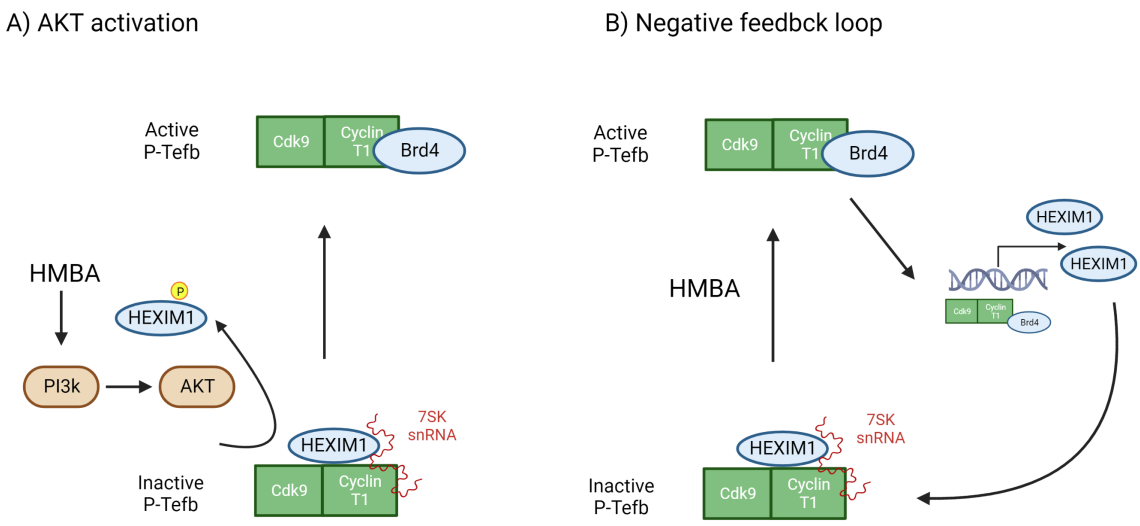


Figure 4.12: Models of HMBA induced P-TEFb activation.

A) Proposed method of P-TEFb activation by AKT. B) Proposed negative feedback loop of HEXIM1 regulation of P-TEFb.

lysines in promoters, and consequently unable to recruit P-TEFb. Ren et al., suggested in 2016 that the increase in free Brd4 caused by JQ1 is responsible for the increase in viral transcription. They propose the free Brd4, although bound with JQ1, is able to promote transcription from viral genomes by recruiting P-TEFb (figure 4.13). However, I have presented data which contradicts results found within this paper (figure 4.4 C). This proposed model also introduces several new questions, such as how Brd4 is able to recruit P-TEFb to viral promoters when the normal means of doing so, by binding acetylated lysines, is inhibited.

In this chapter I observe extreme transcriptional changes within a very short time frame. Although the well characterised induction of HEXIM1 may be playing a role, perhaps as described above, there is variation in the timeframes for expression induction profiles for HEXIM1 in different cell lines in the literature. Therefore, in HaCaT cell line the induction may not be rapid enough. An important future experiment would make use of an HEXIM1 antibody and examine HEXIM1

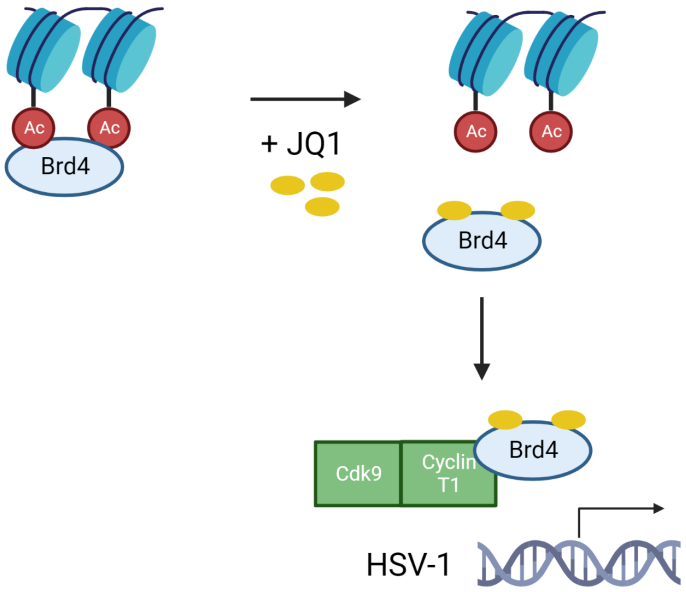


Figure 4.13: Model of JQ1 induced HSV-1 IE transcription

A) Proposed method of JQ1 mediating the release of Brd4 from chromatin, the subsequent activation of P-TEFb and the promotion of IE transcription [200].

expression levels by Western blot.

With the proteomics analysis I undertook, I attempted to analyse the whole cell proteome following a short HMBA treatment. In my analysis I discovered HEXIM1 levels did not increase significantly. Of the 44 proteins that were significantly different in the mock conditions plus or minus HMBA, they were not significantly different in the infected samples plus or minus HMBA. The results between the triplicates were too variable to allow conclusions to be made between the two biological sets. In future analysis there would be strict adherence to protocols and conditions to ensure all the sets and triplicates were precisely controlled.

Chapter 5

The role of cellular protein PML on transcriptional output from HSV-1 genomes

Following the successful combination of RNAscope with click chemistry in Chapter 3, I next wished to combine such analysis with the simultaneous investigation of protein localisation by immunofluorescence. The successful implementation of such three-way analysis would allow me to investigate the relationship between individual genomes, transcription output and the recruitment, or indeed lack of recruitment, of specific viral and host cell proteins. This will enable the assessment of the spatial proximity of host proteins, such as PML, with the transcriptional activity of viral genomes.

5.1 The fate of PML in early HSV-1 infection

PML is the major protein component of nuclear bodies, called ND10 or PML domains, as described in the Introduction. PML was analysed using a monoclonal antibody 5E10 [208]. 5E10 was the widely used PML antibody in the field but had severely limited supplies. Our lab received a small amount of 5E10 from Prof. Van Driel, and additionally developed a rabbit antibody against raised against recombinant GST-PML, #368. The antibodies were directly compared to ensure the accuracy of #368 against 5E10. The various protocols produced similar staining patterns, with PML domains clearly defined (Fig 5.1 A). The PML bodies in HaCaT cells give a less defined signal, but this is consistent

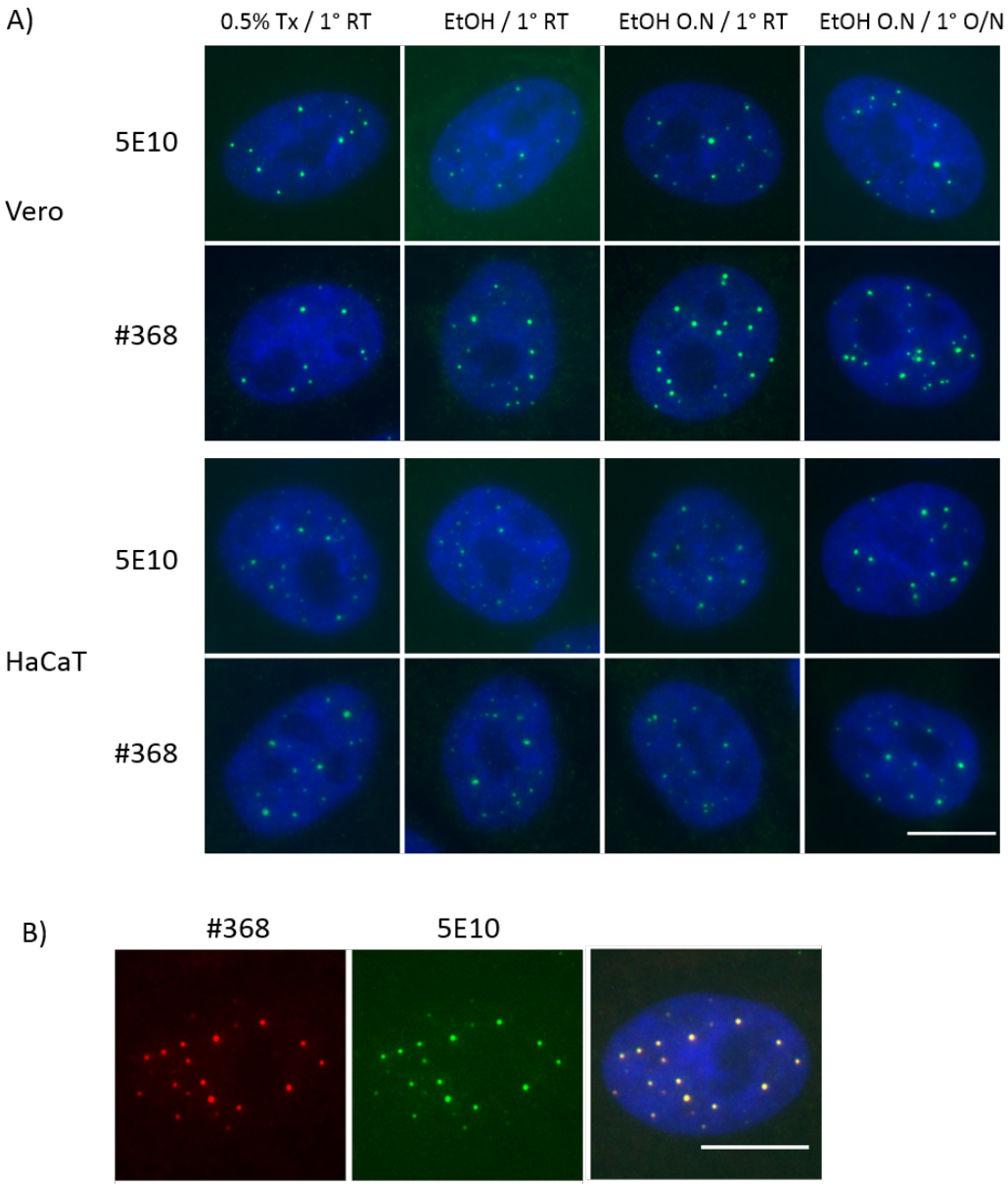


Figure 5.1: Development of PML IF protocols.

A) Optimisation of PML antibody staining in Vero and HaCaT cells. Column 1: permeabilisation with 0.5% Triton, primary antibody incubation 1 h at room temperature. Column 2: Permeabilisation with Ethanol dehydration, primary antibody incubation 1 h at room temperature. Column 3: Permeabilisation with Ethanol dehydration, storage in 100% EtOH overnight. Primary antibody incubation 1 h at room temperature. Column 4: Permeabilisation with Ethanol dehydration, storage in 100% EtOH overnight. Primary antibody incubation overnight at 4°C. Scale bar 10 microns. B) Combined stain using #368 (red) and 5E10 (green) on a Vero cell. Scale bar 10 microns.

across both antibodies. In a dual stain experiment, the PML domains revealed by #368 and 5E10 colocalise exactly (Fig 5.1 B). #368 will be used for the remainder of the thesis.

As described earlier, viral protein ICP0 is an E3 ubiquitin ligase. As ICP0 protein accu-

mulates there is a progressive loss of PML (Fig 5.2 A). If CHX is added to prevent de novo ICP0 synthesis, PML domains are maintained throughout infection (Fig 5.2 B). Therefore, at 3 hpi + CHX when we have previously demonstrated a large quantity of viral transcription to be taking place (Fig 4.1 B), PML bodies are intact. Quantification of PML bodies in the presence of CHX in mock or infected cells confirms the longevity of PML domains, except by 8 hpi in the presence of CHX when we know the cells to be suffering from prolonged CHX exposure.

PML has been previously shown to associate with viral genomes. To confirm this, HSV-1^{EdC} was used to infect Vero cells. At 1 hpi cells were fixed, processed for click chemistry to reveal viral genomes and immunofluorescence for PML. The FIJI plugin Comdet was used to calculate colocalisation of genomes and PML domains (Fig 5.3). In figure 5.3 A, the filled arrow represents a PML domain that is not associated with a genome. The outline arrow shows a genome colocalised with a PML domain, which is detected as a yellow box by the ComDet analysis. Lastly, the arrow head is indicating a genome that is not colocalised with a PML domain. Analysis of over 100 cells infected by HSV-1 at MOI 10 reveals that on average, just under half of the genomes are colocalised with PML at 1 hpi. The genomes that are not associated may never recruit PML, or they have yet to recruit PML. There is also a varying number of PML domains per cell, and in some cells the number of genomes exceeds the number of PML domains as these were high MOI infections.

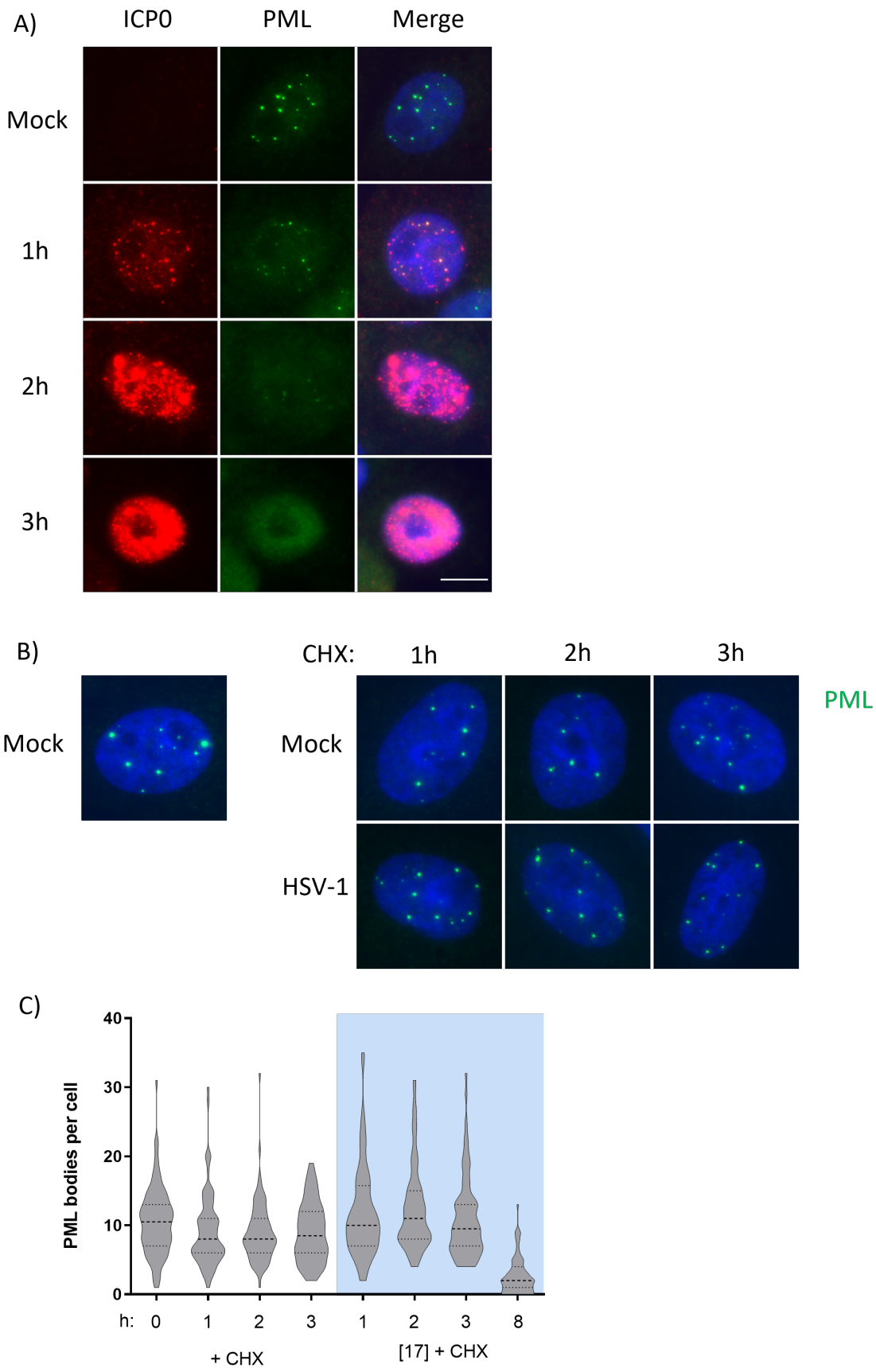


Figure 5.2: PML is degraded during infection by ICP0.

A) Timecourse of infection of HSV-1 in Vero cells, stained for ICP0 protein and PML. Scale bar 10 microns. B) PML in uninfected cells treated with CHX or infected cells treated with CHX. C) Quantification of PML bodies per cell in uninfected cells + CHX (+CHX) or infected cells + CHX ([17] + CHX).

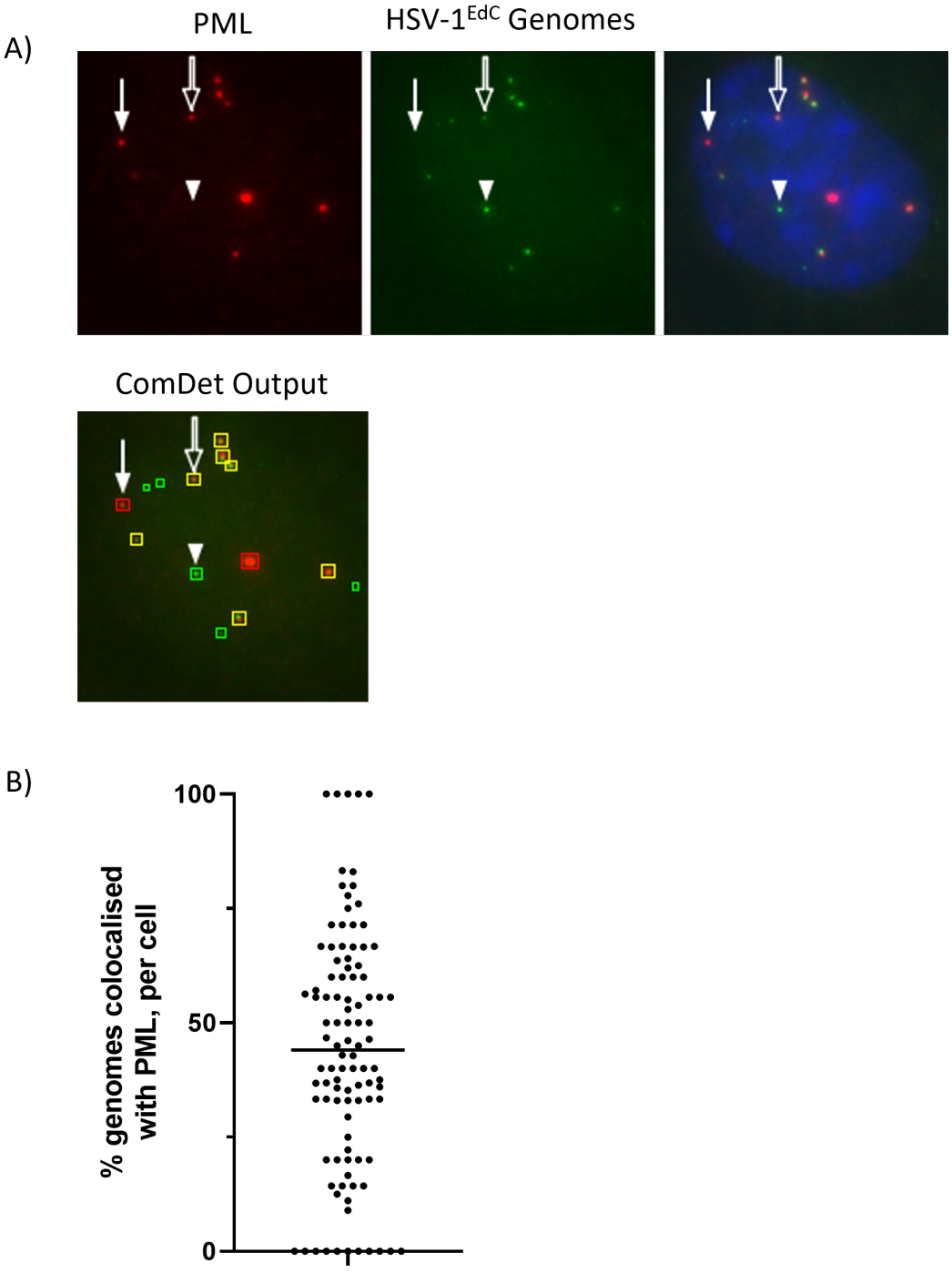


Figure 5.3: PML associates with HSV-1 genomes

A) Vero cells infected with HSV-1^{EdC} at 1 hpi, MOI 10. Click chemistry reveals genome location (green) relative to PML domains (red). Arrow head: a genome that has no PML. Solid filled arrow: PML that is not associated with a genome. Outline arrow: A colocalised genome and PML. Analysis performed using ComDet. B) Quantification of genomes associated with PML. Each point represents an individual infected cell. The plot indicates for each cell with detected genomes, the percentage of those genomes that are associated with PML

5.2 Transcriptional activity of genomes and their proximity to PML domains

PML bodies have a long history within HSV-1 research. The most widely held consensus is that PML domains are restrictive molecules that inhibit viral transcription. The current general proposition is that the genomes that are associated with PML domains will not be transcriptionally active. To investigate the effect of the proximity of PML domains and viral gene expression, RNAscope for IE genes was combined with immunofluorescence for PML.

The RNAscope protocol contains a protease treatment step before the probes are hybridised. The protease is supplied commercially from ACDBio, and there is no information about the strength on the enzymatic activity. IF staining for PML was performed with and without a protease treatment (Fig 5.4 A). There was no difference in PML bodies, demonstrating that the protease treatment is mild enough to not affect the epitope required for antibody binding. When immunofluorescence for PML was performed after the RNAscope protocol, there was a loss of signal intensity of RNA transcripts for cellular gene PP1B compared to the RNAscope protocol alone (Fig 5.4 B). However, a slight increase in exposure time during image acquisition reveals that no detail or resolution is lost when the protocols are combined.

Cells were infected with HSV-1 in the presence of CHX in order to prevent PML degradation. In figure 5.5 A, two cells are showing examples of ICP0 and ICP4 transcripts. The cell probed for ICP0 RNA has one transcription burst, indicated by the arrow. It colocalises with a PML domain. The second cell, probed for ICP4 RNA, has two transcription bursts. The one indicated with the filled arrow also has a PML domain. This cell has a second transcription burst shown by the outline arrow, which does not colocalise with PML. Identification of many transcription bursts and classification as PML negative or positive reveals that the IE transcription bursts are in fact not more likely to be absent of PML domains (Figure 5.5 B). Rather, the results indicate that the transcription bursts are if

anything more likely to be found associated with PML domains.

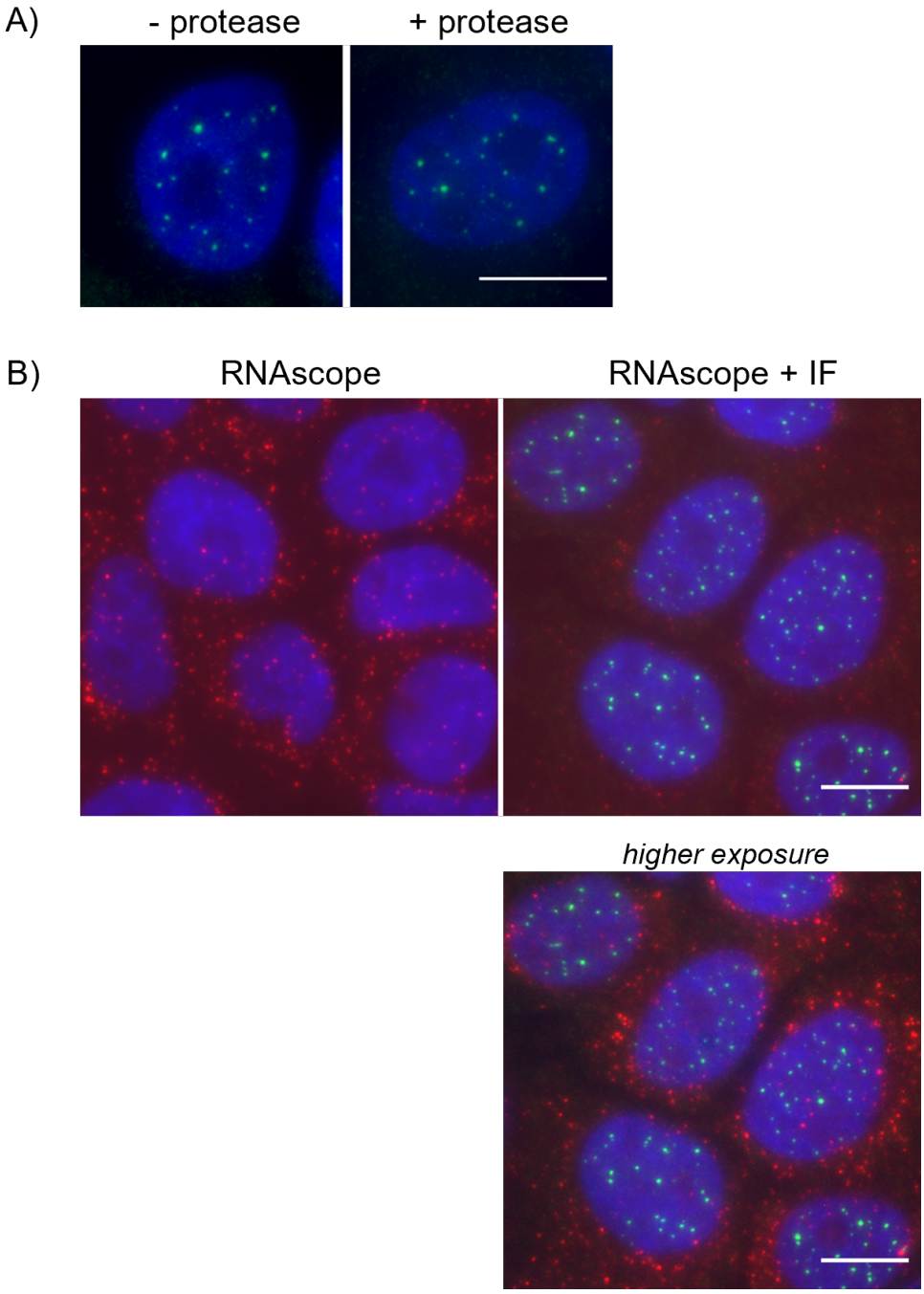


Figure 5.4: RNAscope and IF in combination

A) PML protein (green) in Vero cells with or without a protease treatment. Scale bar 10 microns. B) Uninfected Vero cells processed for RNAscope, or RNAscope with IF. PP1B transcript (red), PML protein (green). An increased exposure panel is shown for this image.

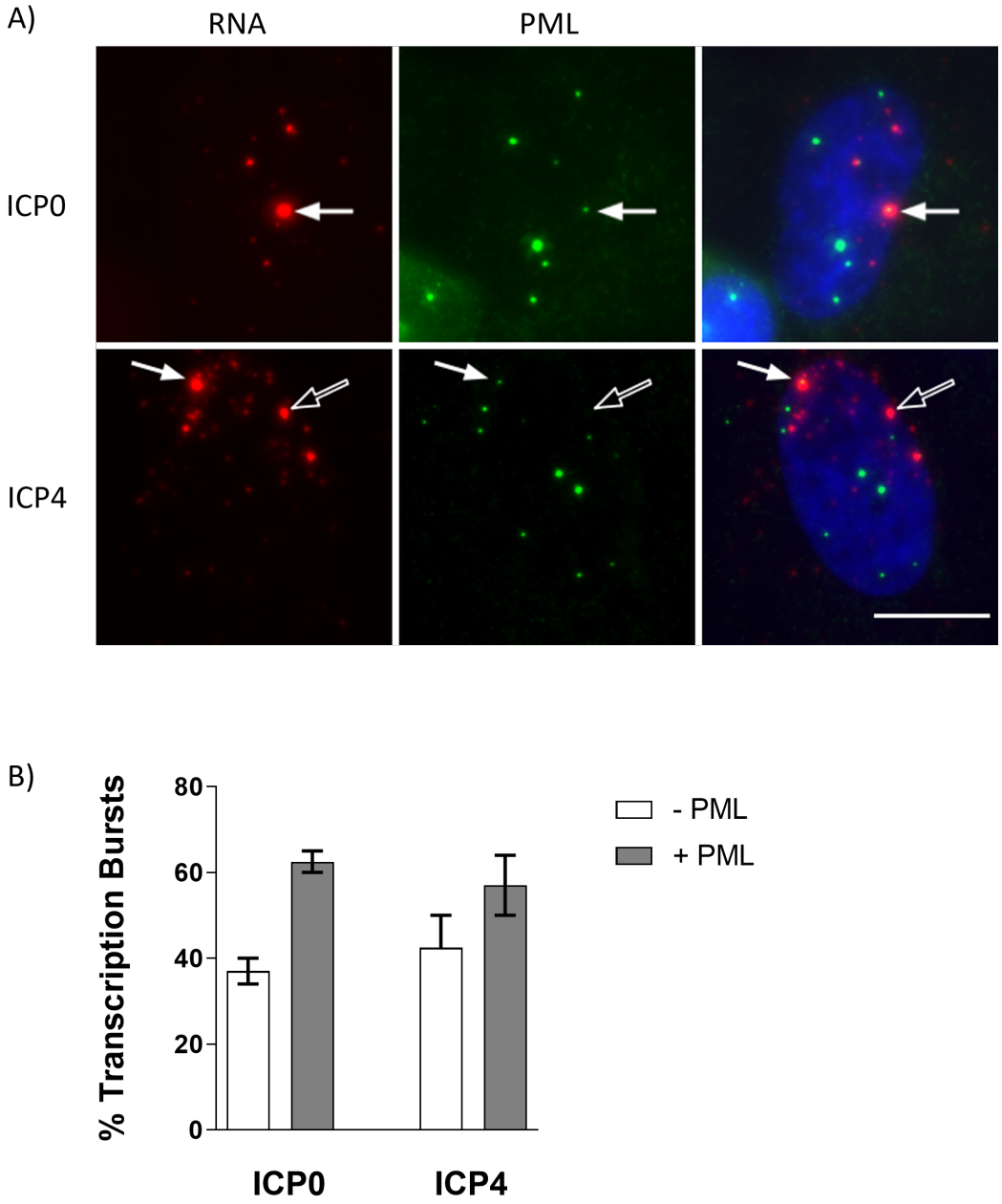


Figure 5.5: PML is associated with IE transcription bursts

A) ICP0 and ICP4 RNA (red) with protein IF for PML (green). Vero cells 1 hpi + CHX. Upper panel: ICP0 RNA transcription burst is colocalised with a PML domain (filled arrow). Lower panel: Two of the ICP4 transcription bursts are indicated by arrows. The filled arrow shows a burst colocalised with PML, the outline arrow indicates a burst that is free of PML. B) Quantification of transcription bursts that are associated with PML for ICP0 and ICP4 at 1 hpi + CHX.

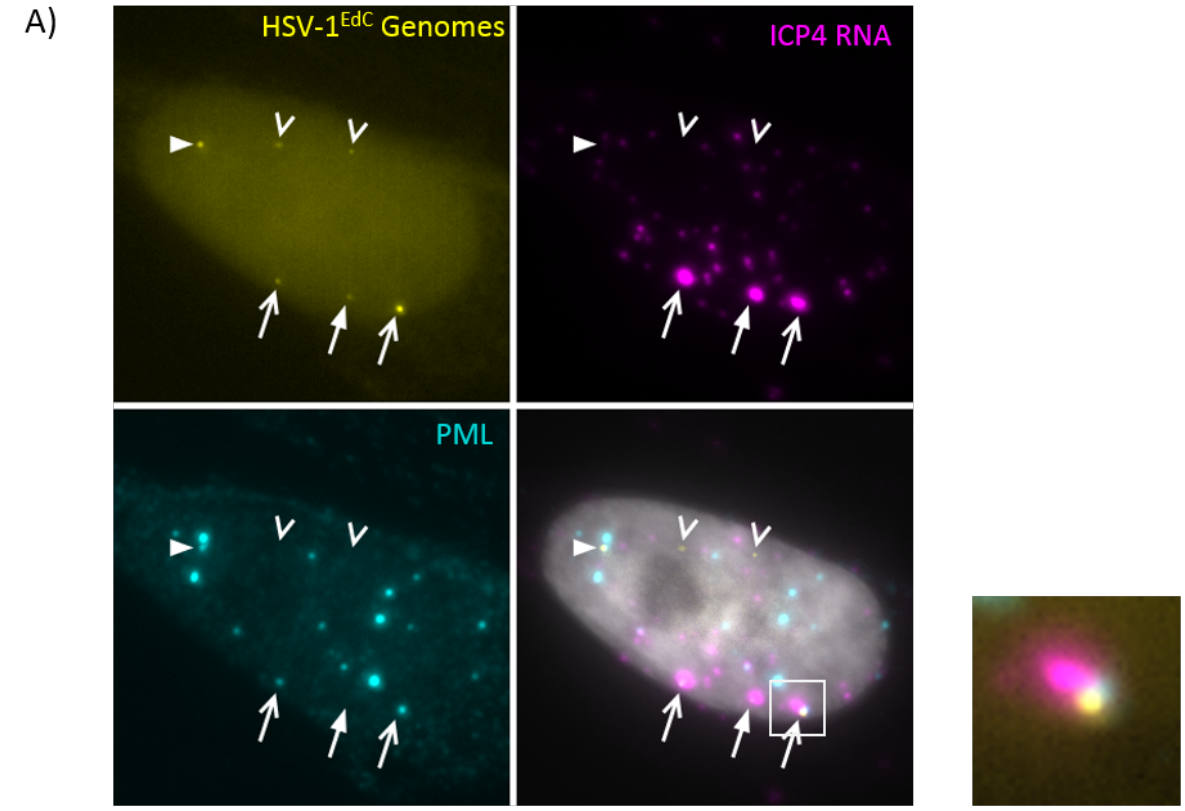
This surprising result goes against the widely accepted view of PML as a transcriptional repressor and the prediction that transcriptional bursts would not be associated with PML. However,

combining RNAscope and PML immunofluorescence does not give any indication about inactive genomes within the cell, and whether such genomes are associated with PML domains or not. To answer this question, RNAscope, click chemistry and protein IF need to be combined into one protocol.

In developing such a three way analysis, I determined the order had to be RNAscope followed by click chemistry and finally the protein IF. To achieve optimal results the cells were processed on the same day as infection and fixation. This successful integration of the three analysis methods reveals for the first time HSV-1 viral genome location, transcriptional activity and the location of PML domains.

Vero cells were infected with HSV-1^{EdC} in the presence of CHX, and fixed at 1 hpi (Fig 5.6 A). They were then processed for RNAscope, click chemistry and protein immunofluorescence for PML. In figure 5.6 I am presenting one example cell, followed by quantification of multiple cells. In this cell (Fig 5.6 A) there are six HSV-1 genomes. Three are bursting for ICP4 transcript. Of these active genomes, two are associated with PML (the outline arrows) and one is not associated with PML (filled arrow). The three inactive genomes are positioned along the top of the cell. The filled arrow head is indicating a genome that is inactive and associated with PML. The other two inactive genomes are not associated with PML (v shaped arrow heads). Thus it is revealed that not all of the inactive genomes are associated with PML.

Identification and classification of HSV-1 genomes as transcription burst positive (TB+) or transcription burst negative (TB-) for ICP0 in Vero cells show that the genomes that are bursting are actually more likely to be associated with PML (Fig 5.6 B). The inactive genomes are equally likely to be found with or without PML bodies. To confirm these results in another cell line, HaCaT cells were analysed as described for the Vero cells above. Quantification of transcription bursts, genomes and ICP0 transcript in these cells gives similar results. Therefore, the presence of PML on a viral genomes does not inhibit transcription.



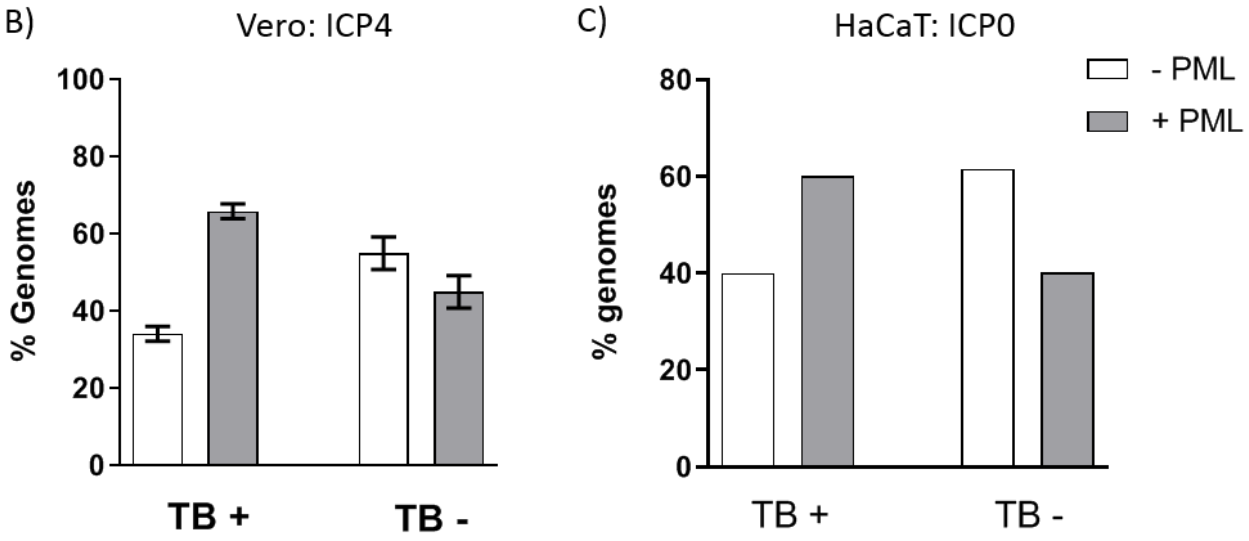


Figure 5.6: Transcriptional activity of genomes and their proximity to PML domains.

A) Vero cell infected with HSV-1^{EdC} MOI 10, and processed for click chemistry, IF (PML) and RNAscope (ICP4) at 1 hpi. Six genomes are visible, the arrow heads show inactive genomes, the arrows show active genomes. The two outline arrows indicate active genomes associated with PML, the filled arrow indicates an active genome not associated with PML. The filled arrow head indicates an inactive genome associated with PML, and the V arrow heads indicate inactive genomes not associated with PML. B-C) Quantification of genomes that are classified as transcriptionally bursting (TB +) or not bursting (TB-), and identification of PML association. B) ICP4 RNA in Vero cells. C) ICP0 RNA in HaCaT cells. Transcription burst (TB).

As described in section 3.6, the spatial relationship between transcription bursts and genomes is of great interest. When combined with PML, a third entity is brought into play. In figure 5.7 A the DAPI signal is represented by greyscale, and is removed for clarity in the expanded box. Here I show an infected cell at 1 hpi (Fig 5.7 A i), and one transcription burst has been enlarged within the box. This active genome is colocalised with the PML body, and the transcription burst is pluming in one direction from the genome. In comparison, there are two active genomes in cell ii in the expanded region. The Comdet analysis (Fig 5.3) would not identify the PML and genomes in cell ii as colocalised, as the pixel distances for the maximum foci signal are too great for the acceptable parameters. However, there is a clear association between the PML and the genome. Therefore, I can distinguish based on pixel distance both colocalised (Fig 5.7 i) and associated (Fig 5.7 ii) genomes and PML domains. In the analysis in figure 5.6 both colocalised and associated measurements are included.

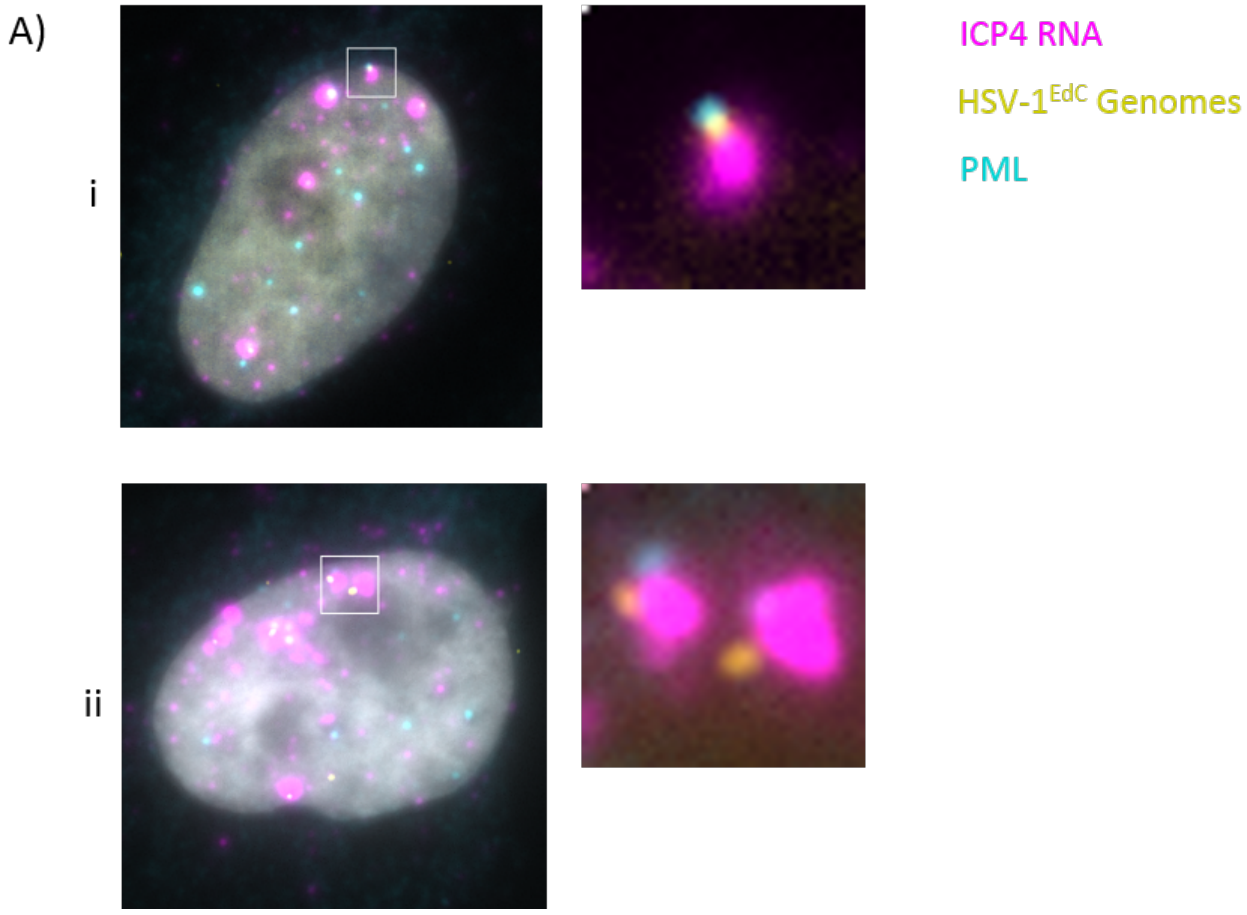


Figure 5.7: Association vs colocalisation

A) Two example Vero cells infected with HSV-1^{EdC} MOI 10, 1 hpi, PML protein and ICP4 RNA. Cell i: Genome and PML are colocalised, and transcription burst is pluming in one direction. Cell ii: Genome and PML are associated, with the transcription burst between.

All of the previous experiments were performed in the presence of CHX to prevent PML degradation. Although CHX does not affect PML bodies within 3 hours (Fig 5.2), infection with an ΔICP0 virus would allow the maintenance of PML domains without CHX addition. The FxE mutant virus has a deletion within the RING finger domain of ICP0, rendering it functionally inactive. FxE has a growth deficit on RPE cells, the cell line used to produce WT HSV-1^{EdC}, so it has to be grown on U2OS cells, a permissive bone cancer cell line. Attempts to produce an FxE^{EdC} virus were unsuccessful, with a very low EdC incorporation rate (Fig 5.8).

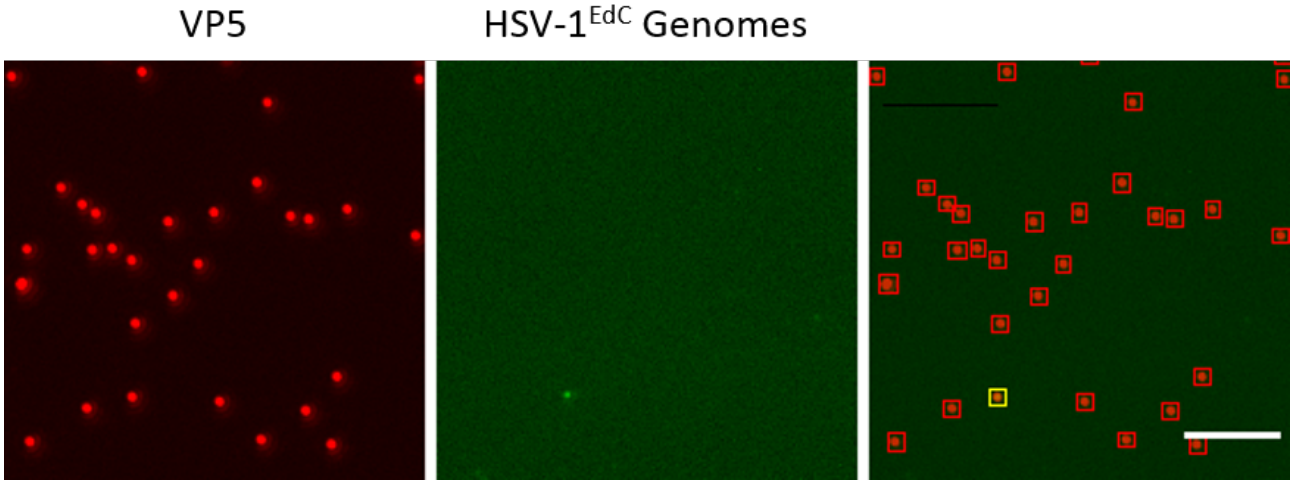


Figure 5.8: Production of FxE^{EdC}

FxE^{EdC} adhered onto a glass coverslip. VP5 (capsid protein) and click chemistry for EdC genomes. Comdet analysis only finds very few capsids with an EdC labelled genome, one in this example field within the yellow box. Scale bar 10 microns.

The analysis of infections with FxE was therefore limited to RNAscope and IF. Three example cells at 1 hpi presented in figure 5.9 A show that the ICP0 transcription bursts, and therefore the sites of the FxE genomes, may be found associated with PML or PML free. In cell i, the filled arrow shows an ICP0 transcription burst that is not associated with PML. In cell iii, there is one transcription burst, indicated by the outline arrow, and it is associated with a PML domain. Finally, cell ii has one example of each. Quantification of these cells shows that 40% of the transcription bursts are found with PML (Fig 5.9 B). In the absence of CHX, ΔICP0 HSV-1 genomes are still transcriptionally

active when associated with PML.

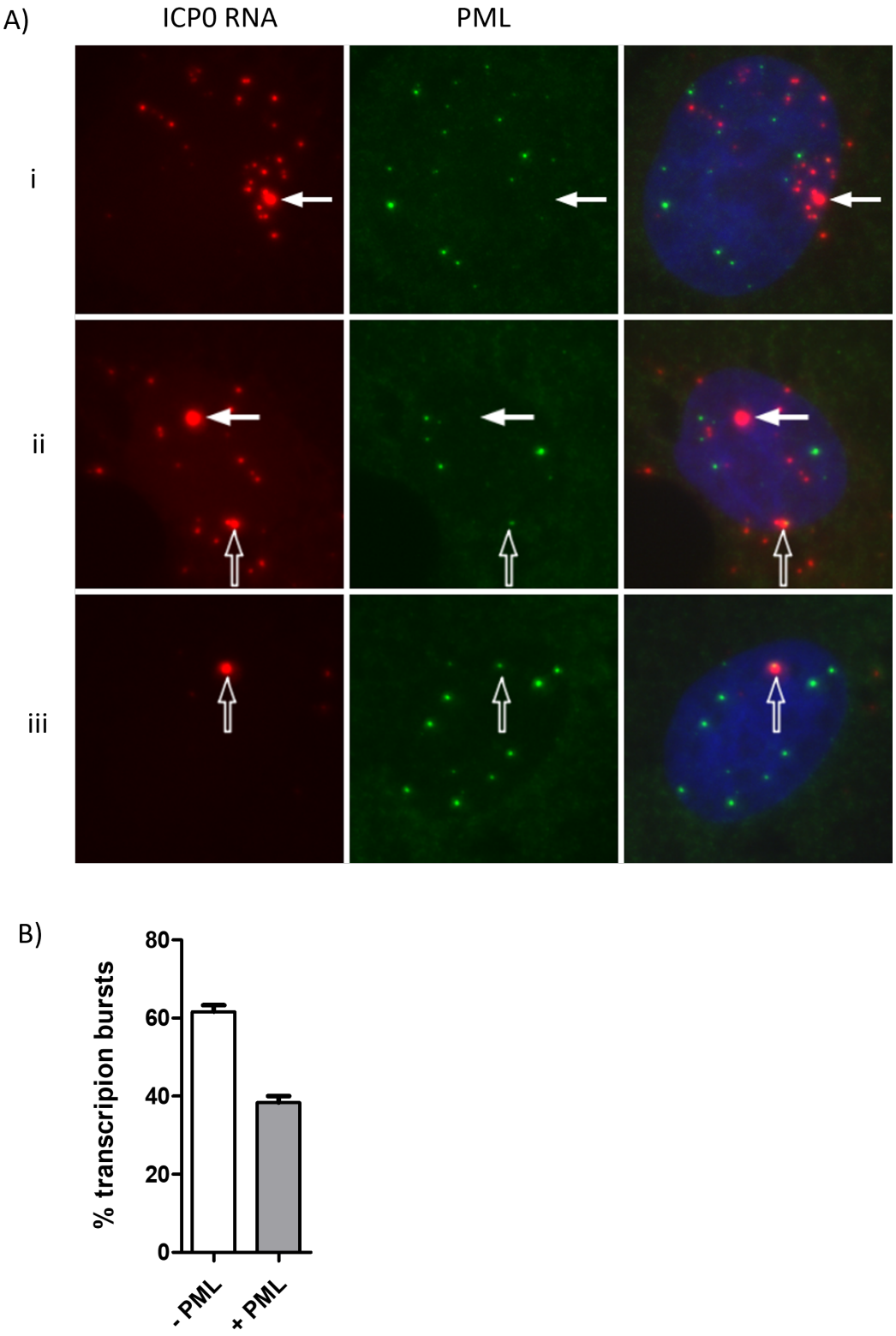


Figure 5.9: PML is associated with IE transcription of an FxE virus

Infection with FxE in Vero cells, 1 hpi, MOI 10. ICP0 RNA (red) and PML protein (green). A) Three example cells of ICP0 RNA and PML association. Filled arrow: transcription burst without PML. Outline arrow: Transcription burst associated with PML. B) Quantification of transcription bursts with or without PML.

5.3 Role of PML recruitment to HSV-1 genomes

The evidence presented here indicate that PML association with viral genomes does not correlate and is not a predictor of suppression of IE transcription. However, it is very clear from both this work and other published works that PML is degraded during infection by ICP0 and that it is recruited to genomes. Therefore, a clear role for PML in HSV-1 infections remains to be determined. One possible role could be linked to the recruitment of cellular proteins in the DNA damage response (DDR).

HSV-1 genomes contain many nicks and gaps in the DNA which can be recognised as damaged DNA and trigger the host cell DDR. γH2AX is a commonly used as marker of DNA damage. HSV-1 infection induces an increase in the total γH2AX stain (Fig 5.10 A). By 6 hpi, γH2AX is pushed out of replication compartments as they grow in size, marking the damaged host chromatin around the areas of virus replication. Phosphorylated DNA-dependent protein kinase (pDNA-PK) is an important protein in the DDR and is recruited to damaged DNA. It also increases during HSV-1 infection (Fig 5.10 B). For both γH2AX and pDNA-PK bright foci appear at 1-2 hpi. The presence of these foci suggests γH2AX and pDNA-PK may be responding to HSV-1 genomes.

Vero cells were infected with HSV-1^{EdC} and processed for click chemistry and the detection of DDR markers. At 1 hpi, γH2AX accumulates around HSV-1 genomes (fig 5.11 A). There is very little colocalisation, as the γH2AX is forming adjacent to the genomes and is therefore on host cell DNA. The viral genomes could be causing a lot of damage to host cell DNA upon entry and through the initiation of infection. In contrast, DNA-PK is being phosphorylated on areas that do colocalsie with genomes (fig 5.11 B). The example cell in figure 5.11 B has two large sites of DNA-PK phosphorylation, shown by the two arrows. These both colocalise with HSV-1 genomes. However, the pDNA-PK signal may form initially on surrounding host cell DNA, as shown by the genomes indicated by the arrow head, which only has a small enrichment of pDNA-PK signal adjacent to the

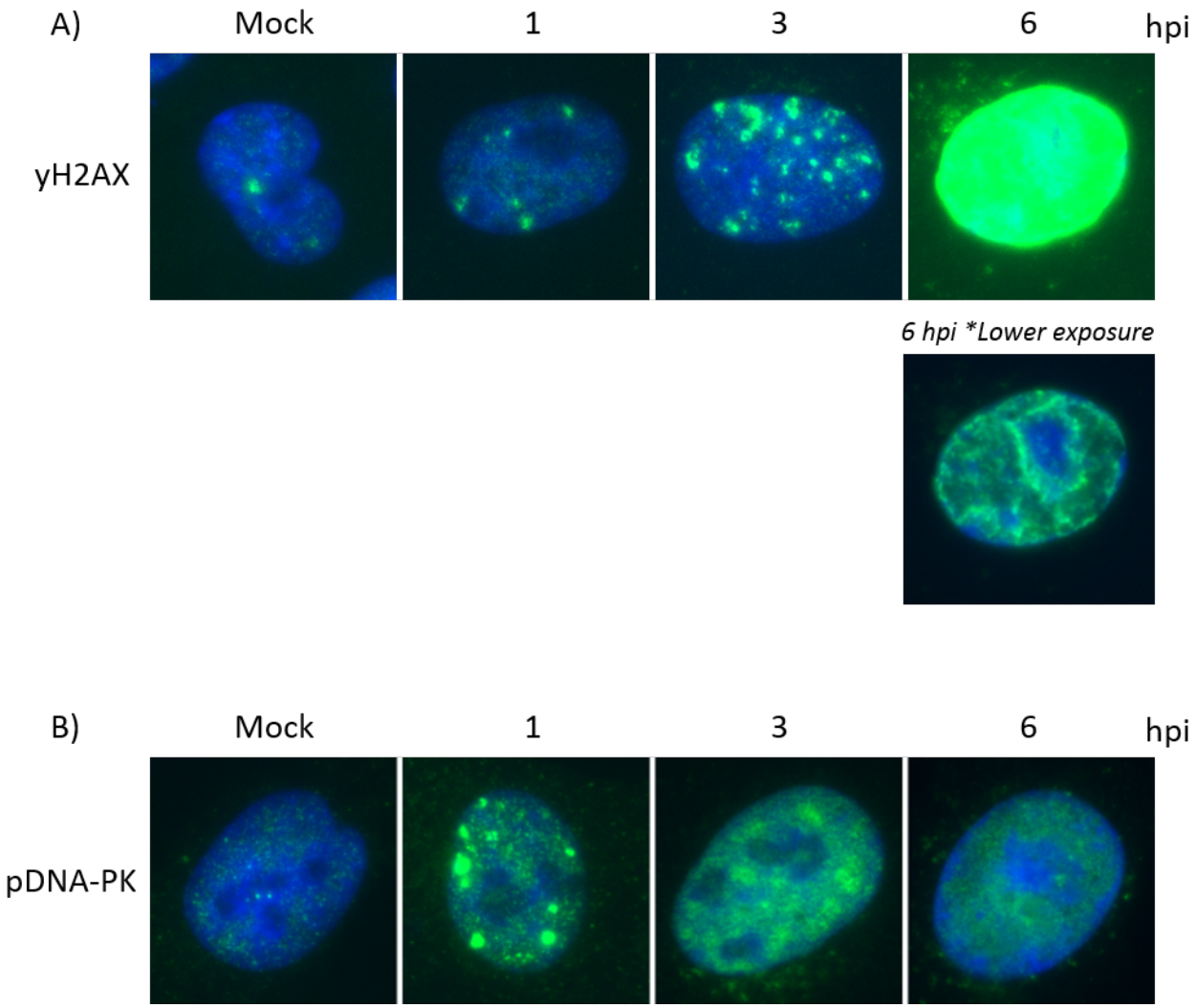


Figure 5.10: HSV-1 infection induces DNA damage and activates the DDR

A) Timecourse of γH2AX IF through a high MOI infection in Vero cells. B) Timecourse of pDNA-PK in a high MOI infection in Vero cells.

genome.

By 1 hpi, these genomes will be transcribing and the first IE genes will be being translated. To identify if the damage surrounding the HSV-1 genomes is triggered by viral transcription, cells were treated with ActD. ActD however induced a large amount of DNA damage in uninfected cells, measured with γH2AX (Fig 5.12 A). It therefore became necessary to inhibit transcription without causing any DNA damage. To this end, the transcription inhibitor 5,6-dichloro-1-beta-D-ribofuranosylbenzimidazole (DRB) was used. Uninfected cells were treated with 50 μg/mL DRB for

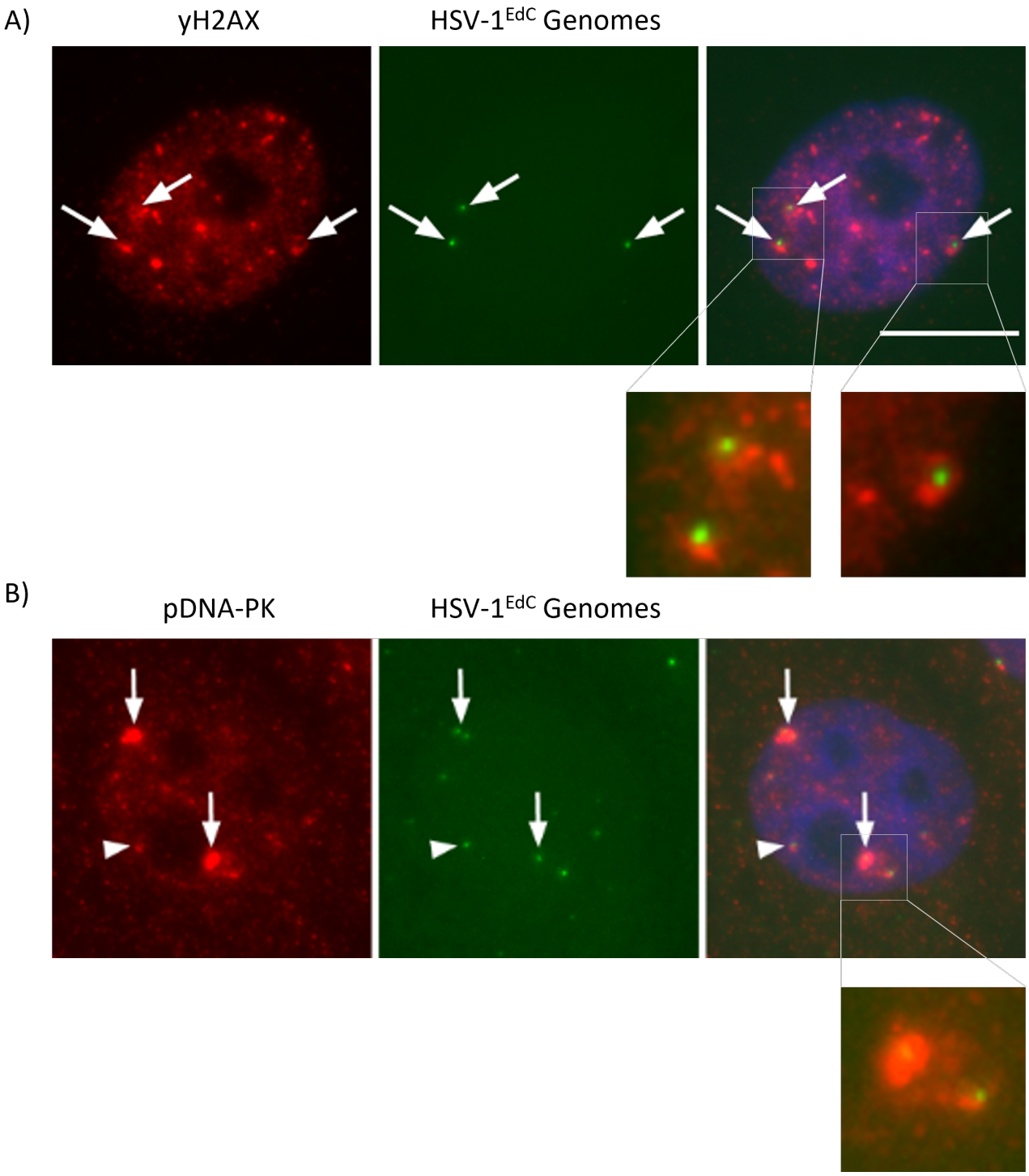


Figure 5.11: DDR markers are recruited to viral genomes

Infection of Vero cells with HSV-1^{EdC}. A) Click chemistry combined with IF for γH2AX. The arrows show EdC genomes. The two expanded boxes show the accumulation of γH2AX around viral genomes. Scale bar 10 microns. B) Click chemistry combined with IF for pDNA-PK. Vertical arrows: large pDNA-PK accumulating on genomes. Arrow head: small pDNA-PK accumulate adjacent to genome.

1 h. The DRB did not induce an increase in γH2AX (Fig 5.12 B). Vero cells were then infected with HSV-1 in the presence of DRB and ICP0 transcript was examined. At 1 hpi, DRB inhibits viral

transcription but without causing damage to host cell DNA (Fig 5.12 C). Infection with HSV-1^{EdC} in the presence of DRB, and then processing with click chemistry and IF for γH2AX revealed that if HSV-1 genomes are inactive and not transcribing, γH2AX still accumulates adjacent to HSV-1 genomes (Fig 5.12 D). This is in direct contrast with work by Lilley et al., who found that mutant viruses which don't express viral proteins do not trigger the DDR. I have shown that host cell DNA damage is triggered by genome presence alone [143].

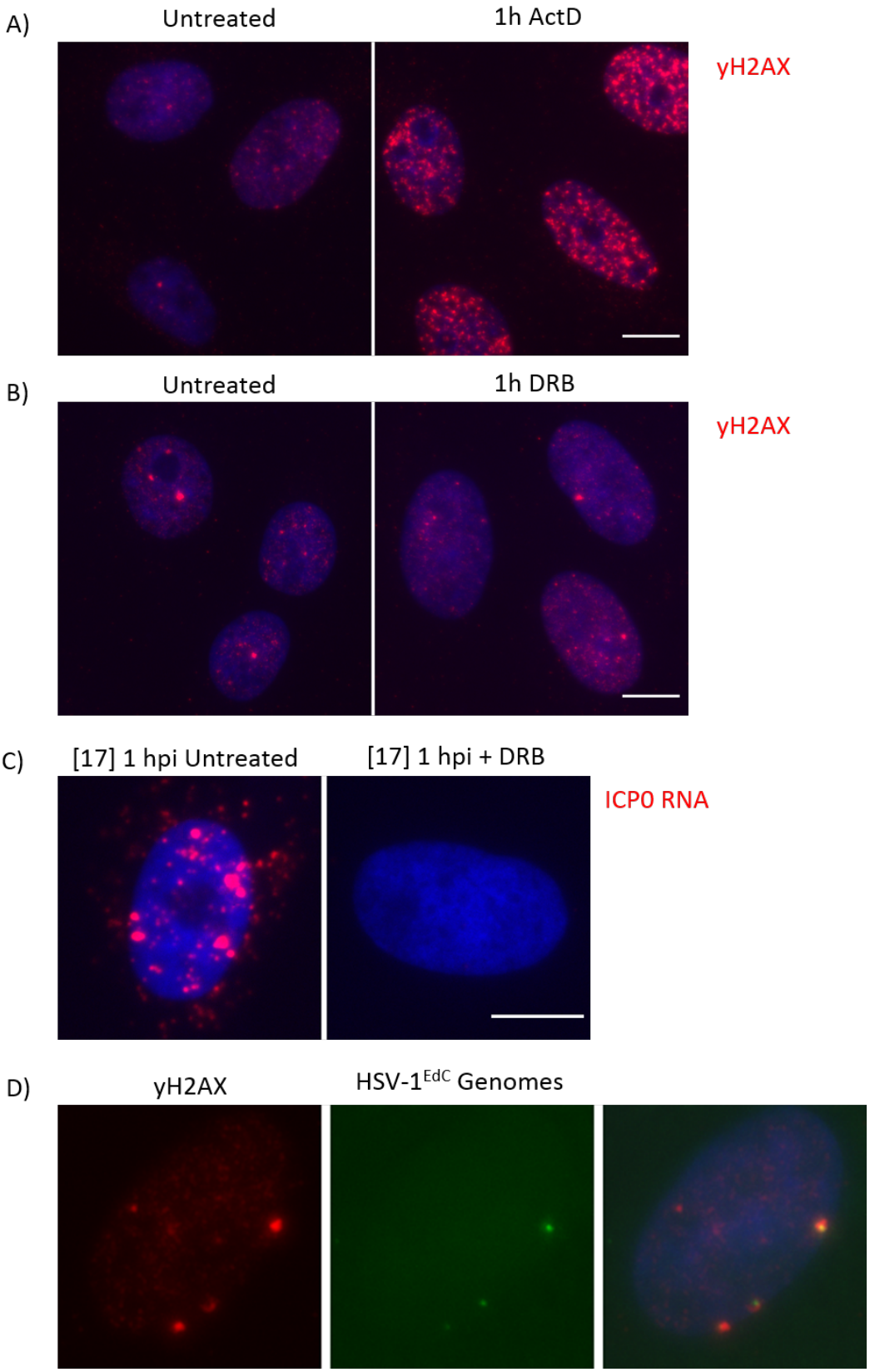


Figure 5.12: Damage accumulates around genomes even if they are transcriptionally silenced

A) γH2AX staining (red) in uninfected cells either untreated or treated with 1 h ActD. B) γH2AX staining (red) in uninfected cells either untreated or treated with 50 μg/mL DRB for 1 h. C) ICP0 RNA (red) in cells infected with HSV-1 MOi 10 at 1 hpi, Untreated or treated with DRB. D) Infection with HSV-1^{EdC} MOI 10 in the presence of DRB, 1 hpi. Click chemistry (green) combined with IF for γH2AX (red). Scale bar 10 microns.

5.4 Discussion and Future Perspectives

The ability to combine RNA FISH with genome detection and protein immunofluorescence provides exciting new opportunities to investigate the roles of many proteins on the transcriptional activity of viral genomes. During the process of optimisation, it became clear that the order of the processing steps was important. The RNAscope protocol should be performed first, followed by the click chemistry and then the immunofluorescence. Although the protease treatment step from the RNAscope protocol as found to have no detrimental effect on the epitope recognition of PML, any other proteins subjected to this analysis should also be evaluated for protease treatment.

The spatial orientation of genomes, PML and transcription bursts is quite diverse. As explained above in figure 5.7, there are genomes and domains that are easily classified as colocalised. Yet, there are another population of actively transcribing genomes that are not colocalised but closely associated with PML bodies. Although I have included both in my analysis, I believe further work is needed to understand this class of genomes. It could be that this captures the recruitment of a PML body that has not yet arrived at the genome. In this scenario, it might be argued that the genome is only transcriptionally active because the PML has yet to arrive. However, the numbers of directly colocalised genomes with PML suggest this is not true.

My conclusions from this data are that the presence of PML on a HSV-1 genome does not prevent viral transcription. This contradicts the widely held view in HSV-1 field of PML as a restriction factor, with many stating it operates at the level of viral transcription. At some unspecified level PML may well be operating as a restriction factor, but not by inhibiting viral transcription. PML body recruitment in response to DNA damage has already been documented, and may be why PML bodies are recruited to viral genomes. The subsequent disruption of PML bodies by the degradation of PML by ICP0 could be releasing multiple factors within the PML bodies, which as they are now adjacent to HSV-1 genomes the virus can utilise for enhanced infection. PML bodies have been shown to con-

tain many chromatin modifying factors, including histone chaperones, histone methyltransferases and acetyltransferases [209]. By degrading PML, there is a reduced chance of chromatin being deposited on the viral genome. There are arguments for HSV-1 to encourage PML recruitment by inducing cellular damage, and many reasons why the virus may want to degrade PML. I have shown no direct link between PML association and transcriptional repression, and I think this work should cause researchers to avoid describing PML as a transcriptional repressor.

The development of this analysis technique will allow the evaluation of many proteins on viral transcription. Schlafen family member 5 (SLFN5) was identified in proteomics screen in 2021 as a restriction factor which suppresses HSV-1 at the level of transcription [210]. SLFN5 forms small discrete foci that colocalise with ICP0 upon infection with HSV-1, making it an ideal candidate to analyse by the RNAscope, IF and click chemistry protocol. I obtained the SLFN5 antibody but was unable to successfully optimise it within this project. Interestingly, by western blot I did not observe the degradation of SLFN5 during infection that was found in the above 2021 paper. The authors of the study used HFF cells, in comparison to the Vero and HaCaT cell lines that I utilised, therefore cell type differences may be partly to blame.

Chapter 6

Spatial Relationship between viral transcription and viral DNA replication

6.1 Transcripts accumulate inside replication compartments

I observed that after the first phase of transcription declined at 3 hpi there was a later phase typified by the accumulation of abundant nuclear transcripts together with some cytoplasmic accumulation retained in specific areas (figures 3.2, 6.1). In a high MOI infection of Vero cells both IE and L gene transcripts accumulate within subnuclear regions (Fig 6.1, A and B). These regions are likely to be replication compartments, and the addition of PAA to prevent viral DNA replication inhibited the accumulation of viral transcript within these nuclear regions (Fig 3.2).

As discussed earlier, ICP4 is a dsDNA binding protein and is recruited to and marks viral replication compartments [211]. Immunofluorescence staining for ICP4 protein demonstrates the lack of replication compartments at 8 hpi in the presence of PAA (Fig 6.2 A). To confirm that the regions where transcript accumulates at late timepoints are replication compartments, VP16 transcript and ICP4 protein was examined in infected cells at 8 hpi. Previous experiments had confirmed that like PML, ICP4 protein is not affected by the protease treatment step in the RNAscope protocol. Therefore, it is possible to combine the RNAscope techniques with immunofluorescence. The sub-

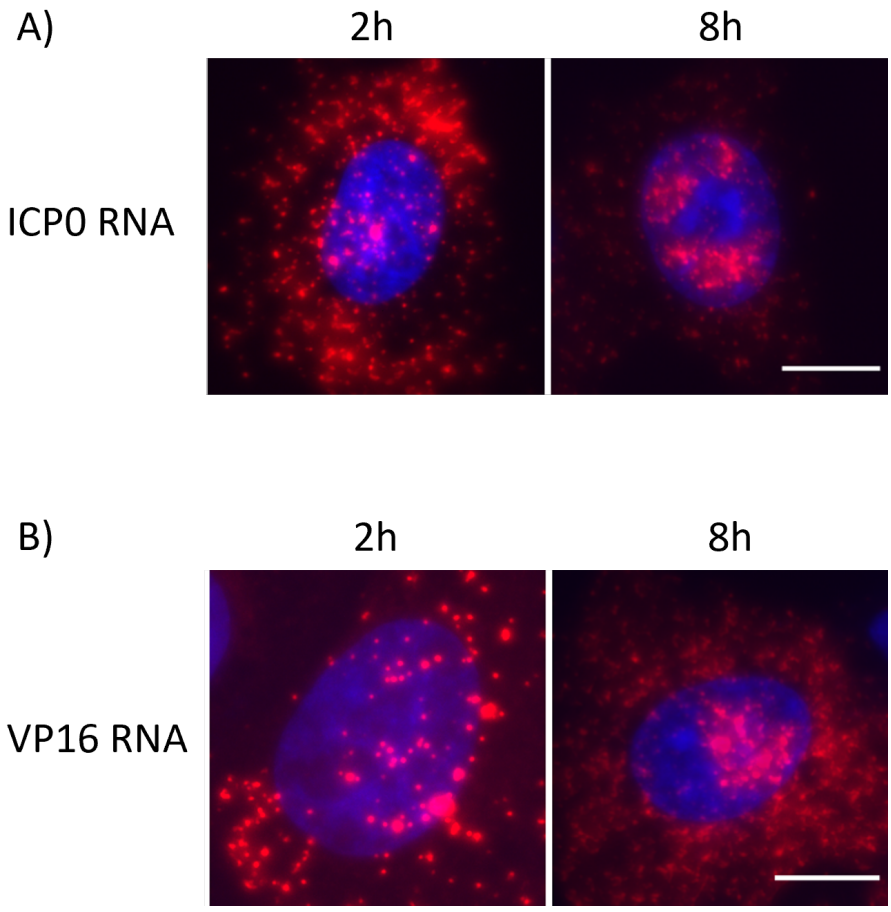


Figure 6.1: Subcellular location of IE and L transcripts pre and post replication

Vero cells infected with HSV-1 at MOI 10. RNAscope at 2 hpi and 8 hpi for A) ICP0 RNA and B) VP16 RNA. Scale bar 10 microns.

nuclear regions where transcript accumulates colocalise with ICP4, confirming that viral transcript is accumulating within replication compartments (Fig 6.2 B). Of note, the RNA is not distributed homogeneously within replication compartments. The expanded region in figure 6.2 B shows two replication compartments. In red are the VP16 transcripts, both single transcripts and small transcript aggregates can be seen. The RNAscope allows highly resolved analysis, discriminating where the majority of transcript signal is in a defined region within a replication compartment.

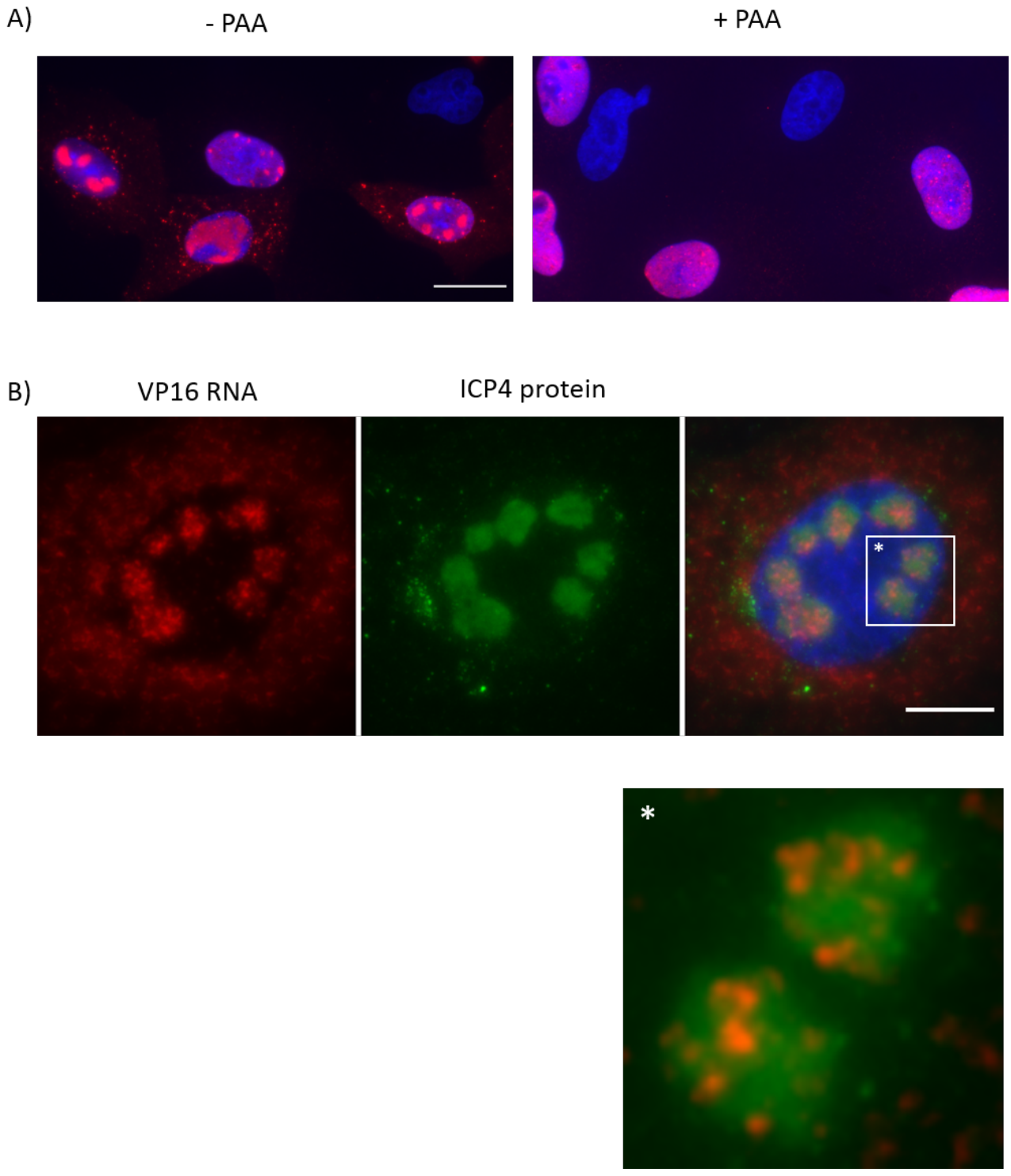


Figure 6.2: Late transcripts accumulate inside replication compartments

A) ICP4 protein (red) in Vero cells infected with HSV-1 MOi 10 at 8 hpi, in the presence or absence of PAA. Scale bar 10 microns. B) VP16 RNA (red) and ICP4 protein (green) at 8 hpi. A small region is expanded (*). Scale bar 10 microns.

6.2 HSV-1 infection in cells undergoing S phase

With the high resolution of transcript location within the replication compartment, the spatial relationship between ongoing viral DNA replication and transcription could be investigated. The modified nucleotide EdC can be used to pulse label nascent DNA replication. When supplied in a 1 h pulse, EdC will be incorporated into newly synthesised DNA, and using click chemistry this DNA can be visualised. Vero cells infected with HSV-1 at 7 hpi were pulsed with EdC for 1 h, and then fixed with PFA at 8 hpi. If a cell had a viral replication compartment that was actively replicating viral DNA during the EdC pulse, the replication compartment (revealed with ICP4 protein) would be labelled with the azide fluorophore, as demonstrated in the example cell in figure 6.3 A.

The infections presented within this thesis are performed in asynchronous cell populations. Therefore, a percentage of the cells will be undergoing mitosis. Any cell in S phase and therefore replicating it's own DNA will also incorporate EdC into newly synthesised cellular DNA. Three examples of uninfected cells after a 1 h EdC pulse are shown in figure 6.3 B. These all represent different EdC staining patterns that can be seen at various stages of S phase, ranging from fairly diffuse to bright discrete foci.

When cells undergoing S phase are infected, EdC will be incorporated into both viral and cellular DNA. Cells with EdC positive replication compartments, which therefore have active viral replication, may also have regions of EdC incorporation which are ICP4 negative, which are likely cellular. An example of this is shown by the cell in Fig 6.3 C. It has two ICP4 positive replication compartments, which are EdC positive. Around the edges of the nuclei and in the space between the replication compartments there are areas of EdC staining that are ICP4 negative. The EdC in these areas takes on more defined staining than the diffuse stain associated with the ICP4 positive areas. Although it cannot be completely ruled out that these areas are viral, it is very likely they are cellular. In a cell with large and highly developed replication compartments, the chance of any other viral

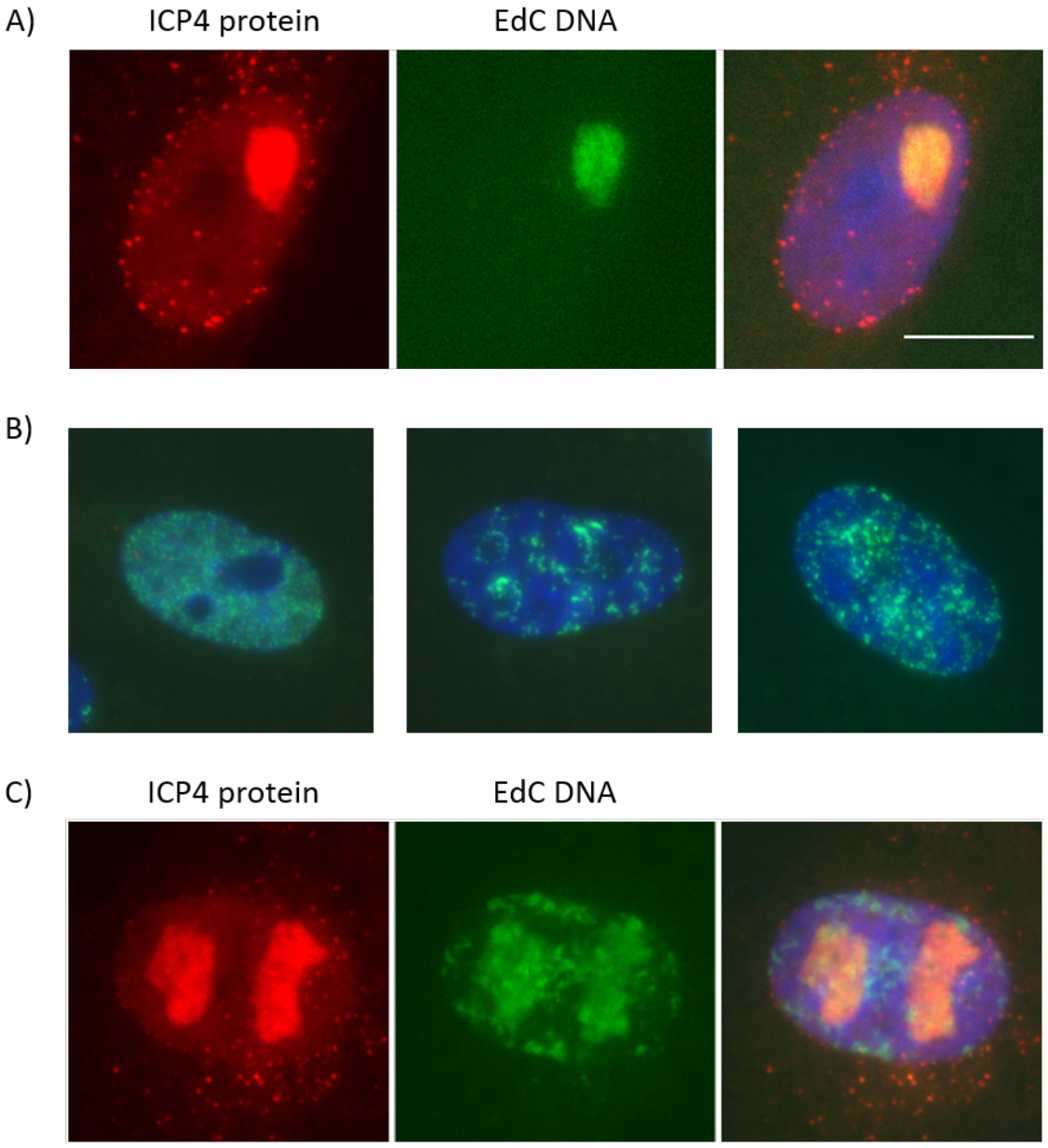


Figure 6.3: EdC pulse labelling reveals newly synthesised DNA

Vero cells are pulse for 1 h with 10 μM EdC. A) Vero cell, 8 hpi, HSV-1. Click chemistry labels the replicating DNA (green) combined with ICP4 protein IF (red). B) Three uninfected Vero cells showing various stages of S phase, with EdC labelled replicating DNA (green). C) Vero cell, 8 hpi, HSV-1. Click chemistry labels the replicating DNA (green) combined with ICP4 protein IF (red).

replication occurring outside of the regions that are ICP4 positive is very low.

The ability of EdC to label both viral and cellular DNA creates a complex cell population, with many different classes of labelled cells. An example field showing roughly fifty nuclei is presented in figure 6.4 A. In red is ICP4 protein, and EdC labelled DNA is presented in green. The

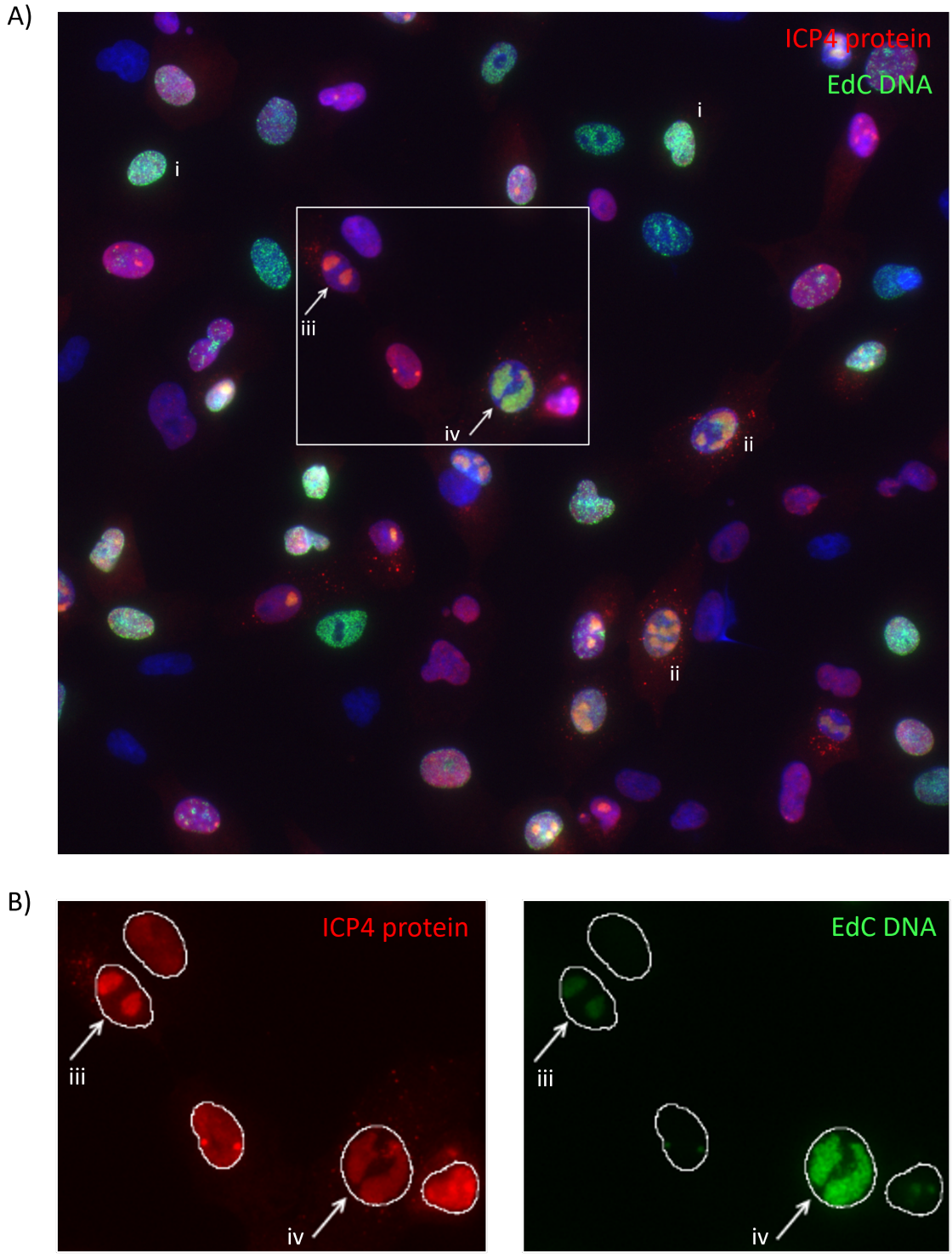


Figure 6.4: Heterogeneity of EdC labelling in an asynchronous population.

Vero cell, 8 hpi, HSV-1. 1h pulse with 10 μM EdC. A) A large filed showing EdC incorporation and ICP4 protein after processing for click chemistry and ICP4 protein. Cell i: Ongoing S phase synthesis, no ICP4. Cell ii: ICP4 replication compartments and both viral and cellular EdC. The two cells, iii and iv, shown by arrows are expanded. B) ICP4 protein and EdC from the box in part (A). White circles outline nuclei.

two cells labelled i are examples of cells undergoing S phase with no ICP4 positive viral replication compartments. The cells labelled ii are examples of cells with multiple ICP4 positive replication compartments which are also positive for EdC and therefore actively replicating DNA. They also have regions of cellular DNA synthesis outside the replication compartments, similar to the cell presented in figure 6.3 C. In addition, there are cells with no EdC incorporation and cells that show very low or no infection. To illustrate some of these features, the inset box shows two cells indicated by arrows and labelled iii and iv. The upper one, cell iii, has large replication compartments but little EdC incorporation. The lower one, cell iv, also has large replication compartments and has a large amount of EdC incorporation, indicating a large amount of viral replication within the EdC pulse duration. Therefore, the size of the replication compartment does not reflect the level of DNA replication.

Classification of different infected and replicating cell types gives rise to 7 cell types (Fig 6.5 A), which are summarised and quantified in figure 6.5 B. Classes a to d all have ICP4 positive replication compartments. The most abundant class is class a, where the EdC pattern shows that the only nascent DNA synthesis is viral and occurring inside the replication compartment. In classes b and d, there is both cellular S phase and viral DNA replication. The difference between b and d lies in the pattern of S phase synthesis. In class b there are regions of high incorporation and regions that are EdC negative, whereas in class d the entire nucleus outside of the replication compartments is diffuse EdC. Class c has fully formed replication compartments, but a diffuse EdC pattern with no enrichment in the viral compartments. These cells could either have a very low level of viral DNA synthesis, or none at all and represent a type of abortive cell, where viral replication began but was then inhibited. Class c has been counted as positive for viral DNA synthesis for this analysis, but an asterisk in figure 6.5 B shows there is some uncertainty here. This class is discussed further in section 6.5 below. Classes e and f do not have replication compartments, but have a diffuse ICP4 staining pattern. These cells could be slower in infection progression and have not yet formed replication compartments, which is the most likely, or infection could have been repressed by cellular mechanisms and they will

never progress to replication. Together, e and f comprise 25% of the cell population. Class e cells are not undergoing S phase, whereas class f have ongoing cellular DNA synthesis. Finally, cell class g are ICP4 negative and therefore may be uninfected with no detectable ICP4 protein expression. They are in S phase based on the EdC staining pattern. Class g accounts for 8% of the cell population. Overall, 65% of cells within this analysis have replication compartments, 25% have not yet formed replication compartments and the final 8% are negative for ICP4 (Figure 6.5 C). With regards to EdC incorporation, 11% have no ongoing DNA synthesis. 24% of the cells in the population have only viral replication, just over 40% have both viral and cellular DNA synthesis and 23% are only replicating cellular DNA (Fig 6.4 D).

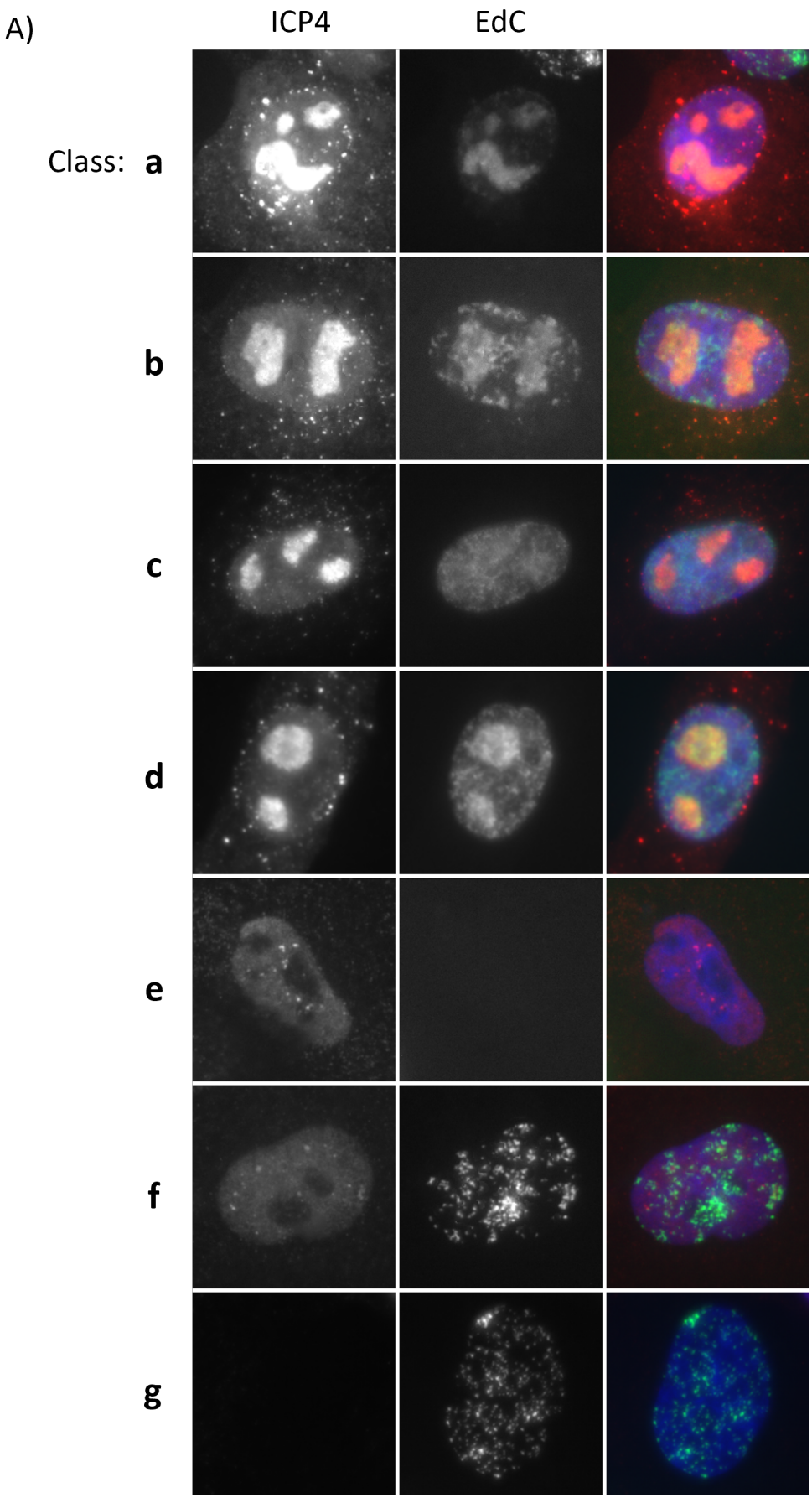
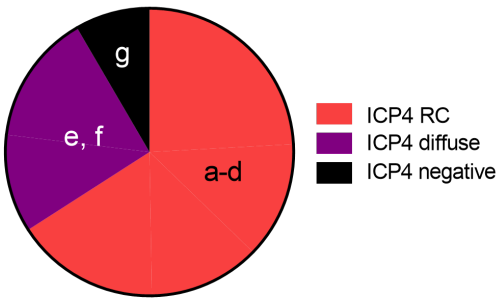


Figure 6.5: Continued on following page.

B)

Class	%	Viral DNA synthesis	Cell DNA synthesis	Characteristics
a	24.1	+	-	EdC incorporation within viral RC
b	13.1	+	+	EdC incorporation within viral RC and discrete regions of cellular EdC incorporation
c	12.5	+*	+	Diffuse EdC incorporation throughout the cell
d	16.1	+	+	EdC incorporation within viral RC and diffuse cellular EdC incorporation
e	11.0	-	-	No EdC incorporation, diffuse ICP4 protein with no viral RC
f	14.7	-	+	Discrete regions of cellular EdC incorporation, diffuse ICP4 protein with no viral RC
g	8.4	-	+	Discrete regions of cellular EdC incorporation, no ICP4 protein expression

C)



D)

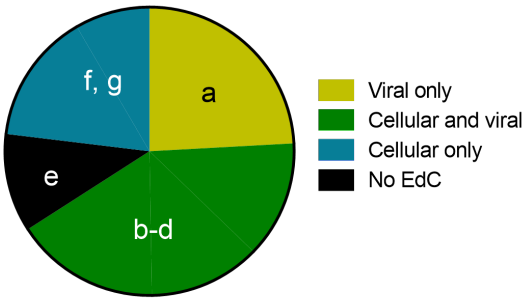


Figure 6.5: Classification of EdC labelled HSV-1 infected cells at 8 hpi.

A) 7 classes of Vero cells at 8 hpi after a 1 h EdC pulse. ICP4 protein (red) and EdC (green). B) Quantification of numbers of cells in each class, expressed as a percentage of the population. C) Proportions of cells with replication compartments (ICP4 RC), infected but without replication compartments (ICP4 diffuse) or uninfected (ICP4 negative). D) Proportions of cell with nascent replication viral, cellular, viral and cellular or no EdC incorporation.

There has been previous work by the labs of David Knipe and others identifying that if cells are infected by HSV-1 in G1, mitosis is blocked. However, if cells are infected in S phase mitosis can continue [212]. To examine this in our system, cells were pulsed with EdC for 1 hour before infection, then the EdC was washed out and the cells were infected with HSV-1. Cells were fixed at 8 hpi and processed for click chemistry and ICP4 protein. Quantification of the intensity of ICP4 and EdC staining using Fiji and analysis of the results led to the creation of 4 cell classes. Examples of each of the 4 classes are illustrated in figure 6.6 A, and summarised in the table in figure 6.6 B. Class A were ICP4 negative and were not in S phase at the start of infection. Class B are also uninfected, but were in S phase during the EdC pulse. Classes C and D are infected and are ICP4 positive. Class C were not in S phase, whereas class D were in S phase. Within class D, sometimes the cellular DNA that has incorporated EdC is pushed out by the replication compartments, leaving visible gaps behind which are occupied by viral DNA. In other cases this is not observed and the EdC labelled DNA remains diffuse throughout the cell. Often these cells have smaller replication compartments, suggesting they are not as advanced as the cells that are actively excluding cellular DNA from replication compartments. When infecting Vero cells, HSV-1 is equally able to form large replication compartments in cells that were in S phase (class D) as cells that were not (class C). 40% of cells lie in class C and 32% in class D (Fig 6.6 C, Pre-infection).

In contrast to labelling cellular DNA with EdC before infection there is an experimental way to specifically identify replicating cellular DNA at the endpoint of infection. Vero cells infected with HSV-1 where pulsed with EdC for 1h, from 7-8 hpi. However, PAA was added to inhibit viral replication just before the EdC pulse, therefore only cellular replication was ongoing and it was possible to examine S phase activity after 8 hours of viral infection. The pie chart in figure 6.6 D shows the quantification of the post-infection + PAA EdC pulse. The same ratio of cell classes is observed. There is no difference in the numbers of infected cells with ongoing S phase versus cells with no cellular replication. Therefore, the virus does not block S phase if the cell has already entered

it.

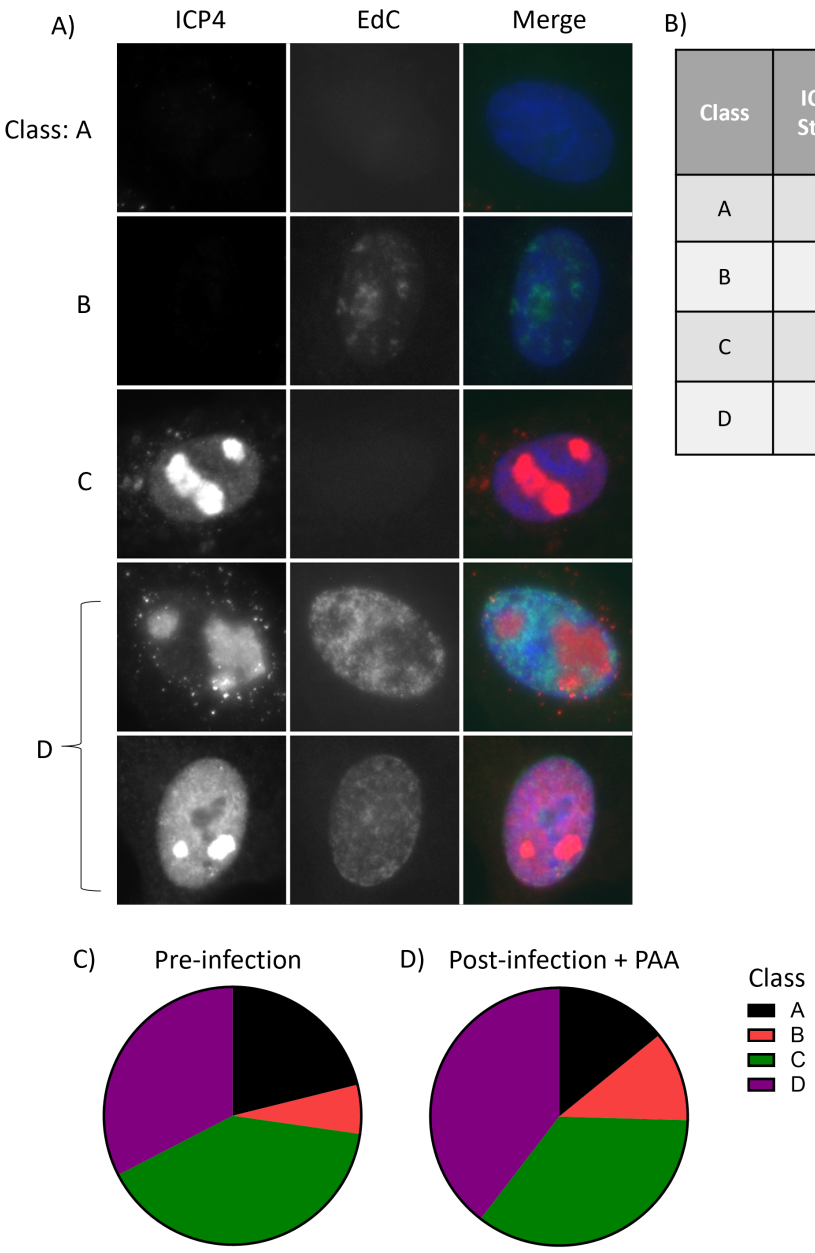


Figure 6.6: There is no preference for HSV-1 infecting mitotic cells.

Vero cells were pulsed with EdC for 1h prior to infection. Cells were fixed at 8 hpi. A) 4 classes of cells determined by infection or EdC incorporation. B) Table summarising the 4 classes of cells illustrated in part (A). C) Quantification of cell classes based on a EdC pulse label pre-infection D) Quantification of cell classes based on an EdC pulse label 7-8 hpi in the presence of PAA.

6.3 ICP8 is recruited to both viral and cell DNA replication sites

The EdC pulse label will reveal both replicating and replicated DNA. A large proportion of DNA that has replicated during the EdC pulse will have incorporated the modified EdC nucleotide, and this will include DNA that replicated at the beginning of the pulse which no longer represents an active site of replication. Therefore, the resolution of the click chemistry signal within replication compartments is low and it is very hard to gain accurate spatial information about the sites of active replication. To improve functional resolution within the replication compartment, an antibody against ICP8 protein was used. ICP8 is a ssDNA binding protein, binding at the replication fork as DNA unwinds. Infected cells pulsed with EdC for 1 h were processed for click chemistry and ICP8 protein by immunofluorescence at 8 hpi (Fig 6.7 A). In this cell there is a large viral replication compartment which is positive for EdC so therefore is replicating viral DNA. ICP8 protein forms many small foci throughout the replication compartment. In cells which have both cellular and viral DNA synthesis, we observed an interesting association. A representative cell has been chose to illustrate this finding. The cell in figure 6.7 B has both viral and cellular DNA replication. It has several relatively small viral replication compartments, marked with diffuse EdC and visible as regions of lower DAPI stain (shown by the solid filled arrows). In addition, there are areas of cellular DNA replication which do not exclude DAPI and have a distinct EdC incorporation pattern, indicated by the outline arrows. All the areas of DNA replication, both cellular and viral, contain ICP8 foci. This suggests that ICP8 binds and is recruited to both cellular and viral nascent DNA synthesis.

The addition of PAA to prevent viral replication reveals where ICP8 will localise when only cellular DNA synthesis occurs. Cell i in figure 6.7 C has no ongoing S phase, therefore ICP8 remains in tight puncta. In cell ii, which is in S phase, ICP8 is redistributed onto replicating cellular DNA. In summary, ICP8 can bind cellular DNA in the absence of viral replication.

As an additional confirmation, ICP8 and ICP4 antibodies were combined alongside an EdC

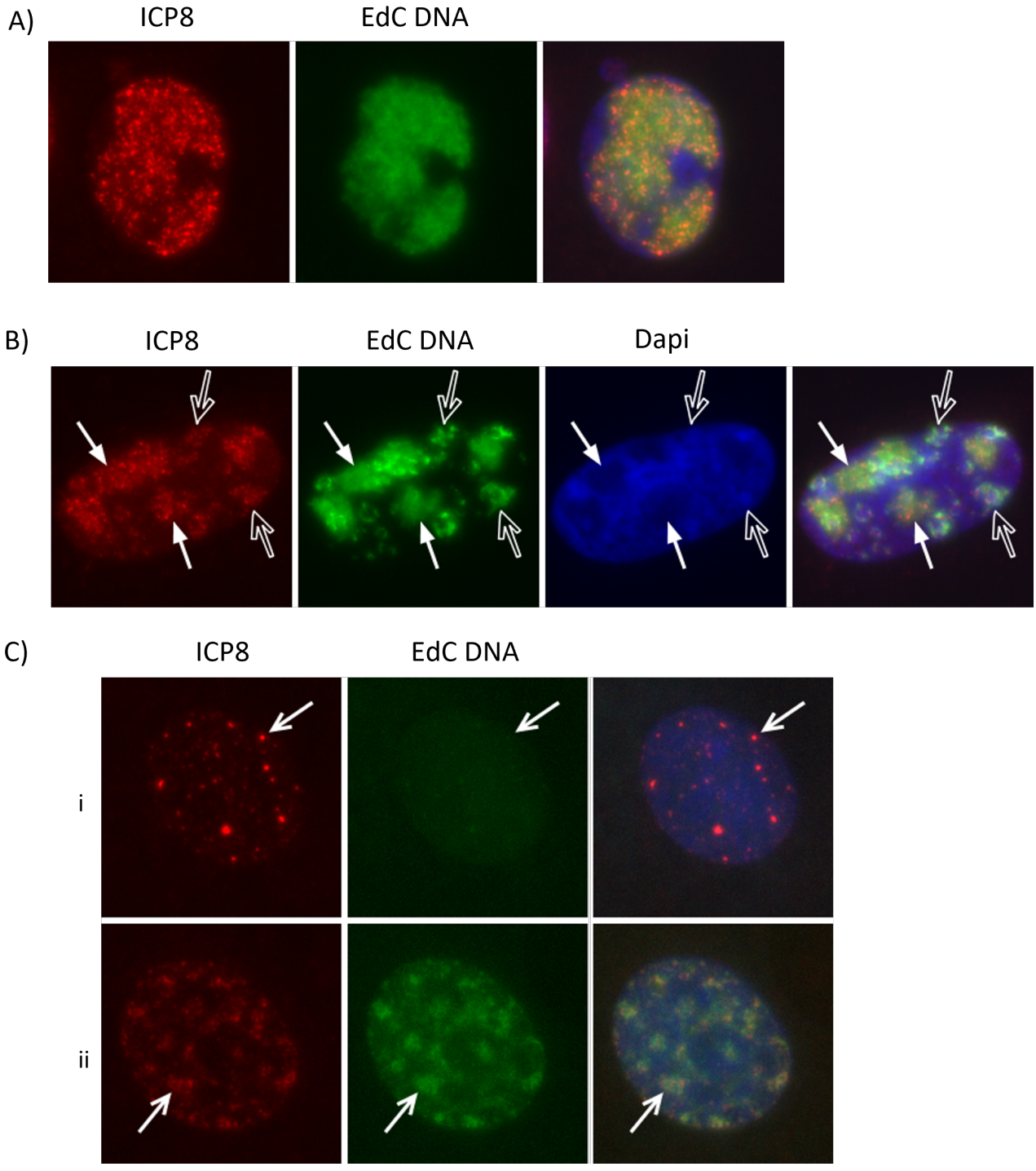


Figure 6.7: ICP8 provides better resolution than EdC patterns.

Vero cells, 8 hpi MOI 10, 1h EdC pulse. Processed for ICP8 protein (red) and click chemistry (green). A) Viral replication compartment positive for ICP8 and EdC signal. B) Viral and cellular DNA replication. Solid filled arrow: Viral replication compartment. Outline arrow: Cellular DNA replication. C) PAA present through infection to prevent viral replication. Cell i: No cellular replication. Arrow indicates a small ICP8 domain. Cell ii: cellular S phase replication. Arrow indicates a regions of EdC incorporation which is ICP8 positive.

pulse (Fig 6.8). In this experiment, a reduced length EdC pulse of 30 minutes was used. In cell i, the only DNA synthesis is occurring inside the ICP4 positive replication compartment. ICP8 protein is also restricted to this region. In cell ii, there are two replication compartments labelled by ICP4, which are positive for EdC, but the rest of the cell nucleus is also positive for EdC illustrating ongoing cellular replication. ICP8 in cell ii is distributed throughout the cell. The reduced pulse length of EdC has increased the resolution of the EdC pattern, and small foci can be identified. The expanded box from cell ii is showing a region of the viral replication compartment, with a small dot of EdC highlighted by the arrow. This EdC domain colocaliases with an ICP8 domain. The colocalistion is evidence that the ICP8 foci represent replication forks. Although the short EdC pulse provided increased resolution, it introduced technical difficulties when combined with RNAscope, therefore in the subsequent experiments ICP8 is used as a surrogate marker for replication forks and nascent replication.

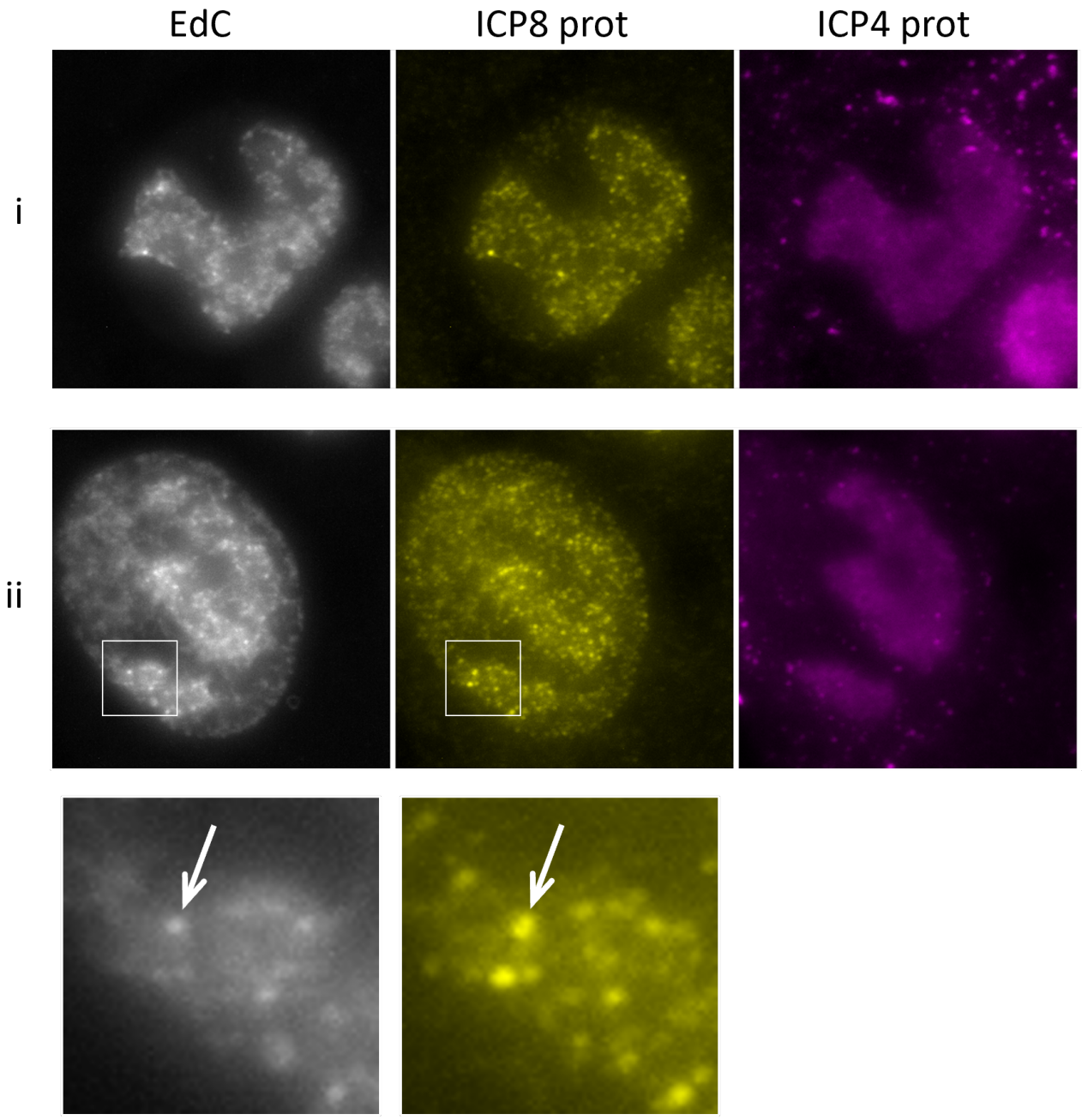


Figure 6.8: ICP8 binds both viral and cellular replicating DNA

Vero cells at 8 hpi, HSV-1 MOI 10. 30 minute EdC pulse. Processed for click chemistry (grey), ICP8 protein (yellow) and ICP4 protein (magenta). Cell i: A large ICP4 and ICP8 positive replication compartment with ongoing viral replication. Cell ii: two viral replication compartments with both viral and cellular DNA synthesis present in the nucleus. A small region is expanded, the arrow indicates colocalised EdC and ICP8 region.

6.4 Spatial separation of nascent replication sites and RNA transcripts

To examine the spatial relationship between transcripts and ICP8 foci, RNAscope needs to be combined with ICP8 protein immunofluorescence. As described previously, the effect of the protease step within the RNAscope protocol on the epitope recognised by an antibody needs to be evaluated for each antibody used in conjunction with RNAscope. In the case of ICP8, removal of the protease step improved the resolution of the protein foci without any loss of transcript signal, as shown in figure 6.9.

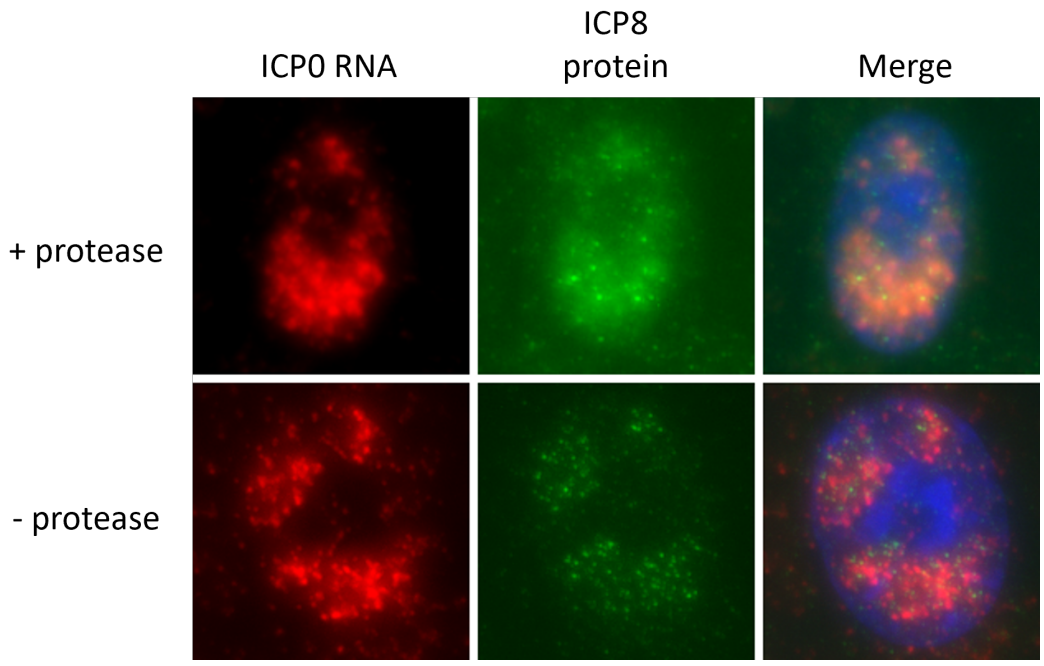


Figure 6.9: Withdrawal of protease step in RNAscope protocol improves ICP8 IF staining

Vero cells at 8 hpi, MOI 10. Processed for ICP) RNA (with or without the protease step) and IF (ICP8 protein).

Replication compartments were examined at 8 hpi for ICP0 RNA and ICP8 protein. Example cells are shown in figures 6.9 and 6.10. An expanded view of two regions from the replication compartment of the cell in figure 6.10, regions i and ii, reveal that there is no colocalisation between the

two channels. Quantification of pixel intensity along a line through region i confirms that the signal intensity peaks of the channels do not overlap (Fig 6.10 B). Therefore, there is a spatial separation of transcripts from nascent replication forks. Transcripts are segregated away from newly synthesised DNA and are instead accumulating on DNA that has already replicated. Although an EdC pulse label was not included in this analysis, it is assumed the replication compartment will be full of recently synthesised DNA, which is where the transcripts are accumulating.

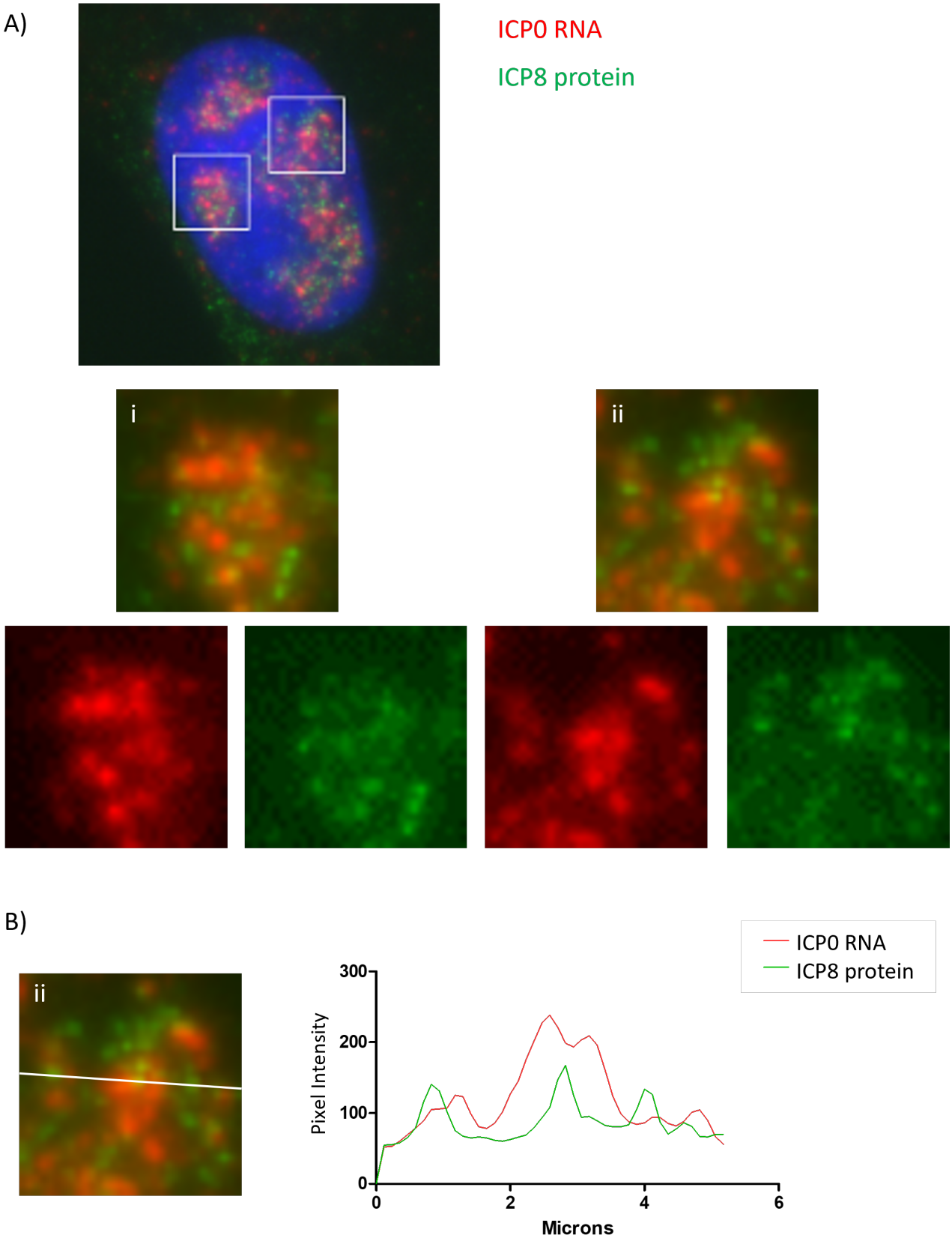


Figure 6.10: Spatial separation between ICP8 foci and RNA transcripts.

A) Vero cell at 8 hpi, HSV-1 MOI 10. ICP0 transcript (red) and ICP8 protein (green). Two expanded regions from the replication compartments, i and ii. Each channel from i and ii are displayed separately. B) Quantification of expanded region ii from (A). Intensity of both channels along the white line is measured and plotted.

6.5 Heterogeneity between replication and transcription

With these tools, various features regarding the relationship between transcription and replication can be investigated. Vero cells infected with HSV-1 were fixed at 8 hpi and processed for ICP0 RNA by RNAscope and ICP8 immunofluorescence. Cells with equivalent levels of ICP8 may have vastly different levels of transcription (Fig 6.11 A). Cells with similar levels of EdC incorporation, therefore similar rates of replication within the pulse duration also may have vastly different levels of transcript. The two cells in Figure 6.11 B have similarly sized replication compartments with similar EdC staining. However, the cell on the left has a large amount of ICP0 transcript in contrast to the right hand cell which has relatively little. The differences between replication and transcription shown by the cells in figure 6.11 A and 6.11 B suggest a degree of uncoupling between the two, that a high replication amount does not directly correlate with a high transcription rate.

In addition to heterogeneity existing between cells, it can be observed between replication compartments within one cell. The cell in figure 6.11 C has four ICP4 positive replication compartments, all of which are actively replicating DNA. The replication compartments are outlined in white, as is the edge of the nucleus. There is additional cellular S phase replication. There is relatively little VP16 transcript, with one replication compartment completely negative for transcript. This analysis was only performed with one class of transcript and needs to be extended for other RNA genes. Although negative for VP16, that replication compartment may be highly active for an IE gene, for example.

Class c cells in figure 6.5 may represent a type of abortive infected cell. Abortive infected cells are infected by HSV-1, and will have detectable levels of gene expression, but are restricted at some point during infection and will not produce any progeny viruses. If the abortive cells are cultured the HSV-1 genomes can lie dormant and sporadically reactivate, suggesting a non-neuronal form of latency [213]. It is not known what triggers an abortive infection, but it has been linked to the

expression of anti-viral genes and IFN induction which would normally be blocked [156]. Another example of a class c cell is presented in figure 6.12 A, with replication compartments outlined in white. Although not negative for EdC, there is no enrichment over cellular S phase levels. To investigate the transcriptional activity inside class c cells, ICP0 RNA transcripts were examined, in combination with an EdC pulse and immunofluorescence for ICP4. An example cell is shown in figure 6.12 B, and two replication compartments have been outlined in white. One replication compartment has a small accumulation of transcript, whereas the other only has one single transcript molecule. Therefore the replication compartments in class c cells have a low level of transcription. However, the analysis would need to be extended to a larger number of cells to show this was a common feature of class c cells.

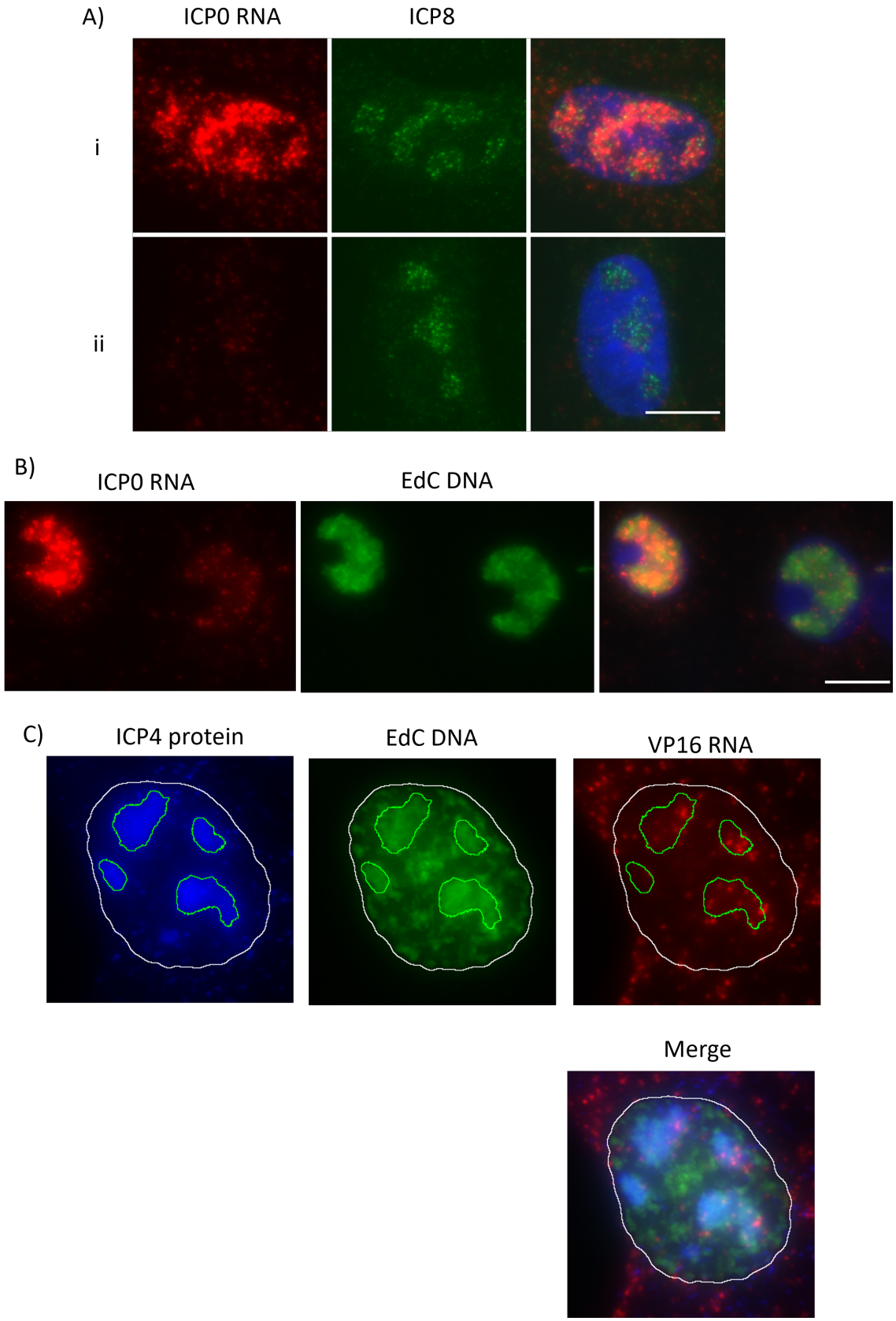


Figure 6.11: Intercellular heterogeneity

Vero cell at 8 hpi, HSV-1 MOI 10. A) ICP0 RNA and ICP8 protein. Scale bar 10 microns. B) 1h EdC pulse. Processed for RNA scope (ICP0) and click chemistry. Scale bar 10 microns. C) 1h EdC pulse. Processed for RNAscope (VP16), IF (ICP4) and click chemistry. Nuclei outline in white, replication compartment outline in green (based on ICP4).

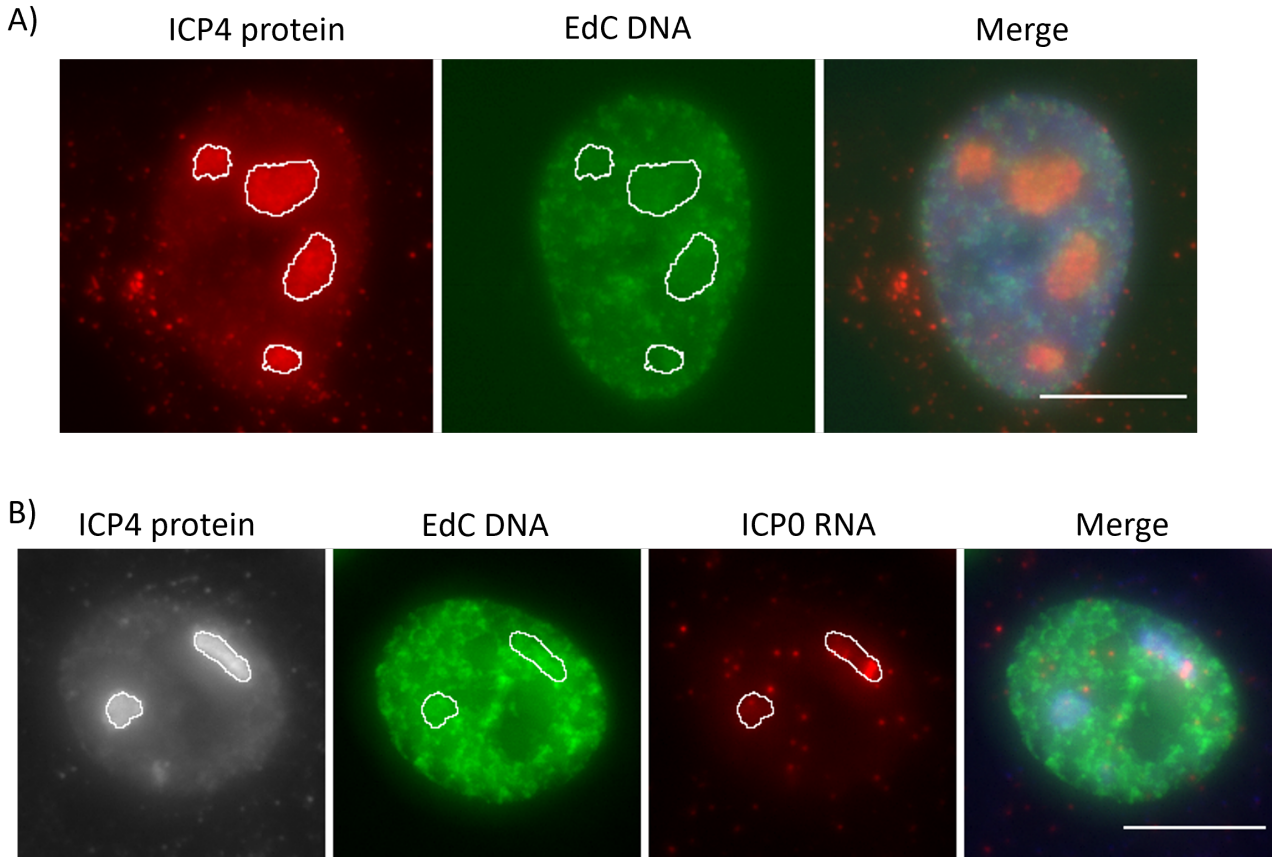


Figure 6.12: Viral Replication compartments may have very low replication.

Vero cell at 8 hpi, HSV-1 MOI 10. 1h EdC pulse. Replication compartments outlined in white. Scale bar 10 microns. A) Processed for click chemistry and IF (ICP4). B) Processed for click chemistry, RNAscope (ICP0) and IF (ICP4).

6.6 Discussion and Future Perspectives

Within this chapter I have examined transcription at late timepoints in a lytic infection. I have achieved high resolution of transcription and nascent DNA replication within replication compartments, allowing conclusions about the organisation of the two processes to be made.

When HSV-1 genomes enter the cell, they begin to decompact. Many host and viral proteins interact with the infecting genome, and eventually will form the replication compartment. As infection progresses the replication compartments expand and merge, although it is thought that the original genomes maintain distinct territories within the compartments. The compartments are the site of DNA replication, transcription and encapsidation [214, 215].

RNAscope on cells fixed at 8 hpi reveals a distinct localisation pattern for transcript. VP16 RNA is found within the replication compartments and in the cytoplasm, yet there is very little transcript present throughout the rest of the nucleus. We believe there is a rapid transport of transcript out of the replication compartment to the cytoplasm. Alternatively, there may be inefficient transport and little nascent transcript production. I was able to begin preliminary experiments using Actinonmycin D to inhibit transcription and examine the longevity and location of both IE and VP16 transcripts. Unfortunately I was not able to complete the analysis, but the initial results showed the amount of nuclear transcript decreased with ActD treatment suggesting that there is active transcription and export. Future work should continue these experiments.

In 2018, Pheasent et al., from the lab of Gill Elliot published RNAscope data from an HSV-1 infection [216]. During their investigations of the viral endouclease virion host shutoff (vhs) they show the inhibition of nuclear export of IE and E transcripts, and the role of viral protein VP22 which specifically allows L transcripts to leave the nucleus for transcription. Their experiments were performed in HFFF cells, which have a different phenotype to the Vero cells I am working with. Differing from my results, they did not observe a retention or accumulation of transcripts within the

replication compartments. However, the differences between the export of IE and L transcripts they discuss are also observable within my results. Figure 6.1 shows the transcripts of ICP0 and VP16 at 8 hpi. There is a greater proportion of VP16 RNA in the cytoplasm than for ICP0, which is almost completely nuclear. At late phases of infection, the preferential export and therefore translation of L genes promotes the production of progeny virions. The transcription inhibition experiments proposed in the previous paragraph could also provide detail on the export of L versus IE transcript, most notably if multiplex analysis of both gene classes was used.

I have presented evidence that ICP4 specifically recognises HSV-1 DNA whereas ICP8 will bind both viral and cellular DNA. If correct, this will have implications on some published HSV-1 research. For example, a proteomics screen for ICP8 binding partners may not be identifying proteins with a role in HSV-1 replication [217]. Immunofluorescence for ICP8 or ICP8 tagged with fluorescent proteins has been used to identify pre-replicative sites [215, 218]. In contrast to ICP8 staining indicating the start of a replication compartments, ICP8 may only be localising to cellular DNA synthesis or repair.

An argument against my hypothesis regarding ICP4 and ICP8 DNA binding may suggest I am not observing S phase replication. DNA repair would also result in the incorporation of EdC into cellular DNA. I would like to highlight two specific examples from the results in this chapter; figure 6.3 C and cell ii from figure 6.8. They both show viral replication compartments with ongoing cellular synthesis, however the cellular replication appears as different patterns. The small patches of cellular synthesis may just be a type of S phase, however it is also possible that this is EdC incorporation that is linked to DNA repair.

Early studies investigating RNA transcription and DNA replication within the replication compartments proposed that the processes are linked at early timepoints, but as infection progresses the virus prioritises DNA replication. Using Br-UTP labelling for RNA and biotin-dUTP for DNA

and antibodies they identified replication compartments that were transcriptionally active, but also described addition areas of DNA replication that were not transcriptionally active. It is likely they were observing replication compartments increasing in size, with an uneven distribution of RNA synthesis within them. The premise for heterogeneity of transcription within replication compartments was therefore proposed over twenty years ago [219]. My data agree with the hypothesis of a high degree of heterogeneity. I observe many cells with replication compartments of similar size and appearance when stained with ICP4 yet have widely varying levels of DNA replication and transcription. Although the majority of the replication compartments I observe are transcriptionally active, there are many which are only transcribing at a very low level.

There is mechanistic uncoupling between DNA replication and transcription. Replication compartment formation and nascent DNA synthesis do not predict rates of late transcription. Such uncoupling can be observed both between neighbouring cells and between replication compartments in one cell. The next steps with this analysis would include multiplexing of RNAscope probes. The replication compartments that I have observed which have no transcript of one particular gene may very well be transcribing another gene. Initially I would propose an experiment with ICP8 protein and the RNAscope probes for ICP0 and VP16, which would generate data on transcription of genes from two temporal classes.

Chapter 7

Spatial analysis of host cell transcription during HSV-1 infection

There is a dramatic change to host cell transcription induced during HSV-1 infection. The viral tegument protein vhs induces rapid mRNA degradation, and the virus recruits RNA polymerase machinery away from host cell DNA therefore shutting down a large proportion of host transcription. This shut off gives multiple advantages to the virus such as increasing availability of resources and preventing the transcription of antiviral genes. Although some research has indicated that there is a complete loss of RNA pol II from host DNA, other work has demonstrated aberrant transcription with defects at termination [220, 221]. It is likely that the virus will allow transcription of genes that promote viral infection. There have been multiple studies examining changes to the host cell transcriptome using RNA sequencing both by single cell and population analysis. There have also been experiments examining the association of viral and cellular proteins across the host and viral genomes by CHIP-seq or PRO-seq. There is a high degree of variability in the omics datasets between cells, cell types and viral dose, making them problematic to analyse and interpret [222].

Within this chapter I aim to examine novel features revealed by spatial single cell analysis. By utilising the techniques developed within this thesis I hope to bring to light new understanding of global transcriptional changes.

7.1 Characterisation of HSV induced transcription territories

The cell nucleus is highly condensed and highly organised. When an HSV-1 genome enters the nucleus, it will encounter this compact environment. Chromatin domains are separated by regions of interchromatin space which provide channels to the nuclear pores and through the dense heterochromatin. The interchromatin space contains many functional regions, including nuclear bodies, splicing speckles and transcriptional factories which contains large amounts of RNA polymerase II [223]. It is likely that HSV-1 viral genomes are utilising transcription factories for their own transcriptional requirements. Most investigations into nascent transcription and the interplay of host polymerase recruitment have used global population analysis. Here, I will use click chemistry to study transcription at the spatial level.

5-Ethynyl-uridine (EU), a metabolic precursor, can be supplied to cells in a defined pulse length. It is incorporated into RNA transcripts, and will react in a copper catalysed click chemistry reaction with an azide fluorophore, revealing the location of RNA transcripts synthesised within the pulse duration. Uninfected cells were pulsed with 1 mM EU for 1 h and then fixed in 4% PFA, followed by a click chemistry reaction. This revealed RNA synthesis within the pulse duration, illustrated by an example cell in figure 7.1 A. There was a large region within the nucleus with an increase in EU staining which is the nucleolus, the site of rRNA transcription by RNA polymerase I. The remainder of the nucleus contains a more diffuse stain, representing RNA pol II transcription. Control cells that were not incubated with EU and processed for click chemistry demonstrated that the background level is very low.

To confirm EU is being incorporated into nascently transcribed RNA, cells were treated with ActD at 5 μg/mL to stop all transcription, followed by an EU pulse in the continued presence of ActD. In figure 7.1 B, no EU is visible. A low dose of ActD at 50 ng/mL inhibited RNA pol I transcription, but not RNA pol II transcription, so there is no nucleolar transcription yet the RNA pol II transcription

throughout the rest of the nucleus is still visible by EU incorporation (Fig 7.1 B).

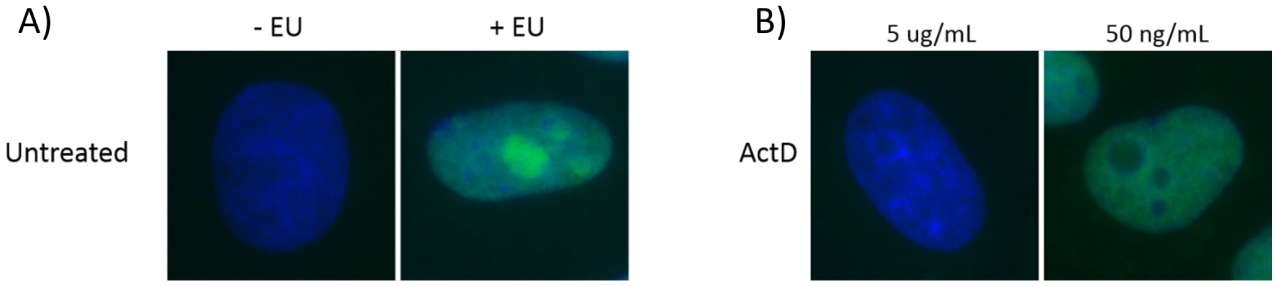


Figure 7.1: An EU pulse labels ongoing RNA synthesis

A) Vero cells, no EU pulse (-EU) and with a 1 h 1 mM EU pulse (+EU). Processed with click chemistry. B) Vero cells pulsed with 1 h 1 mM EU pulse and treated with ActD for 1 h at two concentrations. Processed for click chemistry.

Infection with HSV-1 profoundly affects the synthesis of host cell RNA. Cells were infected with HSV-1 and pulsed with EU for 1 h prior to fixation at 3 hpi, therefore the EU pulse was from 2-3 hpi. As shown in figure 7.2 A there was significant disruption to the compaction of the nucleolus by HSV-1 infection. The boundary around the nucleolar space becomes less defined, with some regions appearing to plume outwards. There is also a drop in RNA pol II transcription, shown by decrease in the EU incorporation in the nucleoplasm. In addition, a novel feature appeared. Small EU foci appeared throughout the cell at 3 hpi, likely representing small active regions of transcription. These regions could represent sites of viral transcription, they could be nucleolar transcripts released from the disrupted nucleolus or they could represent highly active sites of RNA pol II cellular transcription. I will refer to these EU foci subsequently as HSV-1 induced transcription territories, HITTs.

To begin to assess the spatial association of the EU HITTs with viral infection the 1 h EU pulse label from 2-3 hpi was combined with immunofluorescence for ICP4 in cells infected with HSV-1 and fixed at 3 hpi. This revealed that many of the EU HITTs colocalised with ICP4 (Fig 7.2 B). The three example cells in figure 7.2 B all have multiple EU HITTs. In cell i, the outline arrow

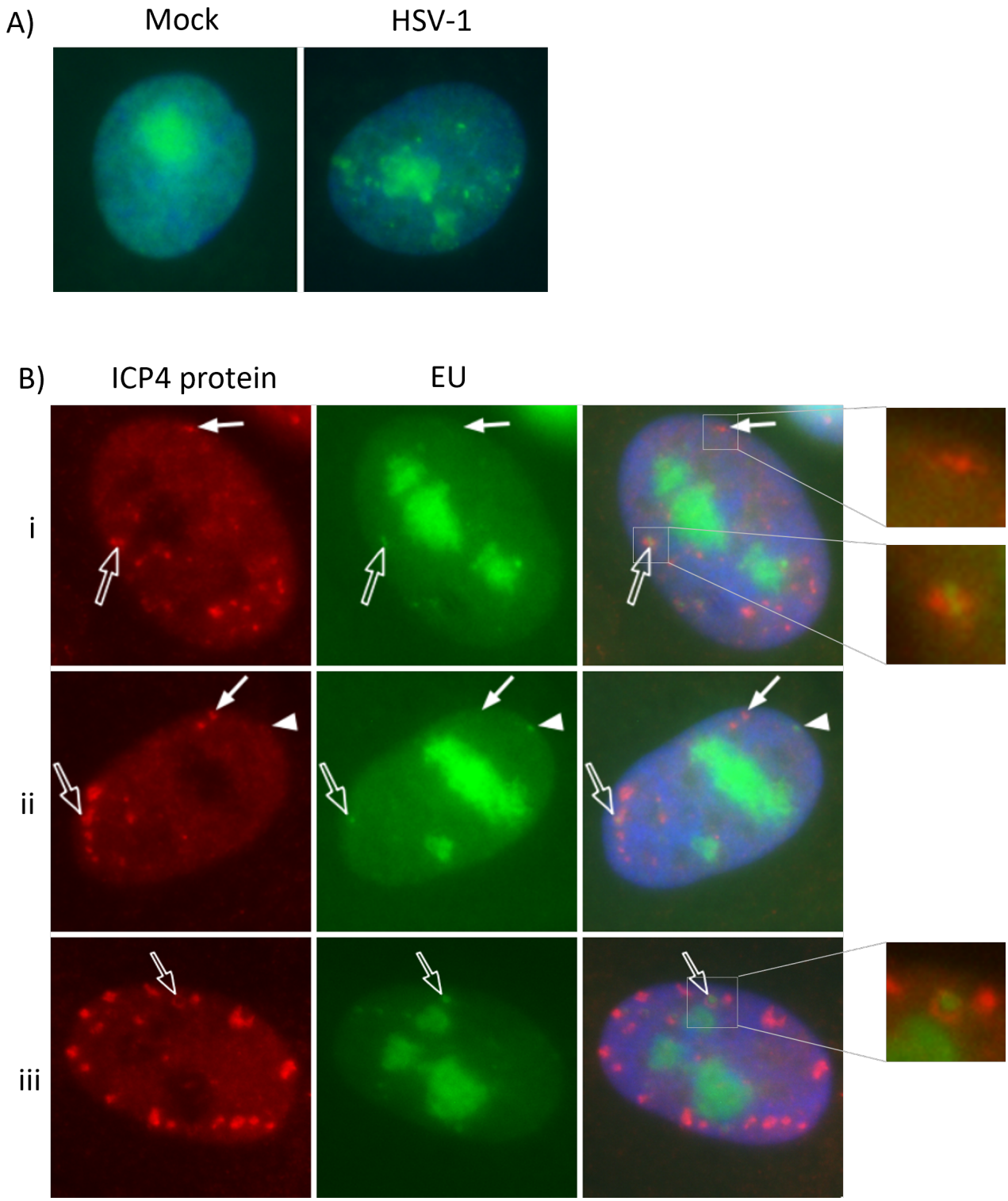


Figure 7.2: EU labels ongoing RNA synthesis

A) Uninfected Vero cell (Mock), 1 h EU pulse (green). HSV-1 MOI 10, 3 hpi, Vero cell, 1 h EU pulse (2-3 hpi). Processed for click chemistry. B) Three example Vero cells infected with HSV-1 MOI 10, 3 hpi, 1h EU pulse (2-3 hpi). Processed for IF (ICP4 protein, red) and click chemistry (green). Outline arrow: colocalising ICP4 and EU HITT. Solid filled arrow: ICP4, no EU. Arrow head: EU, no ICP4.

is showing an EU HITT that is adjacent to small regions of ICP4. There are also ICP4 domains that do not colocalise with EU HITTs, such as the region indicated by the solid filled arrow. In cell ii, there are again colocalising HITTs and ICP4 (outline arrow) and ICP4 without HITTs (filled arrow). Additionally, the arrow head represents a HITT that is negative for ICP4. Cell iii provides an example of how the ICP4 and HITT proximity can sometimes appear, with ICP4 forming a ring around the EU HITT indicated by the outline arrow and shown in the enlarged box. To summarise, ICP4 protein can clearly be found adjacent to the EU HITTs but it is not always the case.

To investigate the hypothesis that EU HITTs may represent the site of viral transcription, Vero cells were infected with HSV-1 and pulsed with 1 mM EU for 1 h before fixing cells at 3 hpi. Cells were processed for ICP0 RNA followed by a click chemistry reaction to reveal total nascent RNA. Two cells are shown as an example in figure 7.3 A. Both cell i and cell ii have multiple transcription bursts and HITTs. HITTs are indicated by the short filled arrows, and it is clear that the HITTs do not colocalise with ICP0 transcription bursts. Several transcription bursts which are indicated with the outline arrows, and therefore the viral genomes, do not colocalise with HITTs. Although other IE and E viral genes have yet to be tested alongside the EU pulse label, it is likely they will all exhibit the same behaviour.

It is not possible to perform two click chemistry reactions simultaneously to visualise both HSV-1^{EdC} genomes and EU incorporation. Therefore, aside from the ICP4 protein staining used above, ICP0 intron RNA is another accurate indicator of HSV-1 genome location. Cells that had been infected with HSV-1 were pulsed with 1 mM EU for 1 h prior to fixation at 3 hpi. The cells were then processed for click chemistry and ICP0 intron transcripts. None of the ICP0 transcripts were adjacent or colocalised with EU foci (Figure 7.3 B). Therefore, it is very likely that viral genomes are not at the sites of the EU HITTs, despite the data showing ICP4 protein colocalisation.

The proximity of ICP4 to some EU HITTs indicates the possibility that ICP4 plays a role in

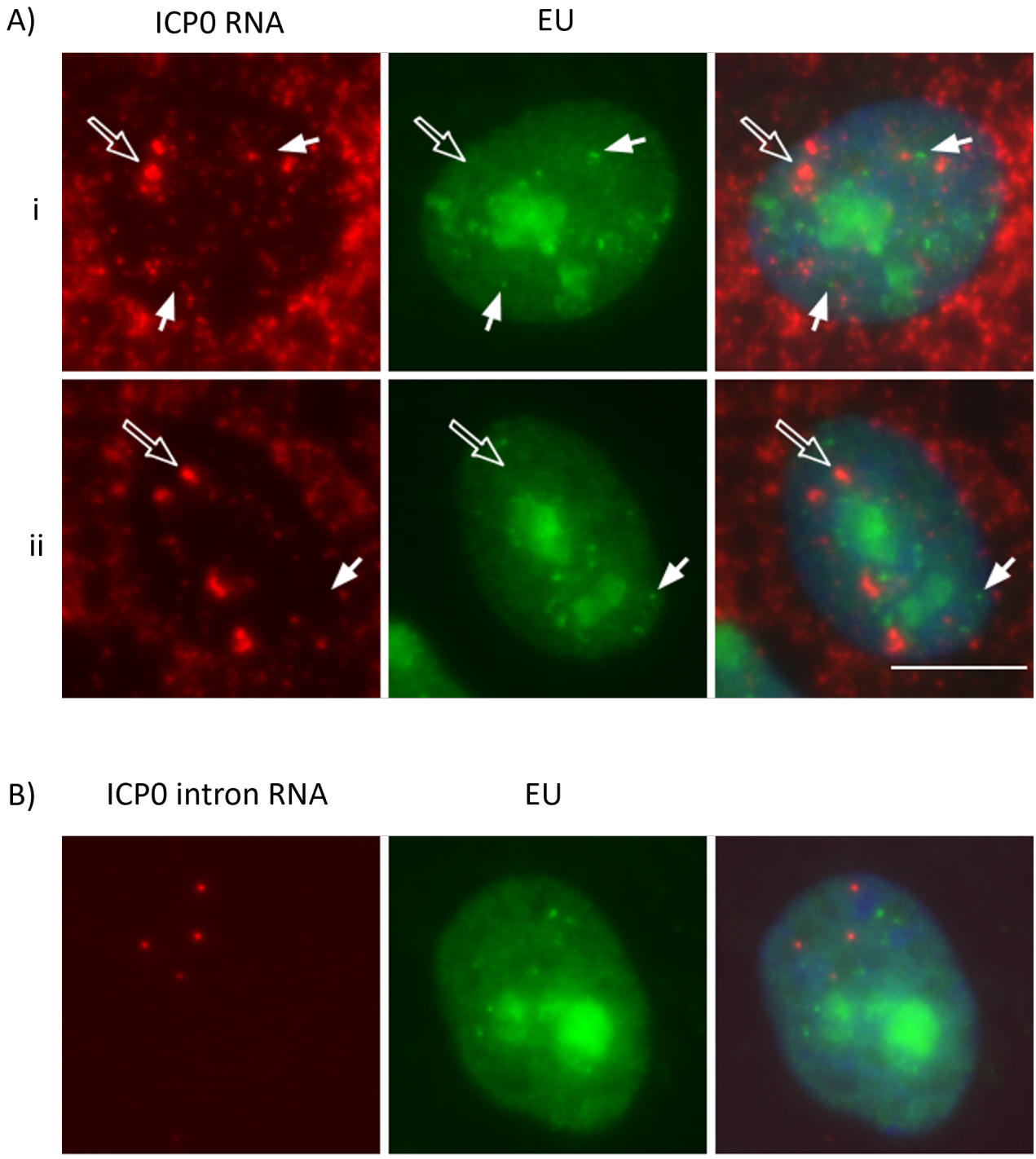


Figure 7.3: EU HITTs are not sites of viral transcription

Vero cells, 3 hpi, HSV-1 MOI 10. 1h EU pulse (2-3 hpi). A) ICP0 exon RNA (red) and click chemistry (green). Short filled arrows: EU HITTS, no RNA. Outline arrow: ICP0 transcription burst, no EU HITT. B) ICP0 intron RNA (red) and click chemistry (green).

their formation. In order to address this question, the n12 mutant virus with a non functional ICP4 was used. The ICP4 gene lacks the NLS containing region and therefore the ICP4 is not able to localise to the nucleus. Cells were infected with n12, pulsed with EU for 1 h and then subjected to

a click chemistry reaction and ICP4 immunofluorescence. In the absence of functional ICP4 protein, no HITTs were observed (Fig 7.4). This is despite the large amount of viral transcription already shown to be present at this timepoint during an n12 infection (Fig 4.2). The results in figures 7.3 and 7.4 strongly indicate that the HITTs are not regions of viral transcription but are induced by viral infection.

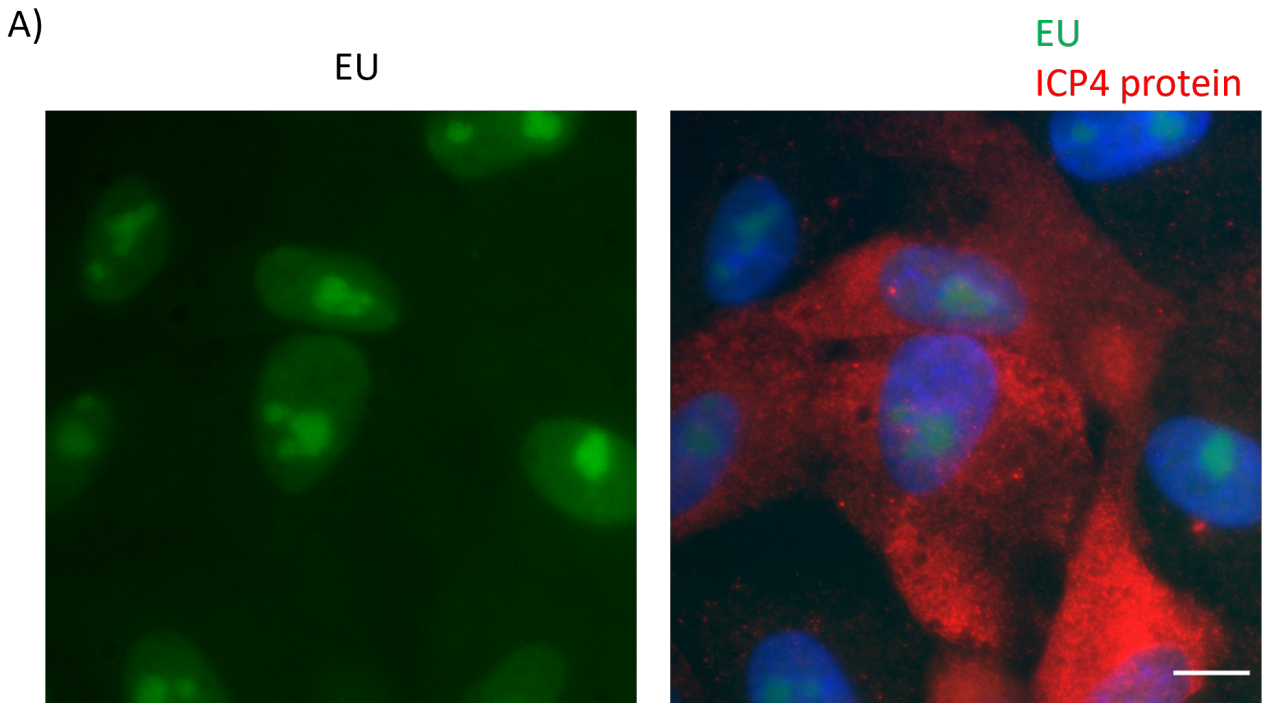


Figure 7.4: ΔICP4 HSV-1 does not induce EU HITTs

A) Infection with n12, MOI 10, 3 hpi. 1h EU pulse (2-3 hpi). Processed for click chemistry (green) and IF for ICP4 protein (red). The EU channel is displayed next to the merged image. Scale bar 10 microns.

7.2 Differential effect of inhibition of Cdk9 on virus versus host transcription

DRB is an inhibitor of transcription through a different mechanism to ActD. Actinomycin D intercalates into DNA, whereas DRB inhibits RNA pol II CTD phosphorylation through inhibition of Cdk9, achieved by binding of DRB near the ATP active site [224, 225]. The aim of using DRB was to determine if the HITTs were host cell nucleolar transcripts and thus due to RNA pol I. It was hypothesised that nucleolar disruption during HSV-1 infection would release aggregates of pol I transcript and therefore the HITTs were not novel transcription territories. Therefore the HITTs could be due to HSV disruption of nucleolar transcription.

To confirm the action of DRB, the levels of phosphorylated Serine 2 (pSer2) in the RNA pol II CTD were assessed by western blot. With increasing DRB treatment length at 50 μg/mL, the level of pSer2 decreased (Fig 7.5 A). IFN treatment activates a large group of IFN inducible genes, including the Mx1 protein. To confirm the activity of DRB on preventing the transcription of inducible cellular genes, protein and RNA levels of Mx1 were examined by immunofluorescence and RNAscope respectively. At the protein level, 6 h of IFN treatment induces a large production of Mx1 yet there is no induction after IFN treatment in the presence of DRB (Fig 7.5 B). At the RNA level using RNAscope probes against Mx1, there is a significant induction of nuclear transcripts of Mx1 in the presence of IFN. When DRB is present, there is no IFN induction of transcription of Mx1 (Fig 7.5 C).

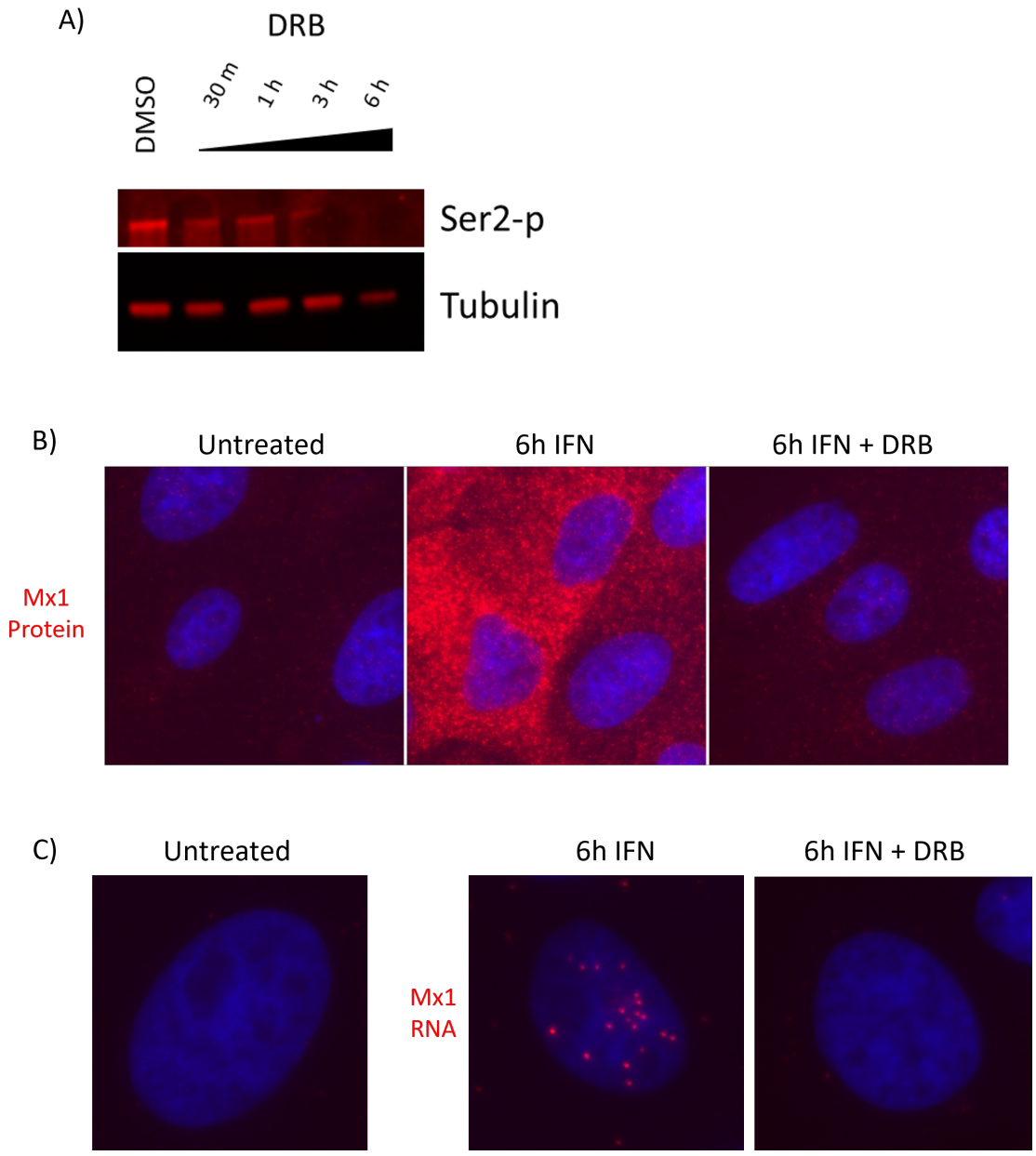


Figure 7.5: DRB inhibits transcription.

A) Abundance of RNA pol II CTD phosphorylated serine 2 (Ser2-p) by western blot. Cells were treated with a DMSO vehicle control for 6h or for DRB at 50 μg/mL for various times. B) Expression of Mx1 protein by IF in untreated cells, cells treated with 6h 500 U IFNα, and cells treated with IFNα + 50 μg/mL DRB. C) Processed for RNAscope (Mx1), same treatment conditions as in part (B).

Cells were infected with HSV-1 at MOI 10 in the presence of varying concentrations of DRB. Cell lysates were collected at 3 hpi and 6 hpi and analysed by western blot. At the protein level, DRB prevented the expression of ICP0 in a dose dependent manner (Fig 7.6 A). At 1 hpi, viral transcription in cells infected with HSV-1 is inhibited by DRB as expected (Fig 7.6 B, Fig 5.12 C). However, RNAscope at 3 hpi in cells infected by HSV-1 in the presence of DRB revealed an interesting result. Rather than transcriptional inhibition by DRB at 3 hpi, in the presence of DRB at 3 hpi there were large intense transcription bursts with very little cytoplasmic transcript (Fig 7.6 C). The bursts were not atypical for IE transcription bursts, they were larger and more intense. This suggests that even with inhibition of the phosphorylation of Ser2 in the CTD of RNA pol II, the virus is able to circumvent the normal requirement of Ser2 phosphorylation to release the paused RNA pol from the elongation checkpoint to transcribe mRNA. However, there is very little cytoplasmic transcript or transcript moving from the sites of the bursts or therefore the genomes. This suggests inefficient release and export of transcripts and that there is still a role for Cdk9 at transcription termination.

Further evidence that viral genomes are transcriptionally active in the presence of DRB is gained by HSV-1^{EdC} infections. Cells were infected with HSV-1^{EdC} in the presence of DRB. By 3 hpi, the two example cells presented in figure 7.6 D show that the genomes that have ICP0 transcription bursts exhibit genome decompaction. This is characterised by the diffuse EdC signal, and was described in [165]. The intriguing effect of DRB mediated inhibition of Cdk9 on viral transcription is discussed further in section 7.4.

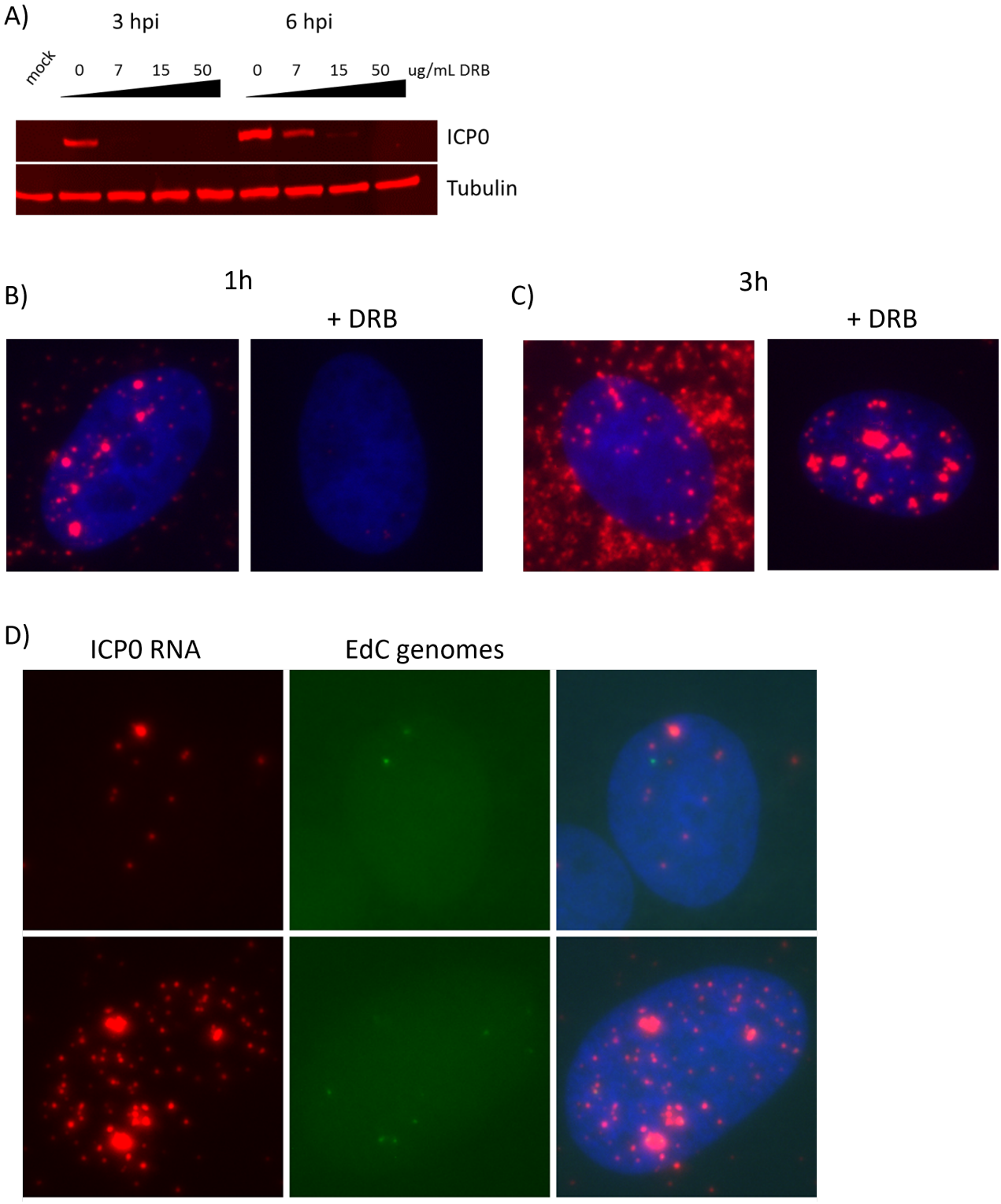


Figure 7.6: DRB has a profound impact on viral transcription.

Vero cells. A) Uninfected cells (mock), and cells infected at MOI 10 with DRB at 7, 15 and 50 μg/mL, or untreated (0 μg/mL) at 3 hpi and 6 hpi. ICP0 and tubulin expression analysed by Western blot. B) 1 hpi, with or without 50 μg/mL DRB. Processed for RNAscope (ICP0). C) 3 hpi, with or without 50 μg/mL DRB. Processed for RNAscope (ICP0). D) Infection with HSV-1^{EdC}, 3 hpi, + 50 μg/mL DRB. Two example cells. Processed for RNAscope (ICP0) and click chemistry.

I have established that the HITTs are not associated with ICP0 viral transcription. To determine if they may be sites of cellular transcription, uninfected cells were treated with DRB and with a 1 h EU pulse label before fixation. As DRB specifically prevents RNA pol II transcription the level of nuclear EU staining is reduced compared to untreated cells, however the nucleolar RNA pol I transcription continues. A phenotype previously described as 'nucleolar necklaces' is observed as the nucleolus loses definition and small subunits spread out, which are thought to be extended linear arrangements of active rRNA genes (Fig 7.7 A) [226]. Figure 7.7 B shows two HSV-1 infected cells; one infection was carried out under standard conditions and the other in the presence of DRB. In the DRB treated cells there are no EU foci present, therefore DRB inhibits the formation of HITTs in HSV-1 infected cells. In this experiment the analysis was combined with RNAscope to validate the effect of DRB at the viral RNA level, with the results confirming the conclusions from figure 7.6. In the presence of DRB when RNA pol II transcription is inhibited but nucleolar transcription, although disrupted, is ongoing, there are no HITTs formed. This strongly suggests that the HITTs are not aberrant releases of RNA pol I transcription released from the nucleolus.

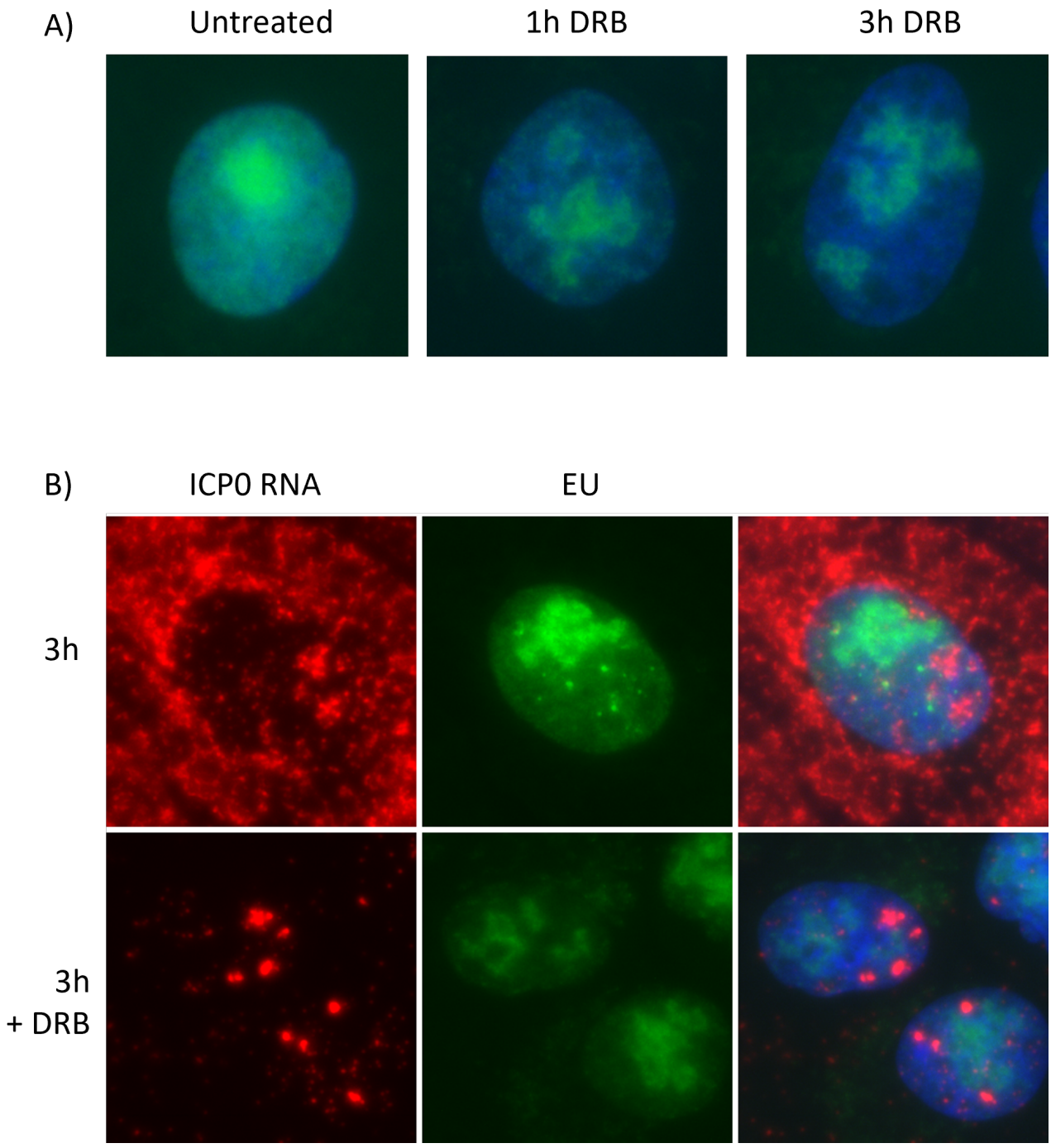


Figure 7.7: EU HITTs are cellular transcription sites.

A) Vero cells, 1h EU pulse. Either untreated, treated with 1h 50 μg/mL DRB or with 3h 50 μg/mLDRB. Processed for click chemistry. B) Vero cells, 3 hpi, +/- 50 μg/mL DRB. 1h EU pulse (2-3 hpi). Processed for ICP0 RNA (red) and click chemistry (green).

7.3 Reorganisation of RNA polymerase II during HSV-1 infection

Having shown that HITTs were not due to RNA pol I, I next wished to investigate processes that were involved in inducing HITTs and in particular the potential involvement and colocalisation with RNA pol II. During HSV1 infection, RNA pol II is recruited for viral transcription and there is a gradual shutoff of host cell transcription. In mock infected cells, RNA pol II protein appears as a diffuse nuclear stain. Small foci of RNA pol II develop by 2 hpi, and at later timepoints the majority of RNA pol II is recruited inside replication compartments (Fig 7.8 A).

Examination of the location of HITTs at 3 hpi in infected cells in relation to the location of RNA pol II CTD foci is presented in figure 7.8 B. Cells were infected with HSV-1 at MOI 10 and pulsed with EU for 1h before fixation at 3 hpi. The cells were then processed for click chemistry to reveal EU incorporation and immunofluorescence for RNA pol II. The first example cell has two arrows, both indicating HITTs. The HITT labelled by the filled arrow has an accumulation of RNA pol II adjacent to it, almost encircling it. The outline arrow is indicating an HITT that has not accumulated any RNA pol II. In the second example cell, the filled arrow is again labelling a HITT with a large RNA pol II CTD domain associated. The arrow head is showing an RNA pol II CTD domain that is negative for EU. The accumulation of RNA pol II CTD around the HITTs adds further evidence to the hypothesis that these are highly active areas of transcription. However, there are EU foci that do not have any colocalising RNA pol II so it is not consistent across all HITTs.

To determine if newly synthesised viral proteins are required for the induction of RNA pol II CTD foci, infections with HSV-1 were performed in the presence of CHX to prevent protein synthesis or with PAA to inhibit viral replication. There is no change to RNA pol II CTD or pSer5 staining in uninfected mock cells treated with either CHX or PAA (Fig 7.9 A). Figure 7.9 B shows untreated cells at 2 hpi and 4 hpi. The CTD foci are visible at 4 hpi, though in this infection they form more

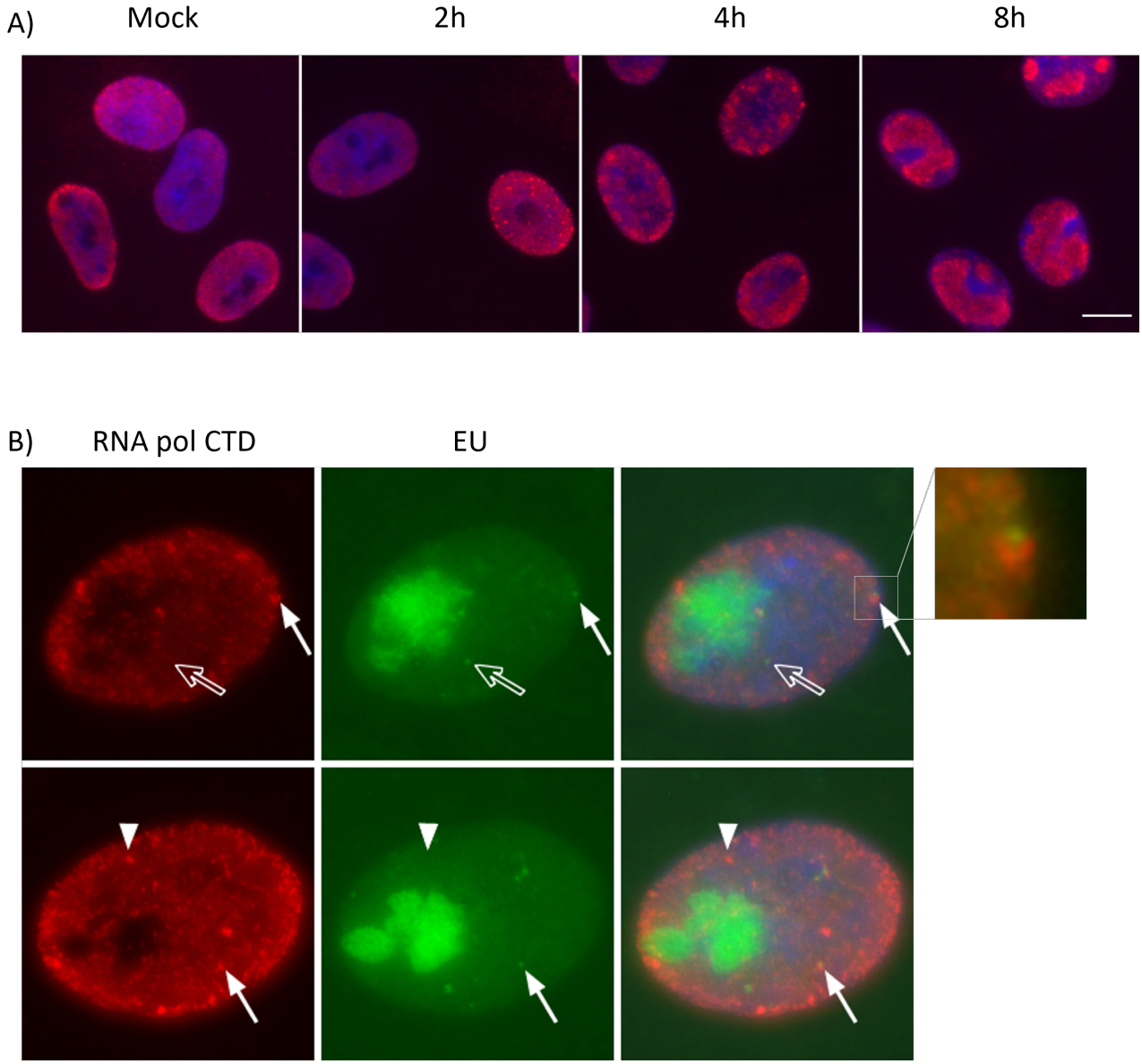


Figure 7.8: RNA polymerase can colocalise with EU HITTs

A) Vero cells, mock or infected with HSV-1 MOI 10 and fixed at 2, 4 and 8 hpi. Processed for IF (RNA pol II CTD). Scale bar 10 microns. B) Vero cells, 3 hpi. 1h EU pulse (2-3 hpi). Processed for click chemistry. Filled arrow: associated RNA pol II CTD accumulation (red) and EU HITT (green). Outline arrow: EU HITT, no RNA pol II CTD. Arrow head: RNA pol II CTD accumulation, no EU HITT.

slowly than the infection in figure 7.8. In uninfected cells, RNA polymerase II with a phosphorylated Serine 5 in the CTD is mostly diffuse throughout the nucleus with some small foci (Fig 7.9 A). Upon infection with HSV-1, more foci of pSer5 form. By co staining for RNA pol II CTD and the pSer5 modification, we conclude that the pSer5 foci do colocalise with the RNA poll II CTD foci (Fig 7.9

B). In the untreated infected cells, the pSer5 is most likely located within the developing replication compartments. The majority of the increase of RNA pol modified with the pSer5 marker is not reflected in the total CTD localisation. The increased pSer5 modification is therefore not indicating a redistribution of total RNA pol II, but rather an increased in pSer5 phosphorylation. However, the CTD foci do correlate with areas of increased pSer5.

In the presence of CHX no RNA pol II foci form during HSV-1 infection (Fig 7.9 C, red channel). I have previously shown the increased viral IE transcription taking place in the presence of CHX, yet in the absence of newly synthesised viral proteins there is no redistribution of CTD into foci. This suggests that the RNA pol II foci are not required for viral transcription, yet like the EU foci they are induced by viral proteins. The number of pSer5 foci increases in the presence of CHX but as there is no replication compartment formation they do not increase in size, suggesting that the pSer5 modification is promoted by viral transcription. In the presence of PAA, the RNA pol II CTD foci appear by 4 hpi (Fig 7.9 D). The phosphorylation of Serine 5 behaves similarly in the presence of PAA as to in the presence of CHX.

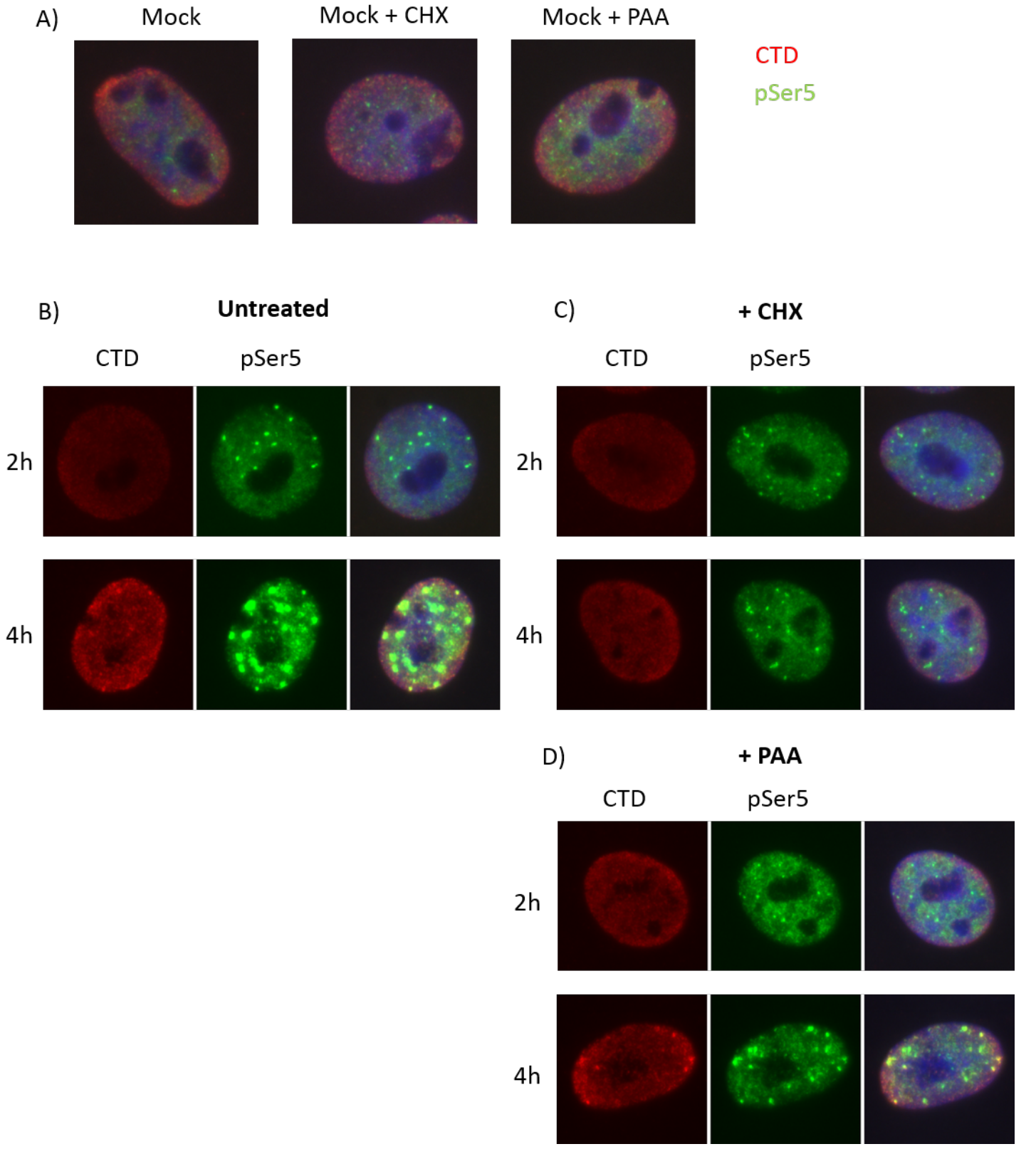


Figure 7.9: IE proteins are required for RNA pol CTD foci formation

A) Uninfected Vero cells, treated with 4h CHX or PAA. Processed for IF (RNA pol II CTD and RNA Pol II pSer5). B-D) Vero cells infected with HSV-1 MOI 10, 2 and 4 hpi. Processed for IF (RNA pol II CTD and RNA Pol II pSer5). B) Untreated, C) Treated with CHX, C) Treated with PAA.

The results above suggest RNA pol II CTD foci are not required for viral transcription. However, the proximity to viral transcription bursts can give insight on the function of CTD foci, both viral and cellular. To address this, HSV-1 infected cells were processed for ICP0 RNA and immunofluorescence for RNA pol II CTD or the pSer5 modification in two separate experiments. In figure 7.10 B, three example cells are showing ICP0 RNA with RNA pol II CTD foci. Cell i has multiple transcription bursts, but no CTD foci, reinforcing the previous conclusion that CTD foci are not required for viral transcription. Cells ii and iii in figure 7.10 B also have multiple transcription bursts, and the ones indicated by the arrows are associated with RNA pol II CTD foci. These cells have additional bursts that are negative for RNA pol II enrichment. Therefore, although not required, there can be some visible recruitment of RNA pol II to transcriptionally active viral genomes.

The RNA pol II CTD modification pSer5 follows a similar pattern. There are some cells, such as cell i in figure 7.10 D, where there are transcription bursts that are not associated with any pSer5 accumulation. Two such bursts are indicated by the outline arrows. These cells tend to have relatively small amounts of cytoplasmic transcript and therefore represent less advanced cells in infection. Cell ii (Fig 7.10 D), which has more cytoplasmic transcript than cell i, has two ICP0 RNA bursts which are associated with small pSer5 foci. These bursts are designated by the solid filled arrow. Cell iii (Fig 7.10 D), the most advanced through infection of the three cells based on ICP0 RNA abundance, has multiple bursts all associated with increased pSer5. One of these bursts is picked out by the filled arrow. The bursts in this cell are relatively smaller, which could suggest that the incoming genomes in this cell are starting to reduce their IE transcription bursting rate before the onset of DNA replication (Section 3.1). There are always small foci of pSer5, even in mock infected cells. Virus infection induces the formation of new pSer5 domains, which begin as small foci and grow in size, and which are located at the sites of viral infection shown by transcription. HSV-1^{EdC} infections could be used to confirm the location of genomes and the proximity of RNA pol II CTD pSer5 accumulation.

The RNA pol II foci do not indicate the location of viral genomes. They may be recruited to

HITTs or for another yet unknown role. However, the phosphorylated Serine 5 marker will ultimately appear on all transcription bursts demonstrating that the RNA polymerase transcribing viral genes carries this modification.

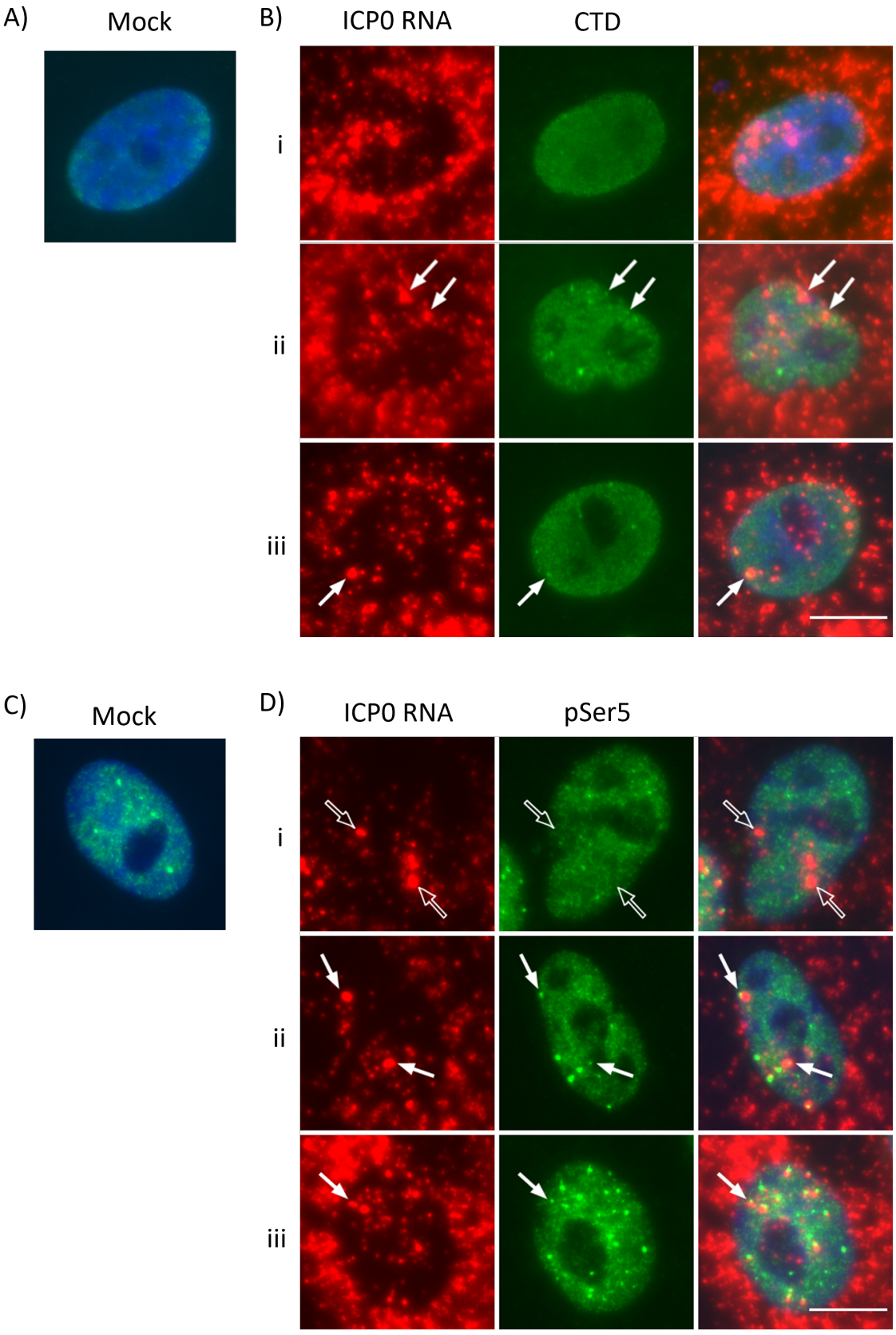


Figure 7.10: Viral transcription bursts are adjacent to RNA polymerase foci.

Vero cells, A + C) Uninfected. B + D) Infected with HSV-1, MOI 10, 2 hpi. B) Three example cells showing ICP0 RNA (red) and RNA pol II CTD protein (green). Arrow: RNA pol II CTD accumulation colocalising with transcription bursts. D) Three example cells showing ICP0 RNA (red) and RNA pol II pSer5 protein (green). Filled arrow: RNA pol II pSer5 foci colocalising with transcription bursts. Outline arrow: Transcription burst only. Scale bar 10 microns.

7.4 Discussion and Future Perspectives

In this chapter I have revealed novel spatial features of RNA pol II transcription during HSV-1 infection. In addition, I would like to propose that HSV-1 alters the requirement for Ser2 phosphorylation during the release of Pol II from the pausing checkpoint before elongation. RNAscope and click chemistry have revealed features that would not be possible to observe during population analysis.

The effect of Cdk9 inhibition on viral transcripton

Cdk9 is the kinase within P-TEFb that phosphorylates NEFL, DSIF and RNA pol II CTD. It has an essential role in productive transcription by controlling the entry into elongation. Inhibition of Cdk9 kinase activity by DRB rapidly halts cellular transcription. However, I propose that the inhibition of Cdk9 does not prove insurmountable to HSV-1. At 1 hpi, DRB dramatically reduces viral transcription. However, at 3 hpi the DRB treated cells have a sizeable amount of viral RNA. I verified the activity of my DRB solutions by showing the reduction in Ser2 phosphorylation by Western blot and by the inhibition of the transcription of the cellular gene Mx1 (Fig 7.5). I also repeatedly added DRB to the culture media of the HSV-1 infected cells to demonstrate that the phenotype observed at 3 hpi is not due to the recovery of cells after either loss of DRB potency or drug turnover. This data is not shown but the 3 hpi phenotype in figure 7.6 C did not change.

My hypothesis is depicted in figure 7.11. At early timepoints the viral genome is in the process of recruiting cellular transcription machinery that is subject to the normal checks and controls. Therefore, the absence of pSer2 and the presence of NELF result in paused polymerases on the HSV-1 genome, which are released from pausing by the action of Cdk9. However, as the virion associated proteins and genome presence begin to alter the nuclear environment there is a mechanistic shift and RNA polymerase is able to transcribe without the checkpoint being cleared. In an untreated infection, showed in the upper diagrams of figure 7.11, this results in a large amount of viral transcription. By

treating with DRB, we reveal the effects of the transcriptional mechanistic shift. Before this shift, at 1 hpi, the virus is unable to transcribe in the presence of DRB. However, by 3 hpi viral transcription has begun in a non-typical manner. The RNAscope images show that in the presence of DRB the transcripts are retained in the nucleus, specifically around the genome. From my protein expression analysis I have shown that viral proteins are not synthesised in the presence of DRB and therefore the transcripts are not being translated. Therefore, I hypothesise that there is still a Cdk9 dependent step that is affected by DRB at later points in transcription preventing the proper export of transcript away from the transcription site and out of the nucleus.

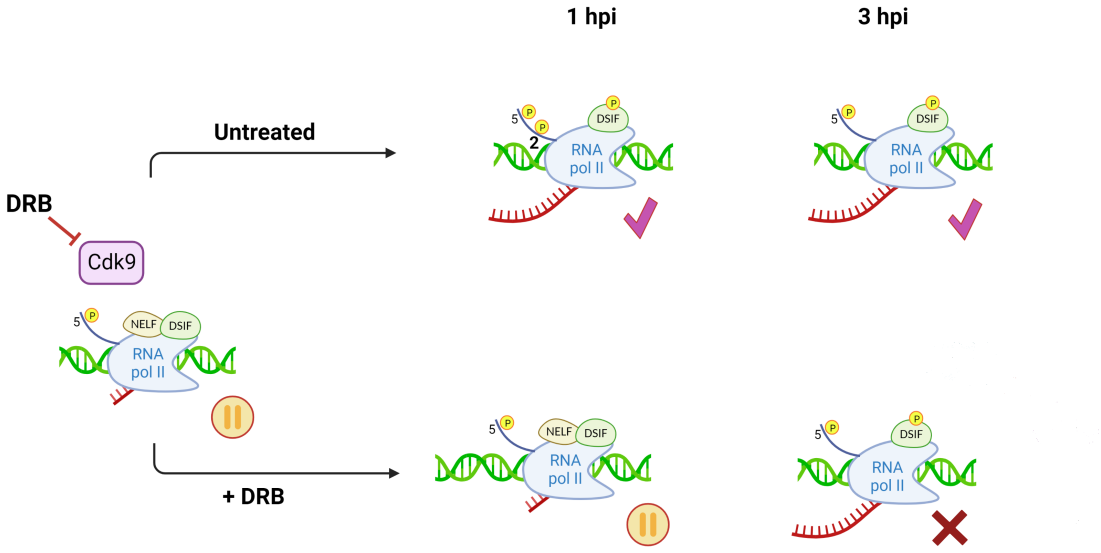


Figure 7.11: Effect of Cdk9 Inhibition on Viral Transcription

There is evidence that HSV-1 transcription can function in the absence of pSer2. A 2005 paper from Fraser and Rice demonstrated a loss of RNA pol II CTD phosphorylation throughout infection. This global loss of phosphorylation has been linked to the shut down of host transcription, however it creates an interesting problem to understand with regard to viral transcription. They hypothesised that if the viral transcription is not restricted by transcriptional pausing this would greatly

benefit the transcriptional output of the virus [227]. If RNA polymerases are recruited and immediately allowed to move down the genome to transcribe this would generate a huge amount of transcript. My evidence highlighting ongoing viral transcription in the presence of Cdk9 inhibition confirms their hypothesis, that viral transcription does not require pSer2. However, this does directly go against some other published work. For example, previous working investigating HSV-1 in the presence of DRB has generally concluded a reduction in viral transcription. A paper by Sandri-Goldin used BrdU labelling to examine nascent transcription. They reported a loss of viral transcription using this method and did not observe any of the spatial features that I have seen [228]. I propose that the high specificity of RNAscope reveals the true picture of viral transcription that methods such as BrdU incorporation and antibody labelling protocols could not detect.

A key aspect to understanding this story lies in an analysis technique I have not been able to perform. It was shown in 2020 that by 3 hpi 30% of cellular RNA pol II can be found on viral genes with a large proportion found at the promoter proximal pausing region. Precision nuclear run-on with sequencing (PRO-Seq) is capable of refining the location of RNA polymerases on genomes to single nucleotide resolution [229]. If RNA pol II is being redirected away from the host genomes but is still subjected to pausing, it is reasonable to suggest different mechanisms are operating on viral and cellular transcription control. Additionally, if what I have hypothesised above regarding a mechanistic shift from the virus being vulnerable to DRB and therefore Cdk9 inhibition of the elongation checkpoint 1 hpi, but the virus becomes resistant to this inhibition and at 3 hpi passes through the elongation checkpoint, PRO-seq analysis of polymerase location at 1 h and 3 h would be a future direction this project could take.

More information could be gained by further development of RNAscope. I have presented data showing the effect of DRB on ICP0 expression, but I have additional data not included here giving the same phenotype for ICP4 expression. It is important to note that both spliced and unspliced genes behave similarly in the presence of DRB. In Chapter 3 I discussed the design of the ICP0 RNAscope

probes. The reduced z probe (Fig 3.9 B) has a narrower binding region. Through a similar process another ICP0 exon probe could be generated, but with the probe binding region restricted to the 3' end of the gene. This would provide information regarding the length of the transcripts produced. If the ICP0 transcript is not full length, then a RNAscope probe targetted to the end of the gene would not be able to bind.

HSV-1 induced transcription territories

I have identified novel transcription territories by EU labelling and click chemistry. These HITTs are induced by viral infection and are visible by 3 hpi but they do not represent the sites of IE viral transcription. They are often but not always associated with ICP4 protein and RNA pol II CTD and require viral gene expression to form.

I hypothesise that HITTs are sites of cellular transcription caused by collapse of traditional transcription factories. In an uninfected nucleus numerous transcription factories line the interchromatin space and do not appear as EU foci or RNA pol II CTD foci. Upon HSV-1 infection and IE protein synthesis, there is huge disruption to the nuclear architecture. This also disrupts transcription factories which releases a large amount of RNA pol II into the interchromatin space. The virus is then able to recruit RNA pol II and associated machinery. It has been shown previously that there is an excess of ICP4 foci over the number of genomes, therefore not all of the ICP4 protein is recruited to viral genomes. The 'genome free' ICP4 is able to recruit RNA pol II transcription associated machinery, but with a limited number of viral genomes to transcribe it can create a new large transcription factory on cellular DNA. I propose that these large domains are the EU HITTs. The side affect of ICP4 modulation of transcription territories is that it decondenses the environment ready for viral transcription. Figure 7.12 summarises this model.

Identification of the transcripts within the EU foci would be a very interesting project to continue. Despite a general shut down of host cell transcription, some genes have been shown to be

elevated, for example antiviral genes. Although the EU HITTs show a small localised transcriptional increase, when averaged over the whole cell they would not counter the overall transcription inhibition. EU pulse labelling and a washout may help monitor the fate of the HITTs, such as stability and size.

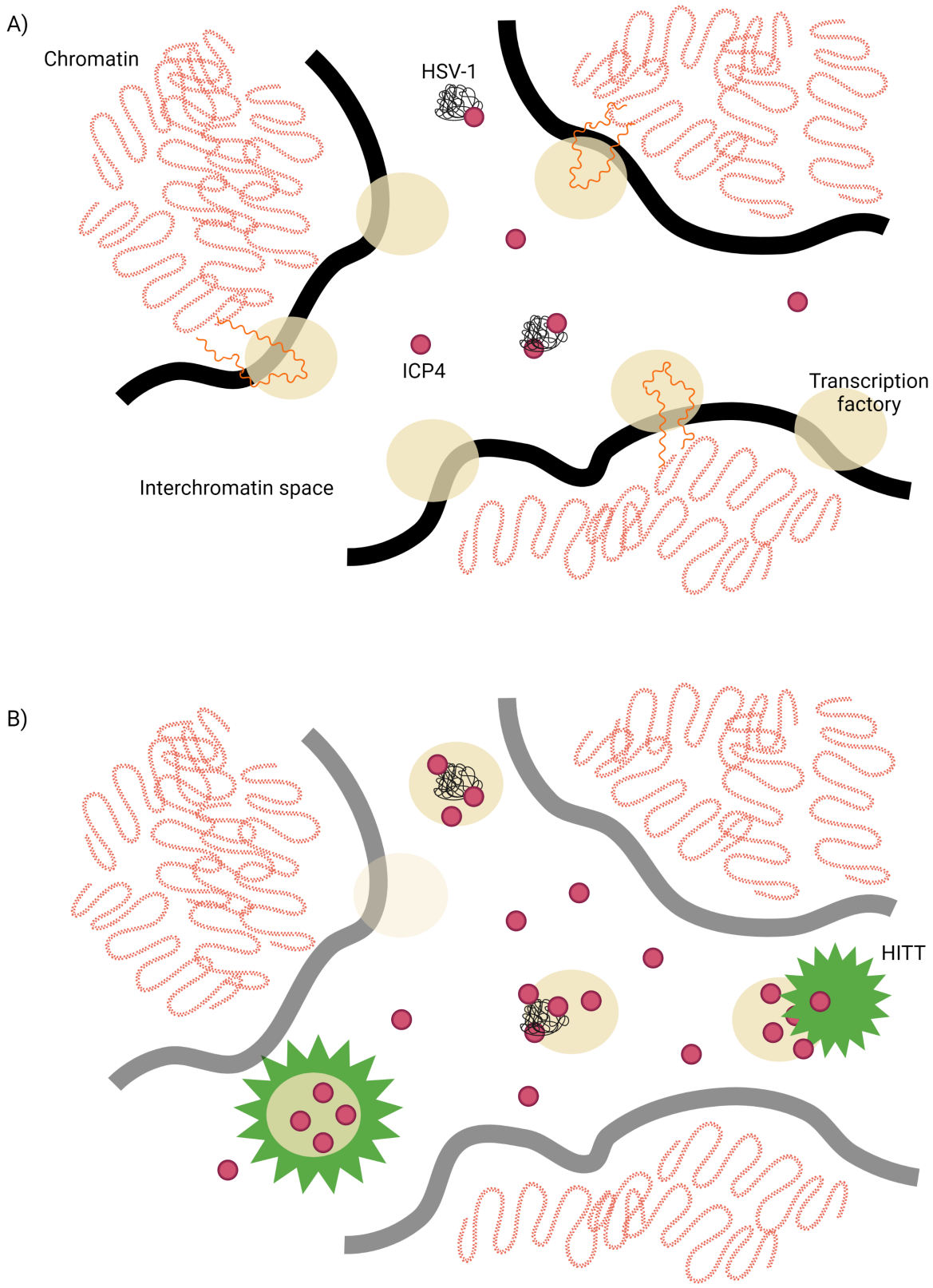


Figure 7.12: HSV-1 Induced Transcription Territories.

A) 1 hpi. Viral genomes (black) are transcribing and ICP4 protein (red circles) is synthesised. Cellular DNA is transcribed in transcription factories (yellow circles) at the edge of the interchromatin space. B) 3 hpi. A large amount of viral ICP4 has been made. Transcription factories have been disrupted, some are recruited by viral genomes. ICP4 recruits transcription machinery to other areas where rapid transcription forms HITTs (green).

Chapter 8

General Conclusions and Closing Perspectives

Within this thesis I have investigated the very earliest phase of transcription after HSV-1 infections. While many studies from genetic and biochemical approaches have contributed to an understanding of broad principles of these early processes, we only have an preliminary understanding of events at the level of single genomes. I have developed a protocol for detecting HSV-1 viral genomes, their transcriptional status and their spatial relationship with proteins.

In chapter 3, I developed and validated the RNA FISH technique RNAscope alongside utilising click chemistry to detect EdC labelled HSV-1 genomes. My results allow detection and quantification of transcriptionally active genomes. Utilisation of multiplex RNA FISH analysis has shown the rapid splicing of ICP0 RNA and the uncoupling of transcription of IE genes at the single genome level. In chapter 5, I extended this analysis by including protein immunofluorescence. I have shown that the presence of PML on a genome does not correlate with transcriptional suppression, a finding which goes against the widely held view of PML as a repressor of transcription.

In further work presented in chapter 6 I examined the spatial relationship between viral transcription and DNA replication. Viral and cellular replication can be separated qualitatively through

EdC pulse labelling. ICP4 is selectively recruited to only viral sites of DNA replication, and these replication compartments are not homogeneous. In pursuing questions relating to similarities or differences in regulatory mechanisms between virus and host I examined the role of P-TEFb in the presence of the specific inhibitor DRB (chapter 7) and in the absence of the viral protein VP16 (chapter 4). It is clear that this molecule is vitally important for HSV-1 transcription and I anticipate future research will bring further insights. Finally, through studying changes to nascent global transcription induced during infection I have examined a completely novel feature of HSV-1 infection, the formation of HITTs, and proposed a model explaining why their formation may provide a pro-viral platform for gene expression and a mechanism for their formation.

With the added insight that stems from high resolution analysis, during these studies one feature became apparent. Whilst general principles and mechanisms can be proposed there was clearly a significant degree of heterogeneity both from cell to cell and between individual genomes. This aspect itself has mechanistic consequences for our general understanding of the nature and progression of virus infection, as discussed below. This work builds the foundations for a wide range of further analysis that can be undertaken, including but not limited to analysis of different viral transcription groups, innate immune responses to viral infection, and the study of many transcription factors to elucidate their role and location during infection.

8.1 Heterogeneity during HSV-1 infection

DNA viral infections are most commonly depicted in schematic formats, where particles enter the cell by fusion or endocytosis and are transported to the nucleus to deliver their genomes which will undergo transcription, replication and eventually produce new progeny [28]. This may falsely lead to the assumption that the pathway is universal across cells in a population, and that each virus will behave in the same manner. However, there is a large degree of heterogeneity across infection which is being demonstrated as novel single cell technologies are established [155]. Variability between

even genetically identically cells at the cell cycle level, at the host RNA transcriptome level and at the protein level all are thought to influence viral infection. For example, a virus may have numerous entry pathways to utilise. A therapeutic entry inhibitor specific to one pathway may not prevent infection and simply divert the virus down an alternative pathway. A full understanding of heterogeneous viral entry pathways for a particular pathogen is vital for therapeutic development. In addition to the host cell, heterogeneity in viral infection can arise from the composition of viral particles. Differences in surface protein composition and internal proteins, as well as particles that may have damaged DNA, all will have different efficiencies of infection which will be reflected in transcriptional output and protein expression.

As an example, in my analysis, in figure 6.5, the percentage of infected cells (defined by the presence of ICP4) is 92% with 8% uninfected (or not expressing ICP4). In a related experiment (figure 6.6), the percentage of ICP4 expressing cells was 75% with 25% not expressing ICP4. This demonstrates some inter experiment variation across experiments which could be due to a number of technical reasons despite following identical experimental protocols. Inevitable variations including cell passage number, age of the virus preparation, number of freeze/thaws cycles and fluctuations in seeding density could all be contributing factors. By using high MOI, statistically all cells will have been infected by multiple particles, eliminating absence of virus as an explanation for the lack of ICP4 expression. Infection with HSV-1^{EdC} and a click chemistry reaction has confirmed this. Population based analysis would not indicate the variability in gene expression and that a significant, though variable, percentage may show no IE protein expression. Precisely why some cells appear relatively resistant to infection, at least as defined by ICP4, is unclear, though these results are in agreement with those of Koblier who recently showed that even in the highly permissive Vero cell line, some cells remained highly refractory to normal progressive infection [213].

What is more pronounced is the heterogeneity in viral transcription between cells which are all clearly classed as positive for viral infection. Even within those cells there is variability in the

activity of individual genomes. The results from visualising transcription have yielded some refined insight into this aspect. Using high MOI infections in an asynchronous cell population, the rate of infection onset and abundance of transcription varied considerably between neighbouring cells. For example figure 3.3 illustrates a typical field of cells at 1 hpi. Some cells have already large transcription bursts whereas others have little or no detectable RNA. At later timepoints, for example 3 hpi in figure 4.2, there are several cells within the field that have very low levels of RNA adjacent to cells with very high levels of RNA. The difference in RNA abundance may be due to differing rates of infection progression, and if examined at later timepoints the numbers of the slower or more resistant cells may decrease. Alternatively, these cells with low RNA at early timepoints may belong to the class of abortive infected cells, described in chapter 6 (fig 6.5, class c). The infecting virions have produced enough viral RNA to develop replication compartments, yet due to the slower rate of infection the cell was able to shut down viral replication before it overwhelmed the cell. Although bulk analysis of transcription whether by RT-PCR or RNA sequencing will not reveal such heterogeneity, single cell RNA sequencing analysis during influenza virus infection has shown such heterogeneity. [171].

In addition to the variability between cells discussed above, my results reveal heterogeneity within a given cell at the level of the genome, where individual genomes may be transcriptionally active or inactive for a particular IE gene (figure 3.8). Moreover, as shown in figure 3.4 by multiplex analysis, genomes that are inactive for one gene may be active for another (Figure 3.8). Thus genomes within the same nucleus are capable of behaving quite differently. Explanation for the differential transcriptional activity of genomes within one cell includes differential association or retention with incoming virus components, the differential deposition or nuclear entry of genomes into distinct nuclear environments or variation in the relative rate of recruitment of both positive and negative host factors. These factors can in future be further studied by combining genome, RNA and protein analysis in a highly multiplexed manner. To that end, I developed assays combining click chemistry with

RNA FISH and protein immunofluorescence. I then investigated the general hypothesis that recruitment of one of the candidate host restriction factors PML would correlate with relative suppression of transcriptional activity of individual genomes [121, 166]. Surprisingly, despite considerable investigation into the role of PML, such direct analysis has not previously been performed in lytically infected cells because the techniques for simultaneous quantitative analysis of genomes, RNA and protein have not been available. My results indicate that while PML protein is recruited to the close vicinity of viral genomes, this does not correlate with inhibition of IE RNA transcription. This analysis can now be extended to examine other protein candidates, as well as expanding the RNA analysis to look at multiple classes of transcripts. Further discussion of the role of the immediate nuclear environment on the transcription from an HSV-1 genome is outlined in more detail in chapter 7.

8.2 Future potential of Azide Biotin Click Chemistry

Click chemistry has proved to be an exceptional tool for visualisation of HSV-1 genomes and for our understanding of detailed mechanism of infection. The applications of inserting clickable ethynyl nucleotides into infecting and replicating genomes extend far beyond the conjugation of a fluorophore for visualisation of spatial localisation by fluorescence microscopy. The corresponding azides with different functional groups apart from a fluorophore allow a wide range of subsequent applications to be performed. Biotin azide has been used to provide a mechanism of capturing and purifying DNA that has incorporated EdC. This technique is providing detailed insight into cellular DNA replication forks and nascent chromatin formation after short EdC or EdU pulses [230]. After fixation, cell suspensions are subjected to a whole cell click chemistry reaction with biotin azide. Following this the chromatin-DNA-EdC-biotin complexes are pulled down by strepatividin beads and processed for subsequent analysis. Several papers utilising this technique to study HSV-1 have been recently published [231, 232]. This work allowed the identification of proteins interacting with replicating HSV-1 genomes by subsequent mass spectrometry after the biotin streptavidin pull down and enrichment.

Therefore the platform I have developed to examine HSV-1 genomes, transcription and protein association will be extremely useful for examining the interaction and function of additional candidate proteins. However, additional hurdles remain to be overcome in their application for the identification of novel targets. During this project I attempted to adapt the technique of azide-biotin click chemistry reactions to isolate the proteins associated with incoming viral genomes, as reported previously using EdC labelled HSV-1 [KOS] [232]. This work isolated nascent EdC incorporating DNA at various timepoints throughout infection, reporting the identification of numerous DNA-associated proteins including viral species and host histone and non-histone factors.

In attempting to repeat such analysis, I spent a significant amount of time optimising a qPCR reaction for the detection of viral DNA, initially using phenol chloroform extracted viral DNA with primers directed against the viral genome. I detected a very clear positive signal. Moreover in the presence of PAA, the signal was substantially reduced confirming that I was detecting replicated DNA and suggesting that the remaining signal was from incoming infecting genomes. However, I encountered several problems with these experiments and interpretation of the data. Alongside the standard infection protocol I performed control experiments at 4 °C. This would allow virus binding to the outside cell surface but prevent fusion and therefore entry to the cell and is used to synchronise infection. However, after DNA extraction and PCR analysis I observed the same level of DNA in these control experiments as cells which had been at 37 °C for 1 hour. This result indicated that the signal that was observed mainly originated from contaminant particles, bound to the cell surface. I attempted multiple methods to remove surface bound virus from cells but was unable to eliminate this contaminating signal. Therefore, if I had continued this project I would not be able to state with any certainty that I was isolating genomes that had entered the cell nucleus. Previous work had combined such selective purification methods with SILAC labelling in order to distinguish between proteins brought in by the virion from proteins in the infected cell ([232]), which unfortunately I did not have the time to pursue.

There are many results in my thesis that this technique, if successful, would be advantageous for. Firstly, identification of proteins bound with the incoming genome. My data examining transcription in the absence of de novo protein synthesis demonstrated a major increase in transcription bursting and burst size. Identifying bound proteins bound under these conditions may reveal novel aspects in the nature of host transcription machinery in the absence of newly made viral proteins. Additionally, my results suggested there may be rapidly synthesised cellular repressors restricting the expression from HSV-1 genomes. Although I concluded the majority of the transcription increase caused by translation inhibition was due to relief of subsequent inhibition by ICP4, comparing the genome bound protein profile in the presence and absence of CHX could identify if there are any candidate proteins for this function.

Secondly, pull down of genomes with biotin could be useful to further the results presented in section 4.2, figure 4.3. In that work, I presented evidence that at least some genomes can resume transcription after a period of general inhibition of transcription by Actinomycin D. I also showed (figure 4.3 E) that if genomes entered nuclei in the presence of ActD, they were eventually able to start transcription when the drug was removed. When HSV-1 DNA enters the cell it is very quickly recognised as naked DNA resulting in rapid deposition of histones, initiation of DNA repair pathways and activation of innate immune signalling. From my results, I concluded that the activity of virion associated VP16 overcame these restrictive processes that associated with the early incoming genome. Using click chemistry with biotin to isolate these genomes would reveal different cellular factors that associated with genomes during periods of transcriptional inactivity, and ultimately how not all genomes were silenced for viral gene expression.

Thirdly, biotin click chemistry reaction could be used to examine nascent RNA transcription with EU pulse labelling. Many studies examining RNA transcription used Global run-on sequencing (GRO-seq), or other similar techniques where RNA is labelled with BrU. However, a major drawback of these techniques is the requirement of nuclei isolation prior to labelling creating an artificial in vitro

environment for studies of viral infection. EU-RNA-seq has been used predominantly to examine transcription during mitosis [233, 234]. I described the use of EU pulse labelling in HSV-1 infected cells in chapter 7 for fluorochrome linked coupling. For the biotin labelling, EU-incorporating RNA is extracted and the Azide-biotin is covalently coupled by the click chemistry reaction. This is followed by the selective isolation of the RNA-biotin by streptavidin beads. Using this technique, it may be possible to identify all nascently transcribed RNA during the pulse length, both cellular and viral. I would not anticipate this as being used for identifying the type of cellular RNA contained within the spatial domains of the HITTs, but rather to examine the global nascent transcriptome. Furthermore performing the pulse labelling and extraction in the presence of DRB would gain further insight into the viral transcription activity that I have observed in the presence of DRB, such as sequence length and content and the difference in DRB sensitivity of host RNA transcription (figures 7.6 and 7.7).

8.3 RNA pol II transcription during HSV-1 infection

HSV-1 recruits and uses the host cell RNA polymerase II and associated machinery for transcription [235]. By attempting to gain further insight into how cellular machinery functions on viral genomes it is possible that unique functional properties of proteins involved with the transcription machinery could be associated for therapeutic purposes.

HMBA and JQ1, two drugs which interfere with the stability of P-TEFb active and inactive forms, only have an effect when VP16 is absent. The strong transcriptional activity of VP16 outcompetes any changes in the P-TEFb composition when these drugs are added, but by studying their effects in the absence of VP16 I have examined the potential roles of P-TEFb on viral genomes. Inhibition of Cdk9 activity by DRB has a dramatic impact on viral transcription, where viral transcription is initially inhibited then is able to resume but is significantly affected and the transcripts are not translated (Chapter 7). Both of these findings have been discussed in chapters 4.5 and 7.4

respectively.

One of the roles of Cdk9 within P-TEFb is phosphorylation within the heptad repeat in the CTD of RNA pol II. Future work examining the necessity and roles of pSer5 and pSer2 phosphorylation during HSV-1 infection will prove very useful. I showed in section 7.3 that the RNA pol II CTD pSer5 was highly elevated on RNA pol II transcribing viral RNA from WT genomes, but the nature of CTD phosphorylation markers on VP16 deficient virus genomes treated with HMBA or JQ1 was not investigated. Additionally the location of pSer5 within the later replication compartments and it's proximity to replication and transcription sites in the presence of drugs affecting P-TEFb should provide information relating to the changing state of transcription on replicated viral DNA. In this regard recent data from super-resolution microscopy examined pSer5 and pSer2 foci in relation to ICP8 within replication compartments [236]. They showed close association of ICP8 foci with HSV-1 genomes, but no association between ICP8 foci and RNA pol II. I would be able to extend this analysis to include RNA transcripts from these later infection stages.

An additional aspect of RNA pol II CTD phosphorylation and the effect of DRB has been shown for snRNAs. U2 snRNA are transcribed by RNA Pol II and are short and intronless genes, which act as components of the spliceosome. While the CTD of RNA pol II is itself required for U2 snRNA transcription, when the phosphorylation of Ser2 and Ser5 is inhibited by DRB transcription of the snRNAs is not affected [237]. In this regard, transcription of snRNAs resemble HSV-1 RNA. The U2 snRNA has an atypically large nucleosome free region with up to 1 kb without nucleosome deposits [238, 239]. In contrast, mRNA genes only have a nucleosome free region of approximately 100 nucleotides. Transcription from eukaryotic genes is highly dependent on chromatin. Because transcription from genes such as U2 snRNA is not dependent on Cdk9 phosphorylation activity, this suggests the lack of nucleosomes around elongation checkpoints may have a significant role in the requirement for CTD phosphorylation markers on the progression through checkpoints. However, studying the regulation of transcription from chromatin free cellular DNA in whole cells is extremely

challenging. It has been suggested that chromatin is required for early elongation checkpoints, and genes devoid of nucleosomes at these points utilise an alternative method of transcription. While there is some nucleoprotein deposition on HSV-1 genomes there is no classical nucleosomal formation [150]. It is tempting to speculate that the DRB-resistant transcription of HSV IE genes may resemble some aspect of the DRB-resistant transcription of the nucleosome free snRNAs. Therefore, I propose that HSV-1 genomes could be a useful tool for studying transcription from non-chromatinised native DNA.

In conclusion, I have developed methods combining click chemistry to visualise individual viral genomes with single molecule RNA transcript analysis and immunofluorescence. The results have yielded more refined and high resolution insight into the earliest processes of RNA polymerase recruitment, transcriptional bursting and RNA transport during the initiation of herpes simplex (HSV) infection. They also provide a platform not only for further studies including HSV transcription, host restriction and DNA replication, but also for similar studies in other virus systems.

Bibliography

[1] G S Stent. A short epistemology of bacteriophage multiplication. *Biophys J*, 2:13–23, 1962. doi: 10.1016/s0006-3495(62)86946-x. URL https://www.ncbi.nlm.nih.gov/pubmed/14039501.

[2] B D Harrison and T M Wilson. Milestones in the research on tobacco mosaic virus. *Philos Trans R Soc Lond B Biol Sci*, 354(1383):521–529, 1999. doi: 10.1098/rstb.1999.0403. URL https://www.ncbi.nlm.nih.gov/pubmed/10212931.

[3] H Sobhy. A comparative review of viral entry and attachment during large and giant dsDNA virus infections. *Arch Virol*, 162(12):3567–3585, 2017. doi: 10.1007/s00705-017-3497-8. URL https://www.ncbi.nlm.nih.gov/pubmed/28866775.

[4] N Pante and M Kann. Nuclear pore complex is able to transport macromolecules with diameters of about 39 nm. *Mol Biol Cell*, 13(2):425–434, 2002. doi: 10.1091/mbc.01-06-0308. URL https://www.ncbi.nlm.nih.gov/pubmed/11854401.

[5] Lara Gallucci and Michael Kann. Nuclear import of hepatitis B virus capsids and genome, 2017. ISSN 19994915.

[6] Merryn Voysey. Safety and efficacy of the ChAdOx1 nCoV-19 vaccine (AZD1222) against SARS-CoV-2: an interim analysis of four randomised controlled trials in Brazil, South Africa, and the UK. *The Lancet*, 397(10269):99–111, 1 2021. ISSN 1474547X. doi: 10.1016/S0140-6736(20)32661-1. URL http://www.thelancet.com/article/S0140673620326611/fulltext.

[7] Tatianna Travieso, Jenny Li, Sneha Mahesh, Juliana Da Fonzeca Redenze E. Mello, and Maria Blasi. The use of viral vectors in vaccine development. *npj Vaccines 2022 7:1*, 7(1):1–10, 7 2022. ISSN 2059-0105. doi: 10.1038/s41541-022-00503-y. URL https://www.nature.com/articles/s41541-022-00503-y.

[8] Jote T Bulcha, Yi Wang, Hong Ma, Phillip W L Tai, and Guangping Gao. Viral vector platforms within the gene therapy landscape. doi: 10.1038/s41392-021-00487-6. URL https://doi.org/10.1038/s41392-021-00487-6.

[9] Hayle Scanlan, Zachary Coffman, Jeffrey Bettencourt, Timothy Shipley, and Debra E. Bramblett. Herpes simplex virus 1 as an oncolytic viral therapy for refractory cancers. *Frontiers in Oncology*, 12, 7 2022. ISSN 2234943X. doi: 10.3389/FONC.2022.940019. URL /pmc/articles/PMC9364694/ /pmc/articles/PMC9364694/?report=abstract https://www.ncbi.nlm.nih.gov/pmc/articles/PMC9364694/.

[10] Aziz A. Chentoufi, Nisha R. Dhanushkodi, Ruchi Srivastava, Swayam Prakash, Pierre Gregoire A. Coulon, Latifa Zayou, Hawa Vahed, Hiba A. Chentoufi, Kathy K. Hormi-Carver, and Lbachir BenMohamed. Combinatorial Herpes Simplex Vaccine Strategies: From Bedside to Bench and Back. *Frontiers in Immunology*, 13:1, 4 2022. ISSN 16643224. doi: 10.3389/FIMMU.2022.849515. URL /pmc/articles/PMC9082490/ /pmc/articles/PMC9082490/?report=abstract https://www.ncbi.nlm.nih.gov/pmc/articles/PMC9082490/.

[11] K Grunewald, P Desai, D C Winkler, J B Heymann, D M Belnap, W Baumeister, and A C Steven. Three-dimensional structure of herpes simplex virus from cryo-electron tomography. *Science*, 302(5649):1396–1398, 2003. doi: 10.1126/science.1090284. URL https://www.ncbi.nlm.nih.gov/pubmed/14631040.

[12] J Rajcani, V Andrea, and R Ingeborg. Peculiarities of herpes simplex virus (HSV) transcription: an overview. *Virus Genes*, 28(3):293–310, 2004. doi: 10.1023/b:viru.0000025777.62826.92. URL https://www.ncbi.nlm.nih.gov/pubmed/15266111.

[13] A V Nicola, A M McEvoy, and S E Straus. Roles for endocytosis and low pH in herpes simplex virus entry into HeLa and Chinese hamster ovary cells. *J Virol*, 77(9):5324–5332, 2003. doi: 10.1128/jvi.77.9.5324-5332.2003. URL https://www.ncbi.nlm.nih.gov/pubmed/12692234.

[14] J Arii, M Uema, T Morimoto, H Sagara, H Akashi, E Ono, H Arase, and Y Kawaguchi. Entry of herpes simplex virus 1 and other alphaherpesviruses via the paired immunoglobulin-like type 2 receptor alpha. *J Virol*, 83(9):4520–4527, 2009. doi: 10.1128/JVI.02601-08. URL https://www.ncbi.nlm.nih.gov/pubmed/19244335.

[15] R S Milne, A V Nicola, J C Whitbeck, R J Eisenberg, and G H Cohen. Glycoprotein D receptor-dependent, low-pH-independent endocytic entry of herpes simplex virus type 1. *J Virol*, 79(11):6655–6663, 2005. doi: 10.1128/JVI.79.11.6655-6663.2005. URL https://www.ncbi.nlm.nih.gov/pubmed/15890903.

[16] P G Spear, R J Eisenberg, and G H Cohen. Three classes of cell surface receptors for alphaherpesvirus entry. *Virology*, 275(1):1–8, 2000. doi: 10.1006/viro.2000.0529. URL https://www.ncbi.nlm.nih.gov/pubmed/11017782.

[17] L V Chernomordik and M M Kozlov. Membrane hemifusion: crossing a chasm in two leaps. *Cell*, 123(3):375–382, 2005. doi: 10.1016/j.cell.2005.10.015. URL https://www.ncbi.nlm.nih.gov/pubmed/16269330.

[18] R P Subramanian and R J Geraghty. Herpes simplex virus type 1 mediates fusion through a hemifusion intermediate by sequential activity of glycoproteins D, H, L, and B. *Proc Natl Acad Sci U S A*, 104(8):2903–2908, 2007. doi: 10.1073/pnas.0608374104. URL https://www.ncbi.nlm.nih.gov/pubmed/17299053.

[19] T Gianni, M Amasio, and G Campadelli-Fiume. Herpes simplex virus gD forms distinct complexes with fusion executors gB and gH/gL in part through the C-terminal profusion domain. *J Biol Chem*, 284(26):17370–17382, 2009. doi: 10.1074/jbc.M109.005728. URL https://www.ncbi.nlm.nih.gov/pubmed/19386594.

[20] D Atanasiu, J C Whitbeck, M P de Leon, H Lou, B P Hannah, G H Cohen, and R J Eisenberg. Bimolecular complementation defines functional regions of Herpes simplex virus gB that are involved with gH/gL as a necessary step leading to cell fusion. *J Virol*, 84(8):3825–3834, 2010. doi: 10.1128/JVI.02687-09. URL https://www.ncbi.nlm.nih.gov/pubmed/20130048.

[21] A Turner, B Bruun, T Minson, and H Browne. Glycoproteins gB, gD, and gHgL of herpes simplex virus type 1 are necessary and sufficient to mediate membrane fusion in a Cos cell transfection system. *J Virol*, 72(1):873–875, 1998. URL https://www.ncbi.nlm.nih.gov/pubmed/9420303.

[22] K Dohner, C H Nagel, and B Sodeik. Viral stop-and-go along microtubules: taking a ride with dynein and kinesins. *Trends Microbiol*, 13(7):320–327, 2005. doi: 10.1016/j.tim.2005.05.010. URL https://www.ncbi.nlm.nih.gov/pubmed/15950476.

[23] B Sodeik, M W Ebersold, and A Helenius. Microtubule-mediated transport of incoming herpes simplex virus 1 capsids to the nucleus. *J Cell Biol*, 136(5):1007–1021, 1997. doi: 10.1083/jcb.136.5.1007. URL https://www.ncbi.nlm.nih.gov/pubmed/9060466.

[24] G W Luxton, S Haverlock, K E Coller, S E Antinone, A Pincetic, and G A Smith. Targeting of herpesvirus capsid transport in axons is coupled to association with specific sets of tegument proteins. *Proc Natl Acad Sci U S A*, 102(16):5832–5837, 2005. doi: 10.1073/pnas.0500803102. URL https://www.ncbi.nlm.nih.gov/pubmed/15795370.

[25] James C. Alwine, William L. Steinhart, and C. W. Hill. Transcription of herpes simplex type 1 DNA in nuclei isolated from infected HEp-2 and KB cells. *Virology*, 60(1):302–307, 7 1974. ISSN 0042-6822. doi: 10.1016/0042-6822(74)90390-0.

[26] Robert W. Honess and Bernard Roizman. Regulation of Herpesvirus Macromolecular Synthesis I. Cascade Regulation of the Synthesis of Three Groups of Viral Proteins. *Journal of Virology*, 14(1):8, 7 1974. ISSN 0022-538X. doi: 10.1128/JVI.14.1.8-19.1974. URL /pmc/articles/PMC355471/?report=abstract https://www.ncbi.nlm.nih.gov/pmc/articles/PMC355471/.

[27] R. W. Honess and B. Roizman. Regulation of herpesvirus macromolecular synthesis: sequential transition of polypeptide synthesis requires functional viral polypeptides. *Proceedings of the National Academy of Sciences*, 72(4):1276–1280, 4 1975. ISSN 00278424. doi: 10.1073/PNAS.72.4.1276. URL https://www.pnas.org/doi/abs/10.1073/pnas.72.4.1276.

[28] F J Ibanez, M A Farias, M P Gonzalez-Troncoso, N Corrales, L F Duarte, A Retamal-Diaz, and P A Gonzalez. Experimental Dissection of the Lytic Replication Cycles of Herpes Simplex Viruses in vitro. *Front Microbiol*, 9:2406, 2018. doi: 10.3389/fmicb.2018.02406. URL https://www.ncbi.nlm.nih.gov/pubmed/30386309.

[29] P Mavromara-Nazos and B Roizman. Activation of herpes simplex virus 1 gamma 2 genes by viral DNA replication. *Virology*, 161(2):593–598, 1987. doi: 10.1016/0042-6822(87)90156-5. URL https://www.ncbi.nlm.nih.gov/pubmed/2825424.

[30] David M. Knipe and Anna Cliffe. Chromatin control of herpes simplex virus lytic and latent infection. *Nature Reviews Microbiology 2008 6:3*, 6(3):211–221, 3 2008. ISSN 1740-1534. doi: 10.1038/nrmicro1794. URL https://www.nature.com/articles/nrmicro1794.

[31] S K Weller and D M Coen. Herpes simplex viruses: mechanisms of DNA replication. *Cold Spring Harb Perspect Biol*, 4(9):a013011, 2012. doi: 10.1101/cshperspect.a013011. URL https://www.ncbi.nlm.nih.gov/pubmed/22952399.

[32] I Muylaert, K W Tang, and P Elias. Replication and recombination of herpes simplex virus DNA. *J Biol Chem*, 286(18):15619–15624, 2011. doi: 10.1074/jbc.R111.233981. URL https://www.ncbi.nlm.nih.gov/pubmed/21362621.

[33] A Severini, D G Scraba, and D L Tyrrell. Branched structures in the intracellular DNA of herpes simplex virus type 1. *J Virol*, 70(5):3169–3175, 1996. URL https://www.ncbi.nlm.nih.gov/pubmed/8627797.

[34] William W. Newcomb, Benes L. Trus, Frank P. Booy, Alasdair C. Steven, Joseph S. Wall, and Jay C. Brown. Structure of the herpes simplex virus capsid. Molecular composition of the pentons and the triplexes. *Journal of molecular biology*, 232(2):499–511, 1993. ISSN 0022-2836. doi: 10.1006/JMBI.1993.1406. URL https://pubmed.ncbi.nlm.nih.gov/8393939/.

[35] M Ogasawara, T Suzutani, I Yoshida, and M Azuma. Role of the UL25 gene product in packaging DNA into the herpes simplex virus capsid: location of UL25 product in the capsid and demonstration that it binds DNA. *J Virol*, 75(3):1427–1436, 2001. doi: 10.1128/JVI.75.3.1427-1436.2001. URL https://www.ncbi.nlm.nih.gov/pubmed/11152516.

[36] A Dasgupta and D W Wilson. ATP depletion blocks herpes simplex virus DNA packaging and capsid maturation. *J Virol*, 73(3):2006–2015, 1999. URL https://www.ncbi.nlm.nih.gov/pubmed/9971781.

[37] J D Heming, J F Conway, and F L Homa. Herpesvirus Capsid Assembly and DNA Packaging. *Adv Anat Embryol Cell Biol*, 223:119–142, 2017. doi: 10.1007/978-3-319-53168-7_6. URL https://www.ncbi.nlm.nih.gov/pubmed/28528442.

[38] Thomas C. Mettenleiter, Barbara G. Klupp, and Harald Granzow. Herpesvirus assembly: a tale of two membranes. *Current Opinion in Microbiology*, 9(4):423–429, 8 2006. ISSN 1369-5274. doi: 10.1016/J.MIB.2006.06.013.

[39] R D Everett. Trans activation of transcription by herpes virus products: requirement for two HSV-1 immediate-early polypeptides for maximum activity. *EMBO J*, 3(13):3135–3141, 1984. URL https://www.ncbi.nlm.nih.gov/pubmed/6098466.

[40] C Boutell, S Sadis, and R D Everett. Herpes simplex virus type 1 immediate-early protein ICP0 and is isolated RING finger domain act as ubiquitin E3 ligases in vitro. *J Virol*, 76(2):841–850, 2002. doi: 10.1128/jvi.76.2.841-850.2002. URL https://www.ncbi.nlm.nih.gov/pubmed/11752173.

[41] A R Cliffe and D M Knipe. Herpes simplex virus ICP0 promotes both histone removal and acetylation on viral DNA during lytic infection. *J Virol*, 82(24):12030–12038, 2008. doi: 10.1128/JVI.01575-08. URL https://www.ncbi.nlm.nih.gov/pubmed/18842720.

[42] M C Smith, C Boutell, and D J Davido. HSV-1 ICP0: paving the way for viral replication. *Future Virol*, 6(4): 421–429, 2011. doi: 10.2217/fvl.11.24. URL https://www.ncbi.nlm.nih.gov/pubmed/21765858.

[43] T. M. Kristie and B. Roizman. Alpha 4, the major regulatory protein of herpes simplex virus type 1, is stably and specifically associated with promoter-regulatory domains of alpha genes and of selected other viral genes. *Proceedings of the National Academy of Sciences of the United States of America*, 83(10):3218, 1986. ISSN 00278424. doi: 10.1073/PNAS.83.10.3218. URL /pmc/articles/PMC323484/?report=abstract https://www.ncbi.nlm.nih.gov/pmc/articles/PMC323484/.

[44] Roger J. Watson and J. Barklie Clements. A herpes simplex virus type 1 function continuously required for early and late virus RNA synthesis. *Nature*, 285(5763):329–330, 1980. ISSN 0028-0836. doi: 10.1038/285329A0. URL https://pubmed.ncbi.nlm.nih.gov/6246451/.

[45] Sarah E. Dremel and Neal A. Deluca. Herpes simplex viral nucleoprotein creates a competitive transcriptional environment facilitating robust viral transcription and host shut off. *eLife*, 8, 10 2019. ISSN 2050084X. doi: 10.7554/ELIFE.51109.

[46] Ilaria Frasson, Paola Soldà, Matteo Nadai, Sara Lago, and Sara N. Richter. Parallel G-quadruplexes recruit the HSV-1 transcription factor ICP4 to promote viral transcription in herpes virus-infected human cells. *Communications Biology 2021 4:1*, 4(1):1–13, 4 2021. ISSN 2399-3642. doi: 10.1038/s42003-021-02035-y. URL https://www.nature.com/articles/s42003-021-02035-y.

[47] P. J. Godowski and D. M. Knipe. Transcriptional control of herpesvirus gene expression: gene functions required for positive and negative regulation. *Proceedings of the National Academy of Sciences of the United States of America*, 83(2):256, 1986. ISSN 00278424. doi: 10.1073/PNAS.83.2.256. URL /pmc/articles/PMC322836/?report=abstract https://www.ncbi.nlm.nih.gov/pmc/articles/PMC322836/.

[48] M S Roberts, A Boundy, P O'Hare, M C Pizzorno, D M Ciufo, and G S Hayward. Direct correlation between a negative autoregulatory response element at the cap site of the herpes simplex virus type 1 IE175 (alpha 4) promoter and a specific binding site for the IE175 (ICP4) protein. *Journal of virology*, 62(11):4307–4320, 11 1988. ISSN 0022-538X. doi: 10.1128/JVI.62.11.4307-4320.1988. URL https://pubmed.ncbi.nlm.nih.gov/2845144/.

[49] N A DeLuca and P A Schaffer. Activation of immediate-early, early, and late promoters by temperature-sensitive and wild-type forms of herpes simplex virus type 1 protein ICP4. *Molecular and cellular biology*, 5(8):1997–2008, 8 1985. ISSN 0270-7306. doi: 10.1128/MCB.5.8.1997-2008.1985. URL https://pubmed.ncbi.nlm.nih.gov/3018543/.

[50] B Gu, R Kuddus, and N A DeLuca. Repression of activator-mediated transcription by herpes simplex virus ICP4 via a mechanism involving interactions with the basal transcription factors TATA-binding protein and TFIIB. *Molecular and cellular biology*, 15(7):3618–3626, 7 1995. ISSN 0270-7306. doi: 10.1128/MCB.15.7.3618. URL https://pubmed.ncbi.nlm.nih.gov/7791769/.

[51] B. Gu, R. Rivera-Gonzalez, C. A. Smith, and N. A. DeLuca. Herpes simplex virus infected cell polypeptide 4 preferentially represses Sp1-activated over basal transcription from its own promoter. *Proceedings of the National Academy of Sciences*, 90(20):9528–9532, 10 1993. ISSN 00278424. doi: 10.1073/PNAS.90.20.9528. URL https://www.pnas.org/doi/abs/10.1073/pnas.90.20.9528.

[52] I H Chen, L Li, L Silva, and R M Sandri-Goldin. ICP27 recruits Aly/REF but not TAP/NXF1 to herpes simplex virus type 1 transcription sites although TAP/NXF1 is required for ICP27 export. *J Virol*, 79(7):3949–3961, 2005. doi: 10.1128/JVI.79.7.3949-3961.2005. URL https://www.ncbi.nlm.nih.gov/pubmed/15767397.

[53] P Malik, A Tabarraei, R H Kehlenbach, N Korfali, R Iwasawa, S V Graham, and E C Schirmer. Herpes simplex virus ICP27 protein directly interacts with the nuclear pore complex through Nup62, inhibiting host nucleocytoplasmic transport pathways. *J Biol Chem*, 287(15):12277–12292, 2012. doi: 10.1074/jbc.M111.331777. URL https://www.ncbi.nlm.nih.gov/pubmed/22334672.

[54] R M Sandri-Goldin. The many roles of the regulatory protein ICP27 during herpes simplex virus infection. *Front. Biosci.*, 14(13):5241–5256, 2008. doi: 10.2741/3078.

[55] S Gupte, J W Olson, and WT Ruyechan. The major herpes simplex virus type-1 DNA-binding protein is a zinc metalloprotein. *J Biol Chem*, 266(18):11413–6, 1991.

[56] Cynthia K Leet and David M Knipe. An immunoassay for the study of DNA-binding activities of herpes simplex virus protein ICP8. *Journal of Virology*, 54(3):731–738, 6 1985. ISSN 0022-538X. doi: 10.1128/JVI.54.3.731-738.1985. URL https://journals.asm.org/doi/10.1128/jvi.54.3.731-738.1985.

[57] G Bayliss, H Marsden, and J Hay. Herpes simplex virus proteins: DNA-binding proteins in infected cells and in the virus structure. *Virology*, 68(1):124–34, 1975. doi: 10.1016/0042-6822(75)90154-3.

[58] Min Gaot and David M Knipe. Distal Protein Sequences Can Affect the Function of a Nuclear Localization Signal. Technical Report 3, 1992.

[59] P J Godowski and D M Knipe. Mutations in the major DNA-binding protein gene of herpes simplex virus type 1 result in increased levels of viral gene expression. *Journal of virology*, 47(3):478–486, 9 1983. ISSN 0022-538X. doi: 10.1128/JVI.47.3.478-486.1983. URL https://pubmed.ncbi.nlm.nih.gov/6312079/.

[60] M Gao and D M Knipe. Potential role for herpes simplex virus ICP8 DNA replication protein in stimulation of late gene expression. *Journal of virology*, 65(5):2666–2675, 5 1991. ISSN 0022-538X. doi: 10.1128/JVI.65.5.2666-2675.1991. URL https://pubmed.ncbi.nlm.nih.gov/1850040/.

[61] Nandakumar Balasubramanian, Ping Bai, Gregory Buchek, George Korza, and Sandra K. Weller. Physical Interaction between the Herpes Simplex Virus Type 1 Exonuclease, UL12, and the DNA Double-Strand Break-Sensing MRN Complex. *Journal of Virology*, 84(24):12504–12514, 12 2010. ISSN 0022-538X. doi: 10.1128/JVI.01506-10. URL https://journals.asm.org/journal/jvi.

[62] Travis J. Taylor and David M. Knipe. Proteomics of Herpes Simplex Virus Replication Compartments: Association of Cellular DNA Replication, Repair, Recombination, and Chromatin Remodeling Proteinswith ICP8. *Journal of Virology*, 78(11):5856–5866, 6 2004. ISSN 0022-538X. doi: 10.1128/JVI.78.11.5856-5866.2004. URL https://journals.asm.org/journal/jvi.

[63] Dengjian Fan, Mingshu Wang, Anchun Cheng, Renyong Jia, Qiao Yang, Ying Wu, Dekang Zhu, Xinxin Zhao, Shun Chen, Mafeng Liu, Shaqiu Zhang, Xumin Ou, Sai Mao, Qun Gao, Di Sun, Xingjian Wen, Yunya Liu, Yanling Yu, Ling Zhang, Bin Tian, Leichang Pan, and Xiaoyue Chen. The Role of VP16 in the Life Cycle of Alphaherpesviruses. *Frontiers in Microbiology*, 11, 8 2020. ISSN 1664302X. doi: 10.3389/FMICB.2020.01910. URL /pmc/articles/PMC7461839/ /pmc/articles/PMC7461839/?report=abstract https://www.ncbi.nlm.nih.gov/pmc/articles/PMC7461839/.

[64] LaBoissière S, Walker S, and O'Hare P. Concerted activity of host cell factor subregions in promoting stable VP16 complex assembly and preventing interference by the acidic activation domain. *Molecular and cellular biology*, 17(12):7108–7118, 12 1997. ISSN 0270-7306. doi: 10.1128/MCB.17.12.7108. URL https://pubmed.ncbi.nlm.nih.gov/9372942/.

[65] W. Herr. The herpes simplex virus VP16-induced complex: mechanisms of combinatorial transcriptional regulation. *Cold Spring Harbor symposia on quantitative biology*, 63:599–607, 1998. ISSN 0091-7451. doi: 10.1101/SQB.1998.63.599. URL https://pubmed.ncbi.nlm.nih.gov/10384325/.

[66] J S Lai and W Herr. Interdigitated residues within a small region of VP16 interact with Oct-1, HCF, and DNA. *Molecular and cellular biology*, 17(7):3937–3946, 7 1997. ISSN 0270-7306. doi: 10.1128/MCB.17.7.3937. URL https://pubmed.ncbi.nlm.nih.gov/9199328/.

[67] S LaBoissiere and P O'Hare. Analysis of HCF, the cellular cofactor of VP16, in herpes simplex virus-infected cells. *J Virol*, 74(1):99–109, 2000. doi: 10.1128/jvi.74.1.99-109.2000. URL https://www.ncbi.nlm.nih.gov/pubmed/10590096.

[68] R Hori and S Pyo. TFIIB facilitated recruitment of preinitiation complexes by a TAF independent mechanism. *Nucleic Acids Res*, 32(13):3856, 2004. doi: 10.1093/nar/gkh711.

[69] Mabrouk M. Elgadi, Christopher E. Hayes, and James R. Smiley. The herpes simplex virus vhs protein induces endoribonucleolytic cleavage of target RNAs in cell extracts. *Journal of virology*, 73(9):7153–7164, 9 1999. ISSN 0022-538X. doi: 10.1128/JVI.73.9.7153-7164.1999. URL https://pubmed.ncbi.nlm.nih.gov/10438802/.

[70] C A Smibert, B Popova, P Xiao, J P Capone, and J R Smiley. Herpes simplex virus VP16 forms a complex with the virion host shutoff protein vhs. *Journal of virology*, 68(4):2339–2346, 4 1994. ISSN 0022-538X. doi: 10.1128/JVI.68.4.2339-2346.1994. URL https://pubmed.ncbi.nlm.nih.gov/8139019/.

[71] J. Knez, P. T. Bilan, and J. P. Capone. A single amino acid substitution in herpes simplex virus type 1 VP16 inhibits binding to the virion host shutoff protein and is incompatible with virus growth. *Journal of virology*, 77(5):2892–2902, 3 2003. ISSN 0022-538X. doi: 10.1128/JVI.77.5.2892-2902.2003. URL https://pubmed.ncbi.nlm.nih.gov/12584313/.

[72] Olga V. Viktorovskaya and David A. Schneider. Functional divergence of eukaryotic RNA polymerases: Unique properties of RNA polymerase I suit its cellular role. *Gene*, 556(1):19–26, 2 2015. ISSN 0378-1119. doi: 10.1016/J.GENE.2014.10.035.

[73] Robert J. White. Transcription by RNA polymerase III: more complex than we thought. *Nature Reviews Genetics 2011 12:7*, 12(7):459–463, 5 2011. ISSN 1471-0064. doi: 10.1038/nrg3001. URL https://www.nature.com/articles/nrg3001.

[74] C. Kedinger, M. Gniazdowski, J. L. Mandel, F. Gissinger, and P. Chambon. α-Amanitin: A specific inhibitor of one of two DNA-dependent RNA polymerase activities from calf thymus. *Biochemical and Biophysical Research Communications*, 38(1):165–171, 1 1970. ISSN 0006-291X. doi: 10.1016/0006-291X(70)91099-5.

[75] François Michel Boisvert, Silvana Van Koningsbruggen, Joaquín Navascués, and Angus I. Lamond. The multifunctional nucleolus. *Nature reviews. Molecular cell biology*, 8(7):574–585, 7 2007. ISSN 1471-0072. doi: 10.1038/NRM2184. URL https://pubmed.ncbi.nlm.nih.gov/17519961/.

[76] Alessandro Vannini and Patrick Cramer. Conservation between the RNA Polymerase I, II, and III Transcription Initiation Machineries. *Molecular Cell*, 45(4):439–446, 2 2012. ISSN 1097-2765. doi: 10.1016/J.MOLCEL.2012.01.023.

[77] P. Cramer, K. J. Armache, S. Baumli, S. Benkert, F. Brueckner, C. Buchen, G. E. Damsma, S. Dengl, S. R. Geiger, A. J. Jasiak, A. Jawhari, S. Jennebach, T. Kamenski, H. Kettenberger, C. D. Kuhn, E. Lehmann, K. Leike, J. F. Sydow, and A. Vannini. Structure of Eukaryotic RNA Polymerases. *Annual Review of Biophysics*, 37:337–352, 5 2008. ISSN 1936122X. doi: 10.1146/ANNUREV.BIOPHYS.37.032807.130008. URL https://www.annualreviews.org/doi/abs/10.1146/annurev.biophys.37.032807.130008.

[78] Kevin M Harlen and L Stirling Churchman. The code and beyond: transcription regulation by the RNA polymerase II carboxy-terminal domain. 2017. doi: 10.1038/nrm.2017.10. URL www.nature.com/nrm.

[79] Jing Ping Hsin and James L. Manley. The RNA polymerase II CTD coordinates transcription and RNA processing. *Genes & Development*, 26(19):2119, 10 2012. ISSN 08909369. doi: 10.1101/GAD.200303.112. URL /pmc/articles/PMC3465734/ /pmc/articles/PMC3465734/?report=abstract https://www.ncbi.nlm.nih.gov/pmc/articles/PMC3465734/.

[80] Alain R. Bataille, Célia Jeronimo, Pierre Étienne Jacques, Louise Laramée, Marie Ève Fortin, Audrey Forest, Maxime Bergeron, Steven D. Hanes, and François Robert. A universal RNA polymerase II CTD cycle is orchestrated by complex interplays between kinase, phosphatase, and isomerase enzymes along genes. *Molecular cell*, 45(2):158–170, 1 2012. ISSN 1097-4164. doi: 10.1016/J.MOLCEL.2011.11.024. URL https://pubmed.ncbi.nlm.nih.gov/22284676/.

[81] Maldonado E, Ha I, Cortes P, Weis L, and Reinberg D. Factors involved in specific transcription by mammalian RNA polymerase II: role of transcription factors IIA, IID, and IIB during formation of a transcription-competent complex. *Molecular and cellular biology*, 10(12):6335–6347, 12 1990. ISSN 0270-7306. doi: 10.1128/MCB.10.12.6335-6347.1990. URL https://pubmed.ncbi.nlm.nih.gov/2247058/.

[82] Xuemei Zhao and Winship Herr. A Regulated Two-Step Mechanism of TBP Binding to DNA: A Solvent-Exposed Surface of TBP Inhibits TATA Box Recognition. *Cell*, 108(5):615–627, 3 2002. ISSN 0092-8674. doi: 10.1016/S0092-8674(02)00648-7.

[83] R ROEDER. The role of general initiation factors in transcription by RNA polymerase II. *Trends in Biochemical Sciences*, 21(9):327–335, 9 1996. ISSN 0968-0004. doi: 10.1016/S0968-0004(96)10050-5.

[84] Yoshiaki Ohkuma. Multiple functions of general transcription factors TFIIE and TFIIH in transcription: possible points of regulation by trans-acting factors. *Journal of biochemistry*, 122(3): 481–489, 1997. ISSN 0021-924X. doi: 10.1093/OXFORDJOURNALS.JBCHEM.A021777. URL https://pubmed.ncbi.nlm.nih.gov/9348072/.

[85] Karen Adelman and John T Lis. Pre-initiation complex Promoter-proximal pausing of RNA polymerase II: emerging roles in metazoans. 2012. doi: 10.1038/nrg3293. URL www.nature.com/reviews/genetics.

[86] Ann E. Rougvie and John T. Lis. The RNA polymerase II molecule at the 5 end of the uninduced hsp70 gene of D. melanogaster is transcriptionally engaged. *Cell*, 54(6):795–804, 9 1988. ISSN 00928674. doi: 10.1016/S0092-8674(88)91087-2.

[87] Daniel S. Day, Bing Zhang, Sean M. Stevens, Francesco Ferrari, Erica N. Larschan, Peter J. Park, and William T. Pu. Comprehensive analysis of promoter-proximal RNA polymerase II pausing across mammalian cell types. *Genome Biology*, 17(1):1–17, 6 2016. ISSN 1474760X. doi: 10.1186/S13059-016-0984-2/FIGURES/5. URL https://genomebiology.biomedcentral.com/articles/10.1186/s13059-016-0984-2.

[88] Barbara Steurer, Roel C. Janssens, Bart Geverts, Marit E. Geijer, Franziska Wienholz, Arjan F. Theil, Jiang Chang, Shannon Dealy, Joris Pothof, Wiggert A. Van Cappellen, Adriaan B. Houtsmuller, and Jurgen A. Marteijn. Live-cell analysis of endogenous GFP-RPB1 uncovers rapid turnover of initiating and promoter-paused RNA Polymerase II. *Proceedings of the National Academy of Sciences of the United States of America*, 115(19):E4368–E4376, 5 2018. ISSN 1091-6490. doi: 10.1073/PNAS.1717920115. URL https://pubmed.ncbi.nlm.nih.gov/29632207/.

[89] Tadashi Wada, Toshiyuki Takagi, Yuki Yamaguchi, Anwarul Ferdous, Takeshi Imai, Susumu Hirose, Seiji Sugimoto, Keiichi Yano, Grant A. Hartzog, Fred Winston, Stephen Buratowski, and Hiroshi Handa. DSIF, a novel transcription elongation factor that regulates RNA polymerase II processivity, is composed of human Spt4 and Spt5 homologs, 1998. ISSN 08909369. URL http://genesdev.cshlp.org/content/12/3/343.

[90] Yuki Yamaguchi, Toshiyuki Takagi, Tadashi Wada, Keiichi Yano, Akiko Furuya, Seiji Sugimoto, Jun Hasegawa, and Hiroshi Handa. NELF, a multisubunit complex containing RD, cooperates with DSIF to repress RNA polymerase II elongation. *Cell*, 97(1):41–51, 4 1999. ISSN 00928674. doi: 10.1016/S0092-8674(00)80713-8.

[91] N F Marshall and D H Price. Control of formation of two distinct classes of RNA polymerase II elongation complexes. *Molecular and cellular biology*, 12(5):2078–2090, 5 1992. ISSN 0270-7306. doi: 10.1128/MCB.12.5.2078-2090.1992. URL https://pubmed.ncbi.nlm.nih.gov/1569941/.

[92] Junmin Peng, Nick F. Marshall, and David H. Price. Identification of a cyclin subunit required for the function of Drosophila P-TEFb. *Journal of Biological Chemistry*, 273(22):13855–13860, 5 1998. ISSN 00219258. doi: 10.1074/JBC.273.22.13855.

[93] Nick F. Marshall, Junmin Peng, Zhi Xie, and David H. Price. Control of RNA polymerase II elongation potential by a novel carboxyl-terminal domain kinase. *The Journal of biological chemistry*, 271(43):27176–27183, 1996. ISSN 0021-9258. doi: 10.1074/JBC.271.43.27176. URL https://pubmed.ncbi.nlm.nih.gov/8900211/.

[94] David H. Price. P-TEFb, a Cyclin-Dependent Kinase Controlling Elongation by RNA Polymerase II. *Molecular and Cellular Biology*, 20(8):2629–2634, 4 2000. ISSN 0270-7306. doi: 10.1128/MCB.20.8.2629-2634.2000/ASSET/167B8111-8C1B-4FC4-A18F-E66114758857/ASSETS/GRAPHIC/MB0801869002.JPEG. URL https://journals.asm.org/doi/10.1128/MCB.20.8.2629-2634.2000.

[95] Tomoko Yamada, Yuki Yamaguchi, Naoto Inukai, Sachiko Okamoto, Takashi Mura, and Hiroshi Handa. P-TEFb-Mediated Phosphorylation of hSpt5 C-Terminal Repeats Is Critical for Processive Transcription Elongation. *Molecular Cell*, 21(2):227–237, 1 2006. ISSN 1097-2765. doi: 10.1016/J.MOLCEL.2005.11.024.

[96] Matjaz Barboric, Robert M. Nissen, Satoshi Kanazawa, Nabila Jabrane-Ferrat, and B. Matija Peterlin. NF-κB Binds P-TEFb to Stimulate Transcriptional Elongation by RNA Polymerase II. *Molecular Cell*, 8(2):327–337, 8 2001. ISSN 1097-2765. doi: 10.1016/S1097-2765(01)00314-8.

[97] Zhiyuan Yang, Jasper H.N. Yik, Ruichuan Chen, Nanhai He, Kyoo Jang Moon, Keiko Ozato, and Qiang Zhou. Recruitment of P-TEFb for Stimulation of Transcriptional Elongation by the Bromodomain Protein Brd4. *Molecular Cell*, 19(4):535–545, 8 2005. ISSN 1097-2765. doi: 10.1016/J.MOLCEL.2005.06.029.

[98] Ballachanda N. Devaiah, Brian A. Lewis, Natasha Cherman, Michael C. Hewitt, Brian K. Albrecht, Pamela G. Robey, Keiko Ozato, Robert J. Sims, and Dinah S. Singer. BRD4 is an atypical kinase that phosphorylates serine2 of the RNA polymerase II carboxy-terminal domain. *Proceedings of the National Academy of Sciences of the United States of America*, 109(18):6927–6932, 5 2012. ISSN 1091-6490. doi: 10.1073/PNAS.1120422109. URL https://pubmed.ncbi.nlm.nih.gov/22509028/.

[99] Ballachanda N. Devaiah, Anne Gegonne, and Dinah S. Singer. Bromodomain 4: a cellular Swiss army knife. *Journal of Leukocyte Biology*, 100(4):679–686, 10 2016. ISSN 1938-3673. doi: 10.1189/JLB.2RI0616-250R. URL https://onlinelibrary.wiley.com/doi/full/10.1189/jlb.2RI0616-250R https://onlinelibrary.wiley.com/doi/abs/10.1189/jlb.2RI0616-250R https://jlb.onlinelibrary.wiley.com/doi/10.1189/jlb.2RI0616-250R.

[100] Nanhai He, Caleb K. Chan, Bijan Sobhian, Seemay Chou, Yuhua Xue, Min Liu, Tom Alber, Monsef Benkirane, and Qiang Zhou. Human Polymerase-Associated Factor complex (PAFc) connects the Super Elongation Complex (SEC) to RNA polymerase II on chromatin. *Proceedings of the National Academy of Sciences of the United States of America*, 108(36):E636–E645, 9 2011. ISSN 00278424. doi: 10.1073/PNAS.1107107108/SUPPL_FILE/PNAS.1107107108_SI.PDF. URL https://www.pnas.org/doi/abs/10.1073/pnas.1107107108.

[101] Zhuojuan Luo, Chengqi Lin, and Ali Shilatifard. The super elongation complex (SEC) family in transcriptional control. *Nature Reviews Molecular Cell Biology 2012 13:9*, 13(9):543–547, 8 2012. ISSN 1471-0080. doi: 10.1038/nrm3417. URL https://www.nature.com/articles/nrm3417.

[102] Ruichuan Chen, Min Liu, Huan Li, Yuhua Xue, Wanichaya N. Ramey, Nanhai He, Nanping Ai, Haohong Luo, Ying Zhu, Nan Zhou, and Qiang Zhou. PP2B and PP1alpha cooperatively disrupt 7SK snRNP to release P-TEFb for transcription in response to Ca2+ signaling. *Genes & development*, 22(10):1356–1368, 5 2008. ISSN 0890-9369. doi: 10.1101/GAD.1636008. URL https://pubmed.ncbi.nlm.nih.gov/18483222/.

[103] Sungyoo Cho, Sebastian Schroeder, Katrin Kaehlcke, Hye Sook Kwon, Angelika Pedal, Eva Herker, Martina Schnoelzer, and Melanie Ott. Acetylation of cyclin T1 regulates the equilibrium between active and inactive P-TEFb in cells. *The EMBO Journal*, 28(10):1407, 5 2009. ISSN 02614189. doi: 10.1038/EMBOJ.2009.99. URL /pmc/articles/PMC2688543/ /pmc/articles/PMC2688543/?report=abstract https://www.ncbi.nlm.nih.gov/pmc/articles/PMC2688543/.

[104] Xavier Contreras, Matjaz Barboric, Tina Lenasi, and B. Matija Peterlin. HMBA Releases P-TEFb from HEXIM1 and 7SK snRNA via PI3K/Akt and Activates HIV Transcription. *PLoS Pathogens*, 3(10):1459–1469, 10 2007. ISSN 15537366. doi: 10.1371/JOURNAL.PPAT.0030146. URL /pmc/articles/PMC2014796/ /pmc/articles/PMC2014796/?report=abstract https://www.ncbi.nlm.nih.gov/pmc/articles/PMC2014796/.

[105] H de The, C Lavau, A Marchio, C Chomienne, L Degos, and A Dejean. The PML-RAR alpha fusion mRNA generated by the t(15;17) translocation in acute promyelocytic leukemia encodes a functionally altered RAR. *Cell*, 66(4):675–684, 1991. doi: 10.1016/0092-8674(91)90113-d. URL https://www.ncbi.nlm.nih.gov/pubmed/1652369.

[106] A Melnick and J D Licht. Deconstructing a disease: RARalpha, its fusion partners, and their roles in the pathogenesis of acute promyelocytic leukemia. *Blood*, 93(10):3167–3215, 1999. URL https://www.ncbi.nlm.nih.gov/pubmed/10233871.

[107] M Stadler, M K Chelbi-Alix, M H Koken, L Venturini, C Lee, A Saib, F Quignon, L Pelicano, M C Guillemin, C Schindler, and et al. Transcriptional induction of the PML growth suppressor gene by interferons is mediated through an ISRE and a GAS element. *Oncogene*, 11(12):2565–2573, 1995. URL https://www.ncbi.nlm.nih.gov/pubmed/8545113.

[108] X Cheng and H Y Kao. Post-translational modifications of PML: consequences and implications. *Front Oncol*, 2:210, 2012. doi: 10.3389/fonc.2012.00210. URL https://www.ncbi.nlm.nih.gov/pubmed/23316480.

[109] G Dellaire, R W Ching, H Dehghani, Y Ren, and D P Bazett-Jones. The number of PML nuclear bodies increases in early S phase by a fission mechanism. *J Cell Sci*, 119(Pt 6):1026–1033, 2006. doi: 10.1242/jcs.02816. URL https://www.ncbi.nlm.nih.gov/pubmed/16492708.

[110] S Yang, C Kuo, J E Bisi, and M K Kim. PML-dependent apoptosis after DNA damage is regulated by the checkpoint kinase hCds1/Chk2. *Nat Cell Biol*, 4(11):865–870, 2002. doi: 10.1038/ncb869. URL https://www.ncbi.nlm.nih.gov/pubmed/12402044.

[111] G Dellaire, R W Ching, K Ahmed, F Jalali, K C Tse, R G Bristow, and D P Bazett-Jones. Promyelocytic leukemia nuclear bodies behave as DNA damage sensors whose response to DNA double-strand breaks is regulated by NBS1 and the kinases ATM, Chk2, and ATR. *J Cell Biol*, 175(1):55–66, 2006. doi: 10.1083/jcb.200604009. URL https://www.ncbi.nlm.nih.gov/pubmed/17030982.

[112] S Zhong, P Salomoni, and P P Pandolfi. The transcriptional role of PML and the nuclear body. *Nat Cell Biol*, 2(5): 85–90, 2000. doi: 10.1038/35010583. URL https://www.ncbi.nlm.nih.gov/pubmed/10806494.

[113] J Wang, C Shiels, P Sasieni, P J Wu, S A Islam, P S Freemont, and D Sheer. Promyelocytic leukemia nuclear bodies associate with transcriptionally active genomic regions. *J Cell Biol*, 164(4):515–526, 2004. doi: 10.1083/jcb.200305142. URL https://www.ncbi.nlm.nih.gov/pubmed/14970191.

[114] P P Kumar, O Bischof, P K Purbey, D Notani, H Urlaub, A Dejean, and S Galande. Functional interaction between PML and SATB1 regulates chromatin-loop architecture and transcription of the MHC class I locus. *Nat Cell Biol*, 9 (1):45–56, 2007. doi: 10.1038/ncb1516. URL https://www.ncbi.nlm.nih.gov/pubmed/17173041.

[115] A M Ishov, R M Stenberg, and G G Maul. Human cytomegalovirus immediate early interaction with host nuclear structures: definition of an immediate transcript environment. *J Cell Biol*, 138(1):5–16, 1997. doi: 10.1083/jcb.138.1.5. URL https://www.ncbi.nlm.nih.gov/pubmed/9214377.

[116] G G Maul, A M Ishov, and R D Everett. Nuclear domain 10 as preexisting potential replication start sites of herpes simplex virus type-1. *Virology*, 217(1):67–75, 1996. doi: 10.1006/viro.1996.0094. URL https://www.ncbi.nlm.nih.gov/pubmed/8599237.

[117] G G Maul, H H Guldner, and J G Spivack. Modification of discrete nuclear domains induced by herpes simplex virus type 1 immediate early gene 1 product (ICP0). *J Gen Virol*, 74 (Pt 12:2679–2690, 1993. doi: 10.1099/0022-1317-74-12-2679. URL https://www.ncbi.nlm.nih.gov/pubmed/8277273.

[118] M K Chelbi-Alix and H de The. Herpes virus induced proteasome-dependent degradation of the nuclear bodies-associated PML and Sp100 proteins. *Oncogene*, 18(4):935–941, 1999. doi: 10.1038/sj.onc.1202366. URL https://www.ncbi.nlm.nih.gov/pubmed/10023669.

[119] J Burkham, D M Coen, C B Hwang, and S K Weller. Interactions of herpes simplex virus type 1 with ND10 and recruitment of PML to replication compartments. *J Virol*, 75(5):2353–2367, 2001. doi: 10.1128/JVI.75.5.2353-2367.2001. URL https://www.ncbi.nlm.nih.gov/pubmed/11160739.

[120] A V Chee, P Lopez, P P Pandolfi, and B Roizman. Promyelocytic leukemia protein mediates interferon-based anti-herpes simplex virus 1 effects. *J Virol*, 77(12):7101–7105, 2003. doi: 10.1128/jvi.77.12.7101-7105.2003. URL https://www.ncbi.nlm.nih.gov/pubmed/12768029.

[121] R D Everett, S Rechter, P Papior, N Tavalai, T Stamminger, and A Orr. PML contributes to a cellular mechanism of repression of herpes simplex virus type 1 infection that is inactivated by ICP0. *J Virol*, 80(16):7995–8005, 2006. doi: 10.1128/JVI.00734-06. URL https://www.ncbi.nlm.nih.gov/pubmed/16873256.

[122] D Cuchet, A Sykes, A Nicolas, A Orr, J Murray, H Sirma, J Heeren, A Bartelt, and R D Everett. PML isoforms I and II participate in PML-dependent restriction of HSV-1 replication. *J Cell Sci*, 124(Pt 2):280–291, 2011. doi: 10.1242/jcs.075390. URL https://www.ncbi.nlm.nih.gov/pubmed/21172801.

[123] G Sourvinos and R D Everett. Visualization of parental HSV-1 genomes and replication compartments in association with ND10 in live infected cells. *EMBO J*, 21(18):4989–4997, 2002. doi: 10.1093/emboj/cdf458. URL https://www.ncbi.nlm.nih.gov/pubmed/12234938.

[124] R D Everett and A Zafiropoulos. Visualization by live-cell microscopy of disruption of ND10 during herpes simplex virus type 1 infection. *J Virol*, 78(20):11411–11415, 2004. doi: 10.1128/JVI.78.20.11411-11415.2004. URL https://www.ncbi.nlm.nih.gov/pubmed/15452264.

[125] P Xu, S Mallon, and B Roizman. PML plays both inimical and beneficial roles in HSV-1 replication. *Proc Natl Acad Sci U S A*, 113(21):3022–8, 2016. doi: 10.1073/pnas.1605513113. URL https://www.ncbi.nlm.nih.gov/pubmed/27162364.

[126] P Xu and B Roizman. The SP100 component of ND10 enhances accumulation of PML and suppresses replication and the assembly of HSV replication compartments. *Proc Natl Acad Sci U S A*, 114(19):E3823–E3829, 2017. doi: 10.1073/pnas.1703395114. URL https://www.ncbi.nlm.nih.gov/pubmed/28439026.

[127] P E Merkl, M H Orzalli, and D M Knipe. Mechanisms of Host IFI16, PML, and Daxx Protein Restriction of Herpes Simplex Virus 1 Replication. *J Virol*, 92(10), 2018. doi: 10.1128/JVI.00057-18. URL https://www.ncbi.nlm.nih.gov/pubmed/29491153.

[128] Q Tang, L Li, A M Ishov, V Revol, A L Epstein, and G G Maul. Determination of minimum herpes simplex virus type 1 components necessary to localize transcriptionally active DNA to ND10. *J Virol*, 77(10):5821–5828, 2003. doi: 10.1128/jvi.77.10.5821-5828.2003. URL https://www.ncbi.nlm.nih.gov/pubmed/12719575.

[129] R D Everett, G Sourvinos, C Leiper, J B Clements, and A Orr. Formation of nuclear foci of the herpes simplex virus type 1 regulatory protein ICP4 at early times of infection: localization, dynamics, recruitment of ICP27, and evidence for the de novo induction of ND10-like complexes. *J Virol*, 78(4):1903–1917, 2004. doi: 10.1128/jvi.78.4.1903-1917.2004. URL https://www.ncbi.nlm.nih.gov/pubmed/14747555.

[130] R D Everett and J Murray. ND10 components relocate to sites associated with herpes simplex virus type 1 nucleoprotein complexes during virus infection. *J Virol*, 79(8):5078–5089, 2005. doi: 10.1128/JVI.79.8.5078-5089.2005. URL https://www.ncbi.nlm.nih.gov/pubmed/15795293.

[131] T Komatsu, K Nagata, and H Wodrich. The Role of Nuclear Antiviral Factors against Invading DNA Viruses: The Immediate Fate of Incoming Viral Genomes. *Viruses*, 8(10), 2016. doi: 10.3390/v8100290. URL https://www.ncbi.nlm.nih.gov/pubmed/27782081.

[132] Nagaraj Kerur, Mohanan Valiya Veettil, Neelam Sharma-Walia, Virginie Bottero, Sathish Sadagopan, Pushpalatha Otageri, and Bala Chandran. IFI16 acts as a nuclear pathogen sensor to induce the inflammasome in response to Kaposi Sarcoma-associated herpesvirus infection. *Cell Host and Microbe*, 9(5):363–375, 5 2011. ISSN 19313128. doi: 10.1016/J.CHOM.2011.04.008.

[133] Tuo Li, Benjamin A. Diner, Jin Chen, and Ileana M. Cristea. Acetylation modulates cellular distribution and DNA sensing ability of interferon-inducible protein IFI16. *Proceedings of the National Academy of Sciences of the United States of America*, 109(26):10558–10563, 6 2012. ISSN 1091-6490. doi: 10.1073/PNAS.1203447109. URL https://pubmed.ncbi.nlm.nih.gov/22691496/.

[134] R D Everett. Dynamic Response of IFI16 and Promyelocytic Leukemia Nuclear Body Components to Herpes Simplex Virus 1 Infection. *J Virol*, 90(1):167–179, 2016. doi: 10.1128/JVI.02249-15. URL https://www.ncbi.nlm.nih.gov/pubmed/26468536.

[135] J M Cabral, H S Oh, and D M Knipe. ATRX promotes maintenance of herpes simplex virus heterochromatin during chromatin stress. *Elife*, 7, 2018. doi: 10.7554/eLife.40228. URL https://www.ncbi.nlm.nih.gov/pubmed/30465651.

[136] Leonie Unterholzner, Sinead E. Keating, Marcin Baran, Kristy A. Horan, Søren B. Jensen, Shruti Sharma, Cherilyn M. Sirois, Tengchuan Jin, Eicke Latz, T. Sam Xiao, Katherine A. Fitzgerald, Søren R. Paludan, and Andrew G. Bowie. IFI16 is an innate immune sensor for intracellular DNA. *Nature Immunology*, 11(11):997–1004, 11 2010. ISSN 15292908. doi: 10.1038/ni.1932. URL https://www.nature.com/articles/ni.1932.

[137] M H Orzalli, N M Broekema, B A Diner, D C Hancks, N C Elde, I M Cristea, and D M Knipe. cGAS-mediated stabilization of IFI16 promotes innate signaling during herpes simplex virus infection. *Proc Natl Acad Sci U S A*, 112(14):1773–81, 2015. doi: 10.1073/pnas.1424637112. URL https://www.ncbi.nlm.nih.gov/pubmed/25831530.

[138] Mitsutoshi Yoneyama, Wakako Suhara, Yukiko Fukuhara, Makoto Fukuda, Eisuke Nishida, and Takashi Fujita. Direct triggering of the type I interferon system by virus infection: activation of a transcription factor complex containing IRF-3 and CBP/p300. *The EMBO Journal*, 17(4):1087, 2 1998. ISSN 02614189. doi: 10.1093/EMBOJ/17.4.1087. URL /pmc/articles/PMC1170457/?report=abstract https://www.ncbi.nlm.nih.gov/pmc/articles/PMC1170457/.

[139] Thomas G.W. Graham, Johannes C. Walter, and Joseph J. Loparo. Two-Stage Synapsis of DNA Ends during Non-homologous End Joining. *Molecular cell*, 61(6):850–858, 3 2016. ISSN 1097-4164. doi: 10.1016/J.MOLCEL.2016.02.010. URL https://pubmed.ncbi.nlm.nih.gov/26990988/.

[140] Andrew Lopez, Randilea Nichols Doyle, Carina Sandoval, Karly Nisson, Vivian Yang, and Oliver I. Fregoso. Viral Modulation of the DNA Damage Response and Innate Immunity: Two Sides of the Same Coin. *Journal of Molecular Biology*, 434(6):167327, 3 2022. ISSN 0022-2836. doi: 10.1016/J.JMB.2021.167327.

[141] Samantha Smith, Nina Reuven, Kareem N. Mohni, April J. Schumacher, and Sandra K. Weller. Structure of the Herpes Simplex Virus 1 Genome: Manipulation of Nicks and Gaps Can Abrogate Infectivity and Alter the Cellular DNA Damage Response. *Journal of Virology*, 88(17):10146–10156, 9 2014. ISSN 0022-538X. doi: 10.1128/JVI.01723-14/ASSET/60AC6E59-14A3-4697-B4CA-C55C356016C8/ASSETS/GRAPHIC/ZJV9990994490009.JPEG. URL https://journals.asm.org/doi/10.1128/JVI.01723-14.

[142] Richard W. Hyman, John E. Oakes, and Linda Kudler. In vitro repair of the preexisting nicks and gaps in herpes simplex virus DNA. *Virology*, 76(1):286–294, 1 1977. ISSN 0042-6822. doi: 10.1016/0042-6822(77)90303-8.

[143] C E Lilley, C T Carson, A R Muotri, F H Gage, and M D Weitzman. DNA repair proteins affect the lifecycle of herpes simplex virus 1. *Proc Natl Acad Sci U S A*, 102(16):5844–5849, 2005. doi: 10.1073/pnas.0501916102. URL https://www.ncbi.nlm.nih.gov/pubmed/15824307.

[144] Jane Parkinson, Susan P. Lees-Miller, and Roger D. Everett. Herpes simplex virus type 1 immediate-early protein vmw110 induces the proteasome-dependent degradation of the catalytic subunit of DNA-dependent protein kinase. *Journal of virology*, 73(1):650–657, 1 1999. ISSN 0022-538X. doi: 10.1128/JVI.73.1.650-657.1999. URL https://pubmed.ncbi.nlm.nih.gov/9847370/.

[145] Oleg Alekseev, Kelly Donovan, and Jane Azizkhan-Clifford. Inhibition of ataxia telangiectasia mutated (ATM) kinase suppresses herpes simplex virus type 1 (HSV-1) keratitis. *Investigative ophthalmology & visual science*, 55(2):706–715, 12 2014. ISSN 1552-5783. doi: 10.1167/IOVS.13-13461. URL https://pubmed.ncbi.nlm.nih.gov/24370835/.

[146] Max E. Mertens and David M. Knipe. Herpes Simplex Virus 1 Manipulates Host Cell Antiviral and Proviral DNA Damage Responses. *mBio*, 12(1):1–22, 2021. ISSN 2150-7511. doi: 10.1128/MBIO.03552-20. URL https://pubmed.ncbi.nlm.nih.gov/33563816/.

[147] Jason S. Iacovoni, Pierre Caron, Imen Lassadi, Estelle Nicolas, Laurent Massip, Didier Trouche, and Gaëlle Legube. High-resolution profiling of gammaH2AX around DNA double strand breaks in the mammalian genome. *The EMBO journal*, 29(8):1446–1457, 4 2010. ISSN 1460-2075. doi: 10.1038/EMBOJ.2010.38. URL https://pubmed.ncbi.nlm.nih.gov/20360682/.

[148] Sandeep Burma, Benjamin P. Chen, Michael Murphy, Akihiro Kurimasa, and David J. Chen. ATM phosphorylates histone H2AX in response to DNA double-strand breaks. *The Journal of biological chemistry*, 276(45):42462–42467, 11 2001. ISSN 0021-9258. doi: 10.1074/JBC.C100466200. URL https://pubmed.ncbi.nlm.nih.gov/11571274/.

[149] C Botting, X Lu, and S J Triezenberg. H2AX phosphorylation and DNA damage kinase activity are dispensable for herpes simplex virus replication. *Virol J*, 13:15, 2016. doi: 10.1186/s12985-016-0470-1. URL https://www.ncbi.nlm.nih.gov/pubmed/26817608.

[150] J Oh and N W Fraser. Temporal association of the herpes simplex virus genome with histone proteins during a lytic infection. *J Virol*, 82(7):3530–3537, 2008. doi: 10.1128/JVI.00586-07. URL https://www.ncbi.nlm.nih.gov/pubmed/18160436.

[151] F J Herrera and S J Triezenberg. VP16-dependent association of chromatin-modifying coactivators and underrepresentation of histones at immediate-early gene promoters during herpes simplex virus infection. *J Virol*, 78(18):9689–9696, 2004. doi: 10.1128/JVI.78.18.9689-9696.2004. URL https://www.ncbi.nlm.nih.gov/pubmed/15331701.

[152] Jennifer S. Lee, Priya Raja, and David M. Knipe. Herpesviral ICP0 Protein Promotes Two Waves of Heterochromatin Removal on an Early Viral Promoter during Lytic Infection. *mBio*, 7(1), 1 2016. ISSN 21507511. doi: 10.1128/MBIO.02007-15. URL /pmc/articles/PMC4725016/ /pmc/articles/PMC4725016/?report=abstract https://www.ncbi.nlm.nih.gov/pmc/articles/PMC4725016/.

[153] Matthew H. Spitzer and Garry P. Nolan. Mass Cytometry: Single Cells, Many Features. *Cell*, 165(4):780–791, 5 2016. ISSN 1097-4172. doi: 10.1016/J.CELL.2016.04.019. URL https://pubmed.ncbi.nlm.nih.gov/27153492/.

[154] Elizabeth H. Finn, Gianluca Pegoraro, Hugo B. Brandão, Anne Laure Valton, Marlies E. Oomen, Job Dekker, Leonid Mirny, and Tom Misteli. Extensive Heterogeneity and Intrinsic Variation in Spatial Genome Organization. *Cell*, 176(6):1502–1515, 3 2019. ISSN 1097-4172. doi: 10.1016/J.CELL.2019.01.020. URL https://pubmed.ncbi.nlm.nih.gov/30799036/.

[155] Efrat M. Cohen and Oren Kobiler. Gene Expression Correlates with the Number of Herpes Viral Genomes Initiating Infection in Single Cells. *PLOS Pathogens*, 12(12): e1006082, 12 2016. ISSN 1553-7374. doi: 10.1371/JOURNAL.PPAT.1006082. URL https://journals.plos.org/plospathogens/article?id=10.1371/journal.ppat.1006082.

[156] Nir Drayman, Parthiv Patel, and Luke Vistain. HSV-1 single-cell analysis reveals the activation of anti-viral and developmental programs in distinct sub-populations. *eLife*, 8, 5 2019. ISSN 2050084X. doi: 10.7554/ELIFE.46339.

[157] Ellen M. Sletten and Carolyn R. Bertozzi. From mechanism to mouse: A tale of two bioorthogonal reactions. *Accounts of Chemical Research*, 44(9):666–676, 9 2011. ISSN 00014842. doi: 10.1021/AR200148Z/ASSET/IMAGES/LARGE/AR-2011-00148Z_0014.JPEG. URL https://pubs.acs.org/doi/full/10.1021/ar200148z.

[158] H C Kolb, M G Finn, and K B Sharpless. Click Chemistry: Diverse Chemical Function from a Few Good Reactions. *Angew Chem Int Ed Engl*, 40(11):2004–2021, 2001. doi: 10.1002/1521-3773(20010601)40:11¡2004::aid-anie2004¿3.3.co;2-x. URL https://www.ncbi.nlm.nih.gov/pubmed/11433435.

[159] Eliana Saxon and Carolyn R. Bertozzi. Cell surface engineering by a modified Staudinger reaction. *Science (New York, N.Y.)*, 287(5460):2007–2010, 3 2000. ISSN 0036-8075. doi: 10.1126/SCIENCE.287.5460.2007. URL https://pubmed.ncbi.nlm.nih.gov/10720325/.

[160] Robert E Bird, Steven A Lemmel, Xiang Yu, and Qiongqiong Angela Zhou. Bioorthogonal Chemistry and Its Applications. 2021. doi: 10.1021/acs.bioconjchem.1c00461. URL https://doi.org/10.1021/acs.bioconjchem.1c00461.

[161] Nicholas J Agard, Jennifer A Prescher, and Carolyn R Bertozzi. A Strain-Promoted [3 + 2] Azide-Alkyne Cycloaddition for Covalent Modification of Biomolecules in Living Systems. 2004. doi: 10.1021/ja044996f. URL http://pubs.acs.org.

[162] Zoltan Cseresnyes, Ulf Schwarz, and Catherine M. Green. Analysis of replication factories in human cells by super-resolution light microscopy. *BMC Cell Biology*, 10(1): 1–12, 12 2009. ISSN 14712121. doi: 10.1186/1471-2121-10-88/FIGURES/5. URL https://bmcmolcellbiol.biomedcentral.com/articles/10.1186/1471-2121-10-88.

[163] Nora Schmidt, Thomas Hennig, Remigiusz A. Serwa, Magda Marchetti, and Peter O'Hare. Remote Activation of Host Cell DNA Synthesis in Uninfected Cells Signaled by Infected Cells in Advance of Virus Transmission. *Journal of virology*, 89(21):11107–11115, 11 2015. ISSN 1098-5514. doi: 10.1128/JVI.01950-15. URL https://pubmed.ncbi.nlm.nih.gov/26311877/.

[164] I. Hsuan Wang, Maarit Suomalainen, Vardan Andriasyan, Samuel Kilcher, Jason Mercer, Anne Neef, Nathan W. Luedtke, and Urs F. Greber. Tracking viral genomes in host cells at single-molecule resolution. *Cell host & microbe*, 14(4):468–480, 10 2013. ISSN 1934-6069. doi: 10.1016/J.CHOM.2013.09.004. URL https://pubmed.ncbi.nlm.nih.gov/24139403/.

[165] Eiki Sekine, Nora Schmidt, David Gaboriau, and Peter O'Hare. Spatiotemporal dynamics of HSV genome nuclear entry and compaction state transitions using bioorthogonal chemistry and super-resolution microscopy. *PLOS Pathogens*, 13(11):e1006721, 11 2017. ISSN 1553-7374. doi: 10.1371/journal.ppat.1006721. URL https://dx.plos.org/10.1371/journal.ppat.1006721.

[166] T Alandijany, A P E Roberts, K L Conn, C Loney, S McFarlane, A Orr, and C Boutell. Distinct temporal roles for the promyelocytic leukaemia (PML) protein in the sequential regulation of intracellular host immunity to HSV-1 infection. *PLoS Pathog*, 14(1):e1006769, 2018. doi: 10.1371/journal.ppat.1006769. URL https://www.ncbi.nlm.nih.gov/pubmed/29309427.

[167] Fuchou Tang, Catalin Barbacioru, Yangzhou Wang, Ellen Nordman, Clarence Lee, Nanlan Xu, Xiaohui Wang, John Bodeau, Brian B. Tuch, Asim Siddiqui, Kaiqin Lao, and M. Azim Surani. mRNA-Seq whole-transcriptome analysis of a single cell. *Nature Methods 2009 6:5*, 6(5):377–382, 4 2009. ISSN 1548-7105. doi: 10.1038/nmeth.1315. URL https://www.nature.com/articles/nmeth.1315.

[168] E. Carol McWilliam Leitch and John McLauchlan. Determining the Cellular Diversity of Hepatitis C Virus Quasispecies by Single-Cell Viral Sequencing. *Journal of Virology*, 87(23):12648, 12 2013. ISSN 0022-538X. doi: 10.1128/JVI.01602-13. URL /pmc/articles/PMC3838117/ /pmc/articles/PMC3838117/?report=abstract https://www.ncbi.nlm.nih.gov/pmc/articles/PMC3838117/.

[169] Sara Cristinelli and Angela Ciuffi. The use of single-cell RNA-Seq to understand virus–host interactions. *Current Opinion in Virology*, 29:39–50, 4 2018. ISSN 1879-6257. doi: 10.1016/J.COVIRO.2018.03.001.

[170] Jiayi Sun, J. Cristobal Vera, Jenny Drnevich, Yen Ting Lin, Ruian Ke, and Christopher B. Brooke. Single cell heterogeneity in influenza A virus gene expression shapes the innate antiviral response to infection. *PLoS Pathogens*, 16(7), 7 2020. ISSN 15537374. doi: 10.1371/JOURNAL.PPAT.1008671. URL /pmc/articles/PMC7363107/ /pmc/articles/PMC7363107/?report=abstract https://www.ncbi.nlm.nih.gov/pmc/articles/PMC7363107/.

[171] Alistair B. Russell, Cole Trapnell, and Jesse D. Bloom. Extreme heterogeneity of influenza virus infection in single cells. *eLife*, 7, 2 2018. ISSN 2050-084X. doi: 10.7554/ELIFE.32303. URL https://pubmed.ncbi.nlm.nih.gov/29451492/.

[172] Fay Wang, John Flanagan, Nan Su, Li Chong Wang, Son Bui, Allissa Nielson, Xingyong Wu, Hong Thuy Vo, Xiao Jun Ma, and Yuling Luo. RNAscope: A novel in situ RNA analysis platform for formalin-fixed, paraffin-embedded tissues. *Journal of Molecular Diagnostics*, 14(1):22–29, 1 2012. ISSN 15251578. doi: 10.1016/j.jmoldx.2011.08.002. URL https://pubmed.ncbi.nlm.nih.gov/22166544/.

[173] Heeva Baharlou, Nicolas Canete, Erica E. Vine, Kevin Hu, Di Yuan, Kerrie J. Sandgren, Kirstie M. Bertram, Najla Nasr, Jake W. Rhodes, Martijn P. Gosselink, Angelina Di Re, Faizur Reza, Grahame Ctercteko, Nimalan Pathma-Nathan, Geoff Collins, James Toh, Ellis Patrick, Muzlifah A. Haniffa, Jacob D. Estes, Scott N. Byrne, Anthony L. Cunningham, and Andrew N. Harman. An in situ analysis pipeline for initial host-pathogen interactions reveals signatures of human colorectal HIV transmission. *Cell Reports*, 40(12):111385, 9 2022. ISSN 2211-1247. doi: 10.1016/J.CELREP.2022.111385.

[174] Karoline Metzger, Cyrine Bentaleb, Kévin Hervouet, Virginie Alexandre, Claire Montpellier, Jean Michel Saliou, Martin Ferrié, Charline Camuzet, Yves Rouillé, Cécile Lecoeur, Jean Dubuisson, Laurence Cocquerel, and Cécile Marie Aliouat-Denis. Processing and Subcellular Localization of the Hepatitis E Virus Replicase: Identification of Candidate Viral Factories. *Frontiers in Microbiology*, 13:467, 2 2022. ISSN 1664302X. doi: 10.3389/FMICB.2022.828636/BIBTEX.

[175] Fengming Liu, Kun Han, Robert Blair, Kornelia Kenst, Zhongnan Qin, Berin Upcin, Philipp Wörsdörfer, Cecily C. Midkiff, Joseph Mudd, Elizaveta Belyaeva, Nicholas S. Milligan, Tyler D. Rorison, Nicole Wagner, Jochen Bodem, Lars Dölken, Bertal H. Aktas, Richard S. Vander Heide, Xiao Ming Yin, Jay K. Kolls, Chad J. Roy, Jay Rappaport, Süleyman Ergün, and Xuebin Qin. SARS-CoV-2 Infects Endothelial Cells In Vivo and In Vitro. *Frontiers in Cellular and Infection Microbiology*, 11:1, 7 2021. ISSN 22352988. doi: 10.3389/FCIMB.2021.701278/FULL. URL /pmc/articles/PMC8292147/ /pmc/articles/PMC8292147/?report=abstract https://www.ncbi.nlm.nih.gov/pmc/articles/PMC8292147/.

[176] Ekaette F. Mbong, Lucille Woodley, Eric Dunkerley, Jane E. Schrimpf, Lynda A. Morrison, and Carol Duffy. Deletion of the Herpes Simplex Virus 1 U L 49 Gene Results in mRNA and Protein Translation Defects That Are Complemented by Secondary Mutations in U L 41 . *Journal of Virology*, 86(22):12351–12361, 11 2012. ISSN 0022-538X. doi: 10.1128/JVI.01975-12/ASSET/6E388379-A994-4955-BE00-DFA07C3F1088/ASSETS/GRAPHIC/ZJV9990968320006.JPEG. URL https://journals.asm.org/doi/10.1128/JVI.01975-12.

[177] Cathryn E. Garvey, Chris L. McGowin, and Timothy P. Foster. Development and evaluation of SYBR Green-I based quantitative PCR assays for herpes simplex virus type 1 whole transcriptome analysis. *Journal of virological methods*, 201:101–111, 6 2014. ISSN 1879-0984. doi: 10.1016/J.JVIROMET.2014.02.010. URL https://pubmed.ncbi.nlm.nih.gov/24607486/.

[178] Fabrice de Chaumont and Stephane Dallongeville. ICY Plugin Spot Detector, 2011. URL https://icy.bioimageanalysis.org/plugin/spot-detector/.

[179] Edward Tunnacliffe and Jonathan R. Chubb. What Is a Transcriptional Burst? *Trends in Genetics*, 36(4):288–297, 4 2020. ISSN 0168-9525. doi: 10.1016/J.TIG.2020.01.003.

[180] Orsolya Symmons, Marcello Chang, Ian A. Mellis, Jennifer M. Kalish, Jihwan Park, Katalin Suszták, Marisa S. Bartolomei, and Arjun Raj. Allele-specific RNA imaging shows that allelic imbalances can arise in tissues through transcriptional bursting. *PLoS genetics*, 15(1), 2019. ISSN 1553-7404. doi: 10.1371/JOURNAL.PGEN.1007874. URL https://pubmed.ncbi.nlm.nih.gov/30625149/.

[181] Roy D. Dar, Brandon S. Razooky, Abhyudai Singh, Thomas V. Trimeloni, James M. McCollum, Chris D. Cox, Michael L. Simpson, and Leor S. Weinberger. Transcriptional burst frequency and burst size are equally modulated across the human genome. *Proceedings of the National Academy of Sciences of the United States of America*, 109 (43):17454–17459, 10 2012. ISSN 00278424. doi: 10.1073/PNAS.1213530109/SUPPL_FILE/APPENDIX.PDF. URL https://www.pnas.org/doi/abs/10.1073/pnas.1213530109.

[182] Joseph Rodriguez and Daniel R. Larson. Transcription in Living Cells: Molecular Mechanisms of Bursting. *https://doi.org/10.1146/annurev-biochem-011520-105250*, 89:189–212, 6 2020. ISSN 15454509. doi: 10.1146/ANNUREV-BIOCHEM-011520-105250. URL https://www.annualreviews.org/doi/abs/10.1146/annurev-biochem-011520-105250.

[183] Abhyudai Singh, Brandon Razooky, Chris D. Cox, Michael L. Simpson, and Leor S. Weinberger. Transcriptional Bursting from the HIV-1 Promoter Is a Significant Source of Stochastic Noise in HIV-1 Gene Expression. *Biophysical Journal*, 98(8):L32, 4 2010. ISSN 15420086. doi: 10.1016/J.BPJ.2010.03.001.

URL /pmc/articles/PMC2856162/ /pmc/articles/PMC2856162/?report=abstract https://www.ncbi.nlm.nih.gov/pmc/articles/PMC2856162/.

[184] Katjana Tantale, Encar Garcia-Oliver, Marie Cécile Robert, Adèle L'Hostis, Yueyuxiao Yang, Nikolay Tsanov, Rachel Topno, Thierry Gostan, Alja Kozulic-Pirher, Meenakshi Basu-Shrivastava, Kamalika Mukherjee, Vera Slaninova, Jean Christophe Andrau, Florian Mueller, Eugenia Basyuk, Ovidiu Radulescu, and Edouard Bertrand. Stochastic pausing at latent HIV-1 promoters generates transcriptional bursting. *Nature Communications 2021 12:1*, 12(1):1–20, 7 2021. ISSN 2041-1723. doi: 10.1038/s41467-021-24462-5. URL https://www.nature.com/articles/s41467-021-24462-5.

[185] Katjana Tantale, Florian Mueller, Alja Kozulic-Pirher, Annick Lesne, Jean Marc Victor, Marie Cecile Robert, Serena Capozi, Racha Chouaib, Volker Bäcker, Julio Mateos-Langerak, Xavier Darzacq, Christophe Zimmer, Eugenia Basyuk, and Edouard Bertrand. A single-molecule view of transcription reveals convoys of RNA polymerases and multi-scale bursting. *Nature Communications 2016 7:1*, 7(1):1–14, 7 2016. ISSN 2041-1723. doi: 10.1038/ncomms12248. URL https://www.nature.com/articles/ncomms12248.

[186] Esther Braselmann, Colin Rathbun, Erin M. Richards, and Amy E. Palmer. Illuminating RNA Biology: Tools for Imaging RNA in Live Mammalian Cells. *Cell Chemical Biology*, 27(8):891–903, 8 2020. ISSN 2451-9456. doi: 10.1016/J.CHEMBIOL.2020.06.010.

[187] Linda S. Forero-Quintero, William Raymond, Tetsuya Handa, Matthew N. Saxton, Tatsuya Morisaki, Hiroshi Kimura, Edouard Bertrand, Brian Munsky, and Timothy J. Stasevich. Live-cell imaging reveals the spatiotemporal organization of endogenous RNA polymerase II phosphorylation at a single gene. *Nature Communications 2021 12:1*, 12(1):1–16, 5 2021. ISSN 2041-1723. doi: 10.1038/s41467-021-23417-0. URL https://www.nature.com/articles/s41467-021-23417-0.

[188] Luca Sardo, Steven C. Hatch, Jianbo Chen, Olga Nikolaitchik, Ryan C. Burdick, De Chen, Christopher J. Westlake, Stephen Lockett, Vinay K. Pathak, and Wei-Shau Hu. Dynamics of HIV-1 RNA Near the Plasma Membrane during Virus Assembly. *Journal of virology*, 89(21):10832–10840, 11 2015. ISSN 1098-5514. doi: 10.1128/JVI.01146-15. URL https://pubmed.ncbi.nlm.nih.gov/26292321/.

[189] Benita Turner-Bridger, Maximillian Jakobs, Leila Muresan, Ho-Wai Wong, Kristian Franze, William A Harris, and Christine E Holt. Single-molecule analysis of endogenous β-actin mRNA trafficking reveals a mechanism for compartmentalized mRNA localization in axons. doi: 10.1073/pnas.1806189115. URL www.pnas.org/cgi/doi/10.1073/pnas.1806189115.

[190] Chris I Ace, Tom A Mckee, J Michael Ryan, Janet M Cameron, and Chris M Preston'. Construction and Characterization of a Herpes Simplex Virus Type 1 Mutant Unable To Transinduce Immediate-Early Gene Expression. *JOURNAL OF VIROLOGY*, 63(5):2260–2269, 1989. URL https://journals.asm.org/journal/jvi.

[191] M. McFarlane, J. I. Daksis, and C. M. Preston. Hexamethylene bisacetamide stimulates herpes simplex virus immediate early gene expression in the absence of trans-induction by Vmw65. *Journal of General Virology*, 73(2):285–292, 1992. ISSN 00221317. doi: 10.1099/0022-1317-73-2-285. URL https://pubmed.ncbi.nlm.nih.gov/1371540/.

[192] Roberta C. Reuben, Richard A. Rifkind, and Paul A. Marks. Chemically induced murine erythroleukemic differentiation. *Biochimica et Biophysica Acta (BBA) - Reviews on Cancer*, 605(3):325–346, 9 1980. ISSN 0304-419X. doi: 10.1016/0304-419X(80)90015-3.

[193] Chris M. Preston and Morag McFarlane. Cytodifferentiating Agents Affect the Replication of Herpes Simplex Virus Type 1 in the Absence of Functional VP16. *Virology*, 249(2):418–426, 9 1998. ISSN 0042-6822. doi: 10.1006/VIRO.1998.9314.

[194] Masatoshi Kusuhara, Koichi Nagasaki, Kensuke Kimura, Nicolai Maass, Tomohiro Manabe, Shiro Ishikawa, Minoru Aikawa, Koji Miyazaki, and Ken Yamaguchi. Cloning of Hexamethylene-bis-acetamide-inducible Transcript, HEXIM1, in Human Vascular Smooth Muscle Cells. *Biomedical Research*, 20(5):273–279, 10 1999. ISSN 0388-6107. doi: 10.2220/BIOMEDRES.20.273.

[195] Rika Ouchida, Kusuhara, Masatoshi, and Hirotoshi Tanaka. Suppression of NFkappaB-dependent gene expression by a hexamethylene bisacetamide-inducible protein HEXIM1 in human vascular smooth muscle cells. *Genes Cells*, 8(2):95–107, 2003. doi: 10.1046/j.1365-2443.2003.00618.x.

[196] Jaromir Vlach and Paula M Pitha. Hexamethylene bisacetamide activates the human immunodeficiency virus type 1 provirus by an NF-tcB-independent mechanism. *Journal of General Virology*, page 74, 1993.

[197] Vladimir Klichko, Nancy Archin, Rupinderjeet Kaur, Ginger Lehrman, and David Margolis. Hexamethylbisacetamide remodels the human immunodeficiency virus type 1 (HIV-1) promoter and induces Tat-independent HIV-1 expression but blunts cell activation. *Journal of virology*, 80(9):4570–4579, 5 2006. ISSN 0022-538X. doi: 10.1128/JVI.80.9.4570-4579.2006. URL https://pubmed.ncbi.nlm.nih.gov/16611917/.

[198] Panagis Filippakopoulos, Jun Qi, Sarah Picaud, Yao Shen, William B. Smith, Oleg Fedorov, Elizabeth M. Morse, Tracey Keates, Tyler T. Hickman, Ildiko Felletar, Martin Philpott, Shonagh Munro, Michael R. McKeown, Yuchuan Wang, Amanda L. Christie, Nathan West, Michael J. Cameron, Brian Schwartz, Tom D. Heightman, Nicholas La Thangue, Christopher A. French, Olaf Wiest, Andrew L. Kung, Stefan Knapp, and James E. Bradner. Selective inhibition of BET bromodomains. *Nature 2010 468:7327*, 468(7327):1067–1073, 9 2010. ISSN 1476-4687. doi: 10.1038/nature09504. URL https://www.nature.com/articles/nature09504.

[199] Jake E. Delmore, Ghayas C. Issa, Madeleine E. Lemieux, Peter B. Rahl, Junwei Shi, Hannah M. Jacobs, Efstathios Kastritis, Timothy Gilpatrick, Ronald M. Paranal, Jun Qi, Marta Chesi, Anna C. Schinzel, Michael R. McKeown, Timothy P. Heffernan, Christopher R. Vakoc, P. Leif Bergsagel, Irene M. Ghobrial, Paul G. Richardson, Richard A. Young, William C. Hahn, Kenneth C. Anderson, Andrew L. Kung, James E. Bradner, and Constantine S. Mitsiades. BET bromodomain inhibition as a therapeutic strategy to target c-Myc. *Cell*, 146(6):904–917, 9 2011. ISSN 1097-4172. doi: 10.1016/J.CELL.2011.08.017. URL https://pubmed.ncbi.nlm.nih.gov/21889194/.

[200] Ke Ren, Wei Zhang, Xiaoqing Chen, Yingyu Ma, Yue Dai, Yimei Fan, Yayi Hou, Ren Xiang Tan, and Erguang Li. An Epigenetic Compound Library Screen Identifies BET Inhibitors That Promote HSV-1 and -2 Replication by Bridging P-TEFb to Viral Gene Promoters through BRD4. *PLoS pathogens*, 12(10), 10 2016. ISSN 1553-7374. doi: 10.1371/JOURNAL.PPAT.1005950. URL https://pubmed.ncbi.nlm.nih.gov/27764245/.

[201] Koen Bartholomeeusen, Yanhui Xiang, Koh Fujinaga, and B. Matija Peterlin. Bromodomain and extra-terminal (BET) bromodomain inhibition activate transcription via transient release of positive transcription elongation factor b (P-TEFb) from 7SK small nuclear ribonucleoprotein. *The Journal of biological chemistry*, 287(43):36609–36616, 10 2012. ISSN 1083-351X. doi: 10.1074/JBC.M112.410746. URL https://pubmed.ncbi.nlm.nih.gov/22952229/.

[202] Akhil Bowry, Ann Liza Piberger, Patricia Rojas, Marco Saponaro, and Eva Petermann. BET Inhibition Induces HEXIM1- and RAD51-Dependent Conflicts between Transcription and Replication. *Cell Reports*, 25(8):2061, 11 2018. ISSN 22111247. doi: 10.1016/J.CELREP.2018.10.079. URL /pmc/articles/PMC6280123/ /pmc/articles/PMC6280123/?report=abstract https://www.ncbi.nlm.nih.gov/pmc/articles/PMC6280123/.

[203] Mimmo Turano, Giuliana Napolitano, Cyprien Dulac, Barbara Majello, Olivier Bensaude, and Luigi Lania. Increased HEXIM1 expression during erythroleukemia and neuroblastoma cell differentiation. *Journal of cellular physiology*, 206(3):603–610, 3 2006. ISSN 0021-9541. doi: 10.1002/JCP.20502. URL https://pubmed.ncbi.nlm.nih.gov/16222702/.

[204] Wannarasmi Ketchart, I. Ju Yeh, Haoyan Zhou, Praveena S. Thiagarajan, Justin Lathia, Ofer Reizes, Agata Exner, Bin Su, and Monica M. Montano. Induction of HEXIM1 activities by HMBA derivative 4a1: functional consequences and mechanism. *Cancer letters*, 379(1):60, 8 2016. ISSN 18727980. doi: 10.1016/J.CANLET.2016.05.029. URL /pmc/articles/PMC4988685/ /pmc/articles/PMC4988685/?report=abstract https://www.ncbi.nlm.nih.gov/pmc/articles/PMC4988685/.

[205] Nanhai He, Andrea C. Pezda, and Qiang Zhou. Modulation of a P-TEFb Functional Equilibrium for the Global Control of Cell Growth and Differentiation. *Molecular and Cellular Biology*, 26(19):7068, 10 2006. ISSN 0270-7306. doi: 10.1128/MCB.00778-06. URL /pmc/articles/PMC1592901/ /pmc/articles/PMC1592901/?report=abstract https://www.ncbi.nlm.nih.gov/pmc/articles/PMC1592901/.

[206] Takeshi Kurosu and B. Matija Peterlin. VP16 and ubiquitin; binding of P-TEFb via its activation domain and ubiquitin facilitates elongation of transcription of target genes. *Current biology : CB*, 14(12):1112–1116, 6 2004. ISSN 0960-9822. doi: 10.1016/J.CUB.2004.06.020. URL https://pubmed.ncbi.nlm.nih.gov/15203006/.

[207] Johannes Gräff and Li Huei Tsai. Histone acetylation: molecular mnemonics on the chromatin. *Nature Reviews Neuroscience 2013 14:2*, 14(2):97–111, 1 2013. ISSN 1471-0048. doi: 10.1038/nrn3427. URL https://www.nature.com/articles/nrn3427.

[208] N. Sturman, A. De Graaf, A. Floore, A. Josso, B. Humbel, L. De Jong, and R. Van Driel. A monoclonal antibody recognizing nuclear matrix-associated nuclear bodies. *Journal of Cell Science*, 101(4):773–784, 4 1992. ISSN 0021-9533. doi: 10.1242/JCS.101.4.773. URL https://journals.biologists.com/jcs/article/101/4/773/23268/A-monoclonal-antibody-reco

[209] Armelle Corpet, Constance Kleijwegt, Simon Roubille, Franceline Juillard, Karine Jacquet, Pascale Texier, and Patrick Lomonte. PML nuclear bodies and chromatin dynamics: catch me if you can! *Nucleic Acids Research*, 48(21):11890–11912, 12 2020. ISSN 0305-1048. doi: 10.1093/NAR/GKAA828. URL https://academic.oup.com/nar/article/48/21/11890/5929229.

[210] Eui Tae Kim, Joseph M. Dybas, Katarzyna Kulej, Emigdio D. Reyes, Alexander M. Price, Lisa N. Akhtar, Ann Orr, Benjamin A. Garcia, Chris Boutell, and Matthew D. Weitzman. Comparative proteomics identifies Schlafen 5 (SLFN5) as a herpes simplex virus restriction factor that suppresses viral transcription. *Nature Microbiology 2021 6:2*, 6(2):234–245, 1 2021. ISSN 2058-5276. doi: 10.1038/s41564-020-00826-3. URL https://www.nature.com/articles/s41564-020-00826-3.

[211] R. E. Randall and N. Dinwoodie. Intranuclear localization of herpes simplex virus immediate-early and delayed-early proteins: Evidence that ICP 4 is associated with progeny virus DNA. *Journal of General Virology*, 67 (10):2163–2177, 10 1986. ISSN 00221317. doi: 10.1099/0022-1317-67-10-2163/CITE/REFWORKS. URL https://www.microbiologyresearch.org/content/journal/jgv/10.1099/0022-1317-67-10-2163.

[212] Byeongwoon Song, J. Jian Liu, Kung Chieh Yeh, and David M. Knipe. Herpes Simplex Virus Infection Blocks Events in the G1 Phase of the Cell Cycle. *Virology*, 267(2):326–334, 2 2000. ISSN 0042-6822. doi: 10.1006/VIRO.1999.0146.

[213] Efrat M. Cohen, Nir Avital, Meir Shamay, and Oren Kobiler. Abortive herpes simplex virus infection of nonneuronal cells results in quiescent viral genomes that can reactivate. *Proceedings of the National Academy of Sciences of the United States of America*, 117(1):635–640, 1 2020. ISSN 10916490. doi: 10.1073/PNAS.1910537117/SUPPL_FILE/PNAS.1910537117.SAPP.PDF. URL https://www.pnas.org/doi/abs/10.1073/pnas.1910537117.

[214] Oren Kobiler and Matthew D. Weitzman. Herpes simplex virus replication compartments: From naked release to recombining together. *PLoS Pathogens*, 15(6), 6 2019. ISSN 15537374. doi: 10.1371/JOURNAL.PPAT.1007714. URL /pmc/articles/PMC6546242/ https://www.ncbi.nlm.nih.gov/pmc/articles/PMC6546242/.

[215] Travis J. Taylor, Elizabeth E. McNamee, Cheryl Day, and David M. Knipe. Herpes simplex virus replication compartments can form by coalescence of smaller compartments. *Virology*, 309(2):232–247, 5 2003. ISSN 00426822. doi: 10.1016/S0042-6822(03)00107-7. URL https://pubmed.ncbi.nlm.nih.gov/12758171/.

[216] Kathleen Pheasant, Carla Sofia Möller-Levet, Juliet Jones, Daniel Depledge, Judith Breuer, and Gillian Elliott. Nuclear-cytoplasmic compartmentalization of the herpes simplex virus 1 infected cell transcriptome is co-ordinated by the viral endoribonuclease vhs and cofactors to facilitate the translation of late proteins. *PLoS pathogens*, 14(11), 11 2018. ISSN 1553-7374. doi: 10.1371/JOURNAL.PPAT.1007331. URL https://pubmed.ncbi.nlm.nih.gov/30475899/.

[217] Travis J. Taylor and David M. Knipe. Proteomics of Herpes Simplex Virus Replication Compartments: Association of Cellular DNA Replication, Repair, Recombination, and Chromatin Remodeling Proteins with ICP8. *Journal of Virology*, 78(11):5856, 6 2004. ISSN 0022-538X. doi: 10.1128/JVI.78.11.5856-5866.2004. URL /pmc/articles/PMC415816/ /pmc/articles/PMC415816/?report=abstract https://www.ncbi.nlm.nih.gov/pmc/articles/PMC415816/.

[218] Lauren M Liptak, Susan L Uprichard, and David M Knipe. Functional order of assembly of herpes simplex virus DNA replication proteins into prereplicative site structures. *Journal of Virology*, 70(3):1759–1767, 3 1996. ISSN 0022-538X. doi: 10.1128/JVI.70.3.1759-1767.1996. URL https://journals.asm.org/journal/jvi.

[219] A Phelan, J Dunlop, A H Patel, N D Stow, and J B Clements. Nuclear sites of herpes simplex virus type 1 DNA replication and transcription colocalize at early times postinfection and are largely distinct from RNA processing factors. *Journal of virology*, 71(2):1124–1132, 2 1997. ISSN 0022-538X. doi: 10.1128/JVI.71.2.1124-1132.1997. URL https://pubmed.ncbi.nlm.nih.gov/8995633/.

[220] Robert G. Abrisch, Tess M. Eidem, Petro Yakovchuk, Jennifer F. Kugel, and James A. Goodrich. Infection by Herpes Simplex Virus 1 Causes Near-Complete Loss of RNA Polymerase II Occupancy on the Host Cell Genome. *Journal of virology*, 90(5):2503–2513, 3 2015. ISSN 1098-5514. doi: 10.1128/JVI.02665-15. URL https://pubmed.ncbi.nlm.nih.gov/26676778/.

[221] Andrzej J. Rutkowski, Florian Erhard, Anne L'Hernault, Thomas Bonfert, Markus Schilhabel, Colin Crump, Philip Rosenstiel, Stacey Efstathiou, Ralf Zimmer, Caroline C. Friedel, and Lars Dölken. Widespread disruption of host transcription termination in HSV-1 infection. *Nature communications*, 6, 5 2015. ISSN 2041-1723. doi: 10.1038/NCOMMS8126. URL https://pubmed.ncbi.nlm.nih.gov/25989971/.

[222] Thomas Hennig, Lara Djakovic, Lars Dölken, and Adam W. Whisnant. A Review of the Multipronged Attack of Herpes Simplex Virus 1 on the Host Transcriptional Machinery. *Viruses*, 13(9), 9 2021. ISSN 19994915. doi: 10.3390/V13091836. URL /pmc/articles/PMC8473234/ /pmc/articles/PMC8473234/?report=abstract https://www.ncbi.nlm.nih.gov/pmc/articles/PMC8473234/.

[223] Thomas Cremer, Marion Cremer, Barbara Hübner, Asli Silahtaroglu, Michael Hendzel, Christian Lanctôt, Hilmar Strickfaden, and Christoph Cremer. The Interchromatin Compartment Participates in the Structural and Functional Organization of the Cell Nucleus. *BioEssays*, 42(2):1900132, 2 2020. ISSN 1521-1878. doi: 10.1002/BIES.201900132. URL https://onlinelibrary.wiley.com/doi/full/10.1002/bies.201900132 https://onlinelibrary.wiley.com/doi/abs/10.1002/bies.201900132 https://onlinelibrary.wiley.com/doi/10.1002/bies.201900132.

[224] Olivier Bensaude. Inhibiting eukaryotic transcription. Which compound to choose? How to evaluate its activity? Which compound to choose? How to evaluate its activity? *www.landesbioscience.com Transcription 103 Transcription*, 2(3):103–108. ISSN 2154-1272. doi: 10.4161/trns.2.3.16172. URL https://www.tandfonline.com/action/journalInformation?journalCode=ktrn20.

[225] Sonja Baumli, Jane A. Endicott, and Louise N. Johnson. Halogen Bonds Form the Basis for Selective P-TEFb Inhibition by DRB. *Chemistry & Biology*, 17(9):931–936, 9 2010. ISSN 1074-5521. doi: 10.1016/J.CHEMBIOL.2010.07.012.

[226] Ulrich Scheer, Barbara Hugle, Rachel Hazan, and Kathleen M Rose. Drug-induced Dispersal of Transcribed rRNA Genes and Transcriptional Products : Immunolocalization and Silver Staining of Different Nucleolar Components in Rat Cells Treated with 5, 6-Dichloro-ß-D-Ribofuranosylbenzimidazole 672. *THE JOURNAL of CELL Bioroey*, 99:672–679, 1984. URL http://rupress.org/jcb/article-pdf/99/2/672/1077629/672.pdf.

[227] Kathryn A. Fraser and Stephen A. Rice. Herpes simplex virus type 1 infection leads to loss of serine-2 phosphorylation on the carboxyl-terminal domain of RNA polymerase II. *Journal of virology*, 79(17):11323–11334, 9 2005. ISSN 0022-538X. doi: 10.1128/JVI.79.17.11323-11334.2005. URL https://pubmed.ncbi.nlm.nih.gov/16103184/.

[228] Mark Ou and Rozanne M. Sandri-Goldin. Inhibition of cdk9 during herpes simplex virus 1 infection impedes viral transcription. *PloS one*, 8(10), 10 2013. ISSN 1932-6203. doi: 10.1371/JOURNAL.PONE.0079007. URL https://pubmed.ncbi.nlm.nih.gov/24205359/.

[229] Claire H. Birkenheuer and Joel D. Baines. RNA Polymerase II Promoter-Proximal Pausing and Release to Elongation Are Key Steps Regulating Herpes Simplex Virus 1 Transcription. *Journal of Virology*, 94(5), 2 2020. ISSN 0022-538X. doi: 10.1128/JVI.02035-19. URL /pmc/articles/PMC7022368/ /pmc/articles/PMC7022368/?report=abstract https://www.ncbi.nlm.nih.gov/pmc/articles/PMC7022368/.

[230] Ozlem Yildirim and Robert E. Kingston. Molecular Dissection of Chromatin Maturation Via Click Chemistry. *Current protocols in molecular biology / edited by Frederick M. Ausubel ... [et al.]*, 114:21.33.1, 4 2016. ISSN 19343647. doi: 10.1002/0471142727.MB2133S114. URL /pmc/articles/PMC4968042/ /pmc/articles/PMC4968042/?report=abstract https://www.ncbi.nlm.nih.gov/pmc/articles/PMC4968042/.

[231] J A Dembowski and N A DeLuca. Selective recruitment of nuclear factors to productively replicating herpes simplex virus genomes. *PLoS Pathog*, 11(5):e1004939, 2015. doi: 10.1371/journal.ppat.1004939. URL https://www.ncbi.nlm.nih.gov/pubmed/26018390.

[232] J A Dembowski and N A DeLuca. Temporal Viral Genome-Protein Interactions Define Distinct Stages of Productive Herpesviral Infection. *MBio*, 9(4), 2018. doi: 10.1128/mBio.01182-18. URL https://www.ncbi.nlm.nih.gov/pubmed/30018111.

[233] KC Palozola, G Donahue, and KS Zaret. EU-RNA-seq for in vivo labeling and high throughput sequencing of nascent transcripts. *STAR Protoc.*, 2021. doi: 10.1016/j.xpro.2021.100651.

[234] Carlos Perea-Resa, Leah Bury, Ian Cheeseman, and Michael D Blower. Cohesin removal reprograms gene expression upon mitotic entry. *Mol Cell*, 78(1):127–140, 2020. doi: 10.1016/j.molcel.2020.01.023.

[235] Stephen A. Rice and Kathryn A. Fraser. The Modification of Cellular RNA Polymerase II During HSV-1 Infection. In *Alpha Herpesviruses: Molecular and Cellular Biology*. 2006.

[236] Zhuoran Li, Ce Fang, Yuanyuan Su, Hongmei Liu, Fengchao Lang, Xin Li, Guijun Chen, Danfeng Lu, and Jumin Zhou. Visualizing the replicating HSV-1 virus using STED super-resolution microscopy. *Virology Journal*, 13(1):1–13, 4 2016. ISSN 1743422X. doi: 10.1186/S12985-016-0521-7/FIGURES/7. URL https://virologyj.biomedcentral.com/articles/10.1186/s12985-016-0521-7.

[237] Erica Y. Jacobs, Ikuo Ogiwara, and Alan M. Weiner. Role of the C-Terminal Domain of RNA Polymerase II in U2 snRNA Transcription and 3 Processing. *Molecular and Cellular Biology*, 24(2):846, 1 2004. ISSN 0270-7306. doi: 10.1128/MCB.24.2.846-855.2004. URL /pmc/articles/PMC343789/ /pmc/articles/PMC343789/?report=abstract https://www.ncbi.nlm.nih.gov/pmc/articles/PMC343789/.

[238] Sylvain Egloff, Hadeel Al-Rawaf, Dawn O'Reilly, and Shona Murphy. Chromatin Structure Is Implicated in "Late" Elongation Checkpoints on the U2 snRNA and β-Actin Genes. *Molecular and Cellular Biology*, 29(14):4002, 7 2009. ISSN 0270-7306. doi: 10.1128/MCB.00189-09. URL /pmc/articles/PMC2704739/ /pmc/articles/PMC2704739/?report=abstract https://www.ncbi.nlm.nih.gov/pmc/articles/PMC2704739/.

[239] Dawn O'Reilly, Olga V. Kuznetsova, Clelia Laitem, Justyna Zaborowska, Martin Dienstbier, and Shona Murphy. Human snRNA genes use polyadenylation factors to promote efficient transcription termination. *Nucleic Acids Research*, 42(1):264, 1 2014. ISSN 03051048. doi: 10.1093/NAR/GKT892. URL /pmc/articles/PMC3874203/ /pmc/articles/PMC3874203/?report=abstract https://www.ncbi.nlm.nih.gov/pmc/articles/PMC3874203/.